Terms and Conditions of Use of Digitised Theses from Trinity College Library Dublin

Copyright statement

All material supplied by Trinity College Library is protected by copyright (under the Copyright and Related Rights Act, 2000 as amended) and other relevant Intellectual Property Rights. By accessing and using a Digitised Thesis from Trinity College Library you acknowledge that all Intellectual Property Rights in any Works supplied are the sole and exclusive property of the copyright and/or other IPR holder. Specific copyright holders may not be explicitly identified. Use of materials from other sources within a thesis should not be construed as a claim over them.

A non-exclusive, non-transferable licence is hereby granted to those using or reproducing, in whole or in part, the material for valid purposes, providing the copyright owners are acknowledged using the normal conventions. Where specific permission to use material is required, this is identified and such permission must be sought from the copyright holder or agency cited.

Liability statement

By using a Digitised Thesis, I accept that Trinity College Dublin bears no legal responsibility for the accuracy, legality or comprehensiveness of materials contained within the thesis, and that Trinity College Dublin accepts no liability for indirect, consequential, or incidental, damages or losses arising from use of the thesis for whatever reason. Information located in a thesis may be subject to specific use constraints, details of which may not be explicitly described. It is the responsibility of potential and actual users to be aware of such constraints and to abide by them. By making use of material from a digitised thesis, you accept these copyright and disclaimer provisions. Where it is brought to the attention of Trinity College Library that there may be a breach of copyright or other restraint, it is the policy to withdraw or take down access to a thesis while the issue is being resolved.

Access Agreement

By using a Digitised Thesis from Trinity College Library you are bound by the following Terms & Conditions. Please read them carefully.

I have read and I understand the following statement: All material supplied via a Digitised Thesis from Trinity College Library is protected by copyright and other intellectual property rights, and duplication or sale of all or part of any of a thesis is not permitted, except that material may be duplicated by you for your research use or for educational purposes in electronic or print form providing the copyright owners are acknowledged using the normal conventions. You must obtain permission for any other use. Electronic or print copies may not be offered, whether for sale or otherwise to anyone. This copy has been supplied on the understanding that it is copyright material and that no quotation from the thesis may be published without proper acknowledgement.

The Characterisation of Electrical Energy Consumption in Complex Manufacturing Process Chains

Eoin O'Driscoll

Department of Mechanical and Manufacturing Engineering

Parsons Building

Trinity College

Dublin 2

Ireland

November 2013

A thesis submitted to the University of Dublin in partial fulfilment of the requirements for the degree of Ph.D.

Declaration

I declare that I am the author of this thesis and that all work described herein is my own, unless otherwise referenced. Furthermore, this work has not been submitted, in whole or part, to any other university or college for any degree or qualification. I authorise the library of Trinity College, Dublin to lend or copy this thesis.

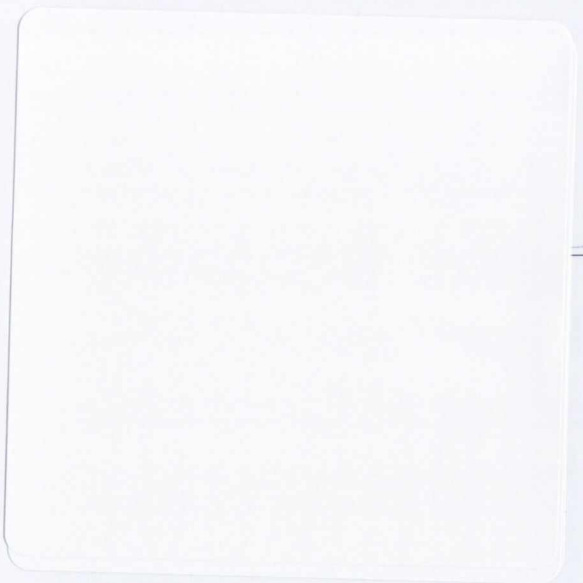

Abstract

The combination of increasing energy costs, corporate image concerns, and environmental legislation is driving a transition towards energy and resource efficiency within the manufacturing sector. Developing a more comprehensive understanding of how energy is consumed within manufacturing facilities is now a core component of research efforts aiming to advance industrial energy efficiency. This thesis reports on the research undertaken to develop a holistic understanding of energy consumption within complex manufacturing facilities at each hierarchical level.

The literature has identified energy transparency as a key enabler of energy efficiency and various studies have highlighted structured submetering as the preferable approach to achieve the necessary level of transparency. The industrial case study described here considered all aspects of the design, installation, and operation of a facility wide energy metering system. The case study presents an effective energy metering system implementation strategy that includes a decision support tool that identifies where metering devices are needed. The case study also develops energy performance indicators based on the data emanating from the installed metering system. The metering infrastructure that is installed in the test facility represents the state-of-the-art in industrial energy metering and comparable projects have not been reported in the literature to date.

A custom power measurement tool facilitated a detailed unit process level energy characterisation. The energy consumption of each machine tool component was assessed during a structured characterisation study. The dynamic behaviour of the machine tool was also investigated during a series of machining tests. The machining tests were performed in order to investigate two phenomena; the relationship between power consumption and depth of cut, and also the relationship between specific energy consumption and material removal rate. Developing a complete understanding of the energy requirements of machining is an essential step towards advancing industrial energy efficiency.

A novel nonintrusive intelligent energy sensor revealed that the operational status of a machine tool could be inferred from information contained within the power signals recorded at the machine tools main incomer. The intelligent energy sensor combines a nonintrusive load monitoring system with condition based inference algorithms in order to identify the operational status. Obtaining transparency on machine tool status during machining will motivate improvements that can reduce the energetic impacts of machining. The research revealed that the information available at the

machine tools electrical service entry is capable of identifying individual component activations in addition to the overall operational status.

Acknowledgments

It would not have been possible to write this doctoral thesis without the help and support of the kind, caring, and inspirational people around me. I would first like to offer my sincere thanks to my PhD supervisor, Dr. Garret O'Donnell. Since meeting Dr. O'Donnell as an undergraduate student he has provided me with unwavering support. Dr. O'Donnell's guidance, motivation, and encouragement at every stage of this work are gratefully acknowledged and appreciated. Special thanks are also offered to Kevin Kelly for his support and constructive advice during some of the most difficult moments of the project.

I would also like to thank my industrial mentor, Dónal Óg Cusack, for his guidance and support. It has been exciting and rewarding to collaborate so closely with industry during this project. Thanks must also be extended to the rest of the team in DePuy Ireland, particularly Donall, Linda, Shane, Norman, Owen, and Joe. At this point I would also like to acknowledge that this project has been funded by the Irish Research Council, DePuy Ireland, and Trinity College Dublin.

To all the mechanical engineering postgrads and workshop staff: Stuart, Barry, Jeff, Robin, Darren, Paul E., Kevin, Darren B., Paul H., Emma, Gio, Seamus, Rayhaan, Peadar, Mick, JJ, Alex, and Seanie. Thank you for all the friendship, words of encouragement, lunchtime company, and support throughout this research project. In particular, special thanks must be extended to Andrew Kelly and Rory Stoney for providing 24/7 technical support, listening ears, laughter, and friendships that I hope last for many years.

To my sister, Tracey, thank you for always looking on the bright side and providing an endless supply of hilarious stories that brightened even the darkest days of my research. Thanks also to my partner, Roxanne, whose love, care, and companionship have been a major source of strength throughout this project. Finally and most importantly, I owe my deepest gratitude to my mother and father, Julie and Michael. Their unequivocal support and endless love have allowed me to get to where I am now. Although I will never be able to adequately express it, I will always be grateful for the opportunities that their hard work has given me.

"Be practical as well as generous in your ideals.

Keep your eyes on the stars

and keep your feet on the ground."

- T.Roosevelt

This work is dedicated to my parents, Julie and Michael O'Driscoll.

Contents

List of Figures

List of Tables

Nomenclature

AHU Air handling unit

CF Crest factor

$CIRP$ International Academy of Production Engineering

$Cos\ (\varphi)$ Power factor

CNC Computer numerical control

CO_2 Carbon dioxide

$d_{Euc}(x, y)$ Euclidean distance

DF Degrees of freedom

EI Energy intensity

FF Form factor

Fv Feature vector

Gt Gigatonne

H_0 Null hypothesis

H_1 Alternate hypothesis

HSS High speed steel

hp Horsepower

I Electric current (Ampere)

$i(t)$ Instantaneous current (Ampere)

$KERS$ Kinetic energy recovery system

LCA Life cycle assessment

MAD Median absolute deviation

MRR Material removal rate

N Spindle speed (RPM)

n Sample size

$NILM$ Nonintrusive load monitor

P Power (Watt)

PCA Principal component analysis

PPC Production planning and control

$p(t)$ Instantaneous power (Watt)

p_m Machining power

p_o Overheads power

p_s Services power

Q Reactive power (Volt-Ampere Reactive)

Q_C Capacitance

Q_L Inductance

RPM Revolutions per minute

S Apparent power (Volt-Ampere)

SEC Specific energy consumption

SEU Significant energy user

SRI Self regulatory initiative

Tm Transformation matrix

THD Total harmonic distortion

V Electric potential difference (Volt)

$v(t)$ Instantaneous voltage (Volt)

μ Sample mean

σ Standard deviation

η Efficiency

Ω Electrical resistance (Ohm)

Chapter 1

Introduction

1.1 Global energy overview

The scale and breadth of the energy challenge is enormous - far greater than many people realise [1]. Over the past twenty years the world's energy landscape has undergone a fundamental change. During the 1990's when the price of oil bottomed out at US$20/barrel, climate change and environmental awareness were only issues for environmentalists. This is in stark contrast to the rapidly expanding industrialised world of 2013 which places climate change and energy security at the forefront of the international agenda [2].

Between 1996 and 2007, the world's total output of primary energy - petroleum, natural gas, coal, and electric power - increased at an average annual rate of 2.3% [3]. The year 2009 saw annual global energy use fall, as a result of the global downturn, for the first time since 1981, however, the International Energy Agency (IEA) have predicted that global energy consumption will grow at a rate of 1.5% until 2030 [4]. The World Energy Council (WEC) recently reviewed the status of the world's major energy resources and addressed the key challenges of the future. The report highlighted the rapid growth of the developing world coupled with the industrialised world's demand for a long term, affordable and secure energy supply as critically important issues [2]. The political complexities of the global energy market also pose dangerous threats; the current state of political turmoil in the Middle East has the potential to instantly destabilise the market.

An additional complication identified by the WEC are logistics bottlenecks within the energy industry. In its logistics bottlenecks report the WEC identified three crucial bottlenecks; oil movement, natural gas and liquefied natural gas (LNG) movement, and electricity transmission [2]. To develop the required oil pipeline and tanker networks, gas pipelines and LNG carrier systems, as well as smart grids boosting the efficiency of electricity distribution, the WEC estimate that more than US$200 billion will have to be spent in the next ten years and an additional US$700 billion in the 2020 to 2050 timeframe [2].

In order to effectively address the challenges posed by the current international environment, the European Union must take a multi-lateral approach to ensure long term development and stability. The Kyoto agreement, signed by over 190 countries with a view to reducing greenhouse

gas emissions, represents one facet of the global approach that is required to combat the energy crisis. The Kyoto protocol established emissions targets for each participating country, relative to their 1990 emissions levels. The Kyoto protocol has had a wide reaching influence simultaneously forcing governments to develop and implement energy efficiency action plans; organisations to adapt energy management strategies; and individuals to become more aware of energy issues.

If global energy consumption trends continue on their current path without any change in government policy there will be significant consequences from a climate change perspective [1]. Having already increased from 20.9 gigatonnes (Gt) in 1990 to 31.2 Gt in 2011, CO_2 emissions are projected to reach 37 Gt in 2035 [5]. Of this projected rise in emissions, 6 Gt is attributed to China, 2 Gt is attributed to India and 1 Gt is attributed to the Middle East [5]. If this trend is realised it would lead to a rapid increase in the concentration of greenhouse gases in the atmosphere, causing significant climatic change and inflicting irreparable damage on the planet [1]. Research studies are already warning that climate change is accelerating with sea levels rising, oceans acidifying and ice caps melting much quicker than initially anticipated [6].

Electricity consumption is also increasing dramatically with a reported rise of over 200% since 1971 [1]. Approximately 66% of this electricity is generated from fossil fuels, primarily from coal, 40%, and gas, 20%. In Ireland, the demand for electricity increased by an average of 0.7% per annum between 2005 and 2010 [7]. In 2010 the Irish electricity generation fuel mix was dominated by gas, with significant contributions from coal, peat, and renewables, see Figure 1.1(a) [7]. In terms of energy security, Ireland is heavily dependent on energy imports with 82% of Ireland's primary energy requirements being met by imported oil and gas in 2010, Figure 1.1(b) [7]. This figure has risen significantly since the mid 1990's when domestic production accounted for 32% of the total primary energy requirement. The key drivers behind this increase are a substantial increase in energy use coupled with a decline in indigenous natural gas and peat production [7]. There is a possibility that this trend could be reversed in the near future with recent exploratory drilling projects off the coast of Ireland at Barryroe and the Porcupine Basin reporting significant oil deposits.

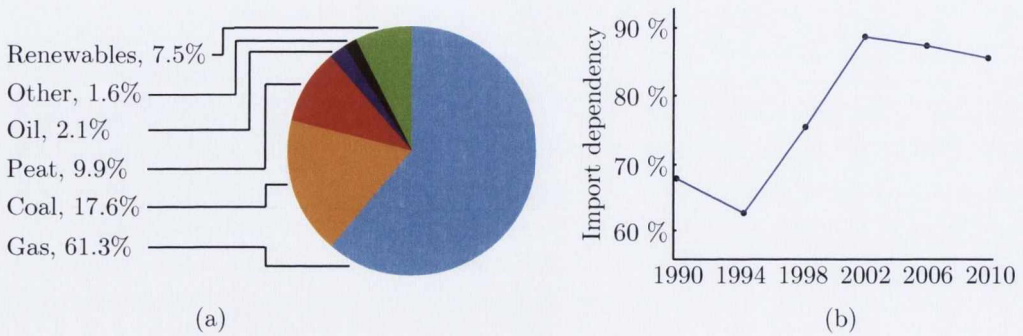

Figure 1.1 – (a) Generation of electricity in Ireland in 2010, (b) Import dependency, adapted from [7]

1.2 Environmentally benign manufacturing

Globally, the industrial sector is the largest consumer of energy [8], see Figure 1.2. The manufacturing sector, which is a subset of the industrial sector covering the mining and quarrying of raw materials, construction, and also the manufacture of finished goods and products is responsible for over one third of global energy use and CO_2 emissions [4]. According to Duflou et al. [9], manufacturing is responsible for 84% of the industrial sectors energy related CO_2 emissions and 90% of the industrial sectors energy consumption.

The manufacturing industry is central to the economy's success, contributing to employment growth, innovation, technological advancement and productivity. Environmentally benign manufacturing is a philosophy that facilitates economic progress while minimising pollution, waste and conserving resources. The implementation of environmentally conscious management strategies, regulatory policies, and operating principles will help protect the environment for future generations.

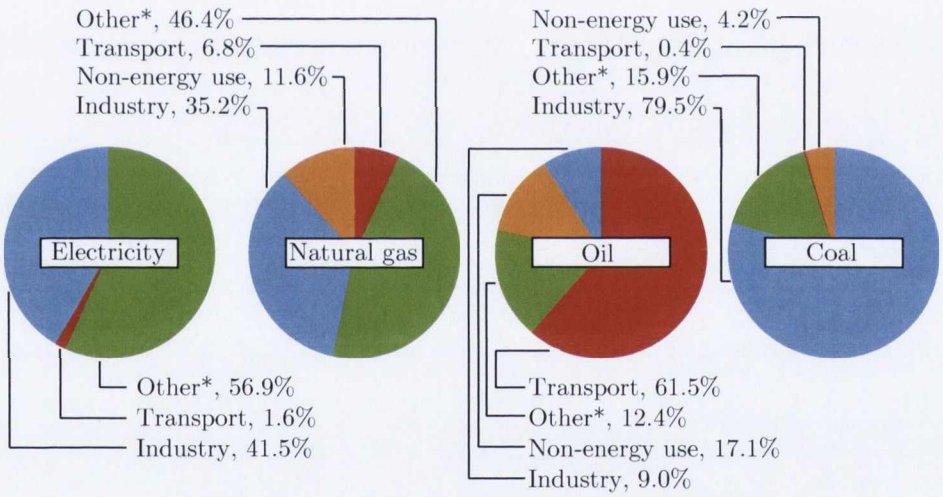

Figure 1.2 – Global total final consumption by sector, adapted from [10]

Manufacturing enterprises require energy in order to produce goods and any increase in production results in increased energy consumption. Herrmann et al. [11] noted that limiting production output is not a feasible option, therefore the improvement of energy efficiency in complex manufacturing facilities is a necessity. Energy efficiency in this context refers to methodologies, frameworks, and procedures that reduce the volume of energy required per unit of production. The opportunities that exist to use energy more efficiently at each stage of product manufacture must be explored as they often represent cost effective ways of cutting emissions and improving productivity. According to the IEA [1], up to 35 exajoules, equivalent to 26% of current primary

energy use in industry could be saved every year if all proven technologies and best practices were implemented throughout the industrial sector. Although reducing energy consumption has typically been promoted as a cost cutting exercise, the future will see the implementation of reduction and optimisation strategies being driven by the need to avoid levies and taxation.

1.3 Energy measurement enabling a sustainable future

In order to overcome the climate and energy challenges already described, significant changes are required. For a successful global transition to sustainable development it is necessary to more efficiently integrate academic results and insights with practical applications in society [12]. Similarly there is an urgent need for decision makers to develop and implement proactive, integrated policies and strategies that will assist societies manage all resources in a more sustainable way [12]. Although there is little doubt that a combination of smart grids, time of use tariffs, and renewable energy generation represent the long term solution to the energy crisis, more efficient energy consumption has the potential to make the most significant contribution in the short term. As a result of this, there is an increased emphasis on adopting environmentally benign processes and products [13].

Manufacturing enterprises typically transition towards environmentally benign processing by reducing utility expenditure in a number of ways: implementing energy efficient technologies, removing out dated equipment, running energy awareness programs for staff, and implementing lean manufacturing initiatives. In an effort to better understand the overall impact a manufacturing facility has on the environment a conceptual model focussing on the flows of material, energy, and waste has been developed and tested [14]. Herrmann et al. [15] observed that a fundamental precondition for accurately identifying and implementing energy efficiency improvement measures is transparency about the energy demands of all processes within a manufacturing facility.

From the perspective of energy consumption, machine tools represent an example of one area where significant savings can be made [16, 17]. Many machine tools are less than 30% efficient [18], and in an effort to reduce energy wastage during production researchers have focused on a wide variety of approaches including: automated energy monitoring [19], energy management [20], simulation [21], ecodesign [22], sustainability [23], and reducing consumables [24].

It is clear that improving energy efficiency is desirable for many reasons, and this improvement can only be realised by accurately quantifying current consumption patterns. The energy and power measurement technologies required to provide this quantification also provide energy transparency locally within manufacturing facilities; this not only improves understanding of energy usage but also provides a broad quantitative perspective on day to day consumption. Therefore power and energy metering technologies not only facilitate process improvements and developments; they also fully support the broader smart grid/time of day pricing implementation infrastructure.

1.4 Research focus

This study is concerned with the development of measurement and characterisation methodologies that facilitate the quantification of energy consumption in manufacturing facilities at various hierarchical levels. The aims of the research are:

- To accurately quantify the energy consumption of a complex manufacturing facility via the implementation of a site wide energy metering system and the development of analytical disaggregation techniques;
- To investigate the component level power consumption of a machine tool representing a unit process within a manufacturing facility;
- To design, develop, and experimentally verify, a nonintrusive intelligent energy sensor capable of recognising the operational status of a machine tool based on the information which exists within the power signals.

An industrial case study was undertaken in a large multinational biomedical device company located in Ireland. A wireless state-of-the-art energy metering system was installed which facilitated a detailed energy analysis. The scale of the installed energy metering system coupled with the resulting process level energy consumption disaggregation represent two areas of novelty in this section of the work.

The second major component of the research involved the design and development of a customised power metering device in order to allow the test machine tool to be characterised from a power consumption perspective. The metering device was calibrated against high end commercially available power measurement equipment. Each machine tool component was investigated independently and the machine tool's performance during machining was also evaluated. The observed results throughout this section align with recently published research studies in the field.

The final stage of the research involved the development of a novel nonintrusive intelligent energy sensor. The system deploys voltage and current sensing elements at the main incomer of the machine tool and assesses the current machine tool status based on the patterns that exist within the acquired time and frequency domain signals. The measurement system employs statistical pattern recognition techniques including principal component analysis and median absolute deviation in order to identify the operational status of the machine tool.

Chapter 2

Literature review

2.1 World energy outlook

The economic, political, and environmental climates currently facing governments worldwide are unprecedented. The need to ensure a secure energy supply is now more urgent than ever. The past decade has brought almost unparalleled uncertainty to the energy industry characterised by the recent turmoil in the Middle East and North Africa, a global recession, and the catastrophic earthquake and tsunami which triggered the Fukushima nuclear disaster in Japan [4]. The global recession has provided an unexpected, and relatively narrow, window of opportunity to take action to concentrate investment on low carbon technologies [2]. A combination of the rate at which economies and populations within the developing world grow, energy efficiency trends, environmental legislation, and the development and deployment of new technologies will all play a role in reducing the projected gap between the supply and demand of energy, Figure 2.1 [2, 4, 25].

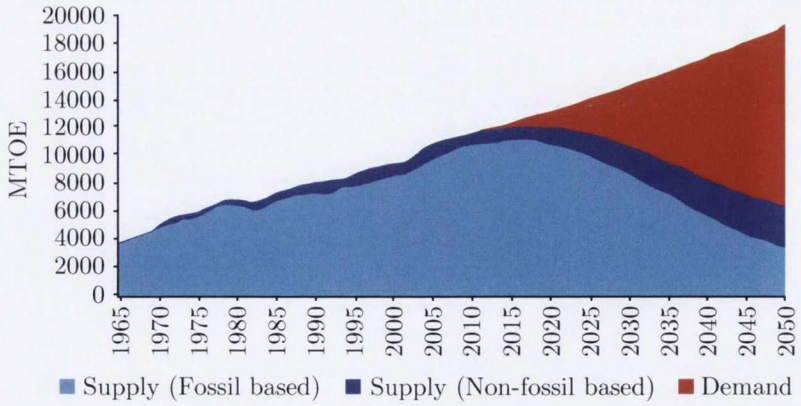

Figure 2.1 – Growing gap between energy supply and demand, adapted from [25]

2.1.1 Primary energy sources

The world's aggregated energy usage is growing steadily. This increased energy consumption is strongly coupled to economic growth in both developing and industrialised countries - the relation-

ship between energy consumption and GDP is illustrated in Figure 2.2. For a more comprehensive analysis of this relationship, the works of Jean-Baptiste and Decroux [26] and Lee and Chang [27] are both informative and concise.

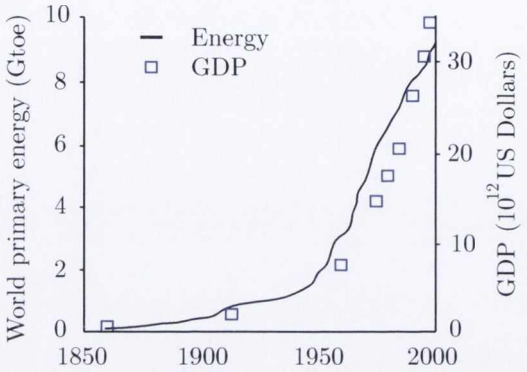

Figure 2.2 – Relationship of GDP and Energy, adapted from [26]

Primary energy is defined as the energy used by the end user plus generation, transformation and distribution losses [28]. Fossil fuels currently supply 80% of global primary energy and this figure is expected to remain largely the same through 2030 [1]. According to the IEA [1], global primary energy demand will increase by 36% before 2035. Almost all of this growth increase, approximately 93%, is attributed to emerging economies. From a European perspective, the primary energy mix has changed significantly over the past 40 years, see Figure 2.3.

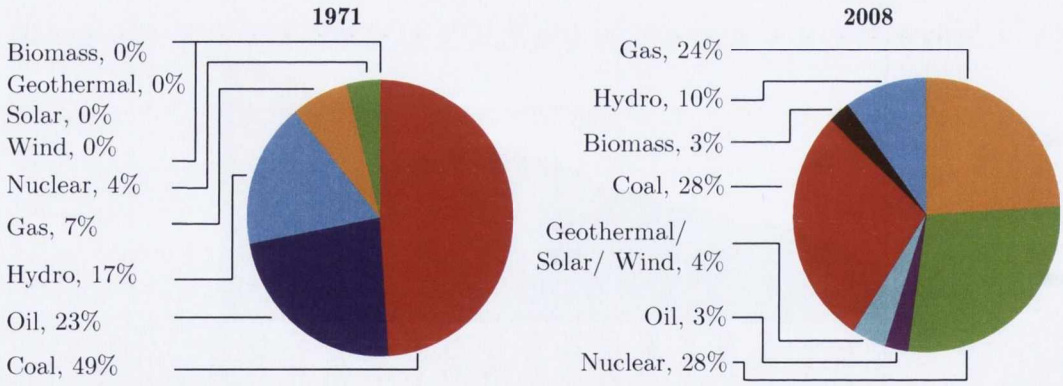

Figure 2.3 – EU27's evolving energy mix (% of electricity consumption), adapted from [6]

In 1971 almost half of Europe's power came from coal, 23% from fuel oil, and 4% from nuclear energy. The generation mix has changed and in 2008, 23% of Europe's electricity came from gas, just 3% from fuel oil, and in the region of 20% from renewable sources [6]. Although a wide range of technological developments and new policies will improve the energy scenario in the coming years, the global energy system is still not on a sustainable path [5]. An overview of recent trends

and the current state of some important primary energy sources is given in sections 2.1.2 and 2.1.3.

2.1.2 Non renewables

Although the proliferation of renewable energy sources is predicted to increase rapidly, the IEA [5] project that the principal source of energy up to 2035 will continue to be fossil fuels. Although the demand for coal, oil, and gas is predicted to grow in absolute terms between 2012 and 2035, their combined share of the global energy mix will decrease from 81% to 75% during the same period [5].

2.1.2.1 Coal

Coal production increased by 1.7 billion tonnes between 1996 and 2006, or at an average annual rate of 2.9% [3]. According to the WEC [2], world coal reserves amount to 860 billion tonnes, of which 405 billion (47%) is classified as bituminous coal, 260 billion (30%) is sub-bituminous, and 195 billion tonnes (23%) is lignite. The USA, Russia and China account for nearly 60% of global reserves [1]. By 2030 the use of coal is expected to rise by over 60% with developing countries responsible for 97% of this increase. It is estimated that coal's share in global electricity generation will increase from 41% to 44% by 2030 [1].

2.1.2.2 Oil

Global reserves of crude oil are reported to be approximately 1,482 billion barrels, with 81% of these reserves held by OPEC member countries [29]. As demand increases and supply diminishes, the price of oil will increase as time progresses; the OPEC Reference Case assumes a nominal price that remains in the US$100/barrel range over the years to 2020, reaching US$155/barrel by 2025 [29]. Oil pricing is a delicate and multifactorial problem. The IEA [30] noted that the price of oil must be sufficiently high to provide an incentive for its development and supply, but oil prices must not be so high that they impair global economic growth. The sector that has the biggest impact on oil demand is the transportation sector, and moving forward it is predicted that this will remain true [30].

2.1.2.3 Oil shale

Oil shale is a sedimentary rock that shale oil and combustible gas can be extracted from by destructive distillation. Oil shale deposits exist in many parts of the world and the size of these areas and their associated ability to generate revenue varies dramatically. Total world resources of shale oil are estimated at 4.8 trillion barrels [1]. Because of the higher costs associated with shale oil, due to the additional costs of mining and extracting the energy, only a small number of oil shale deposits are currently being exploited in Brazil, China, Germany, and Israel [1]. However, with the continuing decline of petroleum supplies and the increased costs of petroleum based products,

oil shale presents opportunities for supplying some of the fossil based energy needs of the world in the future [1].

2.1.2.4 Natural gas

Natural gas is the cleanest and most efficient fossil fuel; it will play a pivotal role in the battle to overcome present and future environmental challenges. According to the IEA [1], natural gas reserves are sufficiently abundant to cover global gas demand for many decades. At the end of 2008, 103 countries were identified as possessing proved reserves of natural gas with a total volume estimated to be in the region of 186 trillion cubic meters. As is the case with coal, some of the world's largest reserves are held by the Russian federation. Natural gas demand is projected to increase by 1.6% per year between 2007 and 2030 to a total of 4.4 trillion cubic meters [1]. In terms of global primary energy demand the share of natural gas is projected to rise from 21% in 2010, to 23% in 2030 [4]. The IEA [4] report that the industrial sector is expected to increase its natural gas demand from 1 trillion cubic meters in 2010 to 1.5 trillion cubic meters by 2030.

2.1.2.5 Nuclear

The generation of nuclear electric power increased by 369 billion kilowatt hours between 1996 and 2006, or at an average annual rate of 1.5% [3]. Due to the low share of fuel costs relative to total generating costs, nuclear power generators continue to be highly cost competitive [1]. Uranium costs account for approximately 5% of total generating costs and because of this plants are insulated from the volatility of fuel costs. This point is illustrated by noting that 2007 saw Uranium spot prices hit an all time high of US$ 350/kgU - compared to US$ 25/kgU in 2003 - and the generating costs of nuclear power plants were barely affected [1].

As of January 1^{st} 2010, the IEA [1] reported that there were four hundred and thirty seven nuclear power reactors in operation worldwide, with a total capacity of 372 GW; the 2,588 TWh of electricity produced by these nuclear reactors in 2009 translated into a market share of 14%. During the year 2009 the UK Nuclear Installations Inspectorate approved an additional 10 years of operation for 2 reactors and the Garona nuclear power plant in Spain was also granted a four year license extension [1]. In addition to this, discussions had started in Germany with a view to postpone the nuclear phase-out policy that required the closure of its reactors between 2015 and 2025 [1].

On the 11^{th} March 2011, a powerful magnitude nine earthquake occurred off the north coast of Japan, which generated a tsunami that struck the shore causing devastating damage. The earthquake and, in particular, the tsunami had a disastrous impact upon the Fukushima Dai-ichi (No. 1) nuclear power station, which was to become the centre of world attention as a consequence [31]. The perception of nuclear power was altered following the Fukushima disaster and it had an immediate impact on the development of nuclear facilities worldwide. In the aftermath

of the accident, China slowed its nuclear spending and revised their goal for generation from solar power from 5 GW to 10 GW [32]. The German government also committed to upgrading the transmission grid, a precondition for replacing nuclear energy with solar, wind, and other renewable power sources [32]. The Fukushima disaster has renewed a global commitment to rigorous nuclear safety and stimulated an increased interest in other carbon free energy solutions.

2.1.3 Renewable energy sources

Manzano-Agugliaro et al. [33] defined a renewable energy source as a sustainable resource available over the long term that can be used for any task without negative effects. Renewable energy resources currently supply 14% of the total world energy demand and this share is expected to increase significantly to between 30% and 80% before 2100 [33]. According to the IEA [5], this increase will be driven by incentives, falling costs, technological advancements, and rising fossil fuel prices.

2.1.3.1 Hydropower

Hydroelectric power plants reliably generate low-cost electricity by harnessing the energy contained in flowing water. Manzano-Agugliaro et al. [33] reported that hydroelectric power is currently the largest renewable energy resource contributing to electricity generation in 160 countries. China is the largest producer of hydroelectricity, followed by Canada, Brazil, and the United States [33]. The IEA [5] reported that 3,190 TWh of hydropower were generated in 2010, corresponding to 16% of global electricity generation and 88% of electricity generated from renewables.

Hydroelectric power systems are characterised by low operations and maintenance costs and long operational life spans. Although hydroelectric power plants do not pollute the water or air they do have a measurable environmental impact. Hydroelectric facilities can change the local environment by affecting the natural habitat in the dam area. The construction of dams can effect fish migration and the operation of hydroelectric generators can change river water temperature often harming plants and animals.

2.1.3.2 Wind energy

The extraordinary growth of wind energy can be demonstrated by noting that the European projection for 2010, set out in the European Commission's 1997 White Paper on renewable energy, was 40 GW [1]. This figure represented a sixteen fold increase in the 1995 capacity, and was achieved by 2005. The total European capacity at the end of 2012 was 106 GW; 101 GW onshore and 4,993 MW offshore [34]. Global wind capacity has been doubling about every three years since 1990, see Figure 2.4, and it is the renewable resource that has grown at the fastest rate. Total capacity at the end of 2012 was over 282 GW [35].

Figure 2.4 – Growth of world wind capacity, adapted from [35]

Numerous estimates exist to try and assess the total energy available from the wind. One estimate presented by Archer and Jacobson [36], suggested that the global wind resource, exploiting only the best sites, with wind speeds above 6.9 m/s at 80 m, could cover the world's electricity needs seven times over. The International Energy Agency's Reference Scenario [1] suggested a global capacity of 422 GW by 2020, but other studies projected higher. The European Wind Energy Association [37] estimated that there will be 230 GW in Europe by 2020, 40 GW of which will be offshore. According to the EIA [38], offshore wind farms are over 150% more expensive than comparable onshore wind developments. In order to achieve the installed capacity estimated by the IEA and assuming an installed cost of US$ 2,000/kW, an investment of around US$ 522 billion will be required over the next 10 years [36].

2.1.3.3 Solar

Solar power can be used to generate electricity at a utility scale in two ways; concentrating solar power (CSP) and photovoltaic technologies (PV). CSP technologies use the sun's energy to generate heat that will drive either a steam turbine or an external heat engine. At the start of 2011, the total installed capacity of CSP plants was 1.26 GW. In photovoltaic systems the photons in sunlight are converted directly into electricity. The IEA [5] reported that PV electricity generation increased from 14 GW in 2008 to 70 GW in 2011 [5]. A key benefit of solar power systems is their ability to generate and supply electricity in regions that are not connected to an electricity supply grid.

Turney and Fthenakis [39] noted that solar powered electricity generation is experiencing rapid growth with total worldwide installed capacity increasing by 40% every year. One of the major drawbacks associated with solar power systems is their cost; the EIA [38] have reported that in terms of US$/MWh solar power is approximately 100% more expensive than the price of energy derived from a conventional coal power plant. In addition to this cost constraint, areas with limited sunlight are also problematic. The largest producers of solar energy in the world are Germany, Japan, and the USA.

2.1.3.4 Geothermal

Geothermal energy is the energy contained as heat inside the earth. The commercial harnessing of geothermal energy for electricity generation has existed since early in the 20^{th} century. Thermal energy from the earth's core heats up underground water sources producing steam. This steam is then channeled towards turbines where it generates electricity. One major drawback associated with geothermal power is the resources limited availability, mainly in harsh geographical locations at high altitude, beside active volcanoes, or in tectonically active regions. According to Manzano-Agugliaro et al. [33], the exploitable potential of geothermal energy systems will increase over the next decade as a result of technical innovations however, the resources limited availability will result in a steady decrease of growth rates.

2.1.3.5 Biomass

Biomass represents an abundant carbon-neutral renewable resource for the production of bioenergy and biomaterials. Currently forestry, agricultural and municipal residues, and purpose grown energy crops are the main feedstocks for the generation of electricity and heat from biomass. Using bioenergy saves the environmental cost of disposing waste material however the burning of biomass releases large amounts of particulates and gases which have a negative impact on the environment. Of the total global bioenergy produced today, wood biomass accounts for 87%, agricultural crops for 9% and municipal and industrial waste for 4% [33]. The main advantage biomass possesses over other renewable energy sources is its availability; biomass is abundantly available throughout the world unlike wind and geothermal resources [33].

Although renewable energy sources are less harmful to the environment than traditional non-renewable sources, the installation and operation of renewable energy power plants can still have adverse environmental impacts which need to be considered. With respect to large scale solar power installations, Turney and Fthenakis [39] identified a series of environmental impacts which fall under five main headings: land use intensity, human health, plant/animal life, geohydrological resources, and climate change. None of the 32 identified impacts are negative relative to traditional power generation, however, the removal of forest spaces to allow the construction of solar power facilities is an example of one indirect cause of CO_2 emissions associated with the development of renewable energy power plants.

The rate of diffusion of renewable energy technologies (RET's) is also a concerning issue. An extensive literature survey was conducted by Negro et al. [40] that categorised the main problems hampering the diffusion of RET's. Market structures, legislative failures, capability problems, and infrastructural failures are all included within the list of systemic problems that are effecting the diffusion rate of RET's [40]. Negro et al. [40] observed that a one size fits all solution does not exist and that it is necessary for stakeholders to focus on the technologies that will provide the largest

benefits. It is inevitable that the exploitation of renewable energy sources will continue to increase over the next twenty years, however energy derived from non renewable sources will continue to meet most of the world's growing energy needs, Figure 2.5.

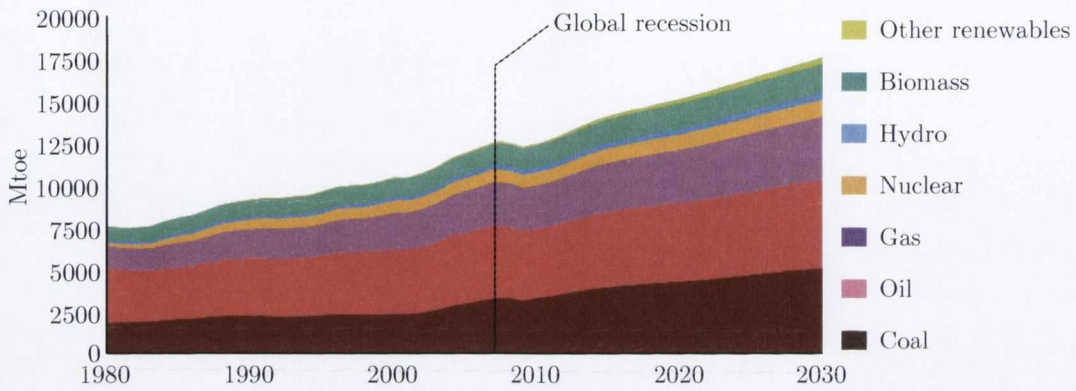

Figure 2.5 – Global primary energy demand, adapted from [1]

2.1.4 EU total final consumption

Total final energy consumption is all energy that is delivered to the end user; it differs from primary energy as it does not include transmission and transformation losses. Consumers of electric power differ widely depending on their requirements for power and for this reason utility companies typically categorise consumers into broad sectors. The residential sector includes private households and apartment buildings where energy is consumed primarily for space heating, water heating, air conditioning, lighting, refrigeration, and cooking. The commercial sector includes non-manufacturing business establishments including hotels, restaurants, retail outlets, social premises, and educational institutions. Finally the industrial sector represents the segment of the economy that includes agriculture, construction, fisheries, forestry, and manufacturing. The sector by sector breakdown of final energy consumption for the EU-27 in 2010 is displayed in Figure 2.6.

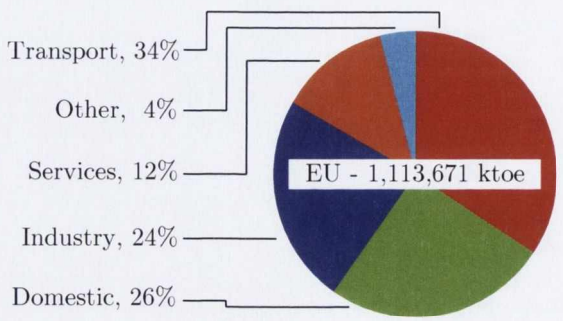

Figure 2.6 – Final energy consumption by sector, adapted from [41]

2.2 Energy use in industry

Industrial facilities consume energy in order to perform a number of tasks; electrical energy is used to power machinery, pumps, belts and fans, gas is used for heating, while compressed air is used for applications including pneumatic actuation and cleaning. Manufacturing companies are therefore financially exposed to energy cost fluctuations; they are affected directly by the energy cost of making products, maintaining office operations, receiving raw materials and delivering finished goods [42]. Herrmann and Thiede [21] reported that energy efficiency is becoming an important area for manufacturing companies as a result of the volatility associated with energy prices. According to the IEA [1], industrial energy consumption will grow at an accelerated rate until 2030, with much of the projected growth occurring in non-OECD countries. Throughout this period electricity will continue to be the essential energy form, see Figure 2.7.

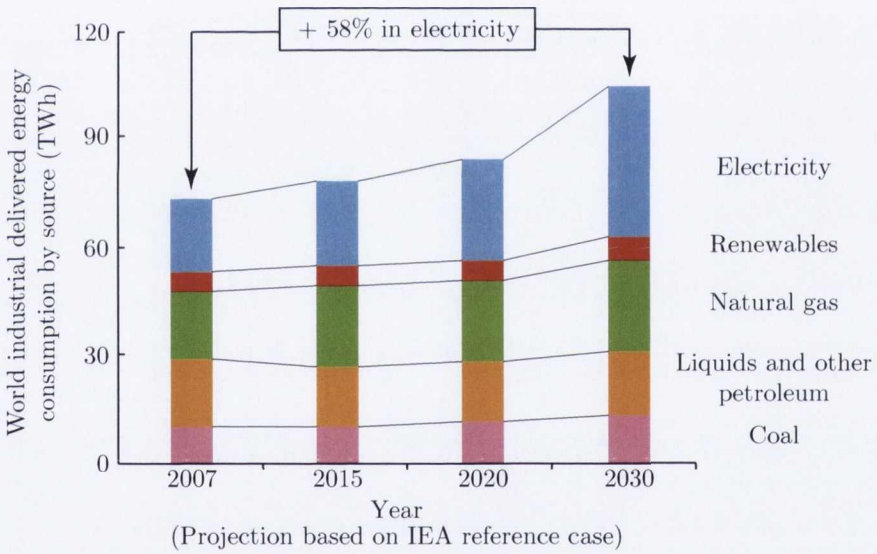

Figure 2.7 – Projection of world industrial energy consumption by sources, adapted from [43]

One of the primary factors that is driving this energy consumption increase is increasing machine tool complexity. A study described by Zein [43] highlighted how the power consumption of manufacturing equipment has grown over the past 70 years. The data presented in Figure 2.8 is derived from three German automotive metalworking manufacturing facilities. The long term trend evident in the dataset identifies a significant amplification of power ratings for both grinding and turning machines. It is the opinion of Zein [43] that this trend is interrelated to the introduction of CNC controls in machine tools at the end of the 1970's.

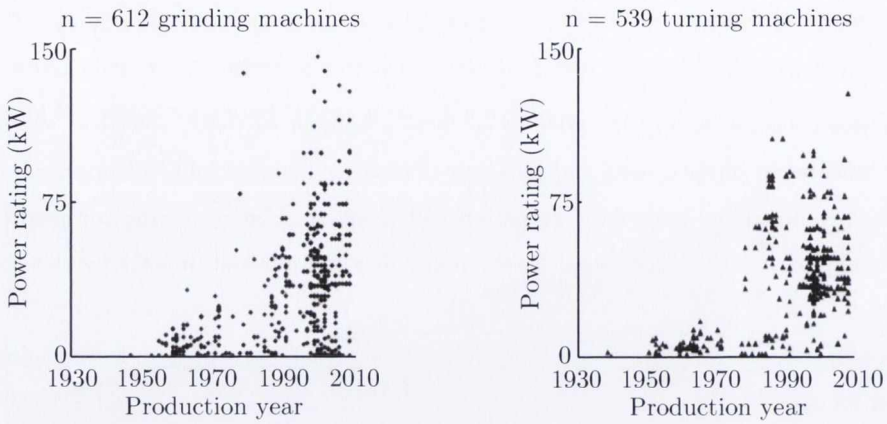

Figure 2.8 – Empirical long term trends in machine tool power ratings, adapted from [43]

2.2.1 Defining energy efficiency

A number of different definitions exist for energy efficiency. At a macro level the definition of energy efficiency is quite general, for example, the Energy Information Administration (EIA) in the United States define energy efficiency as *"the ratio of the amount of energy services provided to the amount of energy consumed"*. The International Standard Oranisation (ISO) use *"the ration or other quantitative relationship between an output of performance, service, goods or energy, and an input of energy"* [44]. From an economic standpoint, energy efficiency is defined as the energy used per unit of economic output; also known as energy intensity. Finally from a physics and engineering perspective energy efficiency is defined by the first law of thermodynamics, measuring the relationship between the total amount of energy inputs and the corresponding amount of useful energy outputs.

2.2.2 Drivers for and barriers to improving energy efficiency in industry

Delivering goods and services more efficiently, using less energy, is a core component of today's attempts to reduce global carbon emissions [45]. Improving energy efficiency remains the largest and least costly strategy for realising reductions in carbon emissions, according to the IEA [46]. In manufacturing, energy cost has traditionally been only a small portion of the total production cost, and therefore, energy cost has received relatively little attention. The combination of increased energy prices, corporate responsibility, and environmental legislation have forced senior management in manufacturing facilities to become energy conscious and focus time and capital on energy efficient optimisation projects [47].

Within the manufacturing sector there still remains scepticism around the effectiveness of energy efficiency projects which hinders the implementation of energy reduction strategies; this barrier results in the creation of an energy efficiency gap. This phenomenon has been defined as the

deviation between actual and ideal energy system requirements [43]. Taylor [48] reported that the energy efficiency gap exists primarily because the seemingly obvious benefits of implementing energy efficiency improvement projects - cost savings, improved compliance, reduced liability, etc., - are not sufficient to ensure cleaner production practices are adopted. The energy efficiency gap represents an unexploited opportunity to improve energy performance that remains untapped. The main drivers to improving energy efficiency in the manufacturing sector have been described in the literature as either economic or environmental; the most prominent barriers can be partitioned into organisational or economic categories [49].

2.2.2.1 Economic and environmental drivers

The economic drivers for energy efficiency in the European manufacturing sector can be loosely divided into three sections: energy prices, economic climate, and policies and regulation. Energy markets and market prices influence the decisions made by manufacturing companies regarding whether or not to invest in energy efficiency projects. As with all economic problems, the economics of energy efficiency is a question of balancing costs and benefits. For the end user this involves weighing the higher initial costs of purchasing energy-efficient components against the projected future cost savings associated with the components improved energy performance. High energy prices do not just influence the procurement decisions of the end user, Gillingham et al. [50] reported that higher energy prices have a significant impact further upstream in the technology development process; forcing manufacturers to produce more efficient goods. As a result of the increasing global resource constraints, it is probable that energy prices will continue to grow at an accelerated rate. A recent research study presented by Altmann et al. [51] highlighted the development of oil price projections between the year 2000 and 2010, see Figure 2.9. If these projections are realised, the level of capital investment injected into energy efficiency improvements will be forced to increase in order to combat the inflated price of energy.

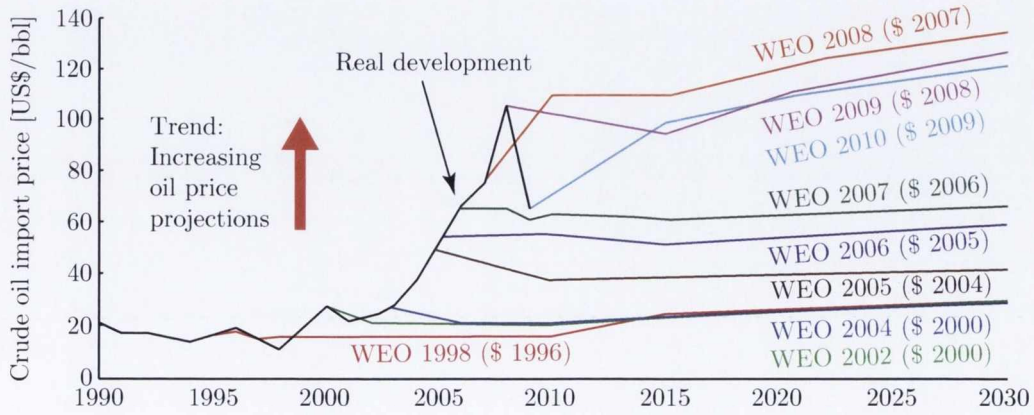

Figure 2.9 – Development of oil price projections over time, adapted from [51]

The economic climate also has a measurable impact on energy efficiency within the manufacturing sector. Studies have shown that periods of economic growth have a positive impact on efficiency due to an increased level of investment in efficiency [51, 52]. This increase in efficiency is not usually seen as a reduction in energy consumption as periods of economic growth invariably result in increased production which stabilises the energy consumption. This fact is illustrated by noting that since the year 2000, industrial growth has averaged slightly less than 2% annually whereas energy consumption has remained constant [51]. Periods of economic decline result in an overall reduction in energy consumption without efficiency improvements, see Figure 2.10.

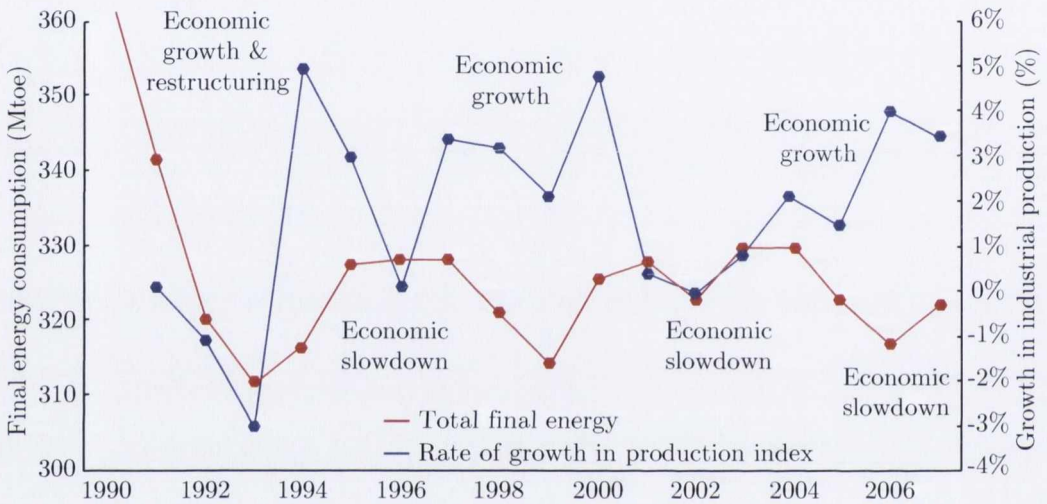

Figure 2.10 – Development of industrial final energy consumption and production index, adapted from [51]

From a policy standpoint, the EU has a total of around 260 measures that have been implemented or considered in the industrial sector, of which 180 measures are being applied [52]. Most of the ongoing measures are relatively recent; nearly 70% have been implemented since 2000 and more than 40% since 2005 [51]. In a recent EU policy overview document, the number of ongoing energy efficiency measures by type were presented, see Figure 2.11.

The most widely recognised and influential measure within the financial measures category is the EU Emissions Trading Scheme (EU-ETS). The EU-ETS, which aims at the energy generation industry and also large industrial emitters, is by far the most important instrument to reduce GHG emissions in the industrial sector [52]. Another measure that is forecast to have a significant effect on energy efficiency in the industrial sector is the ecodesign directive (Directive 2005/32/EC).

From a regulatory point of view, energy management and the implementation of energy management standards are the key drivers for industrial energy efficiency improvements [53]. Energy management standards comprise a small number of steps that assist a company to actively manage energy use and cost, reduce emissions without incurring a negative effect on operations, and

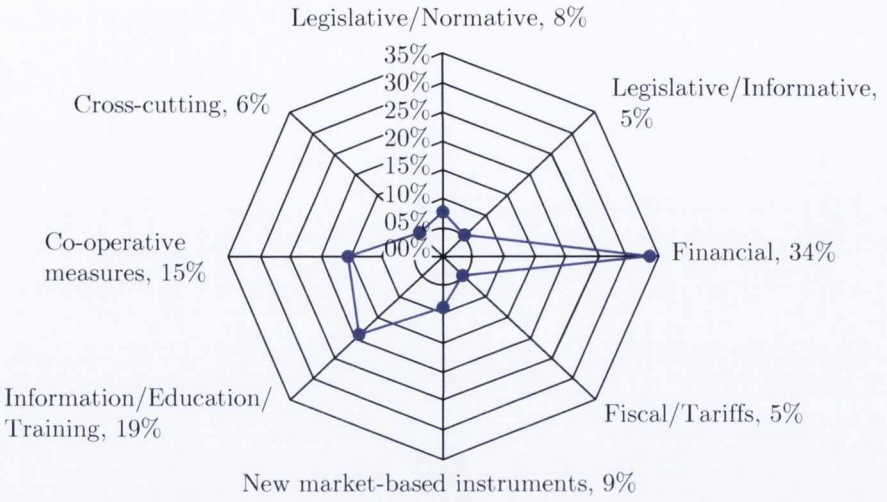

Figure 2.11 – EU policy measures by type, adapted from [52]

document all savings for both internal and external use. Thumann [53] observed that there is no one size fits all solution to energy management and the development of an appropriate program is dependent on the size of the facility, the type of industry, number of employees, and energy sources used. A typical energy management standard includes the following;

- A strategic plan - covering the measurement, management, and documentation of any implemented measures;
- A cross-divisional management team - led by a representative who deals directly with senior management;
- Policies and procedures - addressing energy procurement and consumption;
- Projects - demonstrating the continuous improvement in energy efficiency;
- Energy manual - a document that evolves in parallel with the implementation of energy efficient procedures and projects;
- Key performance indicators - the identification of these indicators provides management with a metric to continuously monitor;
- Periodic reporting - both internal and external audits track progress;

All energy management systems follow a similar methodology; plan, act, check, review. ISO 50001:Energy Management Systems Standard, represents the current state-of-the-art in energy management throughout Europe. This standard is based on existing management standards such as ISO 9001:Quality Management Systems, ISO 14001:Environmental Management Systems, and

replaces the previous energy management systems standard ISO 16001. ISO 50001 defines a standardised framework of systems and processes designed to enable organisations to manage and enhance energy performance by achieving measurable energy savings, Figure 2.12.

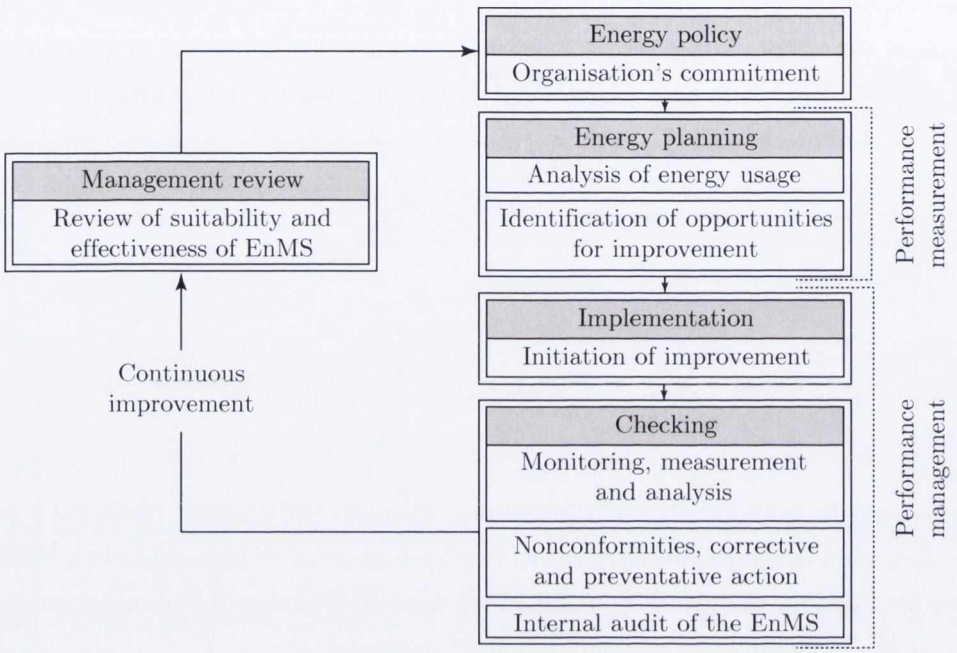

Figure 2.12 – Energy management system model, adapted from [43]

2.2.2.2 Organisational and economic barriers

It is widely accepted that the efficient utilisation of energy is a key method for reducing greenhouse gas emissions and achieving energy policy goals however, the combination of organisational and economic barriers continues to impede the progress of energy efficiency projects. According to Solding and Thollander [54], the aforementioned barriers to energy efficiency are the principal reason why obviously cost-efficient measures are not always implemented and the energy efficiency gap is sustained. Several studies have confirmed that due to the uncertainty of the savings achievable through the implementation of energy efficiency improvements and energy management programs, there is hesitancy from senior management to invest the level of capital required in order to make significant savings [43, 55, 56].

This point of view is supported by a recent survey that also cites the inadequate amount of technical expertise on evaluating projects and the lack of awareness about opportunities as additional barriers [49]. Mecrow and Jack [57] placed further emphasis on this knowledge barrier; a recommendation was made to improve end user awareness in order to dispel incorrect beliefs that exist in the industrial sector. For example, it is a commonly held belief that purchasing a motor rated higher than the application demands, will result in a longer motor lifetime. In practice

however, an over rated motor will have higher iron losses, magnetising losses, and friction losses which will substantially reduce the motors efficiency [57]. Thiede et al. [58] observed that this knowledge gap is particularly prevalent in SME's. Additional barriers identified within the survey of Swedish manufacturing companies conducted by Rohdin and Thollander [49] included the cost of production disruption and inconvenience.

As outlined above, energy efficiency choices fundamentally involve investment decisions that trade off higher initial capital costs and uncertain lower future operating costs. A large proportion of the economic literature covering energy efficiency focuses on behavioural failure and in particular the potential impact policy changes can have to counteract and correct the behaviour of manufacturing companies. Gillingham et al. [50] observed that if behavioural failures lead to under investment in energy efficiency, then a degree of energy consumption reduction could be available at low or even negative cost. At the same time, policies that provide a means of correcting environmental externalities, such as emissions price, may not be well suited to inducing these relatively low-cost energy and emission reductions [50].

Economic market barriers, defined as disincentives to the adoption or use of a good, may in some cases, be beyond the control of policy makers. For example, potential market barriers from an energy efficiency perspective include low energy prices and high technology costs, neither of which can be influenced by policy makers [50]. The economic barriers that can be influenced by policy makers, along with suggested policy options for the removal of these barriers is presented in Table 2.1.

Economic barriers	**Potential policy options**
Energy market	
Environmental externalities	Emissions pricing (cap-and-trade)
Energy security	Energy taxation
Capital	
Liquidity constraints	Financing/loan programs
Innovation	
Research and development	R & D tax credits
Information	
Lack of information	Information programs

Table 2.1 – Overview of economic barriers to energy efficiency [50]

2.3 Characterising the electrical energy requirements of manufacturing systems

Characterising and quantifying the energy consumed within manufacturing facilities has been identified as an area of importance by a number of researchers including Kara et al. [59] and Rahimifard et al. [60]. Within the majority of manufacturing facilities improving the efficiency of electricity consumption is prioritised over other energy forms including gas, as it is used in greater quantities and is significantly more expensive per kWh, see Figure 2.13.

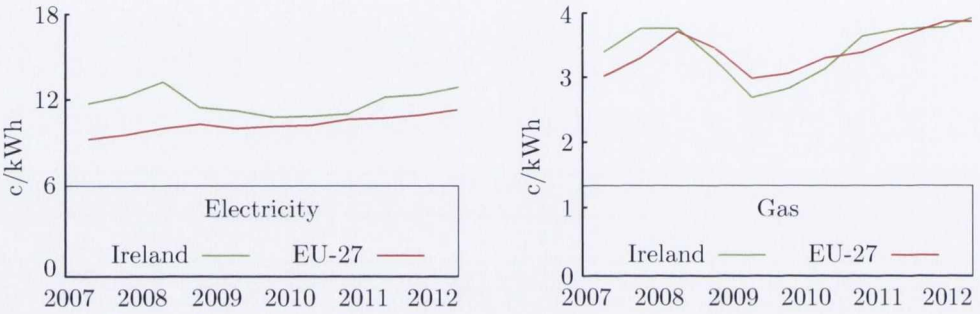

Figure 2.13 – Electricity and gas prices per kWh, adapted from [61]

Electrical energy is used in manufacturing facilities to power machine tools, production supporting equipment, lighting, ventilation and chiller systems, as well as other ancillary devices, see Figure 2.14. The primary function of electricity in industrial facilities throughout the EU however, is to power motors and pumps.

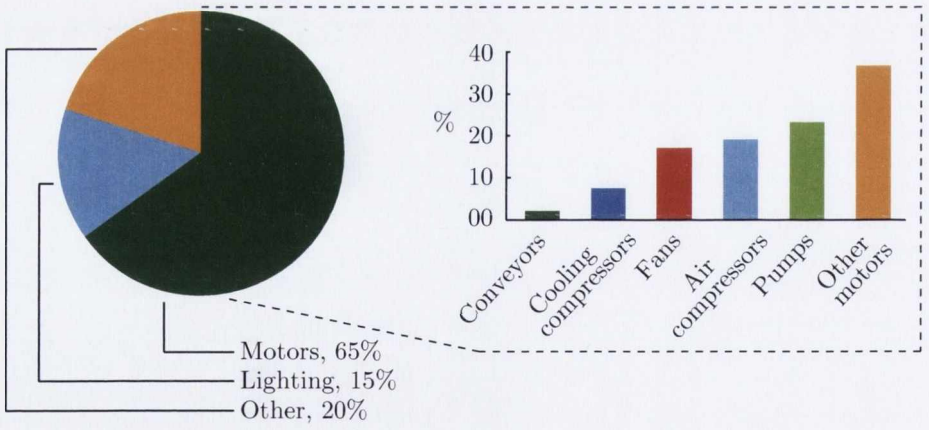

Figure 2.14 – Breakdown of industrial electricity consumption, adapted from [8]

Hesselbach et al. [62] noted that as a consequence of the high levels of energy consumed during manufacturing, companies have an economic motivation to consciously consider energy issues alongside traditional production objectives including cost, quality, and time. In order to increase the efficiency of electrical energy consumption and reduce energy waste, Kopac and Pusavec [63]

suggested that manufacturing companies must follow the resource flow, quantify it, and analyse the data in order to identify opportunities for improvement. As part of this analysis, it is essential to take a holistic approach that considers the electrical energy requirements of equipment required directly and indirectly during production [62, 64]. Figure 2.15 shows a model of a manufacturing facility developed by Herrmann and Thiede [21] that maps the electrical energy consumption requirements of a typical manufacturing facility.

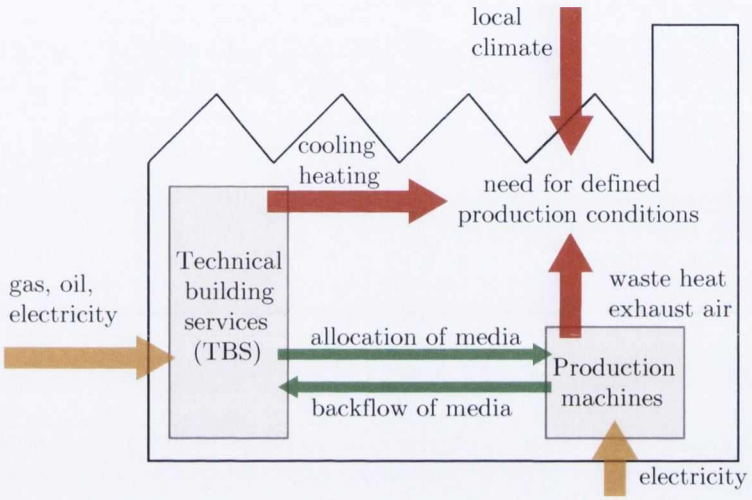

Figure 2.15 – Production facility model, adapted from [21]

One key aspect of the model developed by Herrmann and Thiede [21] is the interdependencies that exist between process energy and enabling energy. For example, machining processes generate heat that is emitted from the machine tool to the local environment, this additional heat forces the HVAC and chiller systems to work harder in order to maintain a constant facility temperature. In order to allow a structured analysis of a manufacturing facility it is possible to decompose the system hierarchically, see Figure 2.16. A perspective on some of the key contributors to energy consumption at a variety of levels follows.

1. Global supply chain (Section 2.3.1)
2. Facility (Section 2.3.2)
3. Significant energy user
4. Value stream (Section 2.3.3)
5. Machine (Section 2.3.4)
6. Machine tool component (Section 2.3.5)

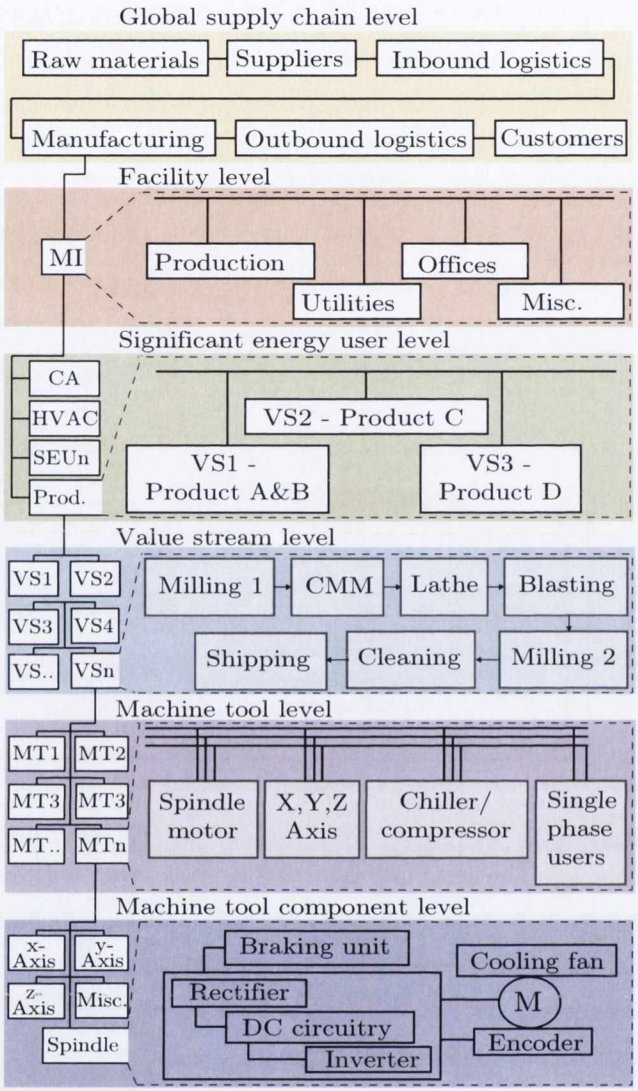

Figure 2.16 – Hierarchical breakdown of a manufacturing system

2.3.1 Global supply chain

Duflou et al. [9] defined a global supply chain as a set of three or more entities directly involved in the upstream and downstream flows of products, services, finances, and/or information from a source to a customer. At this level, a manufacturing organisation consists of a global web of operations and activities including suppliers, production sites, research and development facilities, inventory hubs, and sales centres. The increasing geographical scope of these supply chains is now exposing organisations to a variety of cultural, legal, administrative, linguistic, and political issues that impact on the smooth running of operations [65]. Duflou et al. [9] observed that each country has its own associated environmental impact depending on the primary energy sources used. As a result of this, significant differences exist between countries that rely on conventional

power generation, such as Australia, versus countries that have already moved towards renewable energy, for example Brazil [9].

The movement of goods throughout this global supply chain has a negative impact on the environment that can be reduced by optimising the management of the supply chain. Smith and Schmidt [65] reported that large multinational organisations including Walmart, Ikea, and Tesco are investing in the optimisation of their supply chain energy consumption in order to address corporate level energy efficiency and sustainability targets. Kara and Ibbotson [66] detailed a methodology for quantifying the impact globalised manufacturing has on the embodied energy of products. The study assessed six different products manufactured from various raw materials in a global manufacturing network. The study found that product, material and key supply chain parameters play a crucial role [66].

A study presented by Vanek and Sun [67] developed and implemented an energy consumption model to explore the environmental impact of supplying temperature controlled food products to various locations within the US using surface transportation. The study found that there is significant energy savings potential available from optimising materials souring, transportation choices, and inventory costs. A further study presented by Pearce et al. [68] used Google maps to minimise the embodied energy of transportation by optimising transport routes.

The improvement potential available from optimising logistics was further highlighted in a study by Nuortio et al. [69] which focused on the environmental impacts of municipal waste collection in industrialised cities. The study focused on 169 refuse collection routes in a city located in eastern Finland. The study used matlab to implement improvement heuristics that optimised the distance each refuse collection vehicle traveled in a given day. The experimental results demonstrated that significant energy and cost savings can be achieved by optimising the routing and scheduling of logistics operations [69].

2.3.2 Facility

Research studies at the facility level primarily focus on quantifying and optimising the energy consumed by high-level services such as HVAC and lighting, which are responsible for maintaining the required product conditions and environment. A study presented by Herrmann and Thiede [21] found that process and space heating, lighting, compressed air, and steam are responsible for approximately 35-40% of the total manufacturing industry's energy consumption. Research studies in this area also focus on the effects of energy management systems, the minimisation of peak load surcharges, as well as building design and construction [9, 70].

HVAC systems are one of the largest consumers in typical commercial and industrial facilities. A research project reported by Mathews et al. [71] highlighted a number of ways to improve the energy efficiency of a HVAC system in a commercial building. Within this research project, the provision of HVAC accounted for 54% of the buildings total energy consumption [71]. The majority

of the improvement potential existed in the optimisation of control strategies that simultaneously enhanced the occupiers comfort levels while reducing the systems energy consumption. Examples of control system changes described in this study include setback control, which allows air temperature to increase in unoccupied areas and also enhanced economiser control by varying the amount of outside air that is input to the HVAC system [71]. In a further study concentrating on HVAC systems, Fassiudin and Budaiwi [72] presented technical opportunities for optimising the energy consumption of HVAC systems in non-domestic buildings. Again key findings here included varying the temperature set points during periods of unoccupancy and optimising operating schedules [72].

Lighting systems have also been studied in detail with a view to understanding their impact on facility consumption. Ryckaert et al. [73] observed that in order to accurately assess a lighting installation the power load, P, needs to be calculated. This P value is dependent on:

- The efficiency of the lighting gear, η_{gear};
- The efficacy of the light sources, η_{lamp}, expressed in Lumens per Watt;
- The efficiency of the light fixture;
- The utilance, U, is the efficiency of directing the luminous flux from the light fixture to the task area;
- The maintenance factor, MF, is defined as the ratio of the illuminance on a given area at the end of the maintenance cycle to the initial illuminance of the same area; [73]

Because the lighting gear can have a considerable impact on the lamp efficacy and lamp power, the efficiency of the gear and the efficacy of the lamp are combined in the system efficiency, η_{sys}. The target value proposed in the research of Ryckaert et al. [73] is:

$$\eta_{sys} = \eta_{gear}.\eta_{lamp} > 75lm/W \tag{2.1}$$

The use of this type of system efficiency calculation penalises the use of inefficient gear, including incandescent lamps, while, in general, T5 fluorescent lamps or the most efficient high pressure lamp types easily meet the required value set out in the Ryckaert et al. [73] study. Recently LED's have attracted a lot of attention and interest due to their minimal energy consumption in comparison with existing technologies; for example, a 3 W LED can replace a 40 W halogen lamp. LED's also have an extremely long life span, and can emit coloured light without the use of coloured filters [74]. Apart from the actual light fittings, the energy consumption of a lighting installation is strongly dependant on lightning controls including presence detection and dimming; these controls must also be optimised to maximise efficiency [75]. The work of Duflou et al. [9] is an example of a study that focuses on energy efficient lighting controls. The proposed lighting control system regulates the quantity of artificial light supplied while simultaneously ensuring the overall intensity of illumination is constantly above a minimum threshold [9].

Energy conscious building design is another viable method to reduce energy consumption at facility level. According to the research work of Harvey et al. [76], the single most important factor in the design of low energy buildings is a high performance envelope. For the case of manufacturing facilities, Duflou et al. [9] identified the key functions of the building envelope as thermal and sound insulation, as well as protection from humidity. In particular, the building envelope provides thermal stability for the manufacturing equipment [9]. Harvey et al. [76] reported that effective building design can result in savings of up to 75% by eliminating the need for mechanical heating and cooling equipment. Pachero et al. [70] also reviewed the existing literature on energy efficient building design including building orientation, shape, envelope system, passive heating and cooling mechanisms, shading, and glazing. The influence that each of these parameters has on energy demand was assessed and the best combinations of design options were proposed.

2.3.3 Value stream

The work of Duflou et al. [9] describes value streams as multi-machine ecosystems. Within these ecosystems the goal is to completely utilise all energy inputs and therefore remove environmental wastes. An energy cascade framework is proposed which describes how individual energy inputs can be consumed in multiple processes [9]. Examples presented in the Duflou et al. [9] study include the use of industrial waste heat from a furnace as an energy input for a heat treatment process and also the generation of electricity from industrial waste heat using a Rankine cycle. The work of Vikhorev et al. [77] supports the assertions made by Duflou et al. [9] and suggests scheduling production activities with heat requirements in parallel with other processes that release heat in order to take advantage of energy cascading.

Several research teams have presented frameworks that attempt to holistically quantify value stream level energy consumption. The total equivalent energy tool (TEE), described by Naughton [64] is used to quantify the energy requirements and energetic impact of supporting utilities. The TEE tool is used exclusively for the semiconductor manufacturing industry, which is resource intensive, using large amounts of energy, water, and chemicals [78]. The TEE tool normalises all of the tool configuration differences by establishing an energy boundary condition around each piece of semiconductor manufacturing equipment. The main components of the TEE tool are the energy conversion factors (ECF's), these ECF's are a measure of the total energy required to produce a given utility per unit mass of volume [64]. The basis of the TEE method is summarised in the following formulae [64]:

$$TEE_{SME} = SME_{DE} + SME_{IEU} + SME_{IEH} \tag{2.2}$$

where:

TEE_{SME} = Total equivalent energy

SME_{DE} = Direct energy supplied to equipment

SME_{IEU} = Indirect energy for utilities

SME_{IEH} = Indirect energy for heat removal

Another study that attempts to separate the two discrete components of energy consumption: direct energy and indirect energy was presented by Rahimifard et al. [60]. The primary aim of this particular research project was to map the embodied energy of a product by holistically analysing the total value stream energy requirements. Rahimifard et al. [60] defined the direct energy consumed by a product as:

$$DE_A = \sum_{i=1}^{n} (TE(i)_A + AE(i)_A) \tag{2.3}$$

The indirect energy component, that encapsulates the energy required by supporting activities, for example control systems, lubricants and coolant is defined as [60]:

$$IE_A = \sum_{j=1}^{m} IEzone(j)_A \tag{2.4}$$

where:

DE_A = Total direct energy consumed by product A

TE_A = Theoretical energy consumed by product A

AE_A = Auxiliary energy consumed by product A

The overarching model that describes the research of Rahimifard et al. [60] is included in Figure 2.17 which illustrates the author's method of distinguishing between direct and indirect energy consumption.

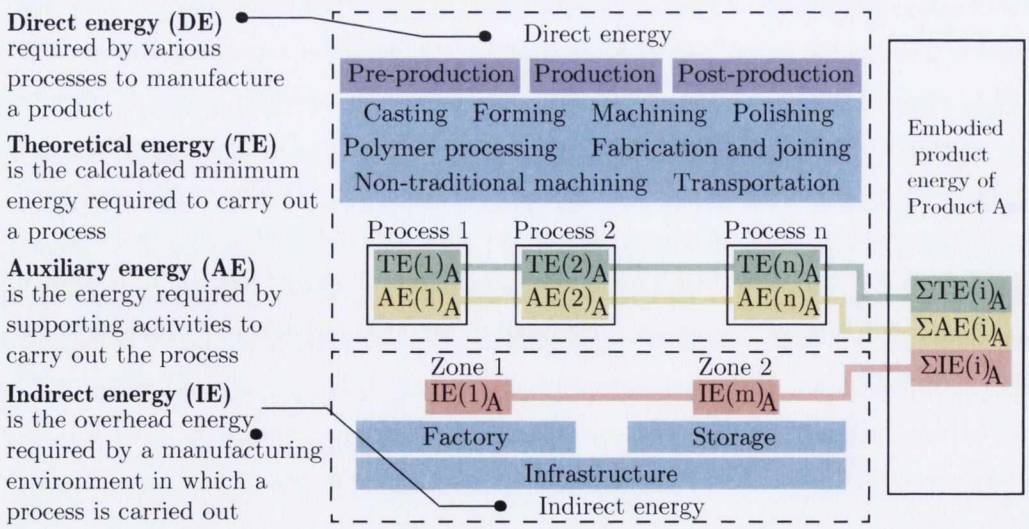

Figure 2.17 – The embodied product energy framework, adapted from [60]

The significant impact that supporting equipment has on the overall process consumption was also assessed by Gutowski et al. [79]. An automobile production line was investigated and the results showed that the proportion of the total energy consumption resulting from machining was only 14.8% of the total for the line in question, see Figure 2.18. Over 31% of the total energy consumption resulted from the use of cooling lubrication fluids to counter the intense heat generated in the cutting zone during the observed machining processes [79].

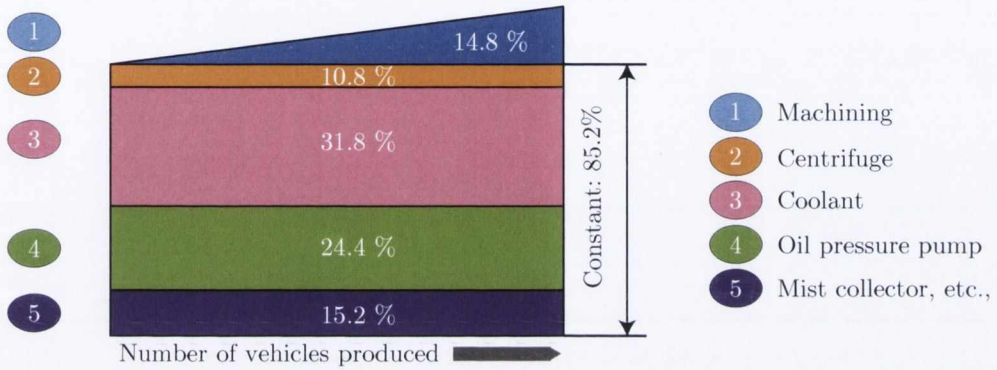

Figure 2.18 – Energy used as a function of production rate, adapted from [79]

Within discrete manufacturing facilities energy consumption at a value stream level is strongly influenced by process planning and production scheduling. Production schedules are typically optimised with respect to cycle times and throughput without considering energy costs. The studies presented by Vikhorev et al. [77], Pechmann and Schoeller [80], and Duflou et al. [9] describe techniques that aim to optimise production schedules in order to minimise value stream energy consumption, see Figure 2.19.

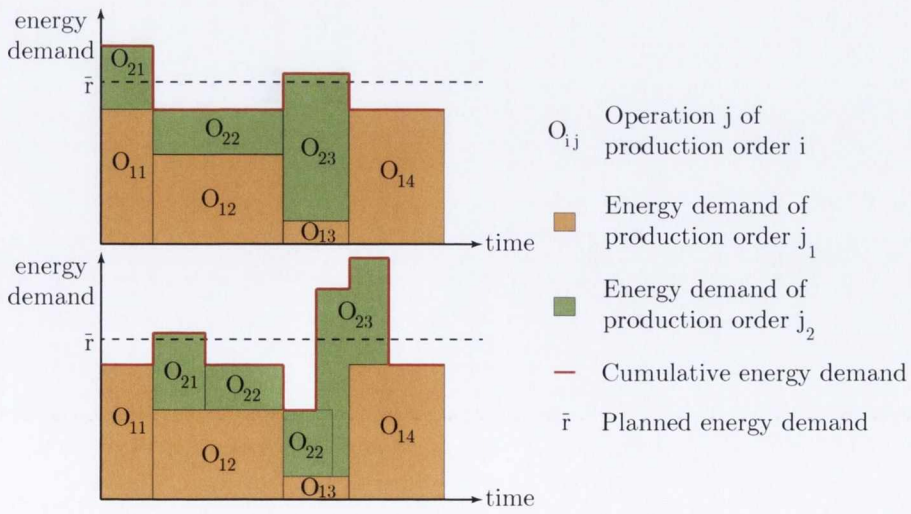

Figure 2.19 – Influence of PPC on energy demand, adapted from [9]

Pechmann and Schoeller [80] investigated the optimisation of energy costs via intelligent production scheduling. The software tool developed in this study allowed a production schedule to be developed that avoids the creation of energy consumption peaks and also allows a twenty four hour energy consumption forecast to be created [80]. An alternative approach that proposes complex event processing as a viable method to dynamically optimise production schedules was presented by Vikhorev et al. [77].

2.3.4 Machine

The majority of research works that focus on the energy consumption and energy efficiency of machine tools concentrate on individual machines and work stations within the context of a broader production system. The key factors for machine tool designers are functionality, cost, accuracy, and safety; until recently, minimising energy consumption has not been a priority. Increasing energy prices and a focus on the environmental impacts of production have ensured that energy consumption is now an important factor for the end user [81, 82]. The energy consumption of manufacturing machines is not normally constant during a production process but rather highly dynamic depending on the state of the machine [62]. Zein [43] described how the overall electrical energy demand of a machine tool results from the temporal accumulation of each components power consumption, see Figure 2.20.

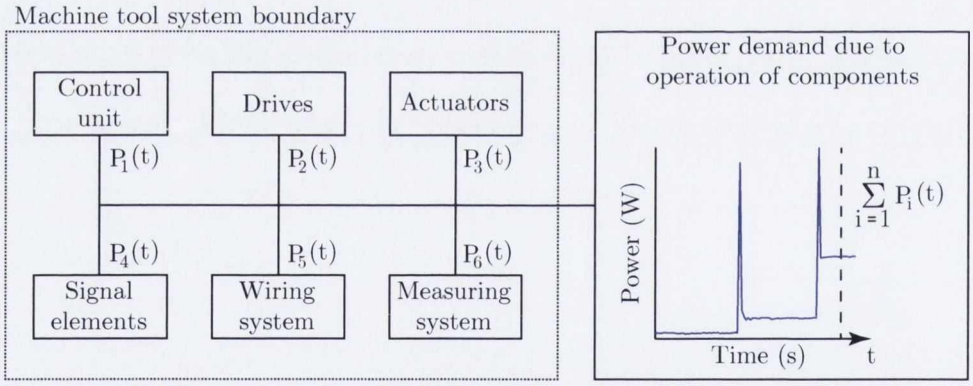

Figure 2.20 – Accumulation of power demands in a machine tool system, adapted from [43]

The consensus amongst the research community is that investigations into the electrical energy consumption of manufacturing machines must go beyond the tool chip interface in order to obtain a full understanding. This is a result of the fact that the energy consumed by machine tools during machining is significantly greater than the theoretical energy required in chip formation [83]. Recent studies have illustrated that the specific cutting energy can account for less than 15% of the total energy consumed by a modern machine tool during machining [83]. Herrmann and Thiede [21] observed that this value is subject to change depending on the process in question, but regardless

of the operation being carried out, the tare consumption, i.e. the energy consumed outside of chip formation, is significant.

Until recently, research projects at a machine tool level have assumed energy requirements are proportional to the physical amount of material being processed, and have therefore neglected this tare consumption, due to unloaded motors, coolant pumps, controllers, fans, and other peripheral equipment [22]. In the case of an automated 5-axes milling machine investigated by Dahmus and Gutowski [84] this constant energy requirement was responsible for between 40% and 90% of the total energy consumption. An additional study which highlighted the impact of using over sized machine tools and the energy intensive nature of peripheral equipment was conducted by Rajemi et al. [85]. The study compared two machines; a conventional Mazak VTC-41 and a micro milling machine. The results of this study illustrated that the conventional machine used 800 times more energy than the micro milling facility [85]. The majority of the energy consumed by the Mazak VTC-41 was required to drive the spindle where most of the torque available was not needed for the job. Within the manufacturing sector it is typically the case that multi-purpose machining centres are purchased to perform single processes and are often substantially over specified.

By performing detailed investigations into the energy profile of manufacturing machines, critical components can be identified. Once these critical components have been identified, optimisation strategies can be designed and implemented, e.g. high efficiency motors, that will act to improve the overall efficiency of the process in question [81]. In order to optimise energy performance, it is critical that machine tools are appropriately specified for their given task. The design and development of low energy footprint machines with high power efficiency presents a significant opportunity to reduce the environmental impact of machining [85].

Within recent research studies, the most widely applied approach to characterising a machine tools energy consumption is to divide it into fixed and variable components. The fixed component includes the energy requirements of machine tool modules such as control units, pumps, and coolers which enable an operational state. The process induced variable energy consumption of a production machine is comprised of the energy required for tool handling, tool positioning, and material removal. The work of Hesselbach et al. [62] provides an example of a study that separates the fixed and variable components of a machine tools power profile, see Figure 2.21.

From the perspective of improving energy efficiency, researchers have been analysing machine tools since the early 1980's. One of the earliest studies that assessed the energy efficiency of machine tools was presented by Filippi et al. [86] in 1981. The authors gathered together data from 10 different NC machine tools involved in various operations. It was concluded that the majority of each machine tools available power was never fully exploited and the machine tools spent on average 40% of the time in idle [86]. Anderberg and Kara [87] provided a quantitative representation of the effects different machining strategies have on machine tool energy efficiency.

Within the literature, researchers also focus on the specific energy consumption of machining,

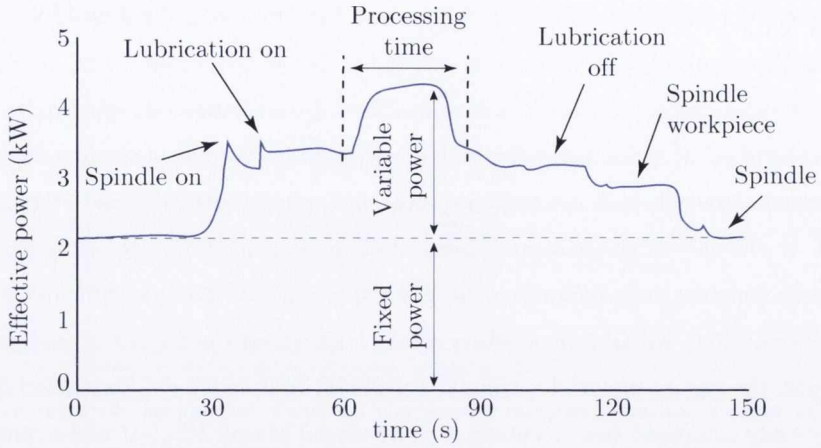

Figure 2.21 – Energy profile of a grinding machine, adapted from [62]

i.e. the energy required to remove material. An example of one such study is the work of Gutowski et al. [79] which proposes a formula that attempts to quantify the energy required to remove material:

$$P = P_o + k\dot{v} \tag{2.5}$$

where:

P_o = Idle power (kW)

$k\dot{v}$ = Rate of material processing (cm^3/s)

In the work presented by Diaz et al. [88] the concepts proposed by Gutowski et al. [79] were developed to include a broader sample of process rates. In this study the total specific energy, which includes cutting and air cutting power consumption was found to have an inverse relationship with the material removal rate, see equation 2.6. Within this equation, k is a constant and b represents the steady state specific energy. The air cutting power demand was found to dominate the specific energy in this study with the cutting power demand only having a minimal impact on the specific energy.

$$e_{cut} = k * \frac{1}{M.R.R.} + b \tag{2.6}$$

Draganescu et al. [89] presented an alternative approach to calculate specific energy based on cutting power, P_c, machine tool efficiency, η, and the material removal rate, z.

$$E_{cs} = \frac{P_c}{60\eta z} \tag{2.7}$$

Kara and Ibbotson [66] focused exclusively on specific energy consumption and presented an empirical approach to develop unit process energy consumption models for different material removal processes. The models developed in this research focused on milling and turning operations.

The resulting models achieved accurate assessments of the environmental impact of the manufacturing processes; the derived models presented were over 90% accurate for predicting the energy consumption [66].

In an additional study presented by Fratila [90], the cutting energy dissipated as heat and its repartition between workpiece, tool, cutting fluid and environment was quantified for a gear milling process with respect to different cooling/lubrication strategies. The effects that coolant and lubrication strategies have on the energy requirements of material removal is a topic that has received significant attention within the literature. Specifically, Pusavec et al. [91] investigated the environmental impacts of modern lubrication strategies which typically result in significant reductions of solid waste, water usage, and acidification but can increase energy consumption.

The current state of the art in the area of energy efficient machine tools is primarily concerned with green mode machines that reduce idle power consumption and also research projects that aim to reduce the mass of moveable objects with a view to reducing the overall power requirements. Dietmair and Verl [92] observed that the efficiency of a manufacturing process can be significantly reduced if a machine with high efficiency components is not switched off or put into a green mode during idle periods. The apparently obvious solution to this problem, i.e. turning off machines whenever they are not needed, is not an ideal solution as there is a significant energy requirement to start-up and maintain equipment in a ready state, as demonstrated by Gutwoski et al. [79].

Already there are a large number of multinational machine developers releasing 'green' machines into the marketplace. For example, Siemens drive technologies unit has developed Sinumerik Ctrl-Energy, a complete range of automation, drives and software components that focus on allowing a machine tool to operate effectively while reducing the power requirements of each operational state [93]. There are also research groups throughout Europe that focus solely on reducing the energy consumed during machining. An example of one such group is the research centre for manufacturing technology (RCMT), part of an EU project group (EcoFIT) which is aimed at the development of manufacturing machines with moveable parts that have significantly less mass than traditional machines [94]. The intention of all the EcoFIT methods is to replace the missing machine structure static stiffness with the so called mechatronic stiffness, which actively employs the control of feed drives. Sulitka et al. [94] noted that the successful completion of research studies in this area will allow manufacturing machines to be controlled by smaller, more accurate, and more energy efficient motors and drives.

2.3.5 Machine tool component

The optimisation of individual machine tool components represents an important area where significant potential exists to improve the overall environmental performance of machine tools [9]. As a result of the increasing number of research studies focusing on the power consumption of individual machine tool components, large organisations including the Yamazaki Mazak Corporation -

a global leader in the manufacture of machine tools - now publish the power consumption of every machine component in their operations manual, see Figure 2.22. Further to this, Mori et al. [95] noted that machine tool manufacturers are now beginning to conduct research studies with the goal of enhancing the energy efficiency of their products.

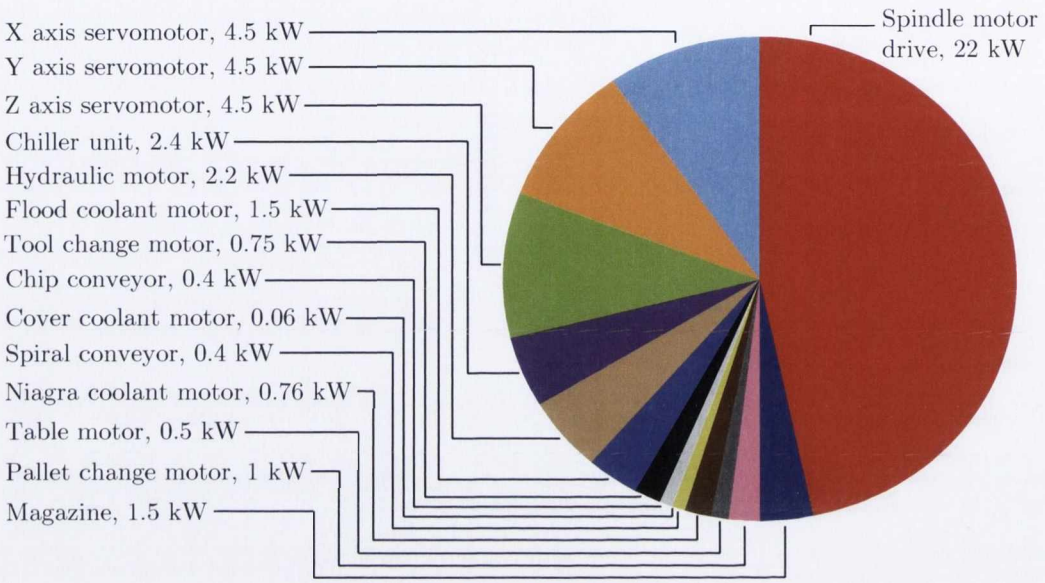

Figure 2.22 – Peak power demand for Mazak FH-4800 machine tool components

The benefits of obtaining component level power consumption information were also highlighted by Byrne et al. [96] who observed that information within the power signals of feed drives and spindle motors can be used for indirect process monitoring. Altintas [97] performed a study that used feed drive current measurements in order to detect tool breakages, whilst Bhattacharyya et al. [98] used spindle motor current and voltage measurements in order to monitor tool condition during face milling operations.

Beyond the implementation of obvious efficiency improvement measures, including high efficiency feed drives and spindle units, researchers have proposed more complex approaches to improve the energy performance of individual components. Diaz et al. [99] proposed a kinematic energy recovery system (KERS) that could recover significant amounts of energy during spindle decelerations and store this energy in super-capacitors. The simulated results showed total power savings of up to 25% however, Diaz et al. [99] concluded that kinetic energy recovery systems would only become viable if energy prices increased or the unit cost of super-capacitors decreased.

Avram and Xirouchakis [17] identified the key factors governing the energy consumption of a machine tool spindle as its inertia, the type and size of bearings, lubrication technique, and its electrical drive and control. Recent research studies have drawn attention to the impact machine tool spindles can have on the power system; particularly focusing on the generation of harmonics

[100]. Standard machine tool spindles are driven by pulse width modulated frequency inverters which electronically alter the width of voltage pulses to the spindle motor in order to control spindle speed.

The standard configuration of pulse width modulated variable frequency drives use six pulse rectifiers. The rectifiers provide the intermediate DC circuit voltage which is filtered in an LC low pass filter. The output voltage and frequency are then controlled electronically, as described in Figure 2.23. In this example, the triangular signal in Figure 2.23 represents the carrier or switching frequency of the inverter. The modulation generator produces a sine wave signal determining the width of the pulses, and therefore the RMS voltage of the inverter. Frequency inverters generate harmonics because of the nature of the front end rectifier design. Characteristic harmonics are based on the number of rectifiers, i.e. the pulse number, and can be determined by the following equation:

$$h = (n\ x\ p) \pm 1 \tag{2.8}$$

where;

n = an integer (1,2,3,4,..,n)

p = number of pulses or rectifiers

For example, the six pulse rectifier within typical frequency converters will have the following characteristic harmonics:

$$\begin{aligned} h &= (1\ x\ 6) \pm 1 \dashrightarrow 5^{th}\ \&\ 7^{th}\ harmonics \\ h &= (2\ x\ 6) \pm 1 \dashrightarrow 11^{th}\ \&\ 13^{th}\ harmonics \\ h &= (3\ x\ 6) \pm 1 \dashrightarrow 17^{th}\ \&\ 19^{th}\ harmonics \end{aligned} \tag{2.9}$$

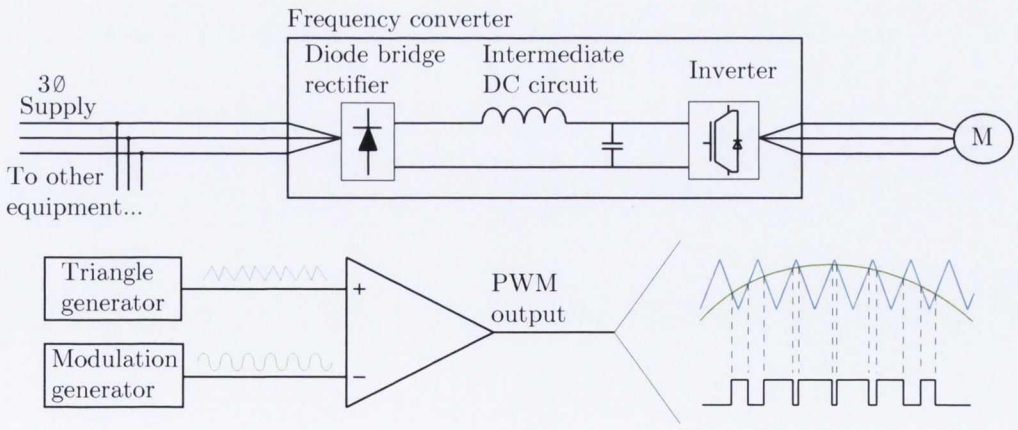

Figure 2.23 – Pulse width modulation

The harmonic losses that result from operating high speed spindles was reported by Chen et al. [101]. Within this study the researchers designed an output filter that improved the total

harmonic distortion from 99.6% to 33.95% for a 24000 rpm spindle. The research work of Wakileh [102] provided a detailed discussion on harmonics in rotating machines which also described typical harmonic reduction methods. The generation of harmonics resulting from the operation of machine tool spindles will continue to rise as manufacturing companies proceed to demand higher and higher processing performance, see Figure 2.24.

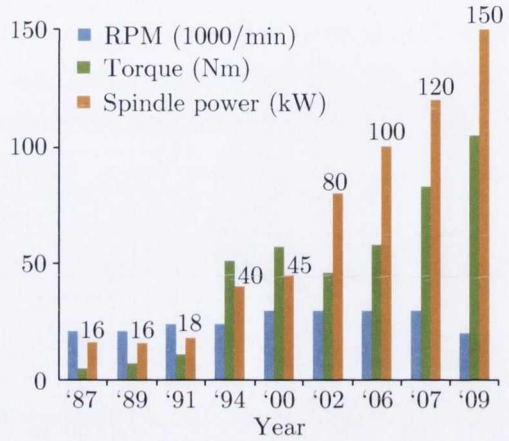

Figure 2.24 – Growth of main spindle performance, adapted from [43]

2.3.6 Environmental evaluation of machine tools

According to Dornfeld [103], a major source of motivation behind the development of environmental machine tool assessment standards comes from Europe's CECIMO organisation. CECIMO - the European association of machine tool builders - covers approximately 99% of total machine tool production in Europe and more than one third worldwide [104]. CECIMO have lead the way with respect to the environmental assessment of machine tools by implementing a self regulatory initiative aiming to improve the energy performance of machine tools.

The high relevancy of machine tool energy consumption has made the development of environmental machine tool evaluation strategies inevitable. According to a recent Franhoffer study, there are gaps in the standardisation of machine tools specifically regarding ecodesign, machine tool energy labeling, power consumption measurements, power modes, power management, consumption of lubricants/compressed air, and the measurement of process waste generation [105]. The work of Herrmann et al. [106] highlighted the importance of machine tool energy labeling as an enabler for energy efficiency improvements.

ISO 14955 aims to address the ecodesign of machine tools, the assessment of the energy consumption of individual machine tool components, and the development of standardised test pieces for the analysis of metal cutting and metal forming tools. The standard is currently under development and will only consider energy consumed during the dominant use phase, ignoring embedded

energy due to raw material extraction, transport, set-up, and end of life energy requirements. The anticipated layout of the ISO 14955 standard is as follows:

- Part 1: Ecodesign methodology of machine tools
- Part 2: Testing of energy consumption of modules
- Part 3: Test pieces and parameters for metal cutting
- Part 4: Test pieces and parameters for metal forming

The system boundaries of the machine tool to be evaluated under the ISO 14955 standard are included in Figure 2.25.

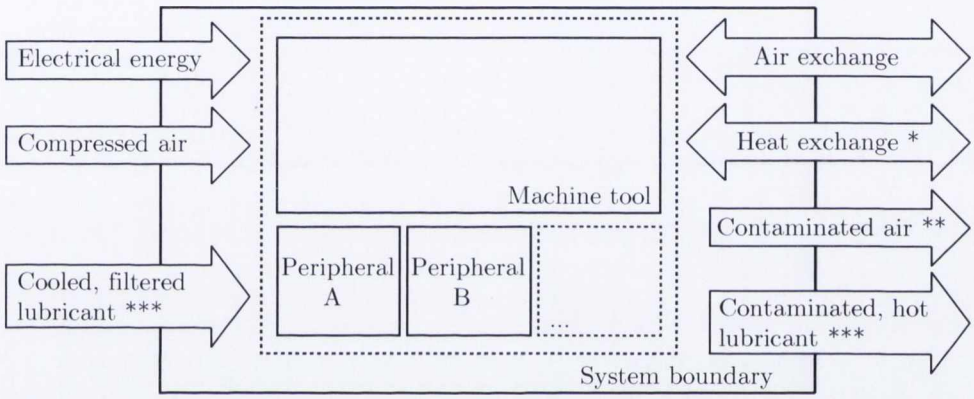

Note: Input of raw parts, new tools, new lubricant, auxillary substances and output of machine parts, used tools, chips, and any other aspects not to be considered if it does not represent a relevant energy flow across the system boundary

* Applies to cases with liquid heat exchangers

** Applies to cases without internal mist filtering

*** Applies to cases with centralised lubricant management only

Figure 2.25 – System boundaries of the evaluated machine tool, adapted from [107]

It is also predicted that machine tools will be the subject of energy efficiency regulations, under the EU Energy using Products (EuP) directive, in the near future. The automotive industry has already adapted to this expected change; prospective machine suppliers are now required to provide data on how much energy their machines consume in order to produce a standard part [92]. Machine tools possess certain characteristics that present a unique set of challenges to the EuP directive policy makers which must be addressed if the directive is to be successful. These challenges include the huge variety of highly customisable machine tools that are available and also the fact that energy consumption is strongly dependent on the end users operating choices.

2.3.7 Life cycle management

Pigosso et al. [108] recently suggested that in order to successfully implement environmentally sustainable business models, a transition must be made from traditional economic values to life

cycle thinking. The full suite of LCM techniques includes life cycle engineering (LCE), life cycle assessment (LCA), life cycle costing (LCC), Life cycle inventory (LCI), and more recently life cycle development (LCD) and life cycle planning (LCP). The goal of all life cycle tools is to protect resources by maximising the effectiveness of their usage [109].

Life cycle analysis is a methodology used to assess the environmental impacts and resource consumption associated with the existence of products throughout their entire life cycle [78, 109]. There are a number of different approaches to the implementation of life cycle analysis including cradle-to-gate and cradle-to-grave type studies. A cradle-to-gate style analysis focuses on the impacts starting from raw material extraction and includes transport form source to manufacturer in addition to the manufacturing processes required to produce the finished product [110]. A cradle-to-grave analysis extends from the cradle-to-gate analysis and includes the usage and the end of life stages. Understanding the environmental impact of each stage of a products life cycle is often complex. One useful way of quantifying the resource consumption in a stage by stage format was presented by Kara et al. [110], see Figure 2.26.

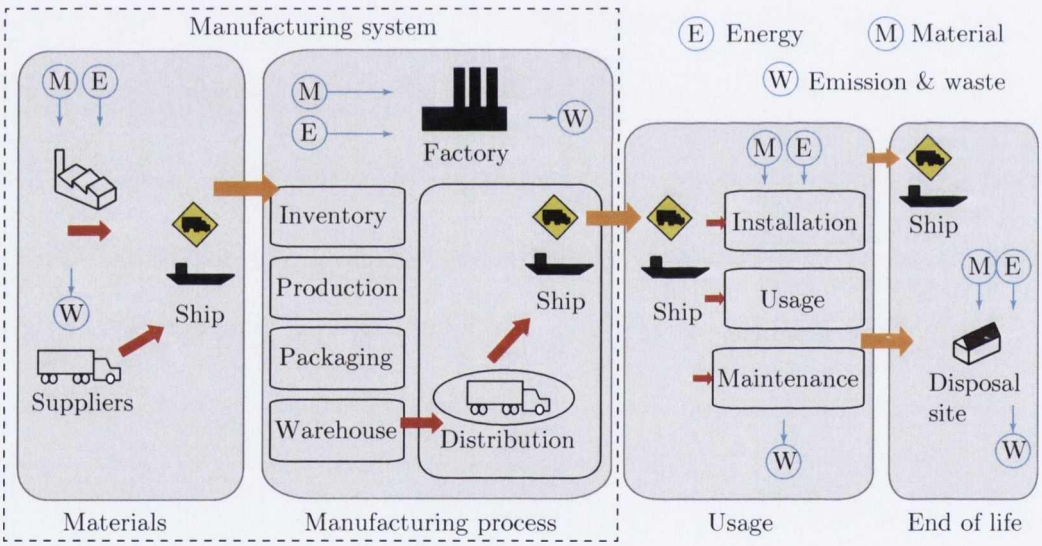

Figure 2.26 – Product life cycle stages, adapted from [66]

In an effort to highlight the importance of life cycle thinking Sullivan [111] presented a research study that assessed the environmental impact of two products over a ten year period using LCA. The two products were a late 1990's U.S. family sedan, assuming the vehicle traveled 120,000 miles at 23 mpg over a ten year life time, and a late 1990's era desktop computer, with a three year life time. The results, in a stage by stage format are included in Figure 2.27.

For the U.S. family Sedan the use phase dominates and therefore the primary carbon responsibility of the manufacturer would be to design a car with higher fuel efficiency. In the case of the desktop computer, the most energy intensive life cycle stage shifts to materials and manufacturing,

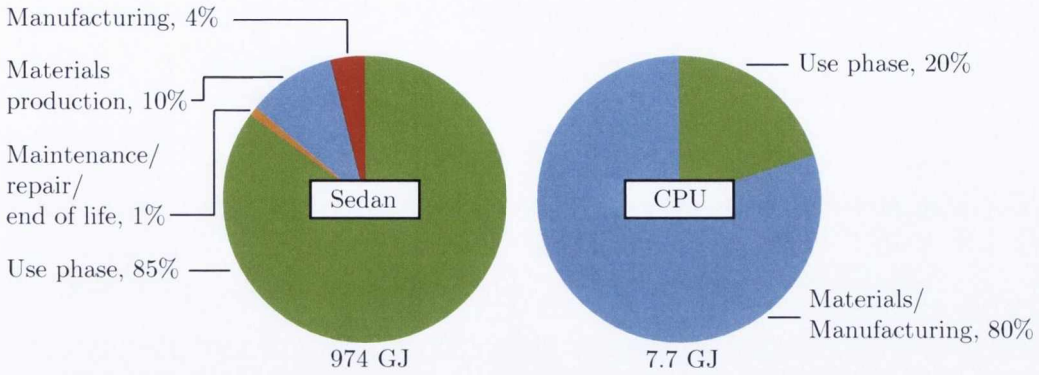

Figure 2.27 – Sedan and CPU life cycle breakdowns, adapted from [111]

which together use about 6.4 GJ or 80% of the total [111], see Figure 2.27. This shift occurs because semiconductor manufacturing is very energy intensive and computers have relatively short lives in the use phase. These examples demonstrate how the carbon load associated with a product may shift to different phases of its life cycle depending upon characteristics of the product and how it is used [112].

The concepts of life cycle development and life cycle planning were comprehensively addressed within a recent CIRP keynote paper by Umeda et al. [113]. The paper proposed a structured life cycle development framework aiming to facilitate more effective life cycle engineering. Specifically the paper encourages product designers to undertake a broad-based re-envisioning of the entire life cycle structure [113]. Within the study, life cycle development is modelled as a three stage process:

1. Life cycle planning
2. Product design/life cycle flow
3. Implementation

Umeda et al. [113] focused on the life cycle planning stage in order to provide a robust approach to a problem which is generally solved in an unstructured manner. Within the proposed framework, Umeda et al. [113] included energy saving during the use phase as an important part of the product design process. The energy savings are identified by performing life cycle evaluations on previous products and locating hotspots where improvement opportunities exist.

A recent study conducted by Cao et al. [114] investigated the quantity of carbon emitted during each phase of a machine tools life cycle. The carbon quantification method proposed by Cao et al. [114] is applied to two machine tools; a basic two axis gear hobbing tool, and a highly complex seven axis gear hobbing tool. The results observed by Cao et al. [114] again identified the use phase as the most influential life cycle stage. The observations made by Umeda et al. [113] and Cao et al. [114] were reinforced by Duflou et al. [9] who reported that over 83% and 60% of the

total life cycle environmental impact for cutting machine tools and press brakes resulted from the use phase. Linke et al. [115] assessed how greening the process chain can reduce this use phase energy consumption.

Several other studies that address the life cycle impacts of machine tools from various perspectives have been proposed within the literature. Abele et al. [9] described a life cycle inventory methodology based on theoretical equations that are used to calculate energy consumption and process waste. Zein [43] reported on a study which assessed the life cycle of machine tools from an economic perspective in the form of a life cycle costing analysis. Figure 2.28 illustrates how the use phase again dominates within this economic analysis with 66% of the life cycle costs occurring during this phase [43].

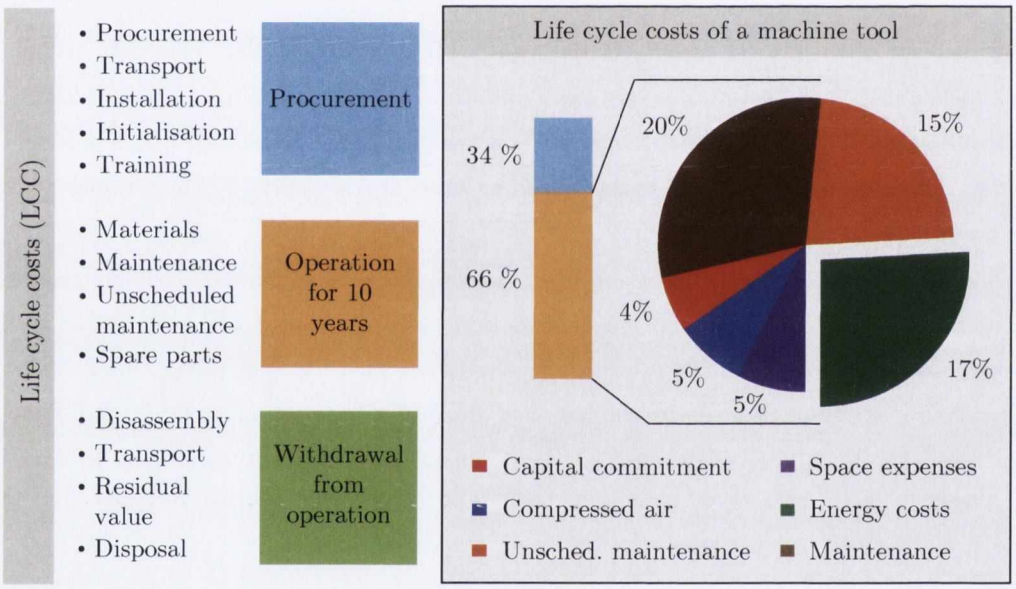

Figure 2.28 – Life cycle costs of machine tools, adapted from [43]

2.4 Measurement and quantification of industrial energy

The quantification of energy consumption within manufacturing facilities is a relatively new process. Traditionally manufacturing companies have been satisfied to pay for electricity without analysing their consumption patterns. The practice of energy management has become increasingly prevalent in all industries as falling profit percentages and an increased emphasis on value for money become the norm [116]. In addition to these financial strains, there is also a parallel drive towards reducing emissions from industrial facilities and meeting governmental climate change targets [45].

Due to this shift toward energy efficiency, there is a need to effectively manage all energy consuming operations. Vikhorev et al. [77] described how energy data is collected at all levels of the

hierarchy from the sub-process level to the global manufacturing sector at a variety of different temporal resolutions depending on the nature of the analysis to be performed. According to Herrmann et al. [15], energy metering facilitates one of the critical components of sustainable manufacturing; the availability of adequate and prompt information on energy demands and consumption patterns at all hierarchical levels.

2.4.1 Power measurement

The electric power consumed by a circuit element is equal to the current in the circuit element, i, multiplied by the voltage across it, v, Equation 2.10.

$$p = vi \tag{2.10}$$

This equation follows from the fact that voltage is work per unit charge, and current is charge transfer per unit time, Equation 2.11.

$$vi = \left(\frac{d_w}{d_q}\right) \cdot \left(\frac{d_q}{d_t}\right) = \frac{d_w}{d_t} = p \tag{2.11}$$

Three phase power systems are the most commonly applied in the industrial sector. A three phase power system is symmetrical or balanced if the three phase voltages and currents have the same amplitudes and are phase shifted by 120^o with respect to each other. A system is asymmetrical or unbalanced if either of these conditions is not met. In a typical balanced three phase system the total instantaneous power is calculated as follows;

$$v_{AN} = \sqrt{2}V_p \cos(\omega t) \tag{2.12}$$

$$v_{BN} = \sqrt{2}V_p \cos(\omega t - 120°) \tag{2.13}$$

$$v_{CN} = \sqrt{2}V_p \cos(\omega t + 120°) \tag{2.14}$$

$$i_a = \sqrt{2}I_p \cos(\omega t - \Theta) \tag{2.15}$$

$$i_b = \sqrt{2}I_p \cos(\omega t - \Theta - 120°) \tag{2.16}$$

$$i_c = \sqrt{2}I_p \cos(\omega t - \Theta + 120°) \tag{2.17}$$

$$p = p_a + p_b + p_c = v_{AN}i_a + v_{BN}i_b + v_{CN}i_c \tag{2.18}$$

$$\begin{aligned} p = 2V_pI_p[&\cos(\omega t)\cos(\omega t - \Theta) + \cos(\omega t - 120°)\cos(\omega t - \Theta - 120°) \\ &+ \cos(\omega t + 120°)\cos(\omega t - \Theta + 120°)] \end{aligned} \tag{2.19}$$

$$\begin{aligned} \therefore p &= V_pI_p[3\cos\Theta + \cos\alpha + 2(-\frac{1}{2})\cos\alpha] \\ &= 3V_pI_p\cos\Theta \end{aligned} \tag{2.20}$$

The power triangle is a method that is used to relate the three key components of power, explaining the relationship between the active, reactive, and apparent power components. The

following equations 2.21-2.23 and Figure 2.29 illustrate the relationships that exist within the power triangle.

$$Active\ power,\ P = V_{rms}\ I_{rms} \cos\Theta\ \ (Watts) \tag{2.21}$$

$$Reactive\ power,\ Q = V_{rms}\ I_{rms} \sin\Theta\ \ (VAR) \tag{2.22}$$

$$Apparent\ power,\ S = V_{rms}\ I_{rms}\ \ (VA) \tag{2.23}$$

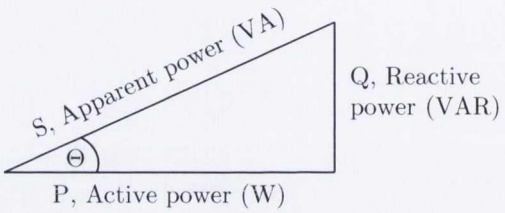

Figure 2.29 – Power triangle

Researchers have been proposing methodologies to link machine tools and manufacturing processes to electrical energy consumption for many decades [11,117,118], it is only now that industrial enterprises are being forced to consider this link that electrical energy measurement and monitoring have become widespread outside of research labs. It is the opinion of Larek et al. [119] that before power consumption in manufacturing facilities can be reduced it is first necessary to quantify the amount of energy needed, to determine the degrees of freedom for an optimisation. According to Wang et al. [120], the most effective way to obtain an understanding of facility wide energy consumption is through online continuous process-level submetering. Industrial energy and power measurement devices typically consist of two sensors - voltage and current - and a meter containing a microprocessor that calculates the required values from the acquired data. The implementation of a large scale energy metering system should ideally be a keystone of an organisations energy management system (EnMS).

An EnMS is a systematic framework for continuously improving the energy performance of a facility and can help industrial enterprises reduce energy costs and improve performance and productivity [121,122]. ISO 50001, Europe's most advanced energy management standard encourages the implementation of extensive energy metering systems. Within annex A3 of EN50001 [44], the installation of appropriate submetering is advised in order to allow information on energy use and consumption to be derived. Further to this, annex A.3.3 suggests the development of energy consumption targets and alarms forming an advanced notification system capable of monitoring a facilities energy performance; this cannot be achieved without an appropriately designed energy metering system. A schematic diagram of a modern industrial electrical energy metering solution is included in Figure 2.30.

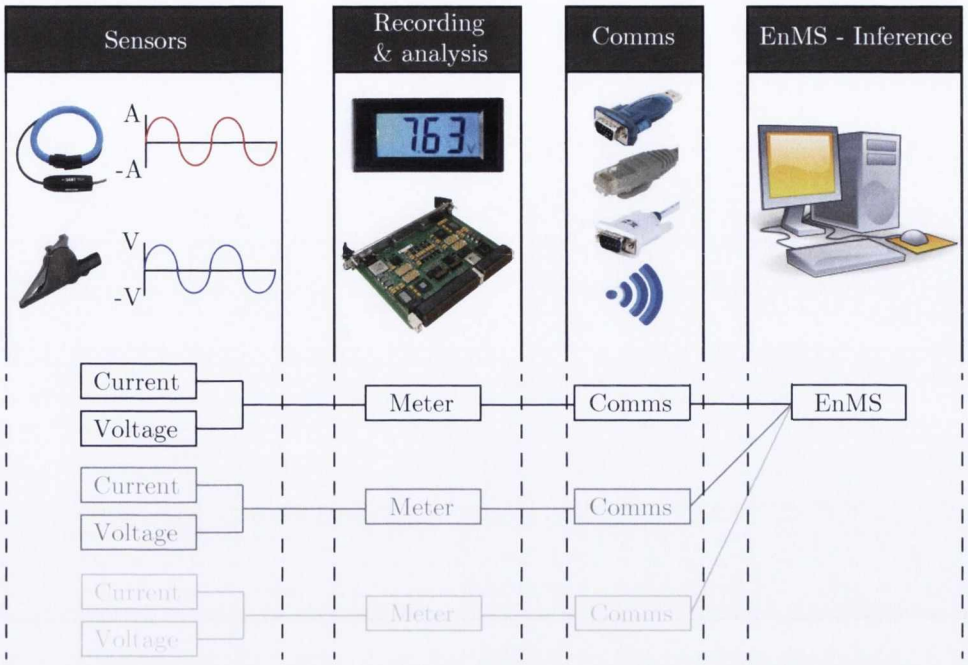

Figure 2.30 – Modern electrical energy metering solution

There are currently a large number of electrical energy meters available on the market with varying degrees of sophistication and functionality. Selecting the correct meter for a given application is not trivial as a number of variables require consideration in order to ensure the metering solution can measure and record the relevant power quality disturbances and events. Due to the constantly increasing number of non-linear and time-variant loads existent within manufacturing facilities, the measurement of power quality is becoming increasingly important. Power quality is defined as a combination of voltage quality and current quality. An ideal voltage source is a single frequency sine wave with constant amplitude, voltage quality is concerned with deviations from this ideal voltage level [123]. Current quality is the complimentary term to voltage quality and is concerned with the deviation of the current waveform from an ideal sine wave, with constant frequency and amplitude, and also the phase relationship between the current and voltage waveforms [123]. As a result of the complex nature of both power and power quality monitoring, it is important to be aware of the complete measuring instrument specifications, including:

1. Sampling rate: the number of samples taken per unit time - typically reported in terms of samples/cycle;

2. Accuracy: the degree of certainty attached to the reported values compared to the true value;

3. Resolution: the smallest change that the device can detect in the quantity it is recording.

2.4.1.1 Current and voltage sensing

According to Kara et al. [59], the accuracy of a power meter is a function of the measurement error associated with the current and voltage sensing equipment. Current sensing is the more difficult of the two as it requires a wider measurement range and also needs to handle a broader frequency range because of the rich harmonic contents of the current waveform [124]. The most common current sensors are now discussed.

Shunt resistors

The underlying principle of operation for a shunt resistor is based on the proportional relationship between the current flow and the voltage drop across the shunt resistor. Shunt resistors have found extensive application in power electronics due to their low cost, small size, and relative simplicity whilst still providing reasonable accuracy [125]. Shunt resistors are introduced into the current conducting path and as a result of this they can generate significant power loss. Ripka [126] noted that it is for this reason that shunt resistors are often avoided in high current applications. Ziegler et al. [125] identified another drawback associated with shunt resistors that relates to the small voltage drop across the resistor; this voltage drop requires amplification, altering the bandwidth, therefore increasing both the cost and size of the sensor.

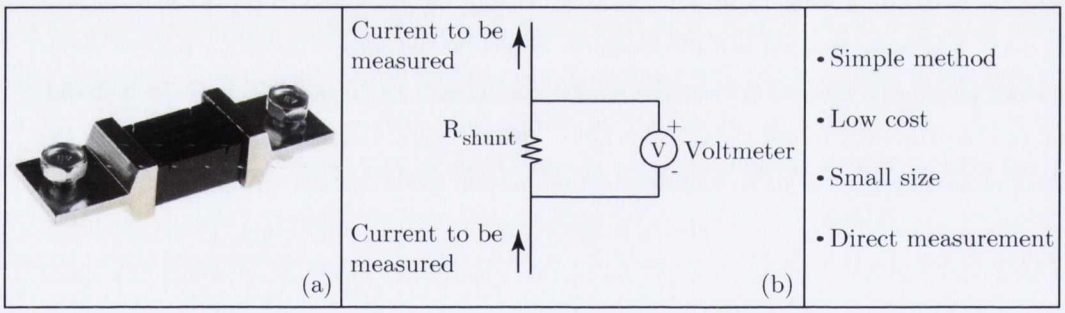

Figure 2.31 – (a) Shunt resistor (b) Principle of operation

Hall-effect sensors

Hall-effect devices can take an open loop or closed loop form and are best suited to DC applications. A Hall-effect sensor consists of three main components; a core, the Hall-effect device, and also a signal conditioner. A constant current excites the device and when this energised sensor is exposed to a magnetic field it produces a measurable potential difference. Figure 2.32(b) illustrates the working principle of a Hall-effect current sensor. One of the main advantages of a magnetic field sensor over a resistive or induction based sensor is the ability to sense currents that generate both static and dynamic magnetic fields as opposed to exclusively dynamic magnetic fields [125]. Hall-effect current sensors are sensitive to external magnetic fields as well as nearby currents and

are therefore not ideally suited to electrically noisy environments [124]. Ripka [126] noted that this type of sensor is also sensitive to the location of the measured conductor within the sensor.

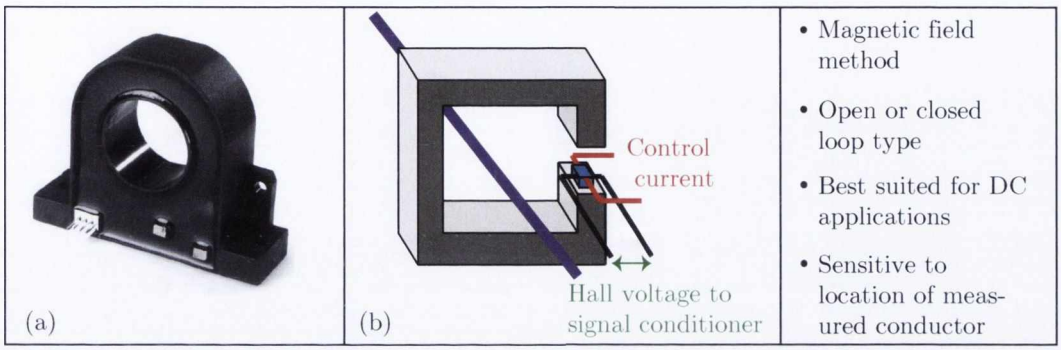

Figure 2.32 – (a) Hall-effect current sensor (b) Principle of operation

Inductive sensors

Induction based current sensors exploit Faraday's law of induction to measure current. There are numerous variations of induction based current sensors including Rogowski coils, but the most commonly used in industrial environments is the current transformer (CT). One significant advantage CT's possess over Rogowski coils is the fact that the output voltage is directly proportional to the primary current; there is no integrator required [125]. Rogowski coils are also sensitive to the location of the measured conductor within the coil and this is another issue that is not encountered when using CT's. Current transformers operate by converting a primary current into a smaller secondary current, see Figure 2.33(b).

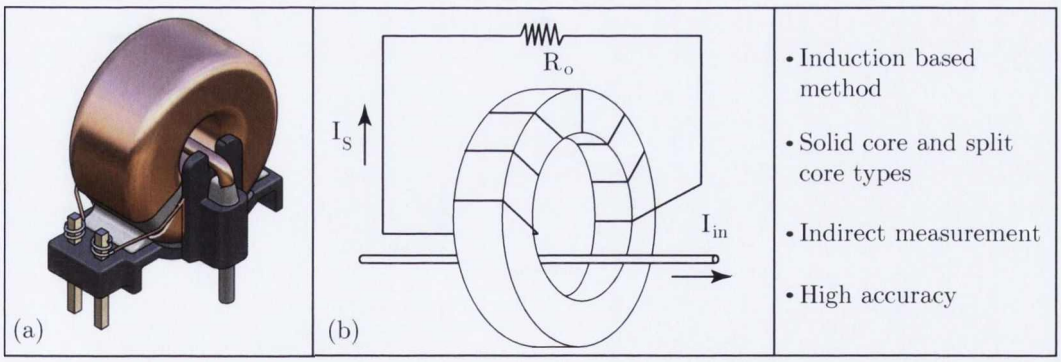

Figure 2.33 – (a) Current transformer [125] (b) Principle of operation

There are two main types of current transformer; solid core and split core. Solid core current transformers tend to be more accurate than the split core variation however, solid core CT's are significantly more difficult to install [124]. The majority of CT's used in industry have an iron core, and in cases where the CT is exposed to currents above its rating, the core can become

magnetically saturated and will need to be demagnetised in order to achieve maximum accuracy levels; in general the lower the magnetising current the higher the accuracy of the CT [124, 127]. Split core CT's are ideally suited to remote power metering applications within industrial facilities where the meter is used to monitor the power consumption of more than one machine.

2.4.1.2 Measurement resolution

Power metering equipment can identify a large variety of events depending on the sampling rate, accuracy, and resolution of the device. Low sampling rates are only necessary in order to obtain basic information including minimum, average and maximum power values. Alternatively, very high sampling rates are required in order to identify transient events that appear and disappear within a fraction of a second. Measurement instruments are available for all possible power measurement scenarios; from the oscilloscope, used for real time measurements to the basic multimeter, useful for network quality analysis [59].

According to Herrmann et al. [15], the amount of information that can be derived from a metering device is highly dependent on the granularity of the measurements in terms of time and amplitude. Within the Herrmann et al. [15] study, granularity is described as a combination of the metering systems sampling rate, resolution, and the digital processing systems capacity. In a study presented by Thiede et al. [58], the accuracy and therefore information content of a measurement device is shown to decrease sharply with lower sampling rates, Figure 2.34.

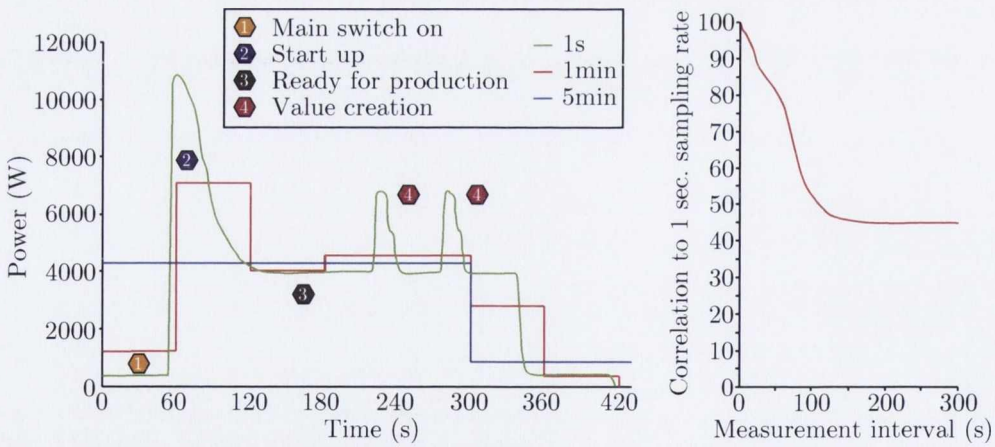

Figure 2.34 – Effect of sampling rate on measurement device accuracy, adapted from [58]

The identification of power quality disturbances requires high sampling rates, typically in the kHz range. Power quality disturbances are broadly categorised into two divisions: variations and events. Bollen [123] describes a power quality variation as a small deviation to either the voltage or current waveform that can be measured at any moment in time. Alternatively, Bollen [123]

describes power quality events as intermittently occurring deviations. Within the IEEE standard 1159 [128], the full range of power quality phenomena are classified. Table 2.2 includes a selection of these events.

S. No.	Categories		Duration	Voltage magnitude
I	*Short duration variation*			
(a)	Sag	Instantaneous	0.5-30 cycle	0.1-0.9 pu
		Momentary	30 cycles - 3 sec	0.1-0.9 pu
(b)	Swell	Instantaneous	0.5-30 cycle	1.1-1.8 pu
		Momentary	30 cycles - 3 sec	1.1-1.8 pu
II	*Long duration variation*			
(a)	Under voltage		$>$ 1 min	0.9 - 0.9 pu
(b)	Over voltage		$>$ 1 min	1.1 - 1.2 pu
III	*Transients*			
(a)	Impulsive	Nanosecond	$<$ 50 nsec	
		Microsecond	50 - 1 msec	
		Millisecond	$>$ 1 msec	
(b)	Oscillatory	Low frequency	0.3 - 50 msec	0 - 4 pu
		High frequency	5 μsec	0 - 4 pu

Table 2.2 – Classification of a selection of power quality events [129]

2.4.1.3 Inference and decision making

The installation of power measurement equipment provides information that is used for various purposes depending on the hierarchical level that is metered. The implementation of a well planned energy metering system within a complex manufacturing facility provides a level of energy transparency and understanding that is typically only available in research labs. As the hierarchical level moves from the macro, at facility level, to the micro, at unit process level, the resulting volume of data increases exponentially. Seow [130] described this exponential relationship and noted the importance of selecting the correct measurement resolution for each hierarchical level, see Figure 2.35.

Facility level metering

At facility level, metering equipment is typically installed between the utility provider and the main facility electrical incomer. The metering device is often used to obtain aggregate data at low sampling rates; a rate of 4 values per hour is not uncommon. This information is then used as a

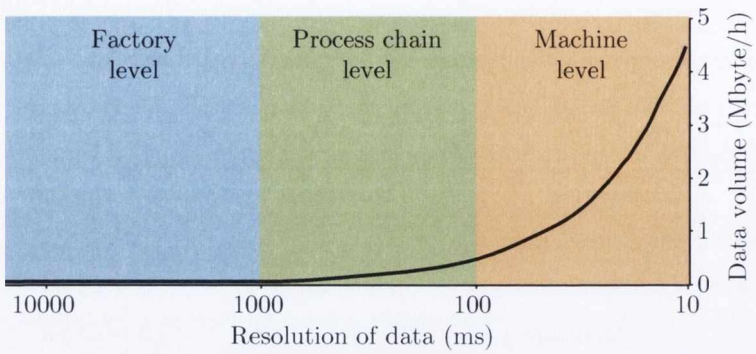

Figure 2.35 – Relationship between data volume and temporal resolution, adapted from [130]

means to query monthly utility bills or for other high level analysis. Kara et al. [59] also suggested that facility level metering can be used to adapt the electricity supply contract and prevent peak charges by rescheduling certain events. More complex metering at facility level can provide an in depth understanding of the power quality within the facility. The analysis of transients is an example of one event that can be quantified through the implementation of suitable power quality meters. Transients can take either an impulsive or oscillatory form; an impulsive transient is unidirectional and can be caused by natural events or the switching of large loads, a typical impulsive transient lasts for less than 200 microseconds [123].

An oscillatory transient is a decaying oscillation imposed on the fundamental. Oscillatory transients are commonly generated by switching events within the electrical system. Low frequency oscillatory transients are generally caused by capacitor switching; the process whereby capacitor banks are switched in and out to improve power factor [131]. It is critical that the correct meter is used otherwise incorrect and misleading information will be relayed to the user. Illustrating this with an example presented by Bickel [132] which investigated the response of two meters with different sampling rates - one sampling at 512 samples/cycle and the other at 83,333 samples/cycle - to an identical transient overvoltage. The meter with the lower sampling rate does not correctly define the true magnitude of the transient over voltage, see Figure 2.36.

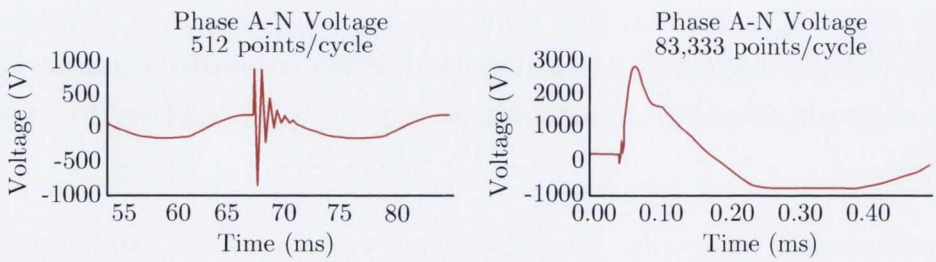

Figure 2.36 – Interpretation of a transient overvoltage, adapted from [132]

Value stream level metering

At value stream level, power consumption information is useful for optimising production schedules and also facilitating value stream competition by benchmarking consumption. Value stream level power consumption information is also used to quantify the energy savings achieved after implementing energy efficiency improvement projects, for example, from the opportunities register created as part of an ISO 50001 EnMS implementation.

The implementation of more complex metering devices at value stream level can identify a wide variety of power quality events that would otherwise go unnoticed. For example, flicker, a power quality event created by short term voltage deviations can have a significant negative impact on the productivity of machine tool operators within a value stream. Bhattacharyya et al. [131] observed that although flicker does not cause harmful equipment damage, it can have adverse effects on humans causing physical sickness and sick building syndrome in extreme cases. The level of harmonic distortion within a value stream is another important issue that should be monitored and analysed. Total harmonic distortion (THD) is expressed as a percentage and can be calculated using Equation 2.24 where V_n is the voltage of the n^{th} harmonic and $n = 1$ is the fundamental.

$$\%THD = \frac{\sqrt{V_2^2 + V_3^2 + ... + V_n^2}}{V_1} x100 \tag{2.24}$$

IEEE standard 519 recommends that harmonic limits on voltage be less than 5% for THD and 3% of for any single harmonic [133]. Bollen [123] reported that harmonic distortion of the current waveform has negative effects on a power system by overheating transformers and cables; for a given active power, the heating increases with increasing current distortion and the higher order harmonics produce more heating per Ampere than the fundamental component. In certain cases the impact of harmonics within a value stream can be so severe as to force equipment derating in order to prevent more serious faults. For example, a large third harmonic current can result in a large current flowing through the neutral conductor and this can cause serious incidents if the neutral conductor is not equipped with overload protection [59, 123]. Using the appropriate power measurement instruments to accurately quantify the level of harmonic distortion within a value streams power system facilitates the mitigation of operational and safety issues arising from the presence of harmonics.

Machine level metering

Power monitoring at machine level provides important information about each machines actual energy requirements including; average power demand, standby power demand, peak power usage, and power factor. This type of information can be used to ascertain a kWh value for each part produced and to facilitate the energy labeling of machine tools. According to Kara et al. [59], machine level metering can also be used to evaluate technical improvements and also to supplement unit process values to LCI databases. Avram and Xirouchakis [17] suggested that developing

a more comprehensive understanding of a machine tools energy requirements facilitates process optimisations and unit process benchmarking. More advanced metering devices can facilitate an investigation into equipment malfunctions and abnormal performance. For example, the presence of long duration voltage sags that last for longer than the maximum duration acceptable by a given appliance will force the appliance to shut down. Table 2.5 shows voltage tolerances for some common manufacturing equipment.

Equipment	Equipment's tolerance limit		Allowable voltage dips (average)
	V_{min}	T_{max}	
Programmable logic controller (PLC)	60%	260ms	40%
3.7 kW AC drive	75%	50ms	25%
AC control relay	65%	20ms	35%
Motor starter	50%	50ms	50%

Table 2.3 – Voltage tolerance of customer's devices [131]

The measurement of harmonics at individual machines can also identify issues causing operational and/or safety problems. Harmonics, primarily caused by electrical inverters and phase controlled modulators have a significant impact on the operation of rotating machines. Wakileh [102] described how harmonics increase the thermal losses by raising the copper, iron and dielectric losses within the machine. Harmonics also produce pulsating torques as a result of the harmonics-generated magnetic fields and this can elevate the audible noise of the machine during operation [102].

2.4.1.4 Metering costs and industrial marketplace

The cost of power metering equipment is highly variable depending on functionality. There are a number of influencing factors that affect the unit cost of a power meter; the primary drivers are the number of samples recorded during each cycle in addition to the meters measurement accuracy and resolution. Choosing the correct metering device for the required analysis is a challenging task that requires an understanding of both the meter characteristics such as measurement resolution, sampling rate, and accuracy and also the characteristics of the electrical event including spectral content and duration. One key difficulty encountered when selecting a power meter is the contrasting measurement requirements of different power system parameters. Delle-Femine et al. [134]

highlighted this by observing that some phenomena, such as transients, require a very fast analysis in a short time interval, whereas others are assessed over a longer time period. Figure 2.37 plots the smallest duration transient identifiable by a meter against its cost in order to highlight the cost impact associated with increasing meter complexity. Table 2.4 includes a sample of the results of a market survey conducted in order to provide an insight into the options available to manufacturing enterprises wishing to monitor their electrical systems.

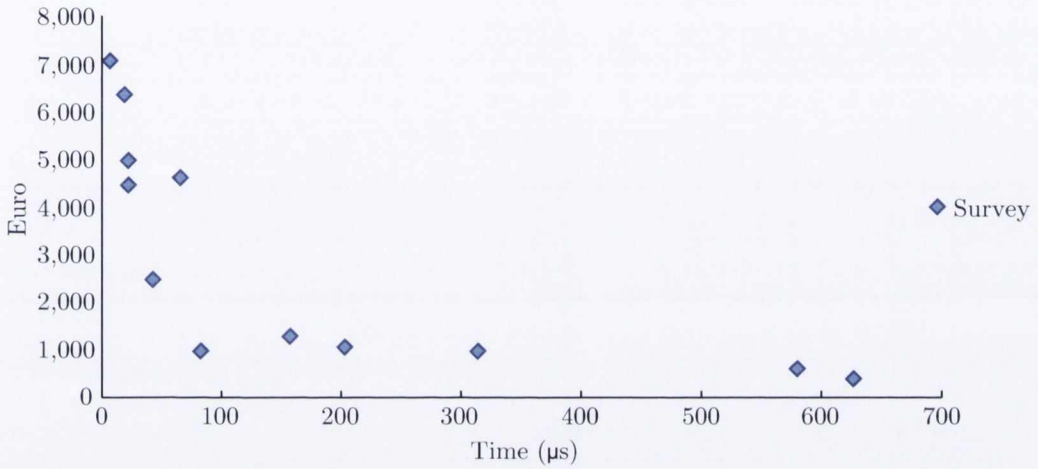

Figure 2.37 – Meter resolution vs price

	Measurement resolution			Harmonics	Samples/	Communication			
Supplier	Low	Med	High	up to	cycle	RS-232	RS-485	Ethernet	Wireless
Socomec									
Countis AM10	•			—	—		•		
Diris A20		•		—	0.02		•		
Diris N600			•	255^{th}	512		•	•	
Schneider									
PM 750		•		15^{th}	32		•		
PM 850		•		63^{rd}	128	•	•	•	
ION 8600 A			•	63^{rd}	256	•	•	•	
CM 4000 T			•	255^{th}	512	•	•	•	
Wi-LEM									
Wi-LEM	•			—	—				•
Siemens									
9350		•		15^{th}	32		•	•	
9200		•		31^{st}	64		•	•	
9610			•	255^{th}	512	•	•	•	
Episensor									
ZEM-61	•			—	—				•
General Electric									
PQM		•		63^{rd}		•	•		
EPM 9650			•	255^{th}		•	•	•	
Rockwell									
1408 PM 1000			•	63^{rd}		•	•	•	

Table 2.4 – Sample of power metering survey

2.4.2 Nonintrusive load monitoring

The concept of an inexpensive, simple to install, and centralised system capable of monitoring electric power systems is very attractive [135]. Nonintrusive appliance load monitoring (NILM) is a relatively new methodology that is used to estimate the load profiles of electrical end use equipment by monitoring the whole load [136]. The nonintrusive load monitor determines the operating schedule of the major electrical loads in an electrical system from measurements made only at the utility service entry. A nonintrusive load monitor is designed to monitor an electrical system that contains a number of devices which switch on and off independently [137].

All NILM systems are based on the discovery that, as electrical end use equipment is turned on and off, the total load changes in predictable ways, i.e. devices have characteristic signatures that make it possible to disaggregate the total load [136,138]. Pihala [136] defined an appliance signature as a measurable parameter of the total load that gives information about the nature and operating state of an individual component within the load. According to its internal circuitry, each piece of end use electrical equipment can be of resistive, inductive, or capacitive, predominance [139]. For example an electrically heated water bath is almost purely resistive while a motor can be predominantly inductive.

Inductive and capacitive loads affect the power consumption by shifting the current waveform with respect to the voltage waveform. In particular, capacitors delay the current with respect to the voltage while the opposite occurs for inductors. Considering that power is the multiplication of voltage and current, if voltage and current waveforms are shifted, the power transferred to the appliance is reduced. This effect is captured by the active and reactive power components, which, in mathematical terms, correspond to the real and imaginary parts of the impedance term respectively [139]. In general, appliances work through the real power, while the reactive power is due to the presence of storage elements in the appliance circuit, i.e. inductors or capacitors.

Conventional energy metering systems require separate submetering devices for every load of interest [140]. This type of submetering system requires a large number of sensors and a means of collecting the data from these sensors to a central location [135, 141]. In order to alleviate the drawbacks of traditional intrusive submetering systems, nonintrusive load monitors that require a maximum of three current and/or three voltage sensors installed at the main electric panel of a consumer were proposed [135, 137, 142]. Lin et al. [142] reported that the NILM approach has several significant advantages including lower cost and ease of installation/maintenance.

Hart [137] observed that the primary application which has driven many NILM studies is monitoring for load research in the residential sector. Utility companies typically monitor hundreds of their domestic customers by installing a submetering system on up to eight major loads including electric heaters, water heaters, refrigerators and air conditioning equipment, see Figure 2.38. This data is then statistically averaged within different demographic classes and used for a range of purposes by many audiences, including load forecasters and appliance designers [137].

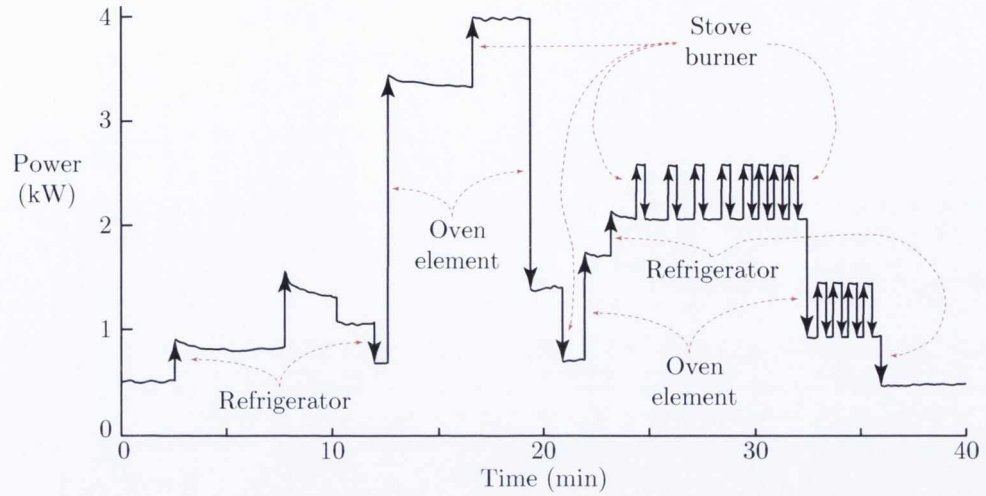

Figure 2.38 – Total domestic load, power versus time, adapted from [137]

2.4.2.1 Existing systems

Pihala [136] observed that within the literature covering nonintrusive load monitoring there is a natural dichotomy according to whether information about an appliances state change is continuously present in the load as it operates, i.e. steady state signatures, or only briefly present during times of state transition, i.e. transient signatures. Since the early 1990's researchers have proposed systems based on steady state, transient, and hybrid systems. In 1992, Hart [137] proposed the first NILM system that examined only the steady state behaviour of loads. Within this study Hart [137] conceptualised a finite state machine to represent a single appliance where power consumption discretely varied with each step change. The system proposed in this study performed well however there were limitations, for example, appliances with very small power consumption could not be identified and the system was also unable to distinguish between different loads with similar real power and reactive power consumptions [142, 143]. Laughmann et al. [143], Chang et al. [141], and Hsueh et al. [144] all provide commentary on the improvement opportunities that arose from this early NILM publication.

The earliest NILM application within the industrial sector was presented by Roos et al. [145] in 1994. The developed NILM used neural networks to recognise the status of industrial loads including fluorescent lights, electric heaters, and arc furnaces. This method, however, was computationally intensive and relatively slow to produce accurate results [141]. In 1996 Robertson et al. [146] proposed a system that employed a wavelet transformation technique to classify transient behaviours for load identification. The system proposed by Robertson et al. [146] was significantly more expensive to implement than the steady state system described by Hart [137] as it required high resolution measurement devices to detect the transient behaviour of the loads [141]. The work of Cole and Albicki [147] focused on steady state load identification algorithms in 1998; the

proposed system provided encouraging results but was limited by the fact that it required extended periods of time to accumulate real power and reactive power values [141]. More recently several authors have proposed new power signature analyses [143, 148, 149], load identification methodologies [150–152] and feature selection techniques [153, 154] to more effectively disaggregate loads via NILM systems.

2.4.2.2 Steady state detection

Under the steady state approach to nonintrusive load monitoring, appliances are distinguished by their steady state power consumption alone [135]. Pihala [136] noted that these steady state signatures are easier to detect than transient signatures; the sampling rates and processing requirements needed to detect a step change in power are far less demanding than those required to capture a transient event. The most common approach to steady state appliance recognition involves the utilisation of a signature space. Generally, observed step changes in real and reactive power are identified by their proximity to clusters in this signature space, see Figure 2.39.

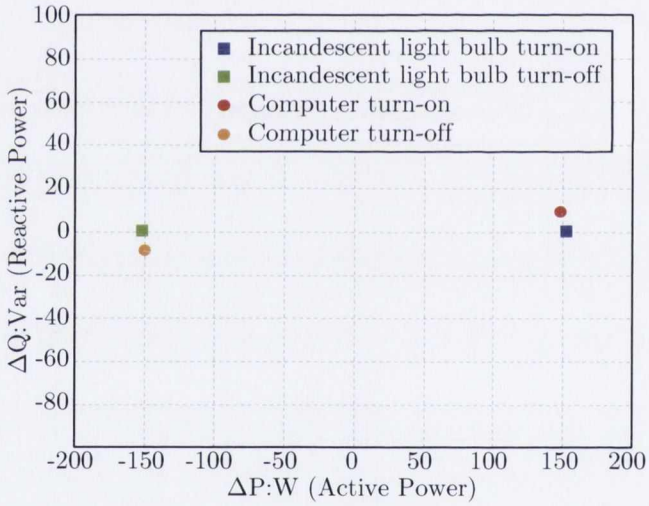

Figure 2.39 – 2-D steady state signature space, adapted from [143]

The steady state technique assumes different appliances exhibit unique signatures in the ΔP - ΔQ plane. Laughmann et al. [143] highlighted that this is not always the case, especially in industrial facilities where the number and variety of loads is greater than in a residential property. Laughmann et al. [143] identified a further limitation associated with the steady state approach; the system must wait until transient behaviour decays so that steady state values can be measured. The steady state approach can be expanded by including additional information obtained by examining the harmonic currents generated by appliances [137].

Virtually all appliances, with the exception of purely resistive loads, produce an assortment of harmonic currents [137]. For example, many motors have triangular current waveforms which

contain significant third, fifth and other low order harmonics [136]. Laughman et al. [143] identified fluorescent lights as another example of a piece of typical end use equipment that generates high third harmonic currents. Hart [137] proposed that by using an appropriate sensor for the frequency range of interest, these harmonic values could be treated as steady state signatures on a par with the fundamental frequency signatures. By including harmonic components, the two dimensional signature space can be expanded to a three dimensional space facilitating a more effective discrimination between similar appliances, see Figure 2.40.

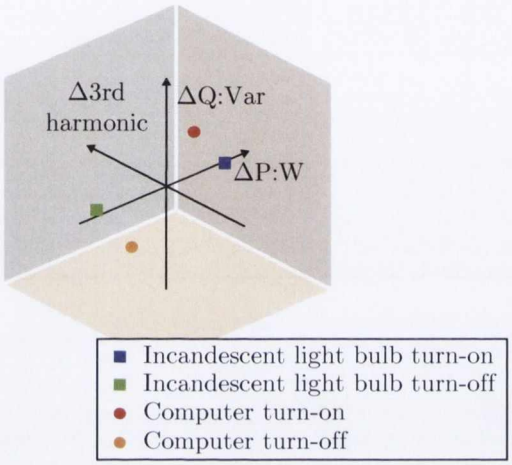

Figure 2.40 – 3-D steady state signature space, adapted from [143]

2.4.2.3 Transient detection

Transient load detection takes advantage of information available immediately after equipment start up [155]. The transient behaviour of an electrical appliance is intimately related to the physical task that the load performs. Load classes performing different tasks are therefore distinguishable by their transient behaviour [137, 141]. For example, the turn on transients associated with a personal computer and an incandescent lamp are distinct because charging capacitors in a computer power supply is a fundamentally different task than heating a lamp filament [143]. Figure 2.41 illustrates two transients; one associated with turning on a personal computer, Figure 2.41(a), and the other for starting an induction motor, Figure 2.41(b).

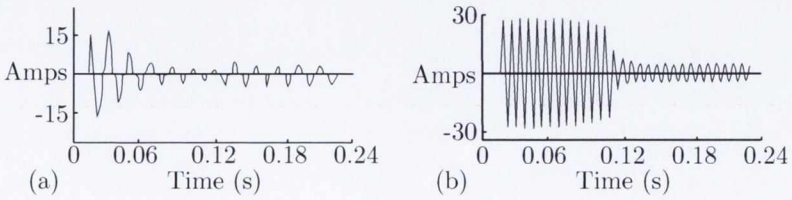

Figure 2.41 – Turn on transients (a) personal computer, (b) induction motor, adapted from [156]

An electric motor driving a pump typically generates a long switch on transient while fluorescent lights have a long two step switching on transient [136]. Purely resistive devices do not generate transients when switching on. Many industrial motors have a starting coil which provides torque for starting but is then switched off automatically after a brief delay and this phenomenon can also be captured with a transient analysis. These transients have a flat character with a sudden step power drop to the steady state operating level [137]. Alternatively, other motors consume sudden large increases in power followed by exponentially enveloped decays lasting several seconds. According to Norford and Leeb [155], these decays are the electrical consequences of the shaft coming up to speed. Figure 2.42 illustrates the turn on transients of two different induction motors, it highlights the characteristic shape of an induction motor start up transient which dilates or contracts in both magnitude and time as a function of motor size [155].

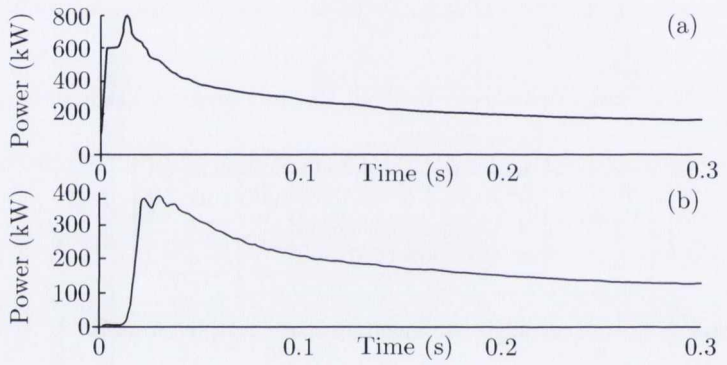

Figure 2.42 – Turn on transient waveforms (a) 160 hp motor, (b) 123 hp motor, adapted from [141]

2.5 Intelligent computation in manufacturing engineering

According to Mekid et al. [157], the future of manufacturing will see an increased proliferation of intelligent devices and sensors supporting the enhancement of manufacturing systems. Cannata et al. [158] predict that future manufacturing systems will be composed of autonomous entities provided with intelligent perception, reasoning, learning, and the ability to seamlessly interact with other system units. Systems of this nature will enable the creation of more flexible and effective production environments. There are two main driving factors behind the increased proliferation of intelligent systems, one is market driven while the other is technology pushed [158]. Within the manufacturing industry there is a drive towards mass customisation and variability which can be facilitated by reconfigurable manufacturing systems. The technology push results from the availability of low power, high performance electronic components which are boosting the creation of intelligent systems [158].

SOCRADES, a European research project with the goal of providing a structured framework allowing the development of intelligent manufacturing systems began in 2006. The SOCRADES

framework supports the development of tools and methods that can achieve flexible, reconfigurable, scalable, and interoperable network enabled collaboration between decentralised and distributed embedded systems [158]. The research work of Mekid et al. [157], coupled with the findings of the intelligent production machines and systems (IPROMS) group suggest that the key technological manufacturing developments will focus on production automation and control. Mekid et al. [157] also identified five critical topics that must be addressed in order to enable the successful development of intelligent manufacturing systems:

1. Intelligent mechatronic production units
2. Intelligent sensor technology
3. Self diagnosis, tuning, and repair
4. Human machine interaction
5. Reconfigurable manufacturing control

The design and development of intelligent sensors with embedded processing capabilities that can monitor applications and assess performance based on experience accumulated during learning periods is a key consideration of this research work. Teti et al. [159] reported that intelligent sensor technology is vital to developing sophisticated manufacturing systems producing high quality goods. The deployment of advanced sensors permits information about process conditions to be relayed to the user enabling optimisation and enhanced control [157].

2.5.1 Machine tool status monitoring

Developing an understanding of the duration of time a machine tool spends in each operational state during processing has been identified as an important research area that can be progressed via the implementation of intelligent sensor technology [19,84]. Researchers have presented a variety of different perspectives and interpretations on the definition of machining states within the literature. Kalla et al. [160] presented a methodology that separates a machine tools power profile into three components; basic energy, idle energy, and tool tip energy, see Figure 2.43. The summation of all three types of energy, Equation 2.25, represents the total process energy consumption.

$$E_{total} = P_{basic} * (t_{basic}) + P_{idle} * (t_{idle}) + P_{milling} * (t_{milling}) \tag{2.25}$$

where,

E_{total} is the total process energy

P_{basic} is the power during the basic mode

t_{basic} is the total process time

P_{idle} is the power during idle periods

t_{idle} is the total time spent during idle stages and milling stages

$P_{milling}$ is the power during milling

$t_{milling}$ is the time which the process spends milling

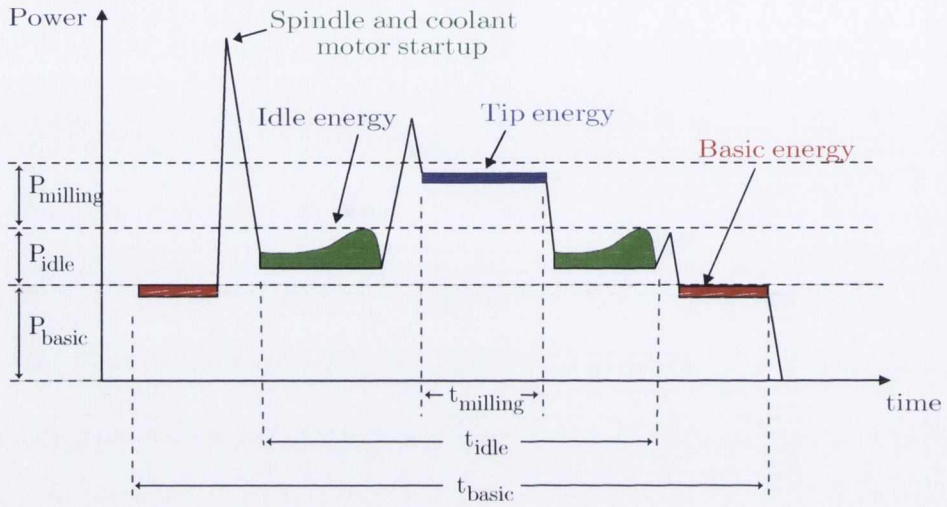

Figure 2.43 – Determination of power characteristics and energy requirements of machine tools, adapted from [160]

Dahmus and Gutowski [84] also proposed a methodology that segregates the power profile of a machine tool into three discrete operational modes: idle mode, run-time mode, and production mode. During idle mode the machine tool is powered on and static. In run-time zones the machine tool is ready for production but not removing material, and finally the machine is in production mode when it is removing material. The study reported by Vijayaraghavan and Dornfeld [19] described a similar interpretation of operational modes however, Vijayaraghavan and Dornfeld [19] proposed a fourth mode of operation reserved for machine tool start up and shut down.

The Vijayaraghavan and Dornfeld [19] study analysed a simulated power profile from a 3-axis precision milling machine during the end milling of aluminium using a 2-flute carbide cutter. The power requirements were recorded during three different levels of spindle operation; idle (0 rpm), low (8000 rpm) and high (16,000 rpm). The resulting power profile, Figure 2.44, illustrates the sharp increase in power consumption during spindle accelerations, a key contributor to peak power demand in manufacturing facilities. Vijayaraghavan and Dornfeld [19] observed that power consumption increased when the spindle was engaged at a higher rpm, and when there was material removal [19].

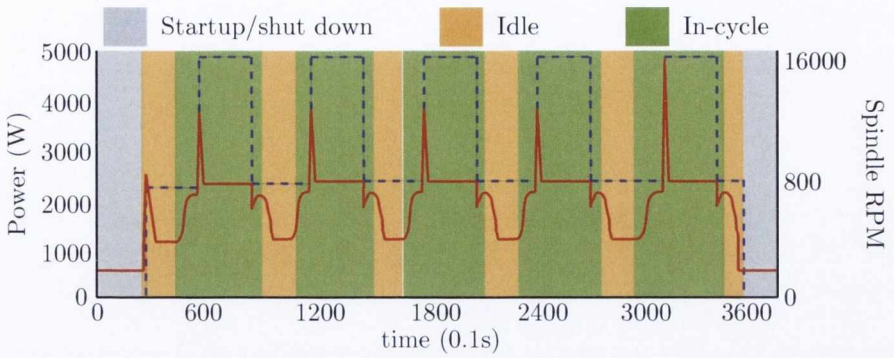

Figure 2.44 – Machine states, adapted from [19]

A different perspective on machine states was proposed by Dietmair and Verl [92]. In this study an extensive number of machine states were proposed and the power requirements of each machine element was quantified during each state, see Figure 2.45. The methodology was proposed as a forecasting tool, however a key limitation of the Dietmair and Verl [92] approach was that it did not take account of acceleration effects; identified by Vijayaraghavan and Dornfeld [19] as key contributors to peak power consumption.

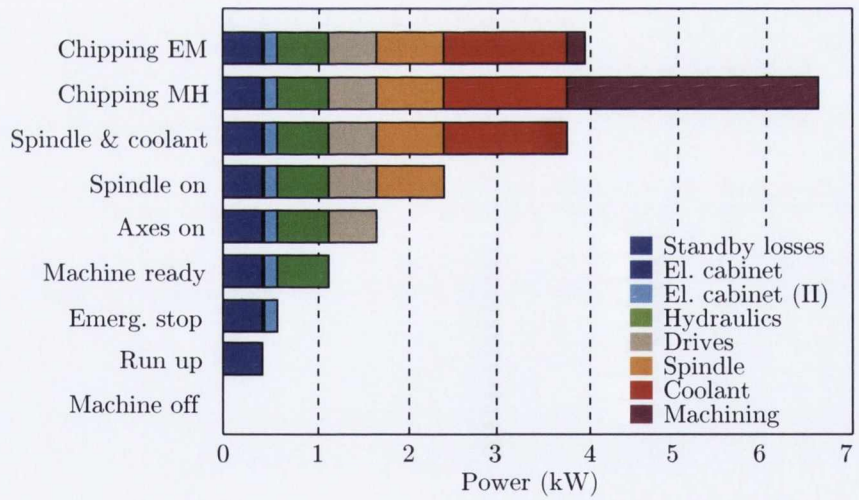

Figure 2.45 – Power consumption of tool machine in different states, adapted from [92]

The research of Weinert et al. [161] progressed some of the ideas proposed in the research studies described previously with the development of the EnergyBlocks methodology. This methodology segregates a production process into individual operations that can be considered independently and works by matching energy consumption to operational state and time. Each operating state is defined as an EnergyBlock and represents the duration of the operation as well as the energy required [161]. A mathematical function is used to calculate the energy required for each Energy-

Block, $P_B(t)$, at a specific time t:

$$P_B(t) = f_m(t), \forall \mathbf{t} \in [T_{m-1}, T_m] \tag{2.26}$$

where:

$P_B(t)$ = Energy required for each EnergyBlock

The EnergyBlocks methodology integrates energy efficiency criteria with evaluation and decision processes during production system planning and scheduling [161]. The most progressive component of this research is the fact that the EnergyBlocks framework allows the energy consumption of a planned, not yet realised production process to be modelled by arranging EnergyBlocks in sequence, see Figure 2.46. Herrmann et al. [21] proposed a similar methodology to that of Weinert et al. [161] which used process chain simulation as a means to link machine movements and electrical energy consumption. The end goal of the research work presented by Herrmann et al. [21] was to identify the most inefficient machine movements with a view to optimising the machine tools G-code and improving the energy performance.

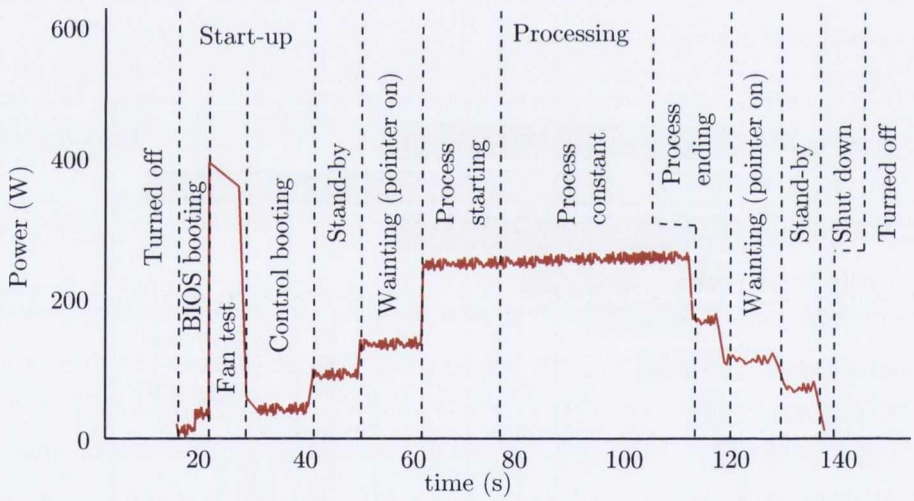

Figure 2.46 – Power profile of a laser for plastics welding, adapted from [161]

In an attempt to overcome the difficulties that exist as a result of the closed architectures of machine tools Vijayaraghavan and Dornfeld [19] introduced the MTConnect standard for data exchange. MTConnect defines an interoperability standard for manufacturing data and a rules engine/complex event processing system that can handle data processing [19]. Within the MTConnect system, data exchange is facilitated by an XML based standard which standardises machine tool data during data collection [19]. MTConnect is an open standard that addresses the need for interoperability and plug-and-play capability within the machine tool industry. An example application was presented by Diaz et al. [99] that used MTConnect to integrate multiple sensors -

x/y/z position, speed, feed, NC information, and a power meter - to create a unified monitoring platform for a Mori Seki NV 1500DCG machining centre, see Figure 2.47.

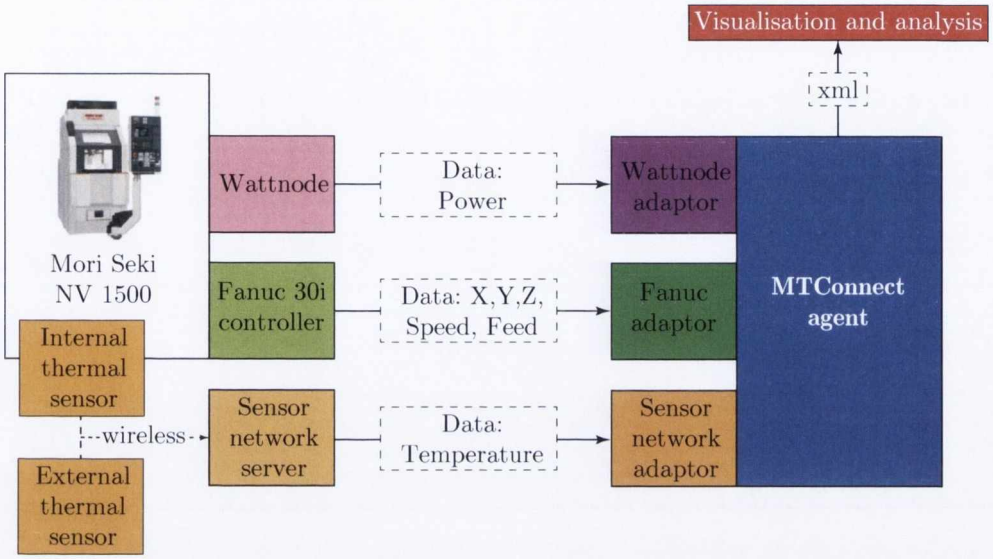

Figure 2.47 – Unified MTConnect based machine tool monitoring system, adapted from [99]

MTConnect was also used in a study conducted by Deshpande et al. [162] that aimed to quantify the duration of time a machine tool spent in different operational modes. The Deshpande et al. [162] study required the user to input threshold values that allowed the smart energy sensor to identify off, idle, and in-cycle machine states. The study also relied on information obtained directly from the machine tool controller in order to infer status information. A fixed energy rate of 10 cents per kilowatt-hour was included in order to allow the sensor to calculate the financial cost of the measured energy consumption. The Deshpande et al. [162] study reported strong results, however, the inference of machine tool status is only achievable by using a combination of sensory inputs.

The application developed by Chiotellis and Grismajer [163] used only power information in order to identify the operational status of a 3-axis CNC milling machine. The application is based on a combination of status-specific power value thresholds and the dynamic time warping similarity metric. The approach proposed by Chiotellis and Grismajer [163] uses low resolution data, 250ms - 1sec, to identify the operating state and high resolution data, 1ms - 250ms, to perform basic process monitoring. Vikhorev et al. [77] built on the work of Chiotellis and Grismajer [163] with a study that attempted to identify the operational status of a series of machine tools in a major European automotive manufacturing facility. The study required the input of energy status threshold values, based on expert knowledge of the process, in order to infer state information. The threshold values defined for the test machine tool described in the Vikhorev et al. [77] study are: idling (0.6 - 1 kW), waiting (3 - 8 kW), and producing (8 - 30 kW). The system reported positive results but

was unable to accurately monitor rapidly occurring status changes. Pang et al. [164] presented an additional intelligent energy sensor that combined a Savizky-Golay filter with neural networks in order to classify the status of an injection moulding machine .

It is clear from the literature that there is an opening for intelligent sensors that can accurately infer machine tool status information and also identify machine tool component activations using only one sensor. In a recent CIRP keynote paper Teti et al. [159] observed that a combination of advanced signal processing techniques and artificial intelligence is required to design and apply the innovative sensing devices that are required to enhance future manufacturing systems. One of the most widely applied advanced signal processing techniques is pattern recognition, which is discussed in section 2.5.2.

2.5.2 Pattern recognition

Pattern recognition is a subject which links statistics, engineering, artificial intelligence, machine learning, computer science, and a number of other fields. The ultimate goal of pattern recognition is to extract patterns based on certain conditions and to separate one class from the others. The process of pattern recognition encompasses data collection, feature extraction and/or selection, classification, as well as the interpretation of results, see Figure 2.48.

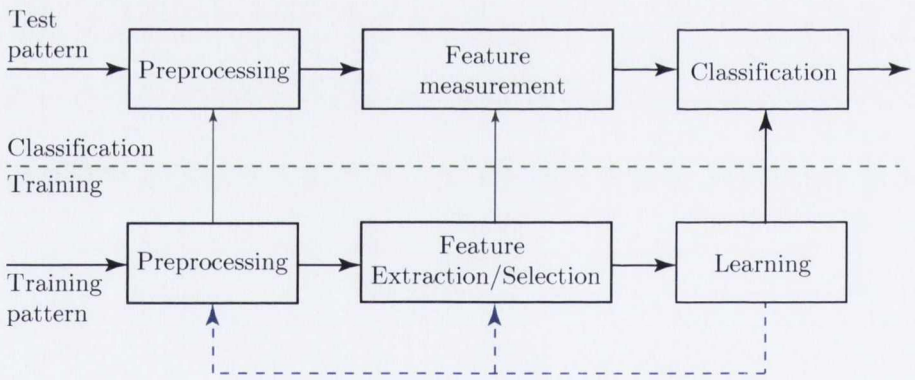

Figure 2.48 – Pattern recognition system, adapted from [165]

The literature suggests that the most natural framework in which to formulate solutions to pattern recognition problems is a statistical one that is capable of recognising the probabilistic nature of both the data being analysed and, of the form in which the results should be presented [166]. In the statistical approach to pattern recognition, each pattern is represented in terms of d-features and is viewed as a point in a d-dimensional space. The goal is to chose a minimal number of features that will allow pattern vectors belonging to different classes to occupy compact and disjoint regions in the d-dimensional feature space [167].

Nadler and Smith [168] defined features as functions of the measurements performed on a class

of objects that enable that class to be distinguished from other classes in the same general category. Features are either selected or extracted from a measured data set. Feature extraction involves the extraction of certain attributes that are then used to map the original data to a feature space, in most cases a dimensionally reduced space, in which the data will be separable so that classification can be performed [167]. Feature selection is the process of identifying the most useful features from the recorded data. Jain et al. [167] described the problem of feature selection as follows: given a set of d features, select a subset of size m that leads to the smallest classification error. Essentially, effective feature selection will create an optimal feature space on which to perform classification.

2.5.3 Dimensionality reduction

The dimension of a data set is the number of variables that are measured on each observation. It is important to minimise the dimensionality of a pattern representation wherever possible for two reasons; measurement cost and classification accuracy [167]. Cunningham [169] noted that from a statistical perspective it is desirable that the number of examples in a training set should be significantly greater than the number of features used to describe those examples.

From a mathematical perspective, the task of reducing dimensionality can be stated as follows: given the n-dimensional variable $x = (x_1, x_2, ..., x_n)$, find a reduced dimensional representation, $y = (y_1, y_2, ..., y_k)$ with $k \leqslant n$, that captures the majority of the information in the original data. Dimensional reduction methods are typically partitioned into the two categories described previously; feature selection and feature extraction. Feature extraction methods are commonly separated with respect to their transformation properties, i.e. linear or non-linear [165]. Linear transformation techniques result in the components of the transformed variable being a linear combination of the original variables [170]. Non-linear transformations operate by either non-linearising linear methods, e.g. kernel PCA, or using manifold based approaches that attempt to preserve neighbourhood information, e.g. Isomaps. An overview of some of the most common extraction tools is summarised in Figure 2.49.

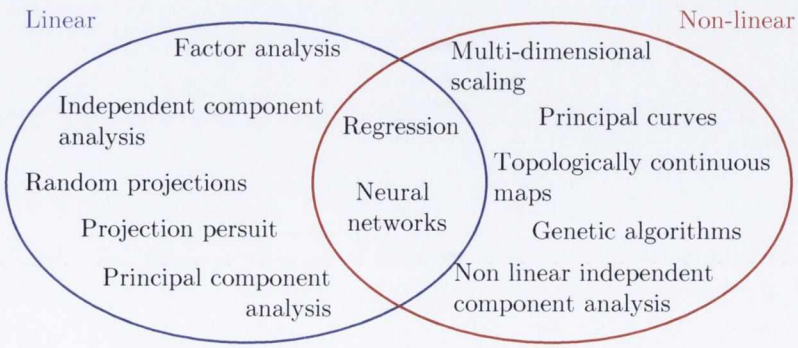

Figure 2.49 – Dimensionality reduction tools, adapted from [165]

According to Jain et al. [167], linear feature extraction techniques are significantly easier to implement than more recent non-linear methods and they achieve similar performance levels in many applications. One of the more frequently used pattern recognition techniques that finds application in manufacturing research studies is principle component analysis (PCA) [170].

2.5.3.1 Principle component analysis

Bishop [165] defined Principle Component Analysis as the orthogonal projection of a dataset onto a lower dimensional linear space, known as the principal subspace, such that the variance of the projected data is maximised. It represents the most commonly used feature transformation technique used in pattern recognition problems. Two key mathematical concepts are central to principle component analysis; covariance matrices and mean vectors. The mean vector consists of the means of each variable and the covariance matrix consists of the variances of the variables along the main diagonal and the covariances between each pair of variables in the remaining matrix positions [165]. In order to compute the covariance of two variables X and Y the following formula is used:

$$COV = S = \frac{\sum_{i=1}^{n}(X_i - \bar{x})(Y_i - \bar{y})}{n-1} \tag{2.27}$$

where $\bar{x}$ and $\bar{y}$ represent the means of X and Y respectively. Once the covariance matrix has been calculated the eigenvectors and eigenvalues of this matrix must be found. In order to briefly explain eigenvalues and eigenvectors consider an n x n matrix $\mathbf{M}$, λ can only be an eigenvalue of $\mathbf{M}$ if there exists a non-zero vector $\mathbf{x}$, such that $\boldsymbol{Mx} = \lambda\boldsymbol{x}$. All of the eigenvalues and associated eigenvectors for the matrix $\mathbf{M}$ exist in the characteristic equation which takes the following form [171];

$$|M - \lambda I| = \lambda^n + m_1\lambda^{n-1} + m_2\lambda^{n-2} + ... + m_{n-1}\lambda + m_n \tag{2.28}$$

The eigenvector with the largest eigenvalue is known as the first principle component and the eigenvector with the second highest eigenvalue is the second principle component and so on. Only the eigenvectors corresponding to the M largest eigenvalues are retained and the input vectors $\mathbf{x}^n$, are projected onto the eigenvectors to give the components of the transformed vectors $\mathbf{x}^n$ in the M-dimensional space [166]. Duda et al. [172] noted that in many cases there are only a small number of large eigenvalues, and this implies that M, the number of principal components chosen, is the inherent dimensionality of the subspace governing the signal, while the remaining D - M dimensions, where D represents the dimensionality of the $d \times d$ covariance matrix, primarily contain noise. Figure 2.50 illustrates this process graphically for the case of a 2-dimensional problem. In this case the maximum variance would be retained by projecting onto the first eigenvector $\mathbf{u}_1$.

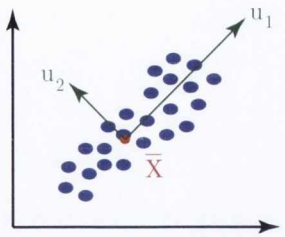

Figure 2.50 – Schematic illustration of PCA applied to 2-dimensional data, adapted from [166]

Within the literature researchers have applied PCA in order to solve a multitude of problems within the manufacturing sector. Tsung [173] presented a study focused on the simultaneous monitoring and diagnosis of automatically controlled processes using PCA. Further to this, Halligan and Jagannathan [174] developed a fault isolation and prognosis tool based on PCA; the developed tool was then applied to a 0.5 horsepower centrifugal water pump in order to identify normal and abnormal operating scenarios.

2.5.4 Classification frameworks

Classification is the final part of the pattern recognition process. During classification a label is assigned to an unknown object according to some representation of the objects properties derived from sensed data. A typical classification tool requires the input of a d-dimensional feature vector, x, composing a number of features extracted from the original sensed data. This feature vector is then used to assign the object to one of the m designated classes C_1, C_2, ..., C_{m-1}, C_m. Duda et al. [172] reported that the ideal class is a set of similar objects having a selection of important common properties. According to Jain et al. [167], the task of choosing the most appropriate classifier is a difficult one and it is generally the most readily available or best known classifier that is chosen for a specific application. The following table includes a sample of some of the more commonly applied classification frameworks.

Method	Property	Comments
Nearest mean classifier	Assign patterns to the nearest class mean	Almost no training needed; fast testing
k-nearest neighbour	Assign patterns to the majority class	Asymptotically optimal
Fisher linear discriminant	Linear classifier using mean square error	Simple and fast

Table 2.5 – Overview of classification methods, adapted from [167]

2.5.4.1 k-nearest neighbours

K-nearest neighbour classification is a member of the family of memory based classification tools, i.e. it relies on an exhaustive search and therefore all of the training data is required at run time [167]. In accordance with the work of Elkan [175], let $\mathbb{R} = \{r_1, r_2, ..., r_m\}$ be a set of m reference points and let $\mathbb{Q} = \{q_1, q_2, ..., q_n\}$ be a set of n query points in the same space, $\mathbb{R}$. The k-nn search problem can then be described as a a search for the k nearest neighbours of each query point $q_i \in Q$ in the reference set $\mathbb{R}$ given a specific distance metric [175]. Figure 2.51 illustrates the k-nn problem with k = 3. The blue circles correspond to the training/reference data and the red cross represents a query point.

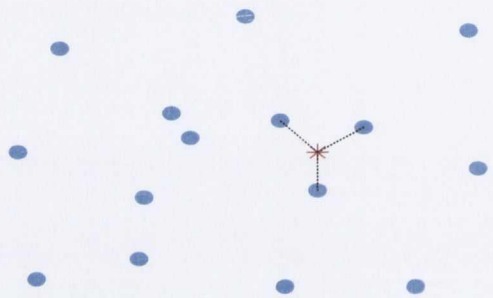

Figure 2.51 – 3-nn illustration

According to He and Wang [176], in general the choice of k is non critical. Larger values of k reduce the effect of noise but also make boundaries between different classes less distinct. The widely accepted best practice is to try several different values of k and choose the value which gives the best cross validation [176]. The one obvious disadvantage of using a k-nn search algorithm for classification is the computational load that results from the fact that all data points are required at run time [175]. Elkan [175] reported that in studies where the dimensionality of the data is greater than twenty, the method is very slow however, in applications where the effective dimensionality of data is low the method performs very well.

Examples of studies that have implemented k-nn classification within the manufacturing industry include the work of He and Wang [176] which used the k-nn rule to detect faults during semiconductor manufacturing processes. This study used the k-nn rule to classify unlabelled samples as either normal or one of a number of known faults and reported strong results in an industrial application [176]. In a study reported by Li and Liao [177], the k-nn rule was used to detect tool failure in a face milling operation. The study investigated the effectiveness of a k-nn based procedure to recognise tool failures based on AE-signals during the milling of high chromium materials [177].

2.5.4.2 Measures of dissimilarity

Several techniques that find application in pattern recognition are based on similarity between objects, for example the nearest neighbour classification method described above, multidimensional scaling, and cluster analysis. For a function calculating the similarity between objects A and B to qualify as a distance metric, Bishop [166] stated that the following must be true;

1. Symmetry - $D(x, y) = D(y, x)$
2. Constancy - $D(x, x) = 0$
3. Positivity - $D(x, y) = 0$ if and only if $x = y$
4. Triangle inequality - $D(x, y) \leq D(x, z) + D(y, z)$

A variety of metrics have been proposed to assess the level of dissimilarity between numeric variables and generally the choice of a particular metric is dependent on the application. Some of the most common metrics are described here.

Euclidean

The contours of equal Euclidean distance from a point are circles in two dimensions. According to Jain et al. [167], Euclidean distance is the most commonly used distance metric in k-nn based studies within the literature.

$$d_{Euclidean}(x, y) = \sqrt{\Sigma_i (x_i - y_i)^2} \tag{2.29}$$

Manhattan

The Manhattan distance, also know as the box-car, city-clock, or absolute value distance uses a distance calculation based on a grid [178]. The contours of equal distance from a point using the Manhattan distance are diamonds in two dimensions. The Manhattan distance is computationally less expensive than the Euclidean distance and may find application in studies where speed is critical.

$$d_{Manhattan}(x, y) = \Sigma_{i=1}^{m} |x_i - y_i| \tag{2.30}$$

Chebyshev

The Chebyshev distance, also known as the maximum value distance, primarily finds application in studies where the execution speed is crucial and the time required to calculate the Euclidean distance is unacceptable [178]. The contour lines of equal Chebyshev distance from a point are squares in two dimensions.

$$d_{Chebyshev}(x, y) = max_{i=1,2,\ldots,m} |x_i - y_i| \tag{2.31}$$

Figure 2.52 illustrates the contours of equal distance in a two dimensional space for the Euclidean, Manhattan, and Chebyshev distance metrics.

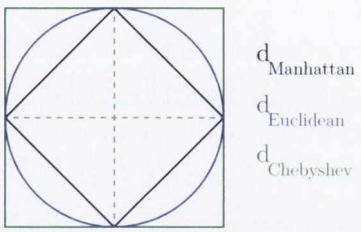

Figure 2.52 – Contours of equal distance, adapted from [178]

2.6 Summary

It is clear that the consumption of energy is a key enabler of economic growth and it represents one of the core components of modern life. The International Energy Agency has predicted that our dependence on energy will continue to grow over the next twenty years and although international governments are devising methodologies to ensure renewable energy sources increase their share of the energy mix, fossil fuels will remain to be a significant contributor. This combination of increasing energy demand and reducing energy supply will create unique challenges that must be addressed globally. As a direct result of these energy challenges, increasing energy efficiency and reducing the environmental impact of production have become major technological and political necessities. This need for change has seen a significant expansion in the number of international research journal publications that aim to address all aspects of energy consumption within the manufacturing sector since the year 2000; Figure 2.53 highlights this rising interest in energy conscious manufacturing.

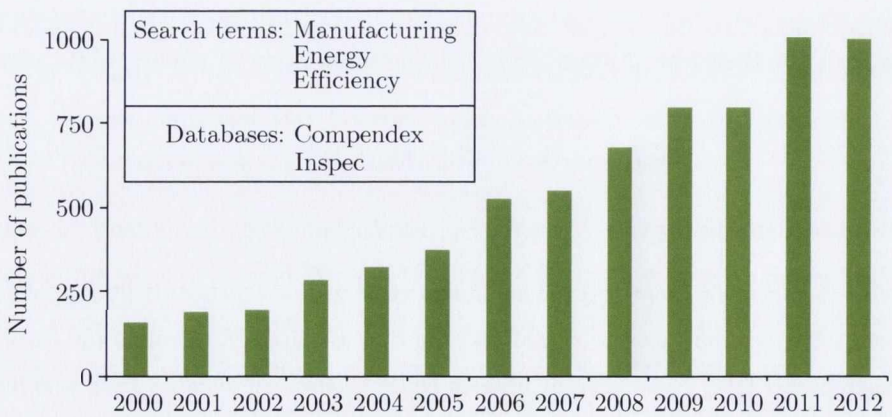

Figure 2.53 – Energy efficiency journal publications

Researchers from Ireland (Naughton [64]), the U.K. (Rahimifard et al. [60]), Germany (Herrmann et al. [21] and Hesselbach et al. [62]), and also the USA (Vijayaraghavan and Dornfeld [19]) are publishing studies that address topics including the power consumption of technical building services and the energy efficient optimisation of manufacturing equipment. These journal papers, along with numerous books, governmental reports, magazines, and other sources have created an extensive manufacturing energy efficiency literature. Researchers have identified numerous areas where opportunities to improve energy performance exist however studies have also highlighted the scepticism that remains within the manufacturing sector around the effectiveness of energy efficiency projects which continues to hinder their implementation [49, 62].

One key pillar of sustainable production is the minimisation of energy and material waste. In order to minimise energy waste, it is first necessary to understand consumption patterns. According to the literature, the most effective way to obtain an understanding of facility wide energy consumption is through online continuous process-level submetering [120]. Although the quantification of energy consumption has been identified as an important task there is scant attention given to the process of industrial energy metering within the literature. The work presented by Kara et al. [59] represents the most comprehensive study, however there is space within the literature for studies which support and develop the observations made by Kara et al. [59].

An additional area that is not comprehensively addressed within the literature relates to the development of energy metering system implementation strategies within manufacturing facilities. Studies that can effectively describe the installation of the metering system infrastructure, the interpretation of the acquired data at each hierarchical level, and the generation of robust energy performance indicators could add significant value to the research area.

The design and development of intelligent sensors with embedded processing capabilities that can monitor applications and assess performance based on experience accumulated during learning periods has been identified as a crucial component of future manufacturing systems. In addition to this, the challenges associated with accurately measuring energy consumption at a machine tool component level have been identified as a key issue for the CIRP Energy and Resource Efficiency and Effectiveness (EREE) focus group [179]. There is a related opening in the literature for contributions that aim to deploy intelligent energy sensors in order to monitor the energy performance and operational status of machine tools.

Chapter 3

Characterising the electrical energy consumption of manufacturing process chains

3.1 Complex manufacturing environments - test facility overview

The objective of the industrial case study was to characterise the electrical energy consumption of a complex manufacturing facility. The investigations examined the multiscale aspects of energy consumption ranging from an entire facility down to an individual machining process. Under the United Nations International Standard Industrial Classification (ISIC) framework the organisation is a class 3250 facility specialising in medical device manufacturing. Energy is required for numerous processes performed on site ranging from the casting of parts through to finishing processes including grinding and polishing, see Figure 3.1.

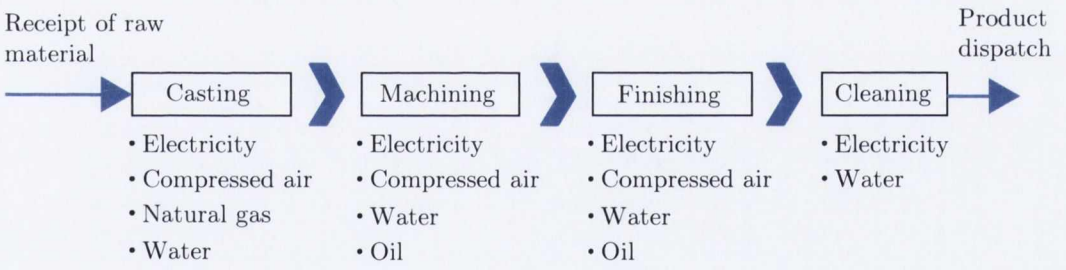

Figure 3.1 – Manufacturing cycle

3.1.1 Identification of system boundaries

Large manufacturing facilities are connected to the national grid, a 6,500km network of high voltage transmission stations and power lines, at a medium voltage. In Ireland, a small number of the largest industrial consumers receive electricity at a higher voltage, approximately 20 kV, due to the type and quantity of operations performed on site. Electricity is received at a main incomer before it is transformed down to the required voltage. Electrical energy is then distributed to a facilities end use equipment via a number of distribution boards, see Figure 3.2.

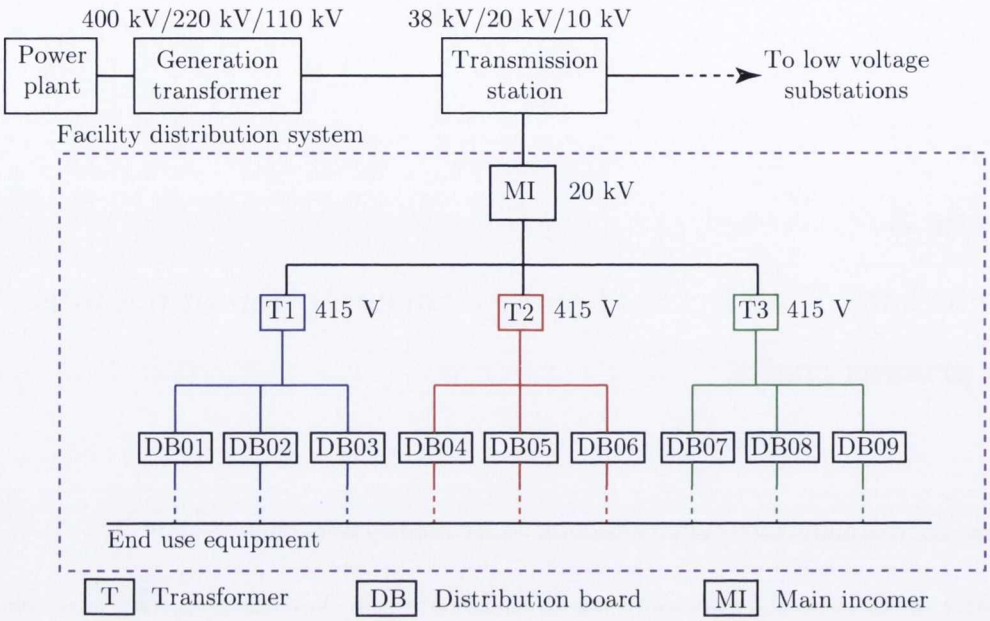

Figure 3.2 – Electricity distribution in case study facility

Electrical energy is consumed during each stage of a products life cycle, this research study concentrates on the electricity consumed during the manufacturing stage of the life cycle. The energy consumed by the sourcing, processing, and transport of raw materials is not considered and neither is the energy consumed during product distribution, end use, and disposal, Figure 3.3.

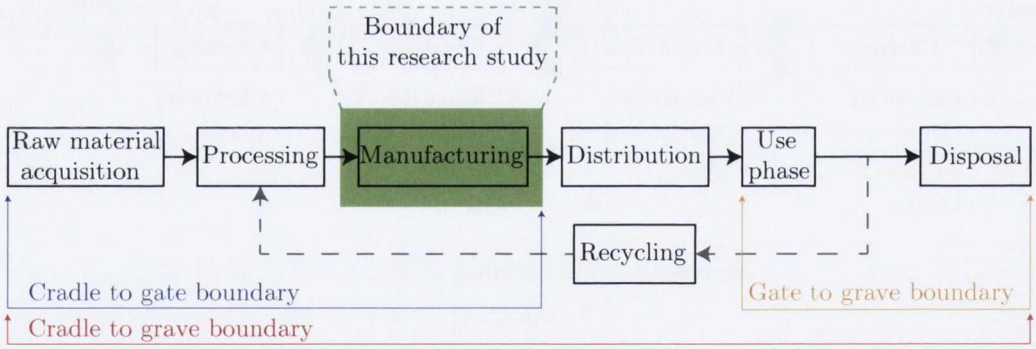

Figure 3.3 – Boundaries of study

3.2 Development of energy measurement strategy

In an effort to assess the energy consumption of the test facility in a systematic manner, a two stage energy measurement strategy was devised. Phase one of this energy monitoring strategy aimed to develop a macro level understanding of the energy requirements of the test facility. This

first phase was performed using a remote power meter and provided a quasi-static picture of energy consumption within the facility. The second stage of the monitoring campaign involved the installation of fixed metering devices capable of relaying continuous data streams to a custom built energy management platform.

The completion of both phases of this monitoring project were needed in order to achieve the required level of energy transparency to facilitate the development of energy performance indicators capable of continuously monitoring the overall energy performance of the test facility. The use of submetering in order to obtain transparency around the energy demands and consumption patterns existent within manufacturing facilities has been identified as an essential energy efficiency improvement enabler in research studies reported by Kara et al. [59], Herrmann et al. [15], and Wang et al. [120].

3.3 Phase one

The first step of the initial investigation consisted of a site walkthrough and an assessment of utility bills. The completion of this phase of the study facilitated the formulation of fundamental energy performance indicators that allowed high level energy performance to be monitored on a monthly basis. During the site walkthrough name plate information from each piece of equipment was collected and stored in a database. The information collected related to the electrical rating of the equipment and also its electrical configuration, single phase, three phase star/delta etc.,. Only major electrical system components including air compressors, extraction fans, and large pumps were considered at this stage of the assessment; this allowed an approximate breakdown of total site energy to be developed.

3.3.1 Measurement equipment

A remote power meter was used in conjunction with a small number of previously installed fixed energy meters to complete the first phase of the monitoring study. The remote power meter used in this study was a Fluke Powerlogger 1735, Figure 3.4. The meter has an 8 channel configuration, with four channels used for monitoring current - 3 phases and 1 neutral - and the remaining four channels used for voltage measurement - again 3 phases and 1 neutral. The meter can accurately measure all single phase, three phase wye, and three phase delta wired equipment. The Fluke Powerlogger 1735 measurement device has a broad range of functions; it is capable of measuring basic energy consumption but it can also monitor more complex events like voltage sags/surges and can uncover harmonic issues that could potentially disrupt or damage critical machinery. The meter has a sampling rate of up to 10.24 kHz used to examine harmonics; at its maximum reporting rate the meter will write three current and three voltage measurement values every 0.5 seconds to a measurement file; a minimum, average and a maximum.

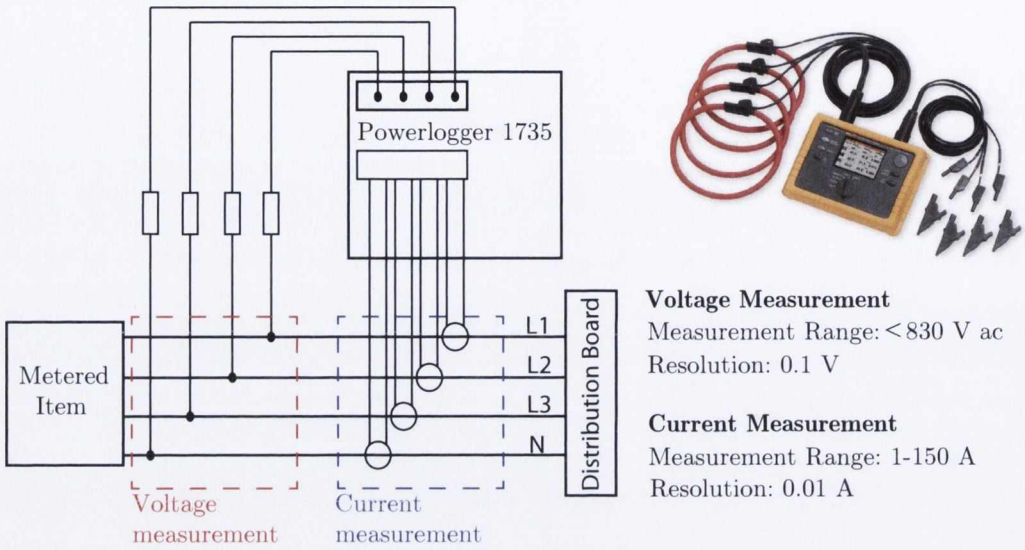

Figure 3.4 – Fluke powerlogger 1735

3.3.2 Fundamental energy performance indicators

The primary goals of energy performance indicators (EnPI's) are to enhance energy consumption understanding, increase energy efficiency, and decrease energy intensity. At a national level energy performance indicator's have found application as useful instruments for measuring the progress of sectoral CO_2 emission reduction efforts [122]. Examples of some existing high level EnPI frameworks are the Global Reporting Initiative (GRI), World Business Council for Sustainable Development (WBCSD), and the International Organisation for Standardisation ISO 14031 environmental management standard.

Although numerous studies have explored the use of EnPI's at national level, scant attention has been given to the concept of designing and implementing EnPI's within a single facility [180]. The most widely applied facility level EnPI is Specific Energy Consumption (SEC) or Energy Intensity (EI); defined by UNIDO [181] as the amount of energy required in order to produce one unit of economic output - in this case kWh/unit shipped. The total electrical energy consumption and the number of units shipped from the test facility in this study have been recorded over the previous six years. The SEC has been calculated each year and the results are included in Figure 3.5.

Specific energy consumption is calculated using the total facility electrical energy consumption, including both value add and non value add operations. This implies that if variables unrelated to production experience change, the SEC will change accordingly. Using this metric as a high level energy performance indicator is useful as it gives one single value that summarises the sites overall energy efficacy however, it is important to exercise caution when applying this statistic as a result of the issues outlined above.

Figure 3.5 also includes summary information on yearly milestones that have improved the overall energy efficiency on site. Specific energy consumption does not decrease each year because other events within the facility - such as the expansion of office operations - negate the impact of improvement projects. If more advanced indicators are to be developed and implemented it is necessary to disaggregate the total facility load in accordance with EN 50001 [44].

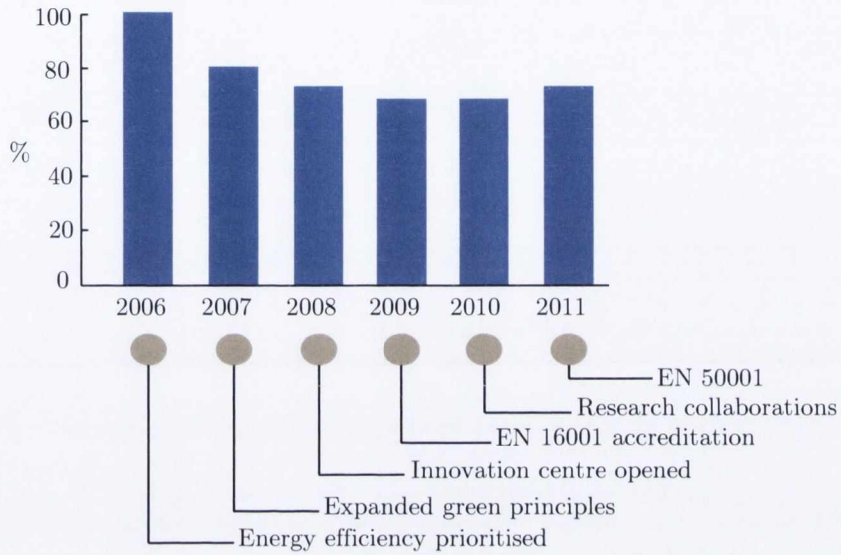

Figure 3.5 – Specific energy consumption - kWh/unit; yearly energy milestones included

3.3.3 Disaggregating total facility load

During phase one of the investigation over 50 individual pieces of equipment were analysed. The power meter was connected to the machine as described in Figure 3.4 and the meter was then set to record a value every ten seconds for a period of twelve hours. Table 3.1 includes a sample list of a selection of the equipment that was investigated as part of this phase of the study.

No.	Name	Average power	Note
1	Dust extraction unit 1	34.98 kW	Figure 3.6
2	Coolant system supply pump	4.15 kW	-
3	Air handling unit 6 supply	31.88 kW	Figure 3.7
4	Air handling unit 6 return	4.45 kW	-
5	Compressed air unit 2	144.95 kW	-

Table 3.1 – Sample of monitored equipment

Figure 3.6 illustrates the recorded power profile from one of the facilities dust extraction units

and the simplified operational sequence. The dust extraction system removes particulate matter from certain machining processes in order to maintain air quality and enhance operator safety. Sand blasting, grinding, and polishing are examples of operations requiring dust extraction within the test facility. Although extraction is only required during and immediately after material removal, it is constantly supplied to each machine. The primary power consuming component of the extraction system analysed here is the large extraction fan that maintains the air velocity required in order to keep the dust particles in suspension until they reach the collection point. The power profile is essentially constant which is to be expected considering the fan is driven by a fixed speed motor. Figure 3.6 also illustrates the meter connection process in addition to the dust extraction units location within the facility's electricity distribution system.

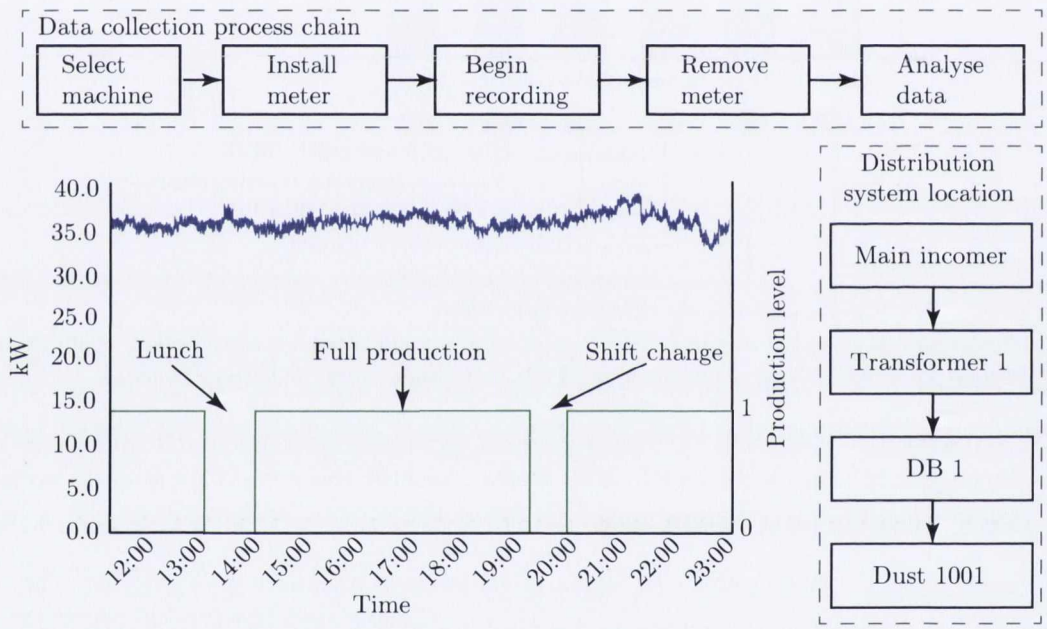

Figure 3.6 – Dust extraction fan power profile

Figure 3.7 illustrates the recorded power profile from one of the facilities air handling units (AHU); integral parts of the facilities heating, ventilation, and air conditioning system. The main purpose of each AHU is to circulate and condition air that is used to maintain the appropriate temperature and humidity in both manufacturing and office areas. Each air handling unit has two fans; one for supply and one return. The power profile included in Figure 3.7, alongside the meter connection process and the distribution system location is for a supply fan.

Completing a similar analysis on all of the key electrical system components and collating the results, allowed a preliminary energy consumption breakdown pie chart to be developed, see Figure 3.8. This preliminary breakdown provides a first perspective on which operations are most significant in terms of energy consumption.

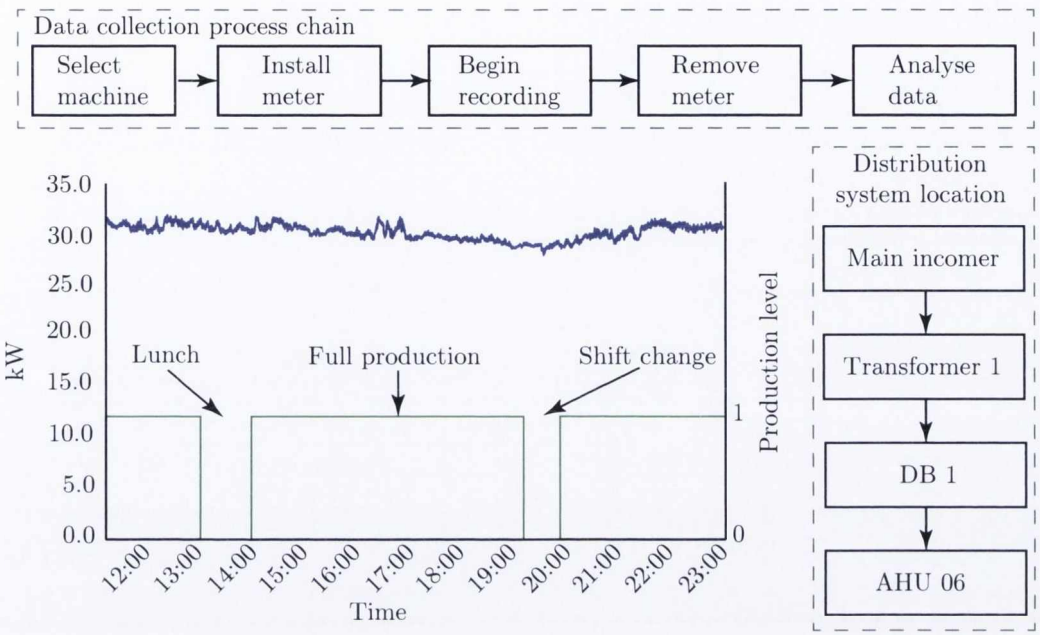

Figure 3.7 – Air handling unit 6 supply fan power profile

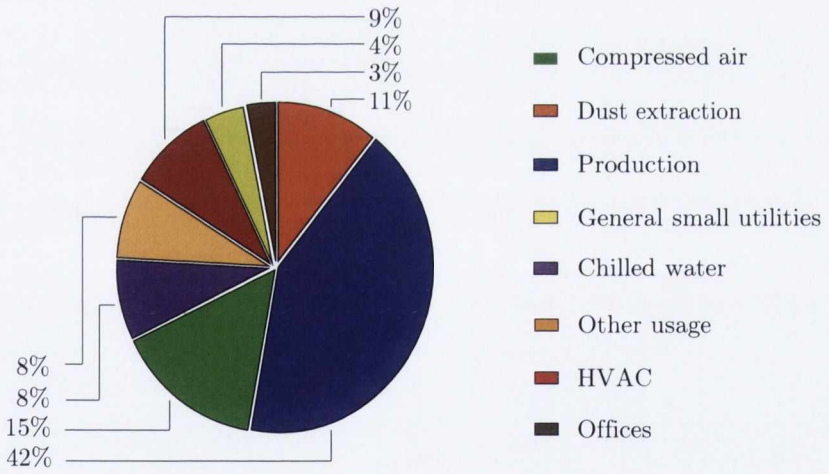

Figure 3.8 – Electricity consumption in case study facility - 48 hour measurement interval

3.4 Phase two

The second phase of the energy monitoring strategy involved the design, specification, and installation of a fixed metering system capable of continuously relaying data to a custom built energy management platform. The installation of a fixed energy metering system facilitates the development of an accurate energy consumption breakdown and also allows more advanced process level energy performance indicators to be established [58].

3.4.1 Energy metering installation strategy

In order to ensure that measurement devices were installed at all of the appropriate locations within the test facility, a metering installation strategy was developed. The installation strategy, which is applicable to any manufacturing facility, is a number of sequential steps ensuring an effective and cost efficient metering system is installed. Thiede et al. [58] observed that the need to maximise energy transparency must be weighted against the level of investment required for acquisition and installation as well as operating costs for continuous evaluation and maintenance.

The first phase of the metering implementation strategy is to install metering devices at each of the main electrical system points, level 1 components; site incomer, transformers, and also distribution boards. Beyond these high level electrical points, all significant energy users, level 2 components, identified in accordance with state-of-the-art European energy management standards must be metered. A basic decision support tool is then required to effectively select the end use equipment, level 3 components, requiring fixed measurement devices, see Figure 3.9. The selection criteria are as follows;

1. Equipment with static power consumption, i.e. a kW demand not more than 3σ from the mean during the screening test, over 20 kW require the installation of a metering device.

2. Equipment with an average power consumption greater than 5 kW and a dynamic power profile, i.e. a kW demand outside of the 3σ limit during the screening test, require the installation of a metering device.

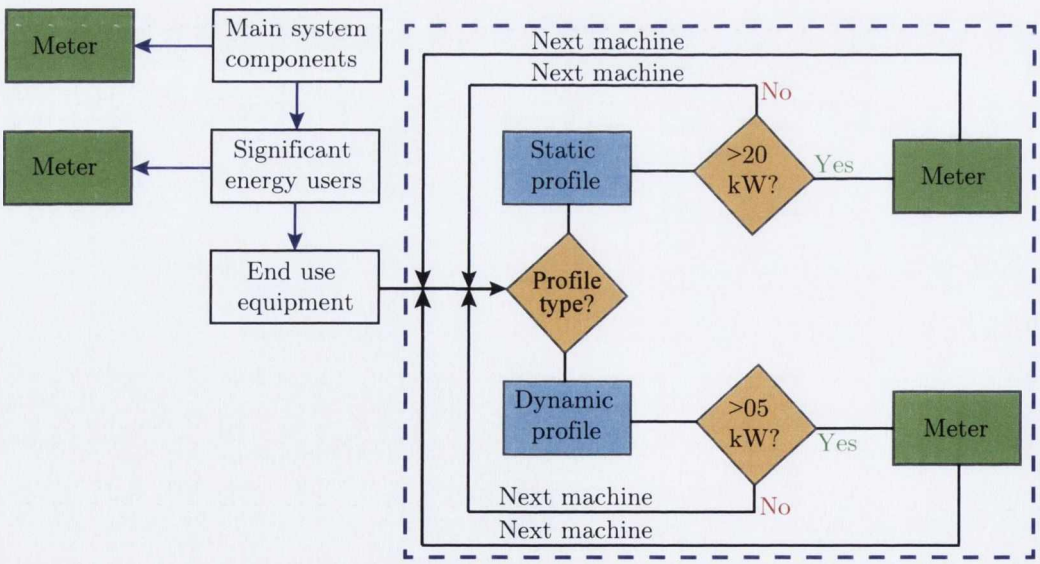

Figure 3.9 – Energy metering implementation methodology

The test facility in this study required a flexible metering solution that could quickly and

easily adapt to the movement of equipment to different locations on the plant floor. The variables required from the meters were kW, kWh, and power factor information to feed into the existing building management system (BMS). The metering system needed to be capable of integrating with the pre-existing quality and site management systems. The meter that provided the optimum solution for the given application from a cost, functionality, installation, and support standpoint was the Episensor ZEM-61 wireless three phase electricity monitor, Figure 3.10.

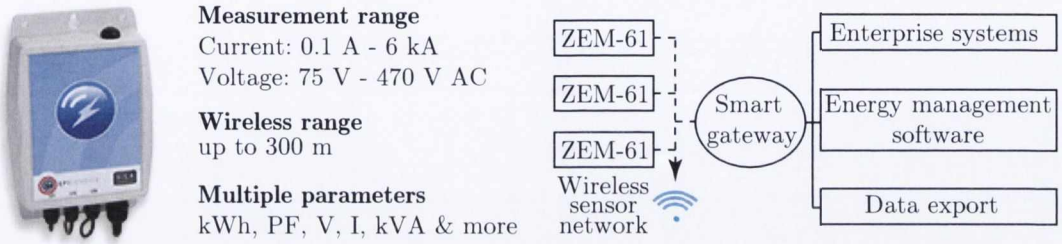

Figure 3.10 – Episensor ZEM-61 three phase electricity monitor

Each ZEM-61 meter sends kW, kWh, and power factor information wirelessly, using 802.15.4 (Zigbee), to a SiCA gateway which is then linked, via ethernet, to a SiCA server that communicates directly with the existing BMS. In accordance with the metering implementation strategy, meters were installed at the main incomer and all of the distribution boards. Measurement devices were also installed at each significant energy user, including air compressors, chillers, extraction fans, etc.,. An example of some of the results obtained during the level 3 screening investigation are included in Table 3.2.

Operation Type	Power Profile	Avg. Power (kW)	Install Meter
Milling	Dynamic	7.42	Yes
Coolant pump	Static	9.87	No
Sand blasting	Dynamic	2.84	No
Extraction fan	Static	34.26	Yes
Cleanline (large)	Dynamic	15.31	Yes

Table 3.2 – Sample of screening investigation results

From a systems integration perspective, the metering system combined seamlessly with the existent quality and management structures on site. The newly installed energy metering system provides a level of energy consumption transparency that is typically only available in research labs and facilitates the use of statistical methods to analyse and forecast past, present, and future energy consumption.

3.4.2 Enhancing energy transparency

Herrmann et al. [15] observed that the temporal resolution of the data coming from the energy metering system controls the level at which indicators can be implemented. Operating at its maximum resolution the metering system described in the previous section outputs data every fifteen minutes. Figure 3.11 illustrates the power consumption profile of a sample month at four different temporal resolutions.

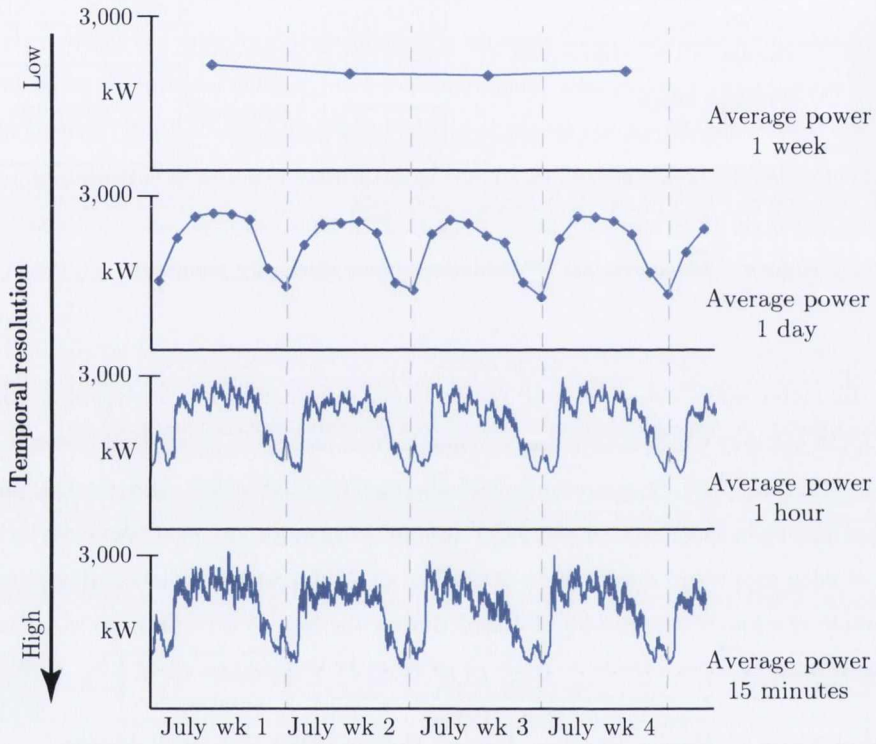

Figure 3.11 – Temporal resolution of energy metering system data

Assessing data over different time scales at multiple temporal levels facilitates a holistic analysis of energy consumption [19]. At a yearly and monthly resolution long term trends and seasonal variation have been observed; this type of information allows the most energy intensive periods of the year to be identified. At a weekly and daily resolution medium term trends can be observed. The normal variation throughout a working week and the baseline energy demand have been identified at this level. Accurately calculating a facility's maximum energy demand is also possible at this resolution, this has allowed the organisation to optimise their maximum import capacity (MIC) agreement with the energy supplier, achieving significant savings.

At an hourly and fifteen minute resolution daily trends can be observed. The typical daily schedule from office start up, break times, and major equipment operation has been observed here. This provides an opportunity to micro manage the facility from an energy perspective and optimise

the production schedule. Optimising production schedules from an energy perspective has been identified as a viable energy performance improvement method by researchers including Vikhorev et al. [77], Pechmann and Schoeller [80], and Duflou et al. [9]. Figure 3.12 illustrates the different information and trends that can be identified by analysing data over a variety of time scales.

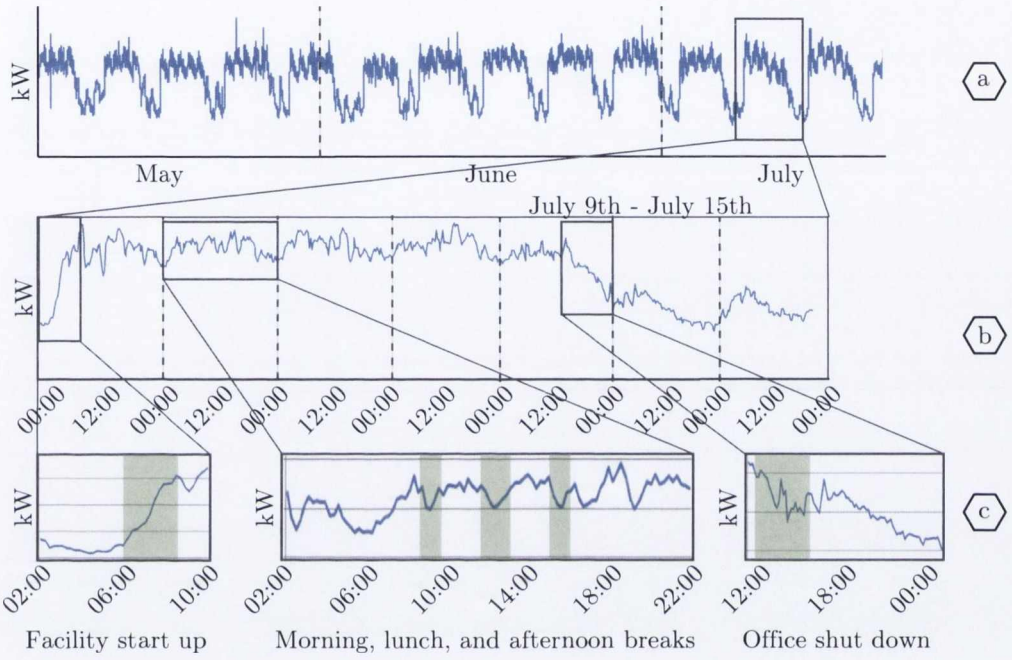

Figure 3.12 – (a) Total power consumption for a three month period; clear weekly trends are visible; (b) Total power consumption data for one week in July; weekly start up, daily patterns, and weekly shut down visible; (c) Individual daily events that can be identified and analysed.

3.4.3 Advanced energy performance indicators

Although it has been illustrated that useful conclusions can be drawn from analysing the total power consumption of a manufacturing facility, there are limitations. In order to further improve the level of information available it is necessary to analyse each significant energy user (SEU) individually. Vikhorev et al. [77] reported that implementing energy management methods at the factory floor level is only possible if energy consumption is continuously monitored. Vikhorev et al. [77] also reported that the identification and monitoring of SEUs is a critical component of any attempt to develop holistic energy efficiency improvement strategies. The previously described energy metering infrastructure has facilitated the disaggregation of total facility load into SEUs. A production correlated indicator, focusing on compressed air, and an environmentally correlated indicator focusing on chilled water are now discussed.

Compressed air

Compressed air is responsible for approximately 10% of the total energy consumed in the industrial sector [15]. Within the test facility compressed air is responsible for approximately 15% of the facility's energy load, and is used for a number of operations including cleaning and purging. The compressed air requirements are met by one variable speed compressor and three fixed speed compressors. The fixed speed compressors operate in a duty-standby cycle with one fixed speed compressor always in operation to satisfy the base load during periods of production. The variable speed compressor is used to fulfil the additional dynamic compressed air load. Figure 3.13 illustrates the total facility compressed air requirements for a sample month and also the energy requirements of each individual compressor over a one week period.

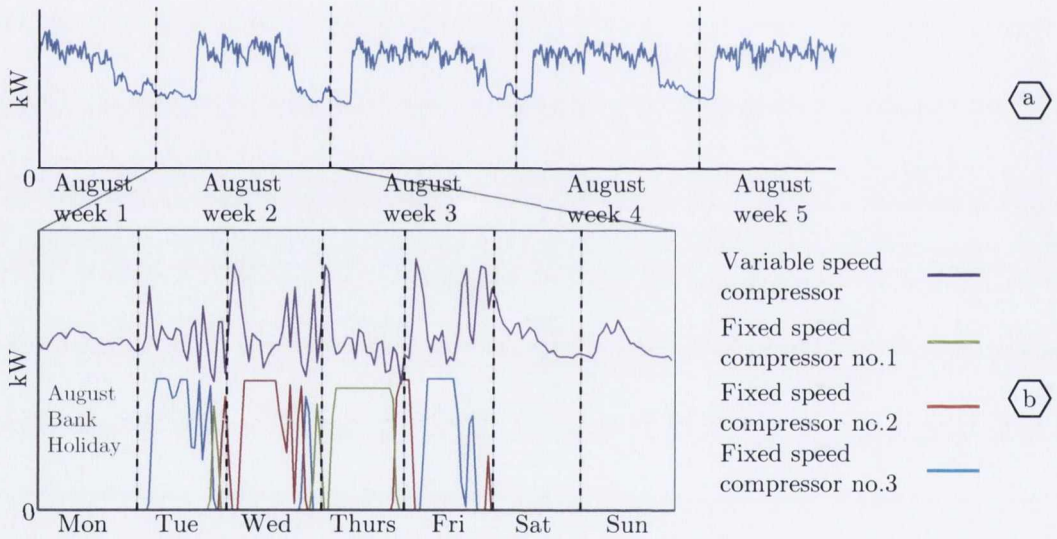

Figure 3.13 – (a) Total compressed air system demand for a sample month; (b) Power consumption for each of the four air compressors over a seven day period

In addition to the electrical power requirements of the compressed air system, the total compressed air flow is also continuously monitored. By recording two compressed air variables the performance of the system can be robustly monitored in a near real-time environment. Regressing the compressed air system flow rate against the associated power consumption yields a strong correlation, $R^2 = 90.9\%$. Monitoring the flow rate and associated power consumption at a variety of system loads on a periodic basis allows the overall system condition to be assessed, see Figure 3.14. An energy performance indicator of this form ensures that the compressed air system is operating optimally and minimises energy wastage.

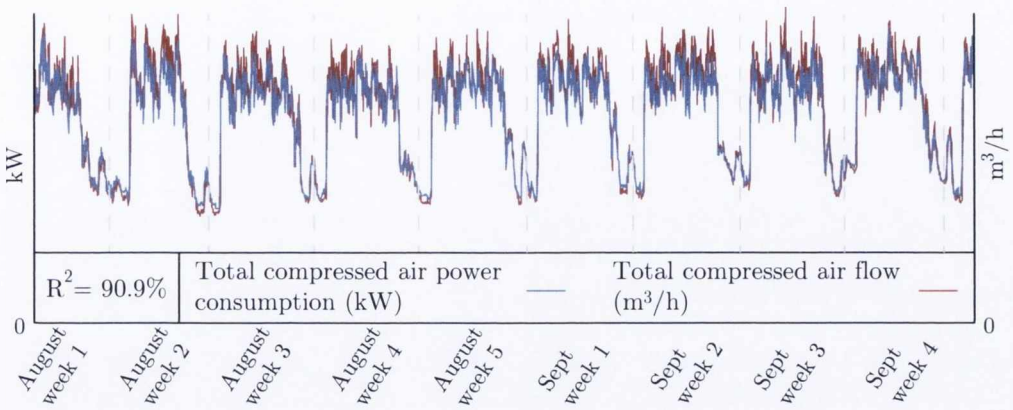

Figure 3.14 – Compressed air system power requirements (kW) and flow rates (m^3/h)

It is important to understand that the overall efficiency of the compressed air system is strongly influenced by the running order of the air compressors. In particular, the kWh/m^3 metric depends on the operational level of the variable speed compressor relative to the total compressed air load. In order to minimise the energetic impacts of compressed air supply it is critical to develop sophisticated control structures that ensure the optimal combination of fixed speed and variable speed air compressors are being used. Figure 3.15 highlights two important compressed air variables, the proportion of the total compressed air requirement that is being serviced by the variable speed compressor (%VSD) and the kWh/m^3 statistic, over a one week period. Figure 3.15 illustrates how the kWh/m^3 metric spikes when the compressed air demand increases above the threshold that one air compressor can supply. During these short periods, the compressed air system is at its least efficient. The results included in Figure 3.15 provide another insight into energy performance that is only possible as a result of the structured energy measurement approach proposed in this research study.

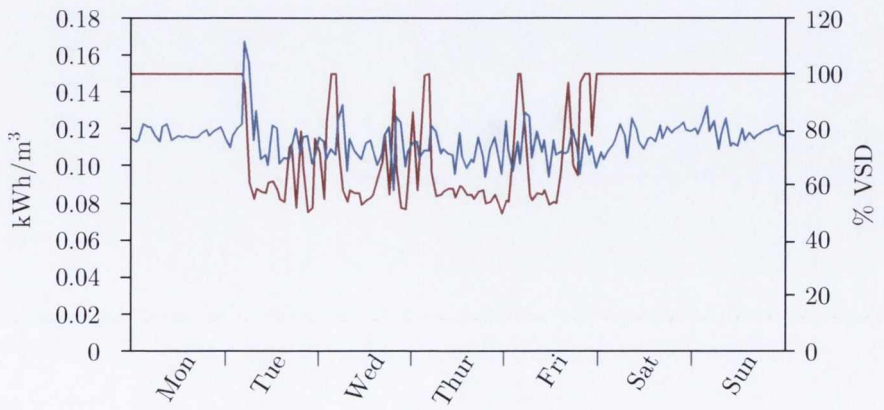

Figure 3.15 – Compressed air system efficiency (kWh/m^3) and %VSD

Chilled water

Chilled water is used within the facility as a coolant for the air conditioning system. As the ambient temperature within the facility increases, the chilled water system consumes more energy in order to maintain the appropriate temperature. Similarly if the ambient temperature decreases, the chilled water system requires less energy in order to maintain the appropriate temperature. Assessing the chilled water power consumption in conjunction with the ambient temperature it is possible to assess the effectiveness and performance of the system continuously, see Figure 3.16.

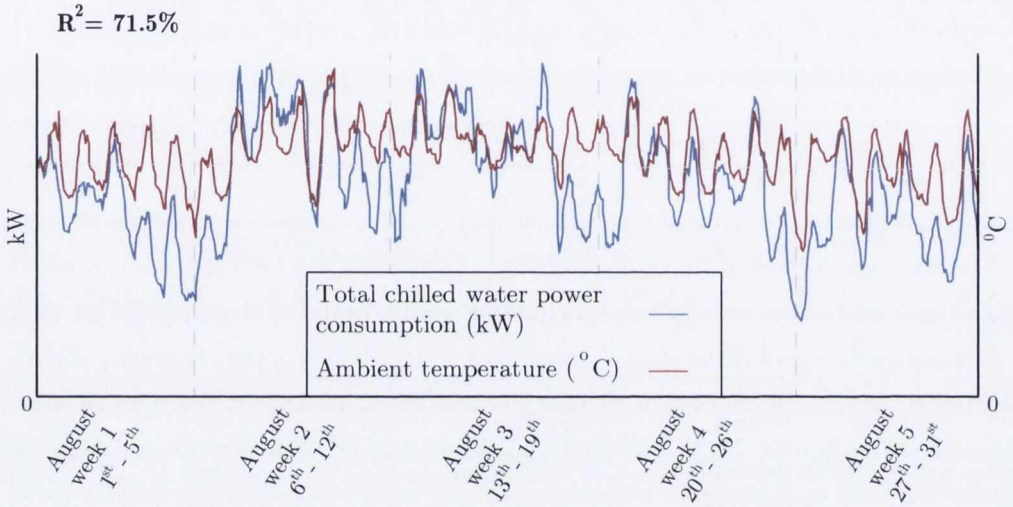

Figure 3.16 – Chilled water system power requirements (kW) and ambient facility temperature (^oC)

3.4.4 Energy performance indicators as forecasting tools

Statistical analysis has been used to analyse previous data in order to locate trends and forecast future needs for many years. Techniques including time series analysis, trend analysis, adaptive filtering, moving averages, and regression find application as statistical forecasting tools. In this study a multiple linear regression analysis was performed; the aim was to predict the energy consumption of a future month, based on the energy data collected from the two preceding months. Throughout a typical year a number of variables effect the overall energy consumption including the level of production and seasonal weather effects.

Considering only the total power consumption at an hourly rate over a three month period a multiple linear regression equation was developed. This equation was able to accurately predict the power consumption of month_N, based on the power consumption of the two preceding months, month_{N-1} and month_{N-2}. The use of two preceding months as predictor variables provides enough input data to the model to ensure that it accounts for short and medium term variation, including seasonal change, see Equation 3.1. Within the model each month is represented by four seven day

weeks and this allows for comparisons between months of different lengths.

$$M_N = -20.8 + 0.0926M_{N-2} + 0.954M_{N-1}; \tag{3.1}$$

Applying the model to an unseen data set, in an attempt to verify its robustness yielded the following results, Figure 3.17.

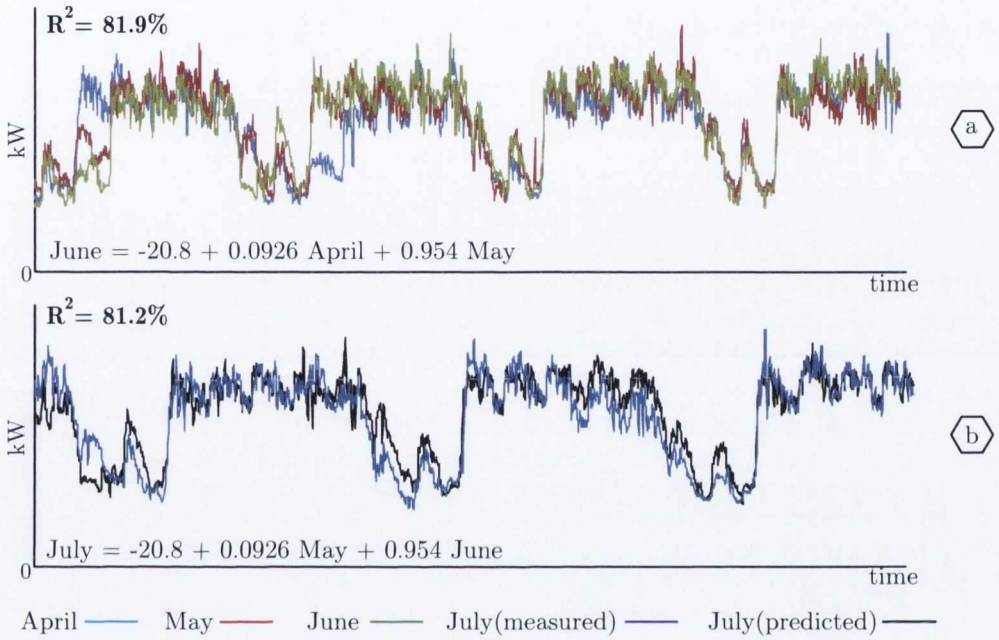

Figure 3.17 – Regression analysis of hourly power consumption (a) data used for model development (b) using model for prediction

The forecasting approach proposed here is a basic two point autoregression. There is scope here to develop and refine the proposed approach, for example, a moving average based autoregression could be used. A more sophisticated approach that attempted to predict each of the variables that contribute to the total electrical energy consumption could also be developed. In this case, more complicated models do not necessarily guarantee more a accurate prediction of energy consumption and this is due to the inherent dynamics and uncertainty that characterise manufacturing facilities. The uncertain nature of weather, building occupancy levels, and production schedules make the task of developing reliable predictive models a challenging task.

3.5 Mapping value stream energy requirements

A variety of different approaches have been taken to the task of quantifying and optimising value stream energy consumption, including simulation [11, 21], planning [161], modeling [118], coordinating building services [62], and mapping process flows [182]. One of the most contemporary

approaches to optimising value stream energy consumption involves empowering machine tool operators with the authority to alter the production schedule in order to make the best use of resources and time [77]. The test facility analysed in this work produces a variety of products, all of which are manufactured in one of five value streams. One of the value streams was selected for an in-depth analysis; the chosen value stream produces two product lines. The two products pass through different processing steps and also require different levels of cleaning and inspection. In order to obtain a better understanding of the energy requirements of the product A and product B value streams a process by process analysis was performed. The process chains for product A and product B are included in Figure 3.18 and Figure 3.19.

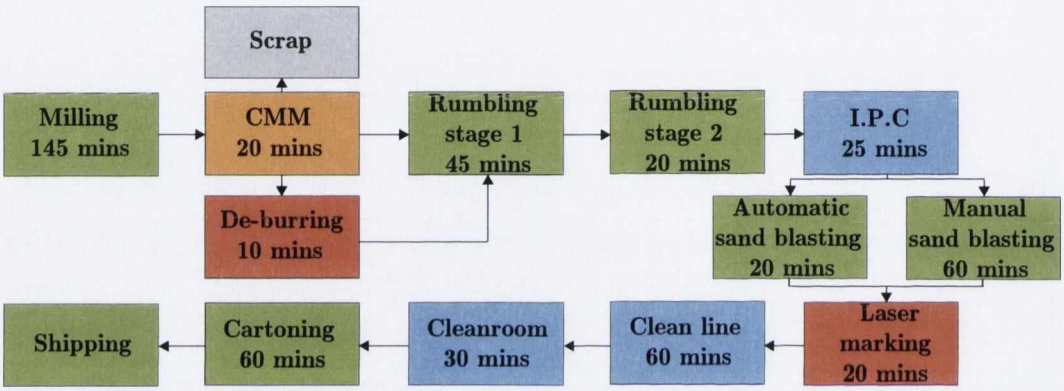

Figure 3.18 – Product A value stream

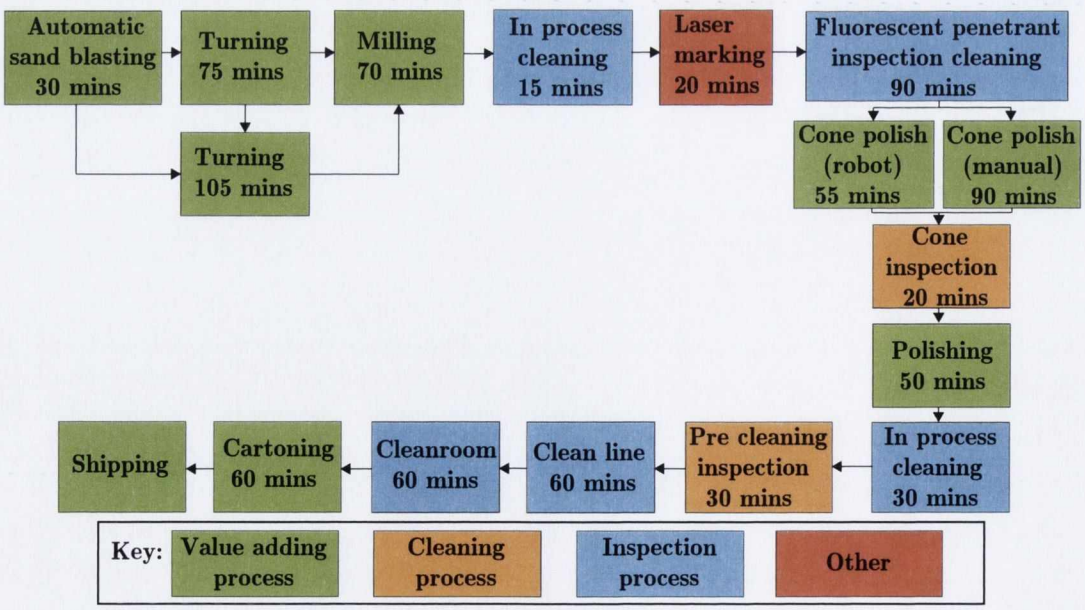

Figure 3.19 – Product B value stream

Each testing period consisted of three complete processing cycles, during this time the machines power profile was measured and recorded. The research studies of Hesselbach et al. [62] and Gutowski et al. [79] identified the ability to segregate the two types of machine tool power consumption - fixed and variable - as a key benefit of machine tool power profiling. The fixed component, that remains constant once the machine is powered on, is the result of keeping the machine in a an operational state whereas the variable component results from of all of the machining operations required to manufacture products. Figure 3.20 illustrates the energy requirements of each process required to manufacture product A and product B. The total kWh required for each product was calculated after the complete process chain was monitored and this allowed a comparison to be performed, see Figure 3.21.

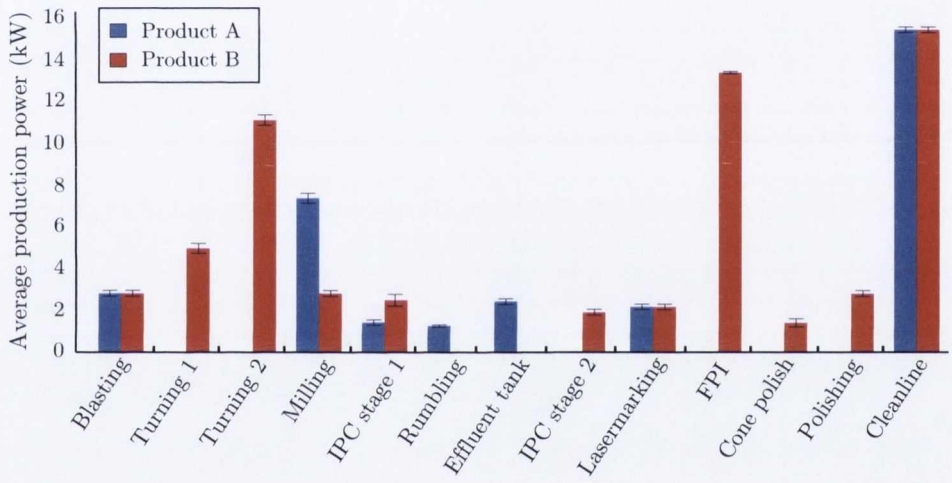

Figure 3.20 – Process power consumption

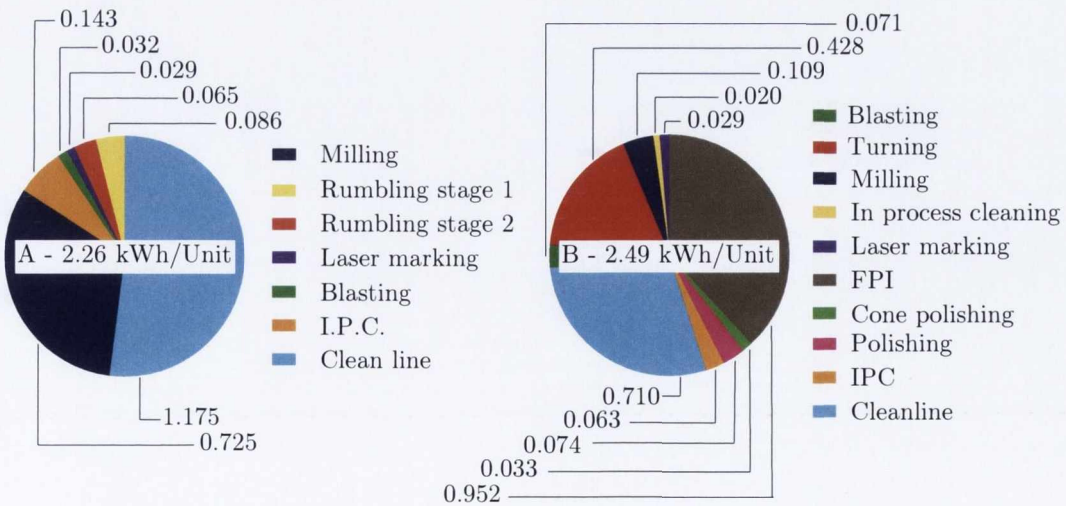

Figure 3.21 – Product A and Product B, kWh/part

The larger number of steps required for product B is evident from Figure 3.20 and another interesting issue that is highlighted here is the large energy consumption of non value adding operations including inspection and cleaning. This finding supports the assertions of Duflou et al. [9] who previously identified technological change and process substitution as methods that can yield significant environmental gains. The results included thus far in this section only take account of the energy consumed directly by each process, there is no consideration of supporting services, lighting, or HVAC.

3.5.1 Quantifying the total energy requirements of machining

Figure 3.22 describes the machine tool energy quantification framework that allows the complete energy requirements of a machine tool to be calculated. Gutowski et al. [79] observed that holistic quantification frameworks are required due to the fact that the energy required to perform the primary task - cutting metal by plastic deformation - only accounts for a small portion of the overall machine tool energy consumption.

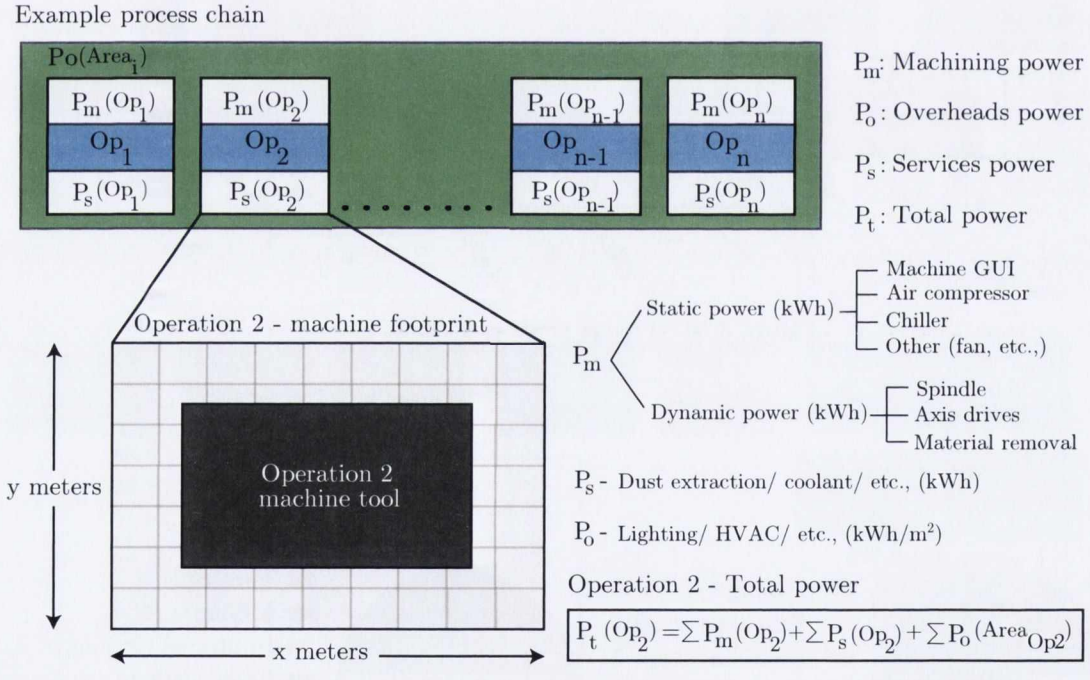

Figure 3.22 – Quantification of total machine energy consumption

The framework presented here accurately quantifies the total energy requirements of an individual machine tool accounting for supporting services, overheads, and the energy consumed directly by the machine tool. This energy quantification framework is based on empirical data as opposed to the theoretical data described in previous research studies [60, 110]. An additional novel aspect of the framework proposed here is the use of the machine tools physical footprint as a means to

allocate the energy consumed by overheads.

Machining and machine tool services power consumption

The sample machine tool was a Mazak FH-4800 milling machine. This machine is used to perform a large number of operations on the workpiece including drilling, milling, tapping and polishing. The electrical load drawn by each Mazak machine is heavily dependent on the machining state. The development of an understanding of the quantity of energy a machine tool consumes in different operational states has been identified as an important research area [19, 84]. Research teams led by Kalla et al. [160] and Dietmair and Verl [92] have presented a variety of different perspectives and interpretations on the definition of machining states within the literature. The power profile for a typical batch, consisting of twelve identical parts, is included in Figure 3.23 showing both the maximum and average machine tool energy consumption.

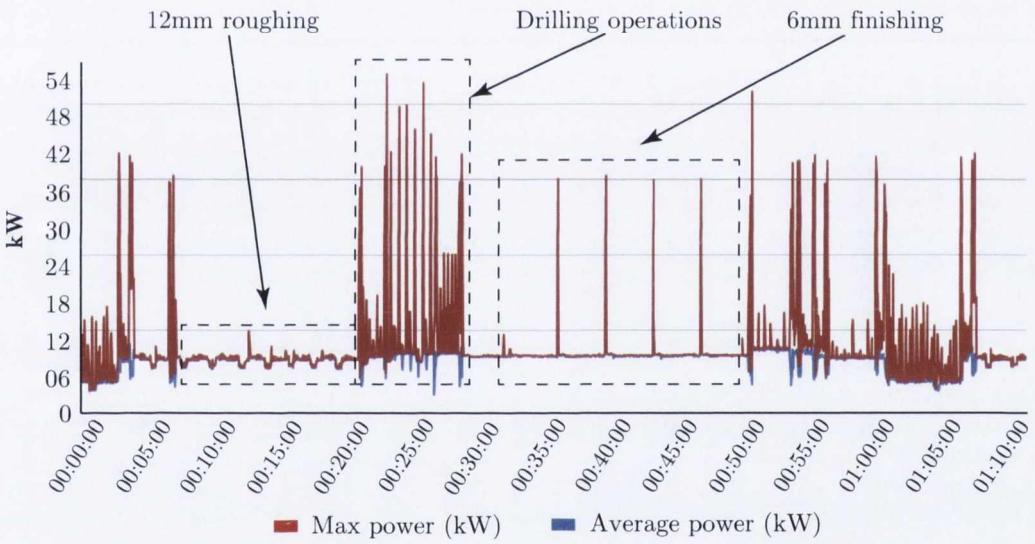

Figure 3.23 – Milling machine power profile

In addition to the energy consumed directly by the Mazak during processing there are additional pieces of support equipment that facilitate the milling operation. According to Duflou et al. [9] it is necessary to quantify the energy consumed by auxiliary support equipment in order to accurately determine the overall energy requirements of a unit process. Each Mazak is linked to a centralised coolant distribution system. The coolant system requires two large pumps, operating on a duty/standby schedule, to distribute the coolant throughout the plant. Coolant is used to enhance cutting performance and maintain acceptable interface temperatures between the machine tool and the workpiece before it is filtered at the base of each machine and returned to the coolant reservoir by another pump.

In order to allocate a proportion of the coolant systems electrical consumption to a single

machine the overall consumption was recorded. The centralised coolant system feeds eighteen similar machines, therefore, the supply pump's power consumption was divided equally between each consumer; giving a per machine value of 0.230 kW. Each machine also has its own coolant return pump which sends the used fluid back to the centralised coolant reservoir. The power profile for one of the coolant return pumps is included in Figure 3.24; the average electrical load is 0.630 kW. The total electrical load per machine, resulting from the supply of coolant is therefore 0.860 kW.

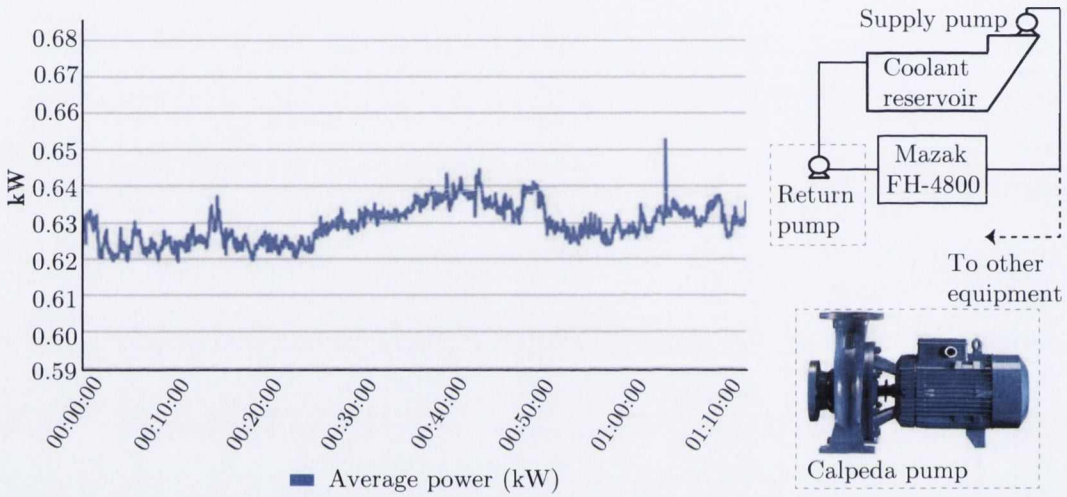

Figure 3.24 – Coolant return pump

Overheads power consumption

For a work environment to be considered safe, it must be adequately illuminated, maintained at an appropriate temperature, and sufficiently ventilated. Numerous researchers have provided comprehensive coverage on the energy requirements of industrial lighting [73], and HVAC installations [71]. Attributing a certain percentage of the electricity consumed by the facility overheads to a certain process or process chain is possible through the use of a suitable metric; within the framework proposed here, the consumption of all utilities is described in terms of a discrete measurable unit - kWh/m^2. The light fittings that illuminate the machining cell containing the Mazak FH-4800 milling machine are 55 Watt fluorescent tubes. There are 24 of these light fittings covering an area of approximately 215 m^2, therefore 6.15 x 10^{-3} kWh's are required per square meter each hour.

The electrical load attributed to HVAC can be established using the same technique. The air handling unit (AHU) that services the product A line is responsible for the HVAC of a large area of the facility; approximately 1,350 m^2. In order to correctly attribute a kWh value to each meter squared of floor space both the supply fan and return fan were metered individually. The supply fan draws an average load of 31 kW and the return fan draws 4.5 kW. This gives a cumulative total

of 35.5 kW for the air handling unit. The total requirement is therefore 2.6 x 10^{-2} kWh's per square meter each hour. Figure 3.25 illustrates the minimum and maximum power consumption during each one second recording interval as well as the average power consumed during the recording interval for the AHU supply fan.

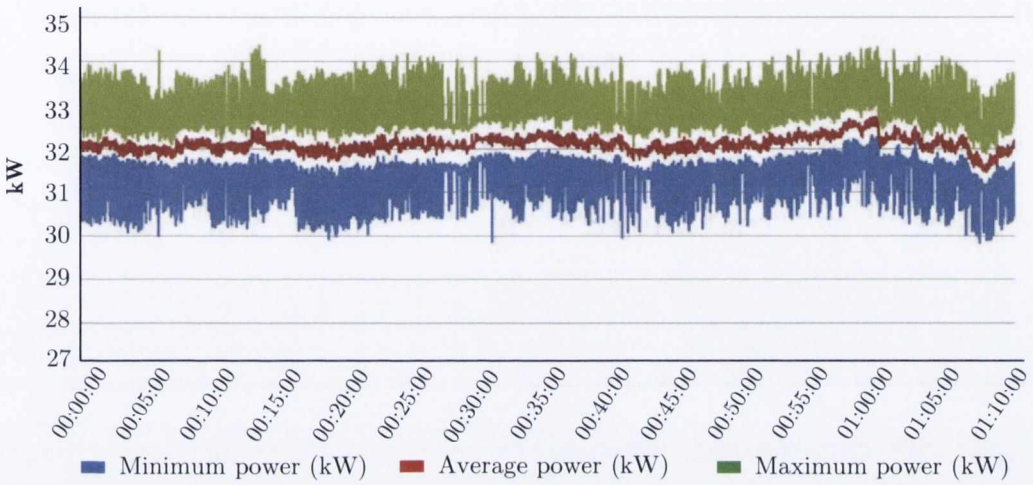

Figure 3.25 – AHU supply fan

The cumulative total consumption for this machine tool is 111.67 kWh per 12 hour shift. The following pie chart, Figure 3.26, illustrates the kWh/shift energy consumption breakdown. A simple assessment that only considered the energy required directly by the machine tool would result in an apparent energy requirement of 89.76 kWh or approximately 80% of the actual energy consumed. The results of this study align with the research work of Gutowski et al. [79] that identified two key strategies to minimise energy use; the redesign of energy intensive support equipment and improving the rate at which machine tools can operate.

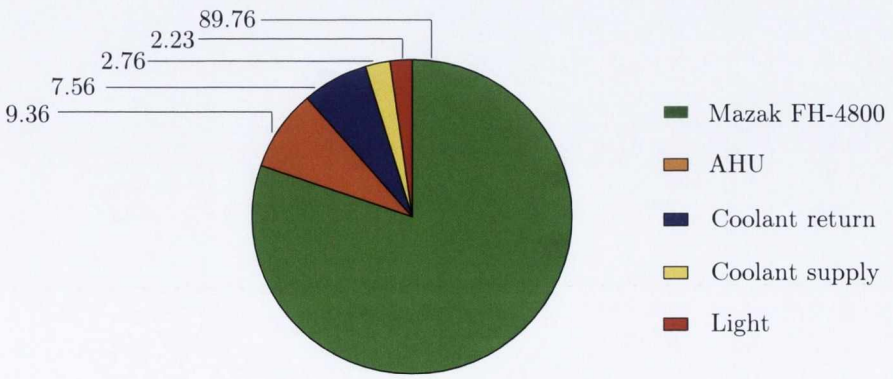

Figure 3.26 – Total machine consumption, kWh/shift

Structured measurement methodologies aimed at quantifying the energy consumption of manufacturing at facility level, value stream level, and process level have been described. The results, which align with state-of-the-art research studies, illustrate the degree of energy transparency that can be achieved via the implementation of robust measurement approaches. The test facility now possesses a level of energy transparency, illustrated in Figure 3.27, that does not typically exist in industry and has not previously been reported in the literature. The work presented in this chapter provides a means to overcome the energy transparency issue highlighted by Thiede et al. [58] as one of the key obstacles that impedes the implementation of energy efficiency improvement projects.

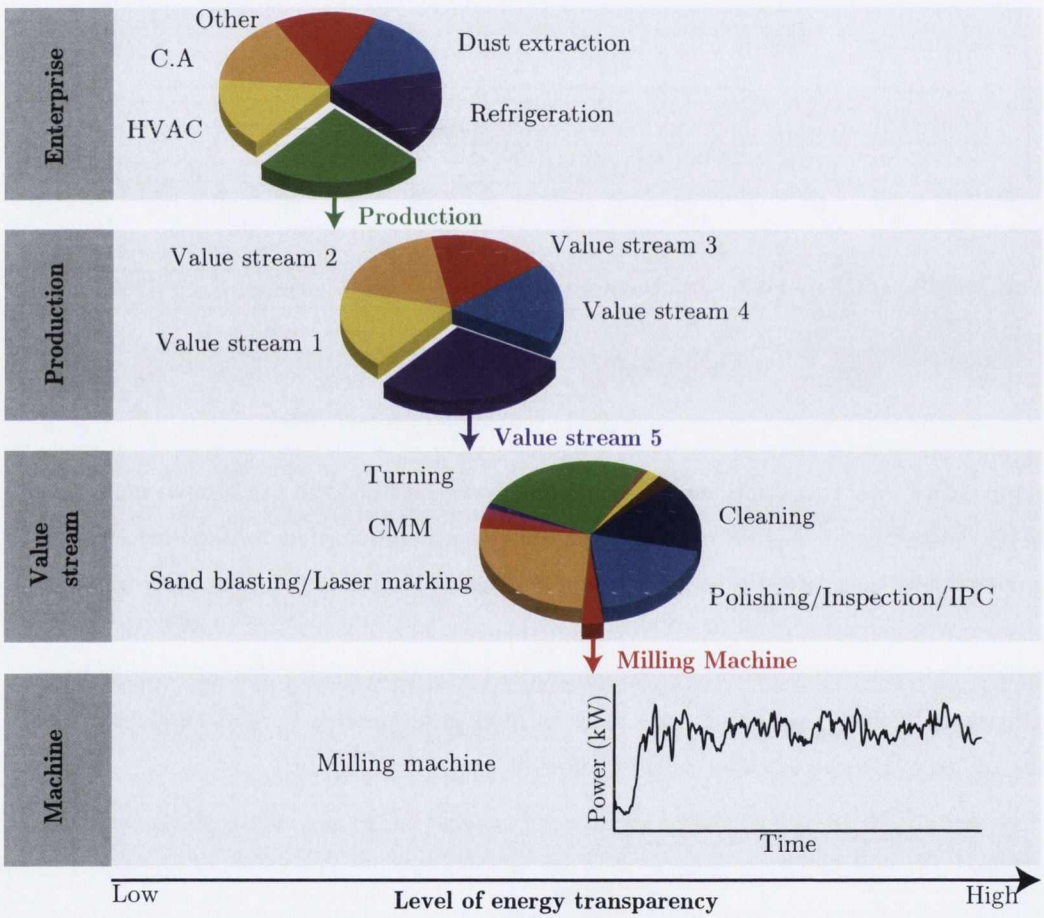

Figure 3.27 – Energy consumption transparency resulting from the state-of-the-art metering installation

3.6 Summary

The work described within this chapter has closely followed the trends that exist in the literature, specifically, energy efficiency projects and research efforts are focused around discrete levels of

the manufacturing facility [59]. Initially the production facility was mapped out and each of the five product lines was identified. The energy consumption of the plant, taken from utility bills, was recorded. This information alone was unable to provide value stream or individual machine information.

A metering strategy was developed and deployed which allowed the total electrical energy consumption to be disaggregated into its significant energy users in accordance with state of the art European standards [44]. The initial phase of the metering strategy used commercially available remote power metering devices to monitor each piece of equipment individually. The second phase of the metering strategy involved the design and installation of a facility wide energy metering system. The majority of these meters were installed on high level distribution points in addition to the sites significant energy using equipment.

The metering infrastructure that is installed in the test facility represents the state-of-the-art in industrial energy management and comparable projects have not been reported in the literature to date. The information emanating from the energy management system was then used to develop energy performance indicators allowing the effectiveness of energy projects to be accurately quantified as well as optimising energy cost savings from the perspectives of both procurement and end use.

A holistic approach was taken to the task of quantifying the total energy requirements of an individual manufacturing process. This section of the research was in line with the most recent research literature from within the CIRP community as well as other relevant academic journals [19, 85, 118]. The total amount of energy consumed directly and indirectly was quantified and the results observed here aligned with the results of the aforementioned research studies.

In order to further develop energy transparency the research needed to progress to the next hierarchical level and assess an individual machine tool at a component level. Characterising individual machine tool components in both the frequency and time domains requires the development of a purpose built measurement tool. The development and application of this tool as well as the obtained results are described in chapter 4.

Chapter 4

Machine tool electrical energy characterisation

4.1 Energy requirements of machine tool systems

Preliminary studies on the environmental performance of machine tools indicate that over 99% of the environmental impacts are due to the consumption of electrical energy during the usage phase of its life cycle [118]. For this reason the European Commission have identified machine tools as a top three priority for inclusion into the product categories regulated by the ecodesign directive [183]. The International Standards Organisation are also developing standards that focus on machine tools; addressing the environmental evaluation of machine tools in ISO 14955-3/4, and the evaluation of manufacturing systems in ISO 20140 [18, 184]. Herrmann et al. [106] reported that characterising the energy consumption of machine tools is a critical step towards improving efficiency. The increasing number of research contributions by different machine tool builders demonstrates the increasing interest in the energy performance of the equipment they develop [95]. CECIMO - the European Association of Machine Tool Builders - has also launched a self-regulatory initiative (SRI) that supports the identification of measures to improve the energy efficiency of the machine tools their members produce. Furthermore, the research community have developed working groups focusing exclusively on the energy consumption of machine tools, for example the cooperative effort on process emissions in manufacturing (CO2PE) group, the University of Wichita's unit process life cycle inventory (UPLCI), and the CIRP collaborative working group on energy and resource efficiency and effectiveness (EREE).

The increased attention given to machine tools by international regulatory bodies and research institutions coupled with the fact that the overall energy efficiency of a typical machine tool is estimated to be less than 30% [18], makes the development of a thorough understanding of their energy use desirable. The performance of a machine tool is dependent on the cooperative interactions between the spindle, feed drives, and peripheral equipment [17]. According to Herrmann et al. [15], the total energy consumption results from the temporal accumulation of the individual power demands of each subordinate component. Studies have also shown the energy consumed by a machine tool system during machining is strongly influenced by cutting parameters, machine tool efficiency, and the rate of material removal [18]. Optimising machining parameters against

a set of environmental criteria was presented as a means to reduce the environmental impacts of machining by Krishnan and Sheng [185]. Krishnan and Sheng [185] presented a case study that reported a 4.5% energy saving by implementing an environmental process plan versus a conventional process plan [185]. Traditionally researchers have focused on specific cutting energy (SCE) [186], and specific energy consumption (SEC) [118] as methods to assess the energy efficiency of machine tools. Balogun and Mativenga [183] observe that there is a need within industry and the research community to accurately relate machine tool motion to energy consumption at a component level.

4.2 Experimental setup

4.2.1 CNC machine

The machine tool that was used in this case study was a Hurco VM2 vertical machining centre, Figure 4.1, available in the advanced manufacturing technology laboratory at Trinity College Dublin.

Hurvo VM2 specifications	
Spindle speed range	400 - 8000 rpm
AC voltage supply	400 V (3 phase)
Machinable area	1168 mm X 457 mm
Tool changer capacity	16
Table load capacity	550 kg
Machine weight	4080 kg

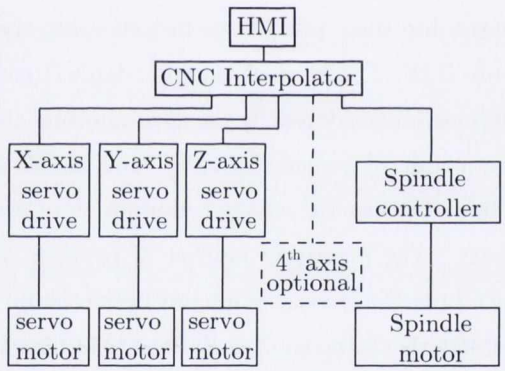

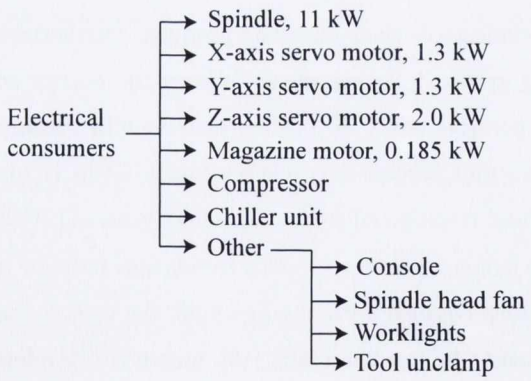

Figure 4.1 – Hurco VM2 CNC Machine Tool

The Hurco VM2 is a 3-axis CNC machine with a table size of 1,168 mm x 457 mm [187]. The machine has a Fanuc 6M model B controller. The spindle of the Hurco VM2 is powered by an 11 kW motor allowing spindle speeds of up to 8,000 rpm. The machine requires a three phase

power supply and can operate in either a delta or wye configuration. Specific information related to travel limits, automatic tool changing, and load capacities have been extracted from the relevant machine tool documentation and included in Figure 4.1.

4.2.2 Data acquisition of electrical energy

Accurately measuring the electrical energy consumption of the test machine described in Section 4.2.1 is a critical aspect of this chapter of the research work. A typical power meter is equipped with an on board processor that will calculate RMS current and voltage values from the raw data waveforms. It is therefore not possible to access the raw waveforms using commercially available power monitoring equipment. In order to obtain the valuable current and voltage waveforms required in this research a custom measurement system was designed and developed, Figure 4.2. This measurement system combines National Instruments data acquisition hardware and software in order to record and display energy consumption information. Voltage was recorded with a NI 9225 DAQ and current was recorded with a NI 9239 DAQ. Data was sampled and analysed using a custom built dedicated software tool.

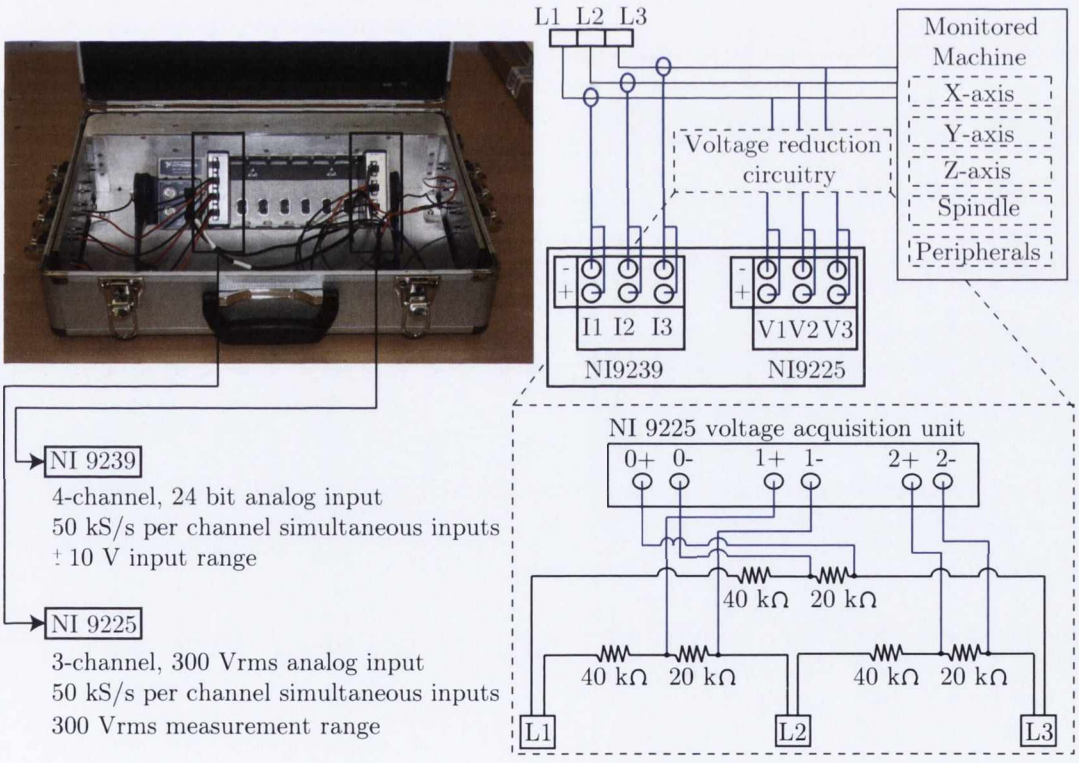

Figure 4.2 – Custom power monitoring device

The measurement of current required a voltage output current transformer; the EL Components 50A/0.33V CT was selected as it was the most suitable product available in terms of the primary

current input range and also the corresponding voltage output. The measurement of voltage required the design and installation of voltage reduction circuitry due to the limitations of the NI 9225 data acquisition module. The NI 9225 is primarily designed to monitor single phase or three phase wye configured voltages, to a maximum of 300 V_{rms}. The voltage reduction circuity illustrated in Figure 4.2 enabled the measurement of the 400 V_{rms} line to line voltages resulting from the Hurco VM2 machine tool's delta configured power supply.

4.3 Measurement system calibration and verification

4.3.1 Current measurement calibration

Attaching a 2.5 kW resistive load to the test circuit, and using a variable autotransformer to modify the circuit voltage allowed known currents to be drawn. The autotransformer used in this study has an analogue dial that is used to vary the voltage. In order to ensure the calibration was accurate a Tenma 72-7725 multimeter and a Metrix MX-22 multimeter were used to monitor the voltage and current respectively, see Figure 4.3.

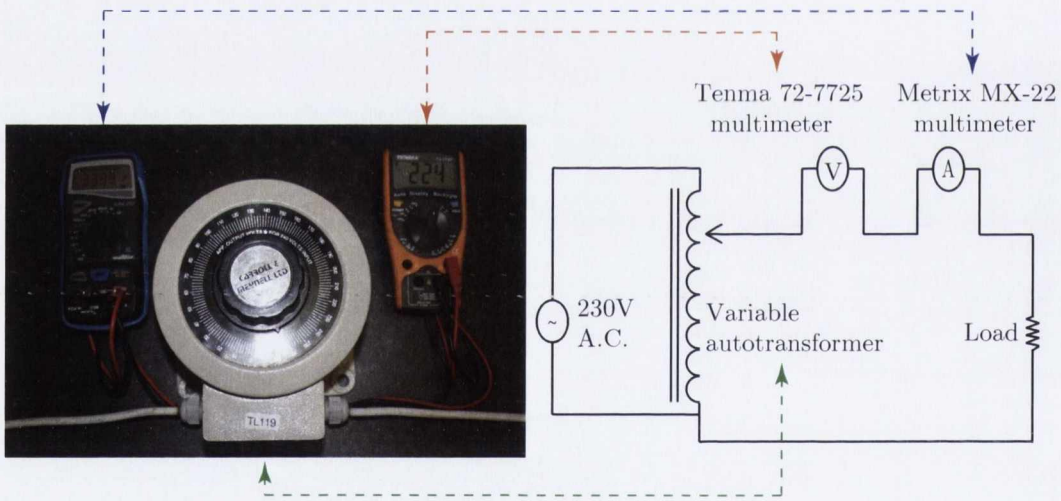

Figure 4.3 – Current Measurement calibration set up

The standardised calibration method has been developed in order to robustly characterise each individual current measurement device. The test operates between 0-9 Amps incrementing in 0.5 Amp steps. During each step of the calibration procedure 49 consecutive data points are recorded alongside the amplutide of current displayed on the Metrix multimeter. This data is then post processed in Matlab where the CT response characteristics are extracted. Loading and unloading each measurement device in a symmetrical manner facilitates the evaluation of sensor linearity, hysterisis, and sensitivity. A typical sensor response from a single calibration cycle for each of the three CT's is shown in figures 4.4, 4.5, and 4.6.

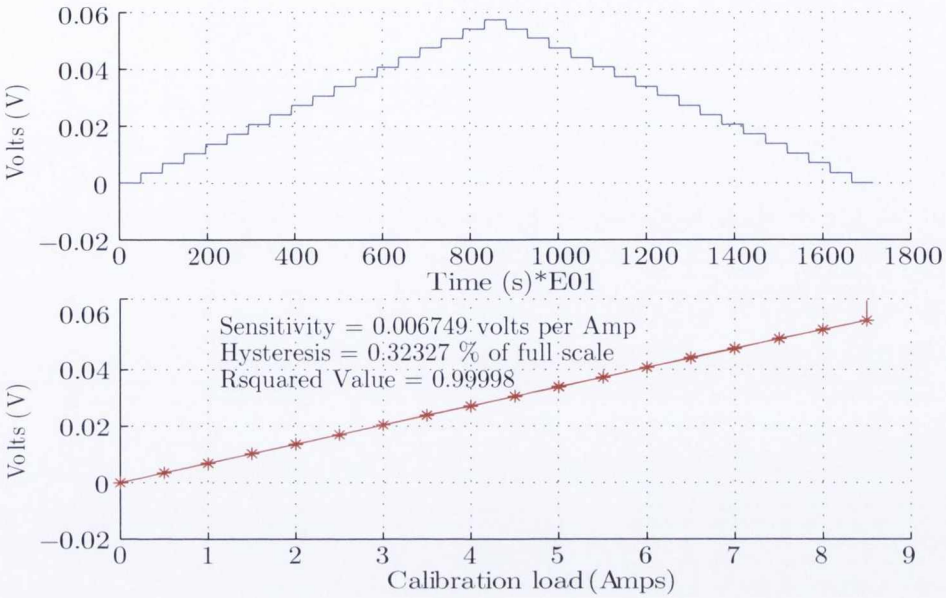

Figure 4.4 – Current transformer no.1 calibration results

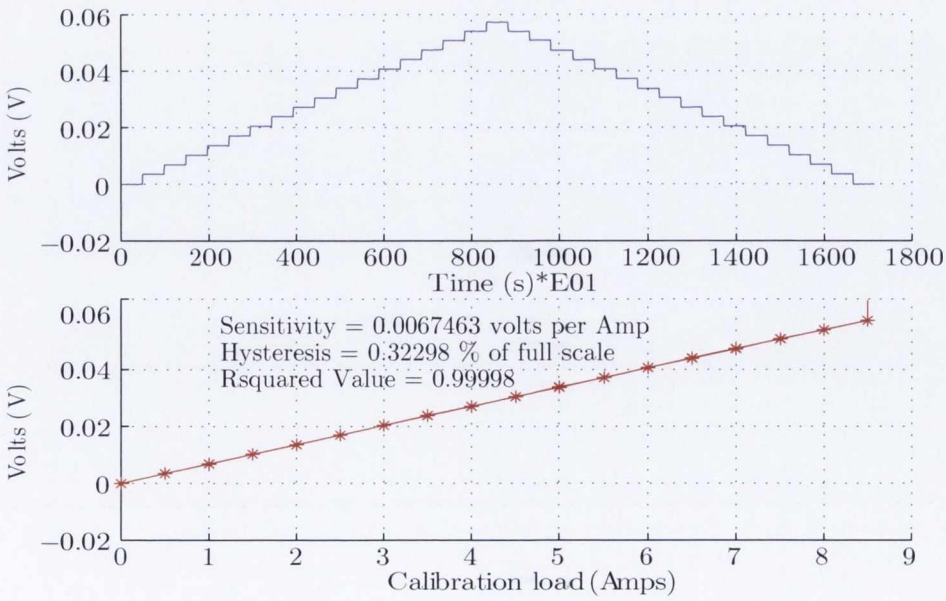

Figure 4.5 – Current transformer no.2 calibration results

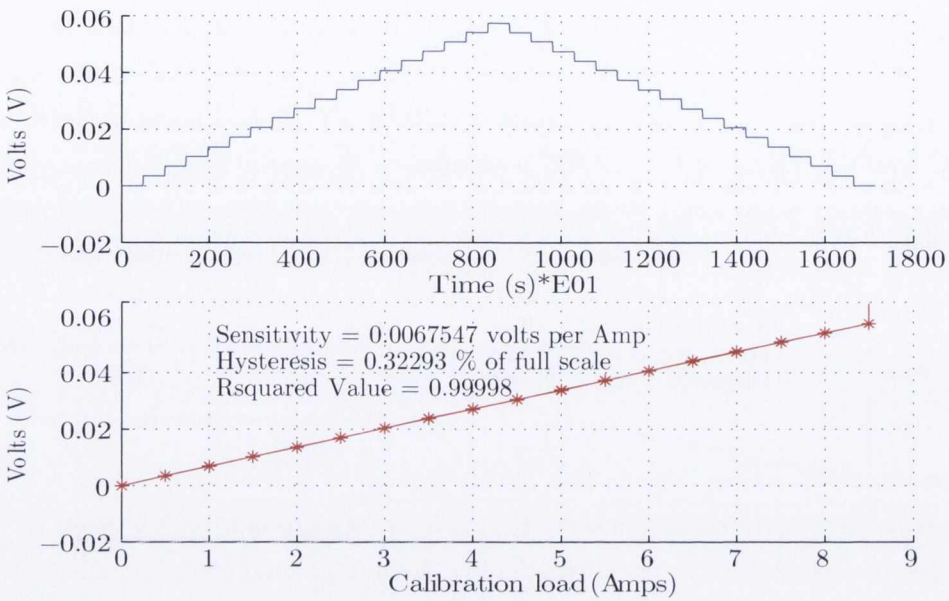

Figure 4.6 – Current transformer no.3 calibration results

4.3.2 Current measurement verification

In order to verify the accuracy of the entire measurement chain a study was conducted that compared the recorded values from the custom power monitoring device with a state of the art meter during a machining process. The machining verification test allowed the custom measurement devices accuracy at higher loads, up to 20 Amps to be assessed. Both measurement devices were installed at the main incomer of the Hurco VM2 machine tool described in Section 4.2.1 and a series of milling operations were performed. The HT Italia power quality analyser, Figure 4.7, is a high end commercially available power monitor allowing the accurate measurement of true RMS current and voltage. The meter can also measure active, reactive, and apparent power consumption in addition to a wide variety of other power related variables including voltage sags, surges, and spikes.

HT Italia PQA 824 specification	
Measurement range	1-300 Amps*
Crest factor	≤ 3
Resolution	0.1 Amp
Accuracy	0.5% reading + 0.6% full scale
*Values under 1 amp are zeroed	

Figure 4.7 – HT Italia PQA 824 power quality analyser

The HT Italia's maximum reporting rate is 1 Hz for RMS voltage and RMS current. In contrast to this, the TCD power meter measures, records, and exports the current and voltage waveforms at a sampling rate of 2 kHz. This sampling rate can be increased up to 25 kHz. In order to allow an accurate comparison between the two power measurement devices, the TCD power metering data was normalised in order to achieve the same resolution as the HT Italia meter. A CAD/CAM drawing illustrating two of the Hurco VM2's test operations is included in Figure 4.8.

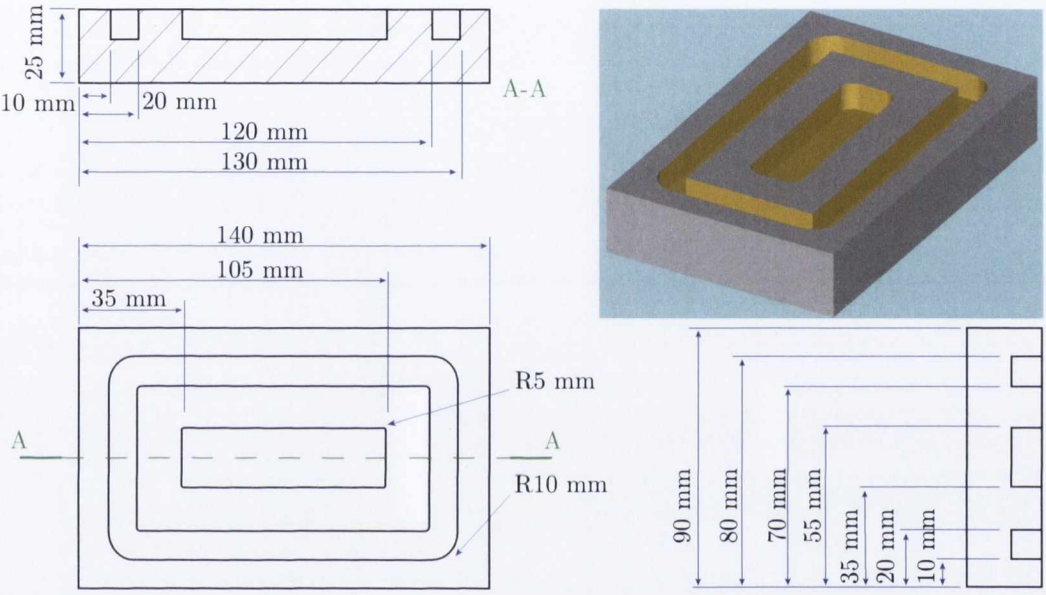

Figure 4.8 – Measurement verification workpiece

The first verification operation used a 10 mm HSS milling tool to machine the inner pocket illustrated in Figure 4.8; the second verification operation machined the rectangular slot. The workpiece material was aluminium (6060). The measured currents from each of the three power supply lines from both the TCD meter and the HT Italia power meter for test one are included in Figure 4.9, the measurements for test two are included in Figure 4.10. The machining parameters are also included in each figure. In both of the test cases there is a strong correlation between the measured values from each metering device. The R-squared values are 95.3%, 97.1%, and 96.2% for operation one and 97.3%, 96.4%, and 96.9% for operation two. The largest source of error within the correlations is intrinsically linked to the limitations of the HT Italia power meter which zeroes all current readings with a magnitude of less than 1 Amp. The current transformers supplied with the HT Italia have an operating range of 1-300 Amps, and therefore 1 Amp represents just 0.33% of the full measurement range. The TCD current transformers have a narrower operating range of 0-50 Amps and do not encounter the same problems when monitoring low amplitude currents.

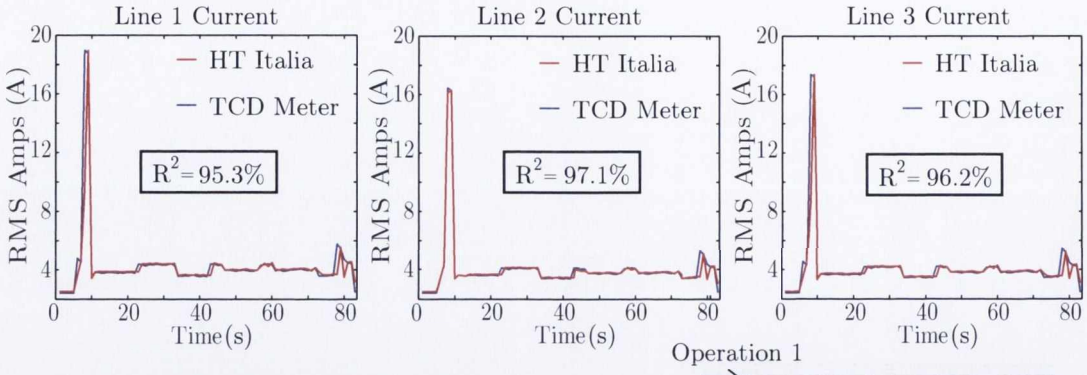

Verification test parameters	
Workpiece material	Aluminium (6060)
Depth of cut	5 mm
Cutting tool	10 mm 2 flute HSS
Spindle speed	4,000 rpm
X,Y axis feed rate	500 mm/min

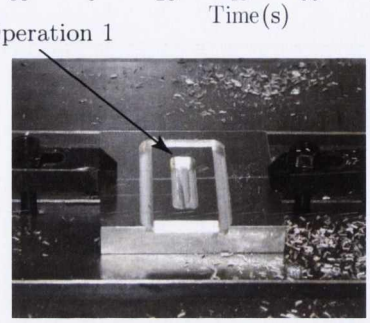

Figure 4.9 – Current verification machining operation no.1

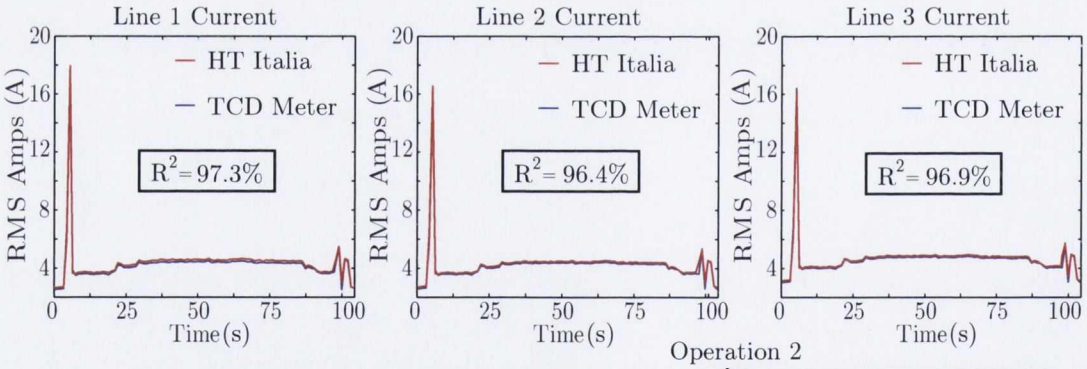

Verification test parameters	
Workpiece material	Aluminium (6060)
Depth of cut	5 mm
Cutting tool	10 mm 2 flute HSS
Spindle speed	4,000 rpm
X,Y axis feed rate	500 mm/min

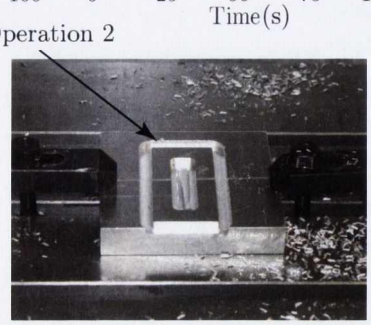

Figure 4.10 – Current verification machining operation no.2

4.4 Machine component analysis

The Hurco VM2 characterisation was completed by conducting a component level energy consumption study. A machine tool energy map was developed after the relevant electrical wiring diagrams were analysed, see Figure 4.11. The analysis of each machine tool component required each component to be activated independently three times under every loading condition investigated. This type of power assessment aligns with recent state of the art research studies published within the CIRP community by Behrendt et al. [188]. Each individual component was characterised in terms of both current and power consumption in the time and frequency domains.

Although the main consumers within the Hurco VM2 machine tool, for example the spindle motor, are balanced loads the machine tool itself is electrically unbalanced. The primary source of this imbalance emanates from the point on the electrical diagram in Figure 4.11 where the single phase supply is created. Phase 1 and phase 3 are used to create the single phase supply that is used to power a number of fans and lights, and as a result of this they carry significantly more current than phase 2 during normal operation. To illustrate this point, Table 4.1 shows the RMS current of each phase during a number of different operating conditions.

Machine state	I1(Amps)	I2(Amps)	I3(Amps)
Idle	2.4051	0.9282	1.7253
Spindle accelerating	19.0652	16.4361	16.6794
Spindle at 8,000 rpm	4.0842	2.2474	2.6764

Table 4.1 – Current load during various operating states

Due to the fact that the Hurco VM2 system is electrically unbalanced, this research uses the two wattmeter method to calculate the total power consumed by the machine tool. The two wattmeter method is based on Blondel's theorem [189], which states that the power in any system containing n wires, can be calculated using n - 1 wattmeters, see Figure 4.12. Blondel's theorem holds true for any system, balanced or unbalanced, given a voltage source and a load of any complexity [190]. Connecting both wattmeters as described in Figure 4.12 will result in the two wattmeters, W1 and W2 reading the following;

$$W_1 = \frac{1}{T}\int_0^T v_{AC}(t) i_{aA}(t) dt \tag{4.1}$$

$$W_2 = \frac{1}{T}\int_0^T v_{BC}(t) i_{bB}(t) dt \tag{4.2}$$

Independently neither reading has any meaningful value but the combined value represents the

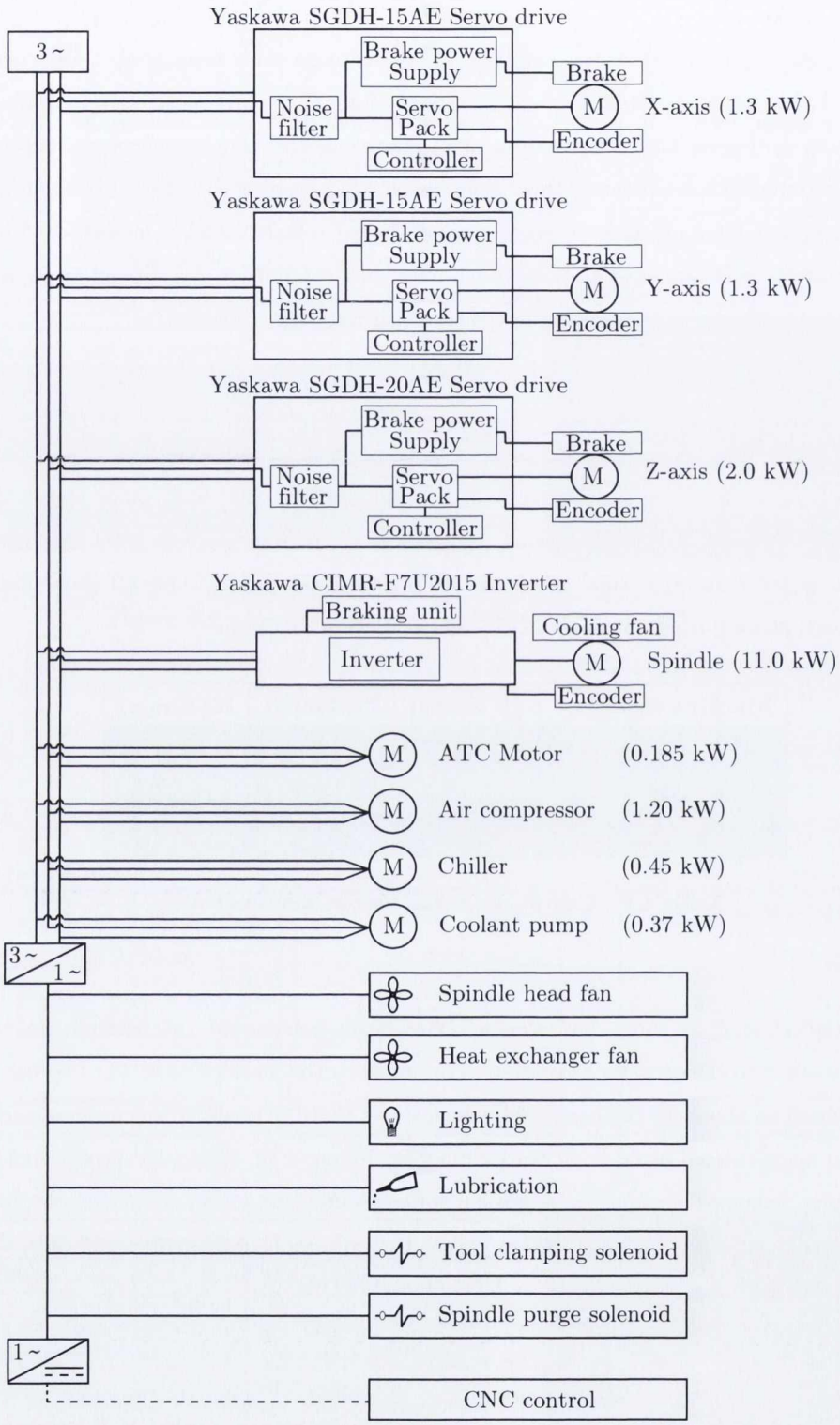

Figure 4.11 – Hurco VM2 Electrical distribution

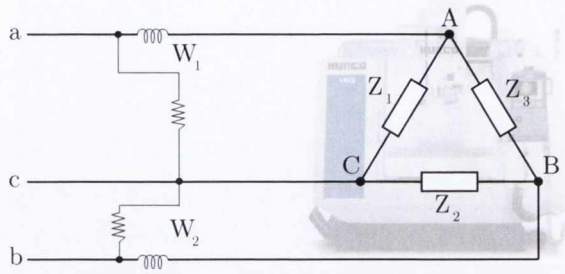

Figure 4.12 – Hurco VM2 two-wattmeter power measurement

total power in the circuit;

$$\begin{aligned} W_1 + W_2 &= \frac{1}{T}\int_0^T v_{AC}i_{aA} + v_{BC}i_{bB}dt \\ &= \frac{1}{T}\int_0^T v_{AC}(i_{AC} + i_{AB}) + v_{BC}(i_{BC} + i_{BA})dt \\ &= \frac{1}{T}\int_0^T v_{AC}i_{AC}dt + \frac{1}{T}\int_0^T v_{BC}i_{BC}dt + \frac{1}{T}\int_0^T (v_{AC}i_{AB} + v_{BC}i_{BA})dt \end{aligned} \tag{4.3}$$

Using the convention of double subscript notation, the integrand of the last integral can also be expressed as follows;

$$\begin{aligned} v_{AC}i_{AB} + v_{BC}i_{BA} &= v_{AC}i_{AB} - v_{BC}i_{AB} \\ &= (v_{AC} - v_{BC})i_{AB} = (v_{AC} + v_{CB})i_{AB} = v_{AB}i_{AB} \end{aligned} \tag{4.4}$$

$$\begin{aligned} \therefore W_1 + W_2 &= \frac{1}{T}\int_0^T v_{AC}i_{AC}dt + \frac{1}{T}\int_0^T v_{BC}i_{BC}dt + \frac{1}{T}\int_0^T v_{AB}i_{AB}dt \\ &= P_{Z_1} + P_{Z_2} + P_{Z_3} \end{aligned} \tag{4.5}$$

4.4.1 Spindle

The Hurco VM2 machining centre uses a precision balanced cartridge spindle that is made of high grade alloy steel [187]. The spindle shaft, located inside the cartridge, is supported by steel bearings. The spindle drive unit contains a closed-loop system that controls and monitors the spindle motor [187]. A microprocessor-based encoder governs the closed-loop control system. Although the majority of modern machine tools are equipped with motorised spindles the Hurco VM2 uses a no slippage gear belt with a 1:1 pulley ratio to couple the spindle motor to the spindle [100, 187].

The Yaskawa F7 drive unit that controls the spindle is pulse width modulated (PWM) and is designed specifically for use with three phase induction motors. The motor is fully enclosed and uses forced-air cooling [187]. According to Avram and Xirouchakis [17] the key factors governing the spindles energy consumption are its inertia, the type and size of bearings, lubrication technique, and also its electrical drive and control. Figure 4.13 illustrates the key components of the Hurco VM2 spindle system; Table 4.2 includes selected spindle specifications.

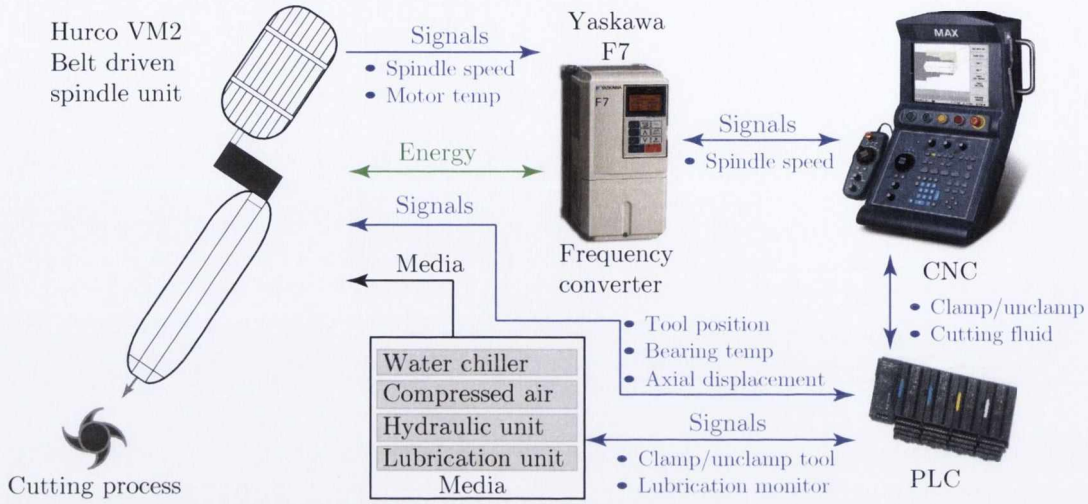

Figure 4.13 – Hurco VM2 spindle components, adapted from [100, 187]

Spindle motor power	
	Hurco VM2
Rpm range	0 - 8000 rpm
Continuous (kW)	11.0
Peak 1 min. rating (kW)	15.0
Spindle torque	
	Hurco VM2
Continuous (Nm)	74.0
Peak 1 min. rating (Nm)	102.0

Table 4.2 – Hurco VM2 spindle specifications [187]

The power consumption of the spindle was investigated from two perspectives; dynamic and steady state. The dynamic component of the spindle consumption is the result of the starting transient that occurs when the spindle is initially energised. The starting transient is composed of two discrete components that are commonly referred to as the inrush current and the locked rotor current. The inrush current is required to establish a magnetic field in the core of the motor each time a voltage is applied. Abele et al. [100] observed that the peak value of inrush current will vary slightly each time the spindle is energised due to the residual magnetism in the core. In certain cases the peak value can be as high as twenty times the rated motor value. This component of the starting transient typically decays within the first few cycles of the line voltage. It is important

to consider inrush current when sizing circuit breakers for motor circuits but it only represents a small part of the starting transient.

The locked rotor current is the larger of the two components of the initial starting transient. When power is first applied to the motor, the stator field will draw very high current since the rotor is not turning. As the rotor begins to turn, it will induce current into its laminated coils and build up torque. This causes the rotor to spin faster, until it approaches the speed of the rotating magnetic field. At the rated load of the motor, the rotor will spin at slightly less than the synchronous speed, this difference is referred to as slip. It is this rotor slip that allows the motor to increase rotor torque and current to match the load requirement [100]. Acceleration time must also be considered when analysing the start up sequence of the Hurco VM2 spindle system.

The acceleration time is the time the motor takes to reach the user defined spindle speed. Faster acceleration time is desirable, but this often results in excessive current peaks and other undesirable effects [100]. In order to combat the undesirable effects of the fastest possible acceleration time, at higher spindle speeds the Hurco's controller limits the amount of current that the motor can draw, Figure 4.14. As a result of this current limiting control, the spindle consumes a fixed level of power during acceleration. Depending on the required spindle speed this max spindle power will be required for a varying time period, see Figure 4.15. When the spindle reaches the required speed, the motor only requires the minimum power necessary to maintain the required rotational speed.

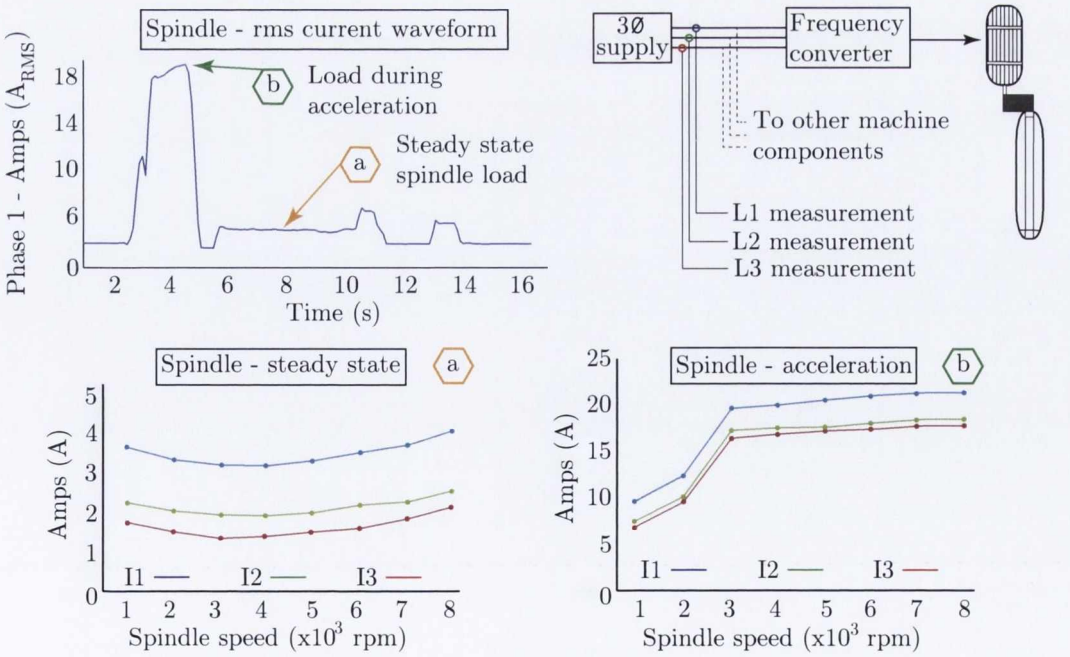

Figure 4.14 – (a)Spindle acceleration power (b)Spindle static load power

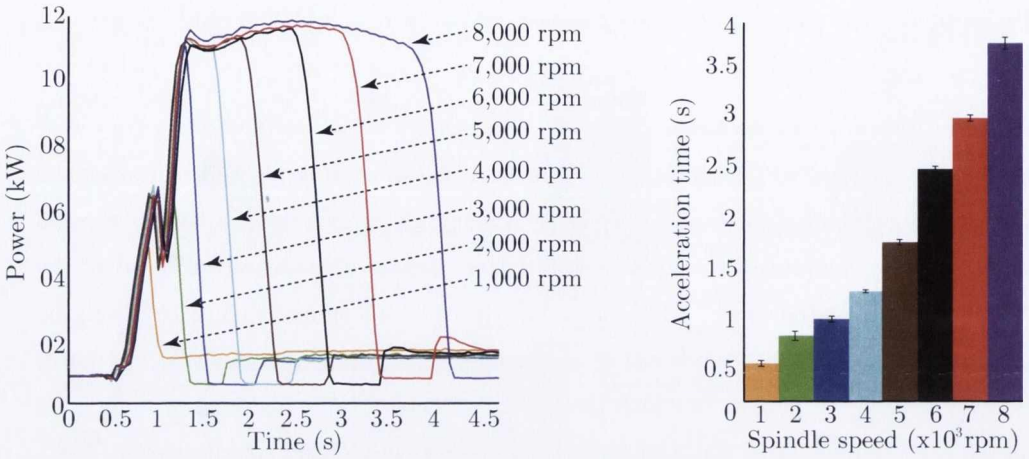

Figure 4.15 – Spindle start statistics - power

There is a dynamic relationship between spindle speed and power consumption which depends on the operating range of the spindle. An analysis of the spindles power-speed characteristics was performed and two independent relationships were observed, Figure 4.16. In zone A there is an inverse relationship between spindle speed and power consumption. The power required to rotate the spindle at 1,000 rpm, 1.798 kW, is significantly more than than the power required at 3,000 rpm, 1.571 kW. In zone B there is a direct relationship between spindle speed and power. At 4,000 rpm the required power is 1.584 kW and at 8,000 rpm the power requirement is 2.021 kW.

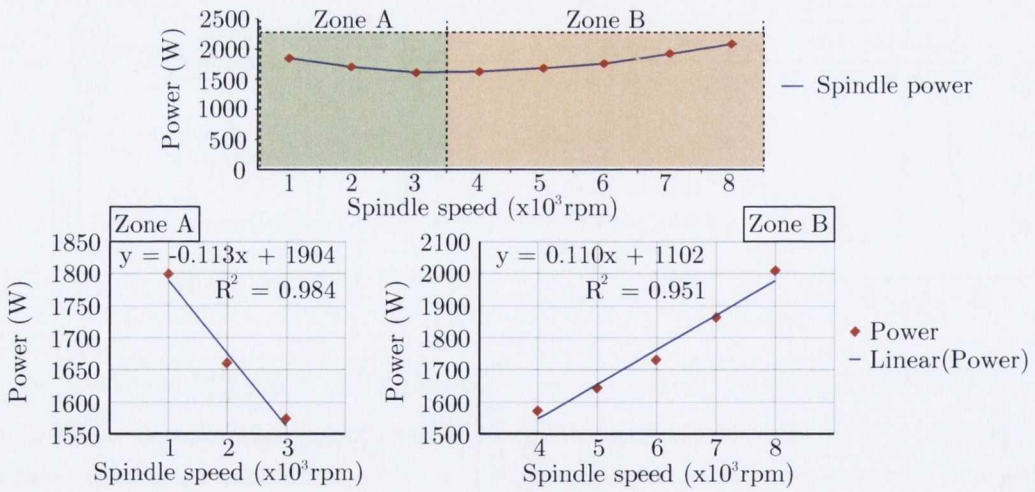

Figure 4.16 – Hurco VM2 power-speed analysis

The varying spindle speed-power relationship observed here is the result of the dynamic interactions between the mechanical and electrical components that form the spindle system. At low speeds the spindle system is less effective at transforming electrical power to mechanical rotation,

whereas above the spindles base speed the system is able to more effectively transform the input electrical energy to mechanical rotation. Equations 4.6 and 4.7 describe the relationships that exist between spindle speed, N, and machine tool power in each zone.

$$Power(W) = -0.113(N) + 1904, \tag{4.6}$$

$$Power(W) = 0.110(N) + 1102, \tag{4.7}$$

The findings observed during the power-speed characterisation described here expand on a portion of the research work presented by Vijayaraghavan and Dornfeld [19]. Vijayaraghavan and Dornfeld [19] suggest that there is a direct relationship between machine tool power consumption and spindle speed. The Hurco VM2 machine tool analysed in this study only exhibits a direct relationship between power consumption and spindle speed at the higher spindle rpm range, 4,000 - 8,000 rpm. In the lower spindle rpm range, 1,000 - 3,000 rpm, the Hurco VM2 demonstrates an inverse relationship between power consumption and spindle speed. These findings align with a recent research study presented by Balogun and Mativenga [183] which found a dynamic relationship between spindle speed and power depending on the operating range.

In addition to the current and power characterisations presented above, a harmonic analysis was performed in order to develop an understanding of the frequency characteristics of the spindle motor system. The Yaskawa F7 inverter, which controls spindle speed, has two power sections; a rectifier section and an inverter section. The AC source voltage is converted into DC voltage by the rectifier circuit; the F7 inverter uses a standard six pulse rectifier. The inverter circuit then converts the DC voltage into a PWM controlled variable voltage AC output. The six pulse rectifier has a nonlinear load characteristic, i.e. it draws a distorted current waveform even though the supply voltage is sinusoidal, causing the generation of harmonic currents in accordance with Equation 4.8.

$$h \; = \; (n \; x \; p) \; \pm \; 1 \tag{4.8}$$

where;

n = an integer (1,2,3,4,..,n)

p = number of pulses or rectifiers

The harmonic analysis was performed by investigating the harmonic content of the current waveforms when the spindle was operating at full load during acceleration and at a reduced load rotating at 4,000 rpm. During this assessment current measurements were taken at the frequency inverters input terminals ensuring that all measured phenomena resulted from spindle system operation. Figure 4.17(a) illustrates the results of the full load harmonic analysis and Figure 4.17(b) illustrates the results of the reduced load test. The magnitudes of the characteristic harmonics, particularly the 5^{th}, 7^{th}, 9^{th}, and 11^{th} are significantly greater than the non-characteristic harmonics at full load.

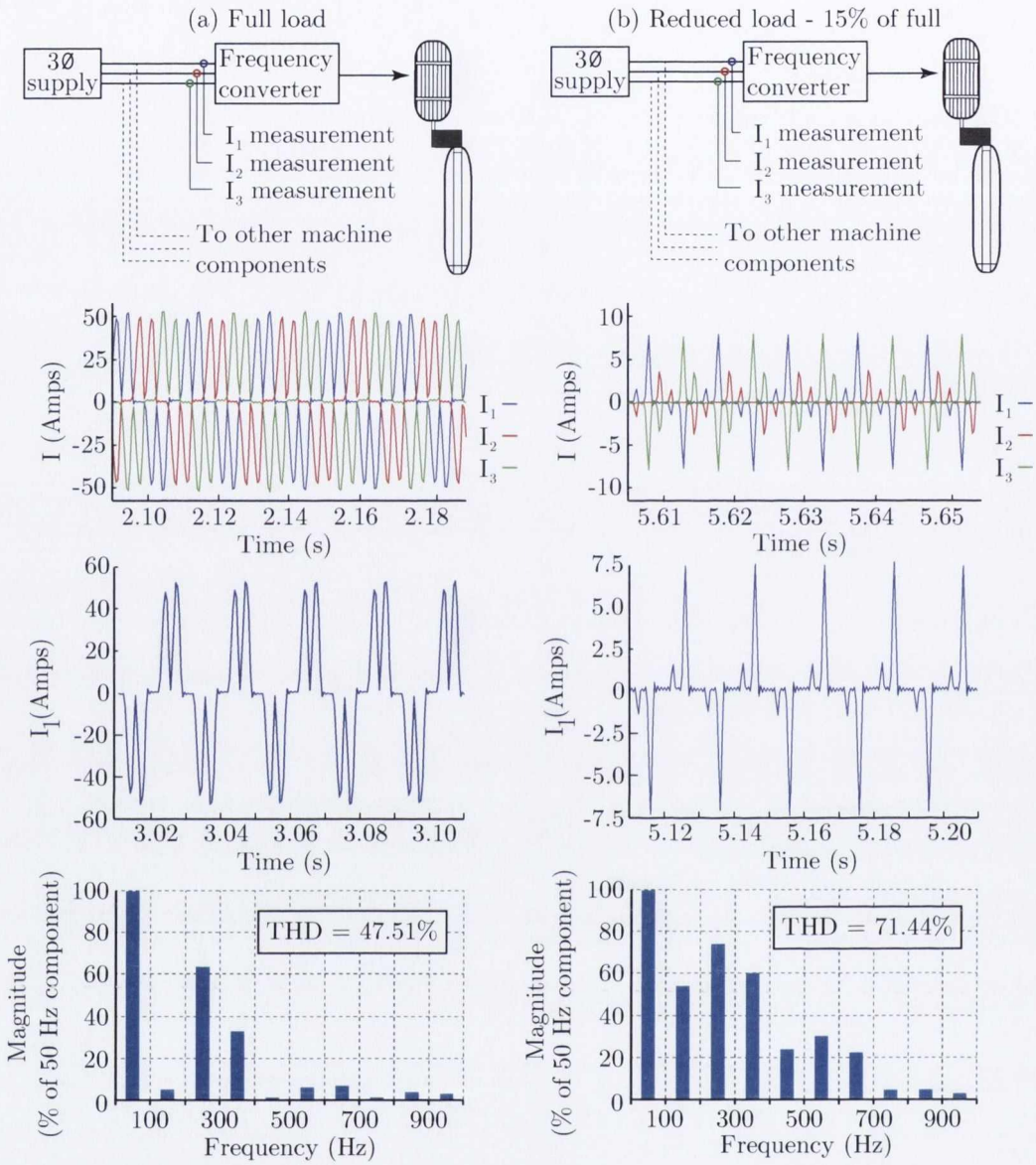

Figure 4.17 – AC current waveform at frequency inverter under different loading conditions

Although the THD is higher in the reduced load scenario the absolute magnitude of the harmonics is dramatically reduced, negating the majority of the adverse impacts on the system. The observed results align with published documentation from Yaskawa [191] and also research studies investigating the generation of harmonics resulting from the use of six diode rectifiers [192]. In order to improve the performance of frequency inverters from the perspective of harmonic mitigation, researchers have proposed numerous different rectifier topologies that significantly reduce the characteristic harmonic magnitudes [192].

4.4.2 Axis motion

The Hurco VM2 uses AC servo drive systems to position the machine tool components and workpiece in the required position. The positional accuracy of each feed drive is a function of the trajectory generation and control algorithms, mechanical drives and guides, amplifiers, motors, and sensors [193]. Abele et al. [100] noted that the positional accuracy and speed of the feed drives are key determinants of machine tool quality and productivity. The trajectory generation algorithm considers the machine tool kinematics in decoupling the spatial tool motion into each feed drive [193]. Each axis motor is equipped with a rotary encoder that provides velocity and position feedback signals for each closed-loop system, see Figure 4.18.

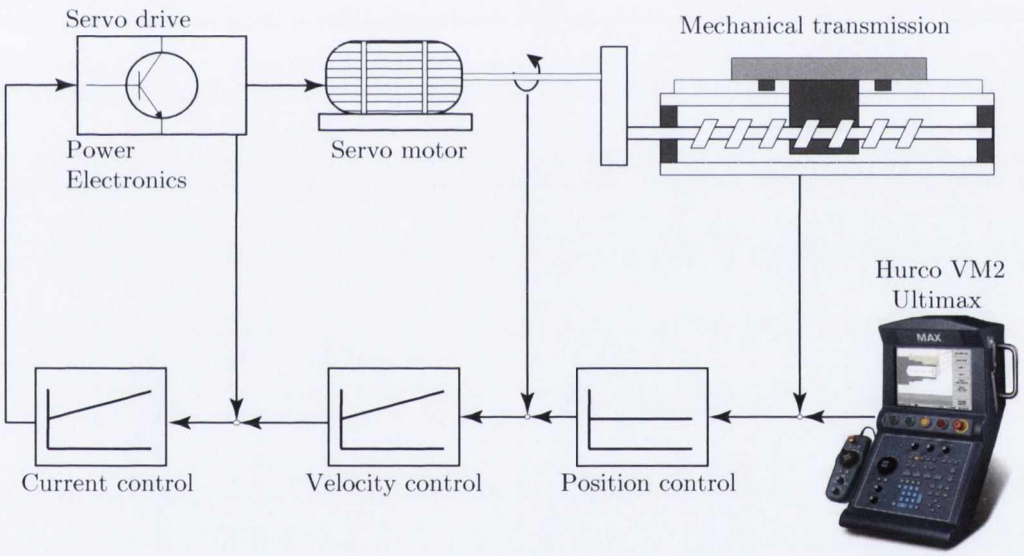

Figure 4.18 – Hurco VM2 feed drive components, adapted from [193]

The Hurco VM2 uses the Ultimax system to control axes velocity and travel direction [187]. The servomotors are enclosed, transistor-driven, and self-cooled; as a result of the motors brushless design they are free from flashover and commutation losses [187]. The servomotors power the x, y, and z axis ballscrews by belt drive. The x and y axes are both driven by 1.5 kW Yasakawa servo motors. According to Altintas et al. [193], ballscrew drives are currently the most commonly used in machine tools; they are characterised by high efficiency (η = 95-98%), low heating, minimal wear, and a long service life. Approximate positioning and travel specifications appear in Table 4.3.

Axis feed rate		
Axis	**X, Y**	**Z**
Cutting (m/min)	7.6	7.6
Rapid traverse (m/min)	24.0	19.0
Maximum travel		
Axis	**X**	**Y, Z**
Distance (mm)	1016	457

Table 4.3 – Hurco VM2 axis specifications [187]

This section describes a power consumption characterisation conducted on the y-axis, and a current consumption characterisation conducted on the x-axis. Figure 4.19 illustrates the average power consumption of the y-axis drive system at a variety of different feed rates. Each test was performed three times in order to obtain statistically significant results. The measurement device was connected at the y-axis servo drive input terminals as shown in Figure 4.19. The power consumption was observed to increase linearly as the feed rate increased from 250 mm/min to 1000 mm/min.

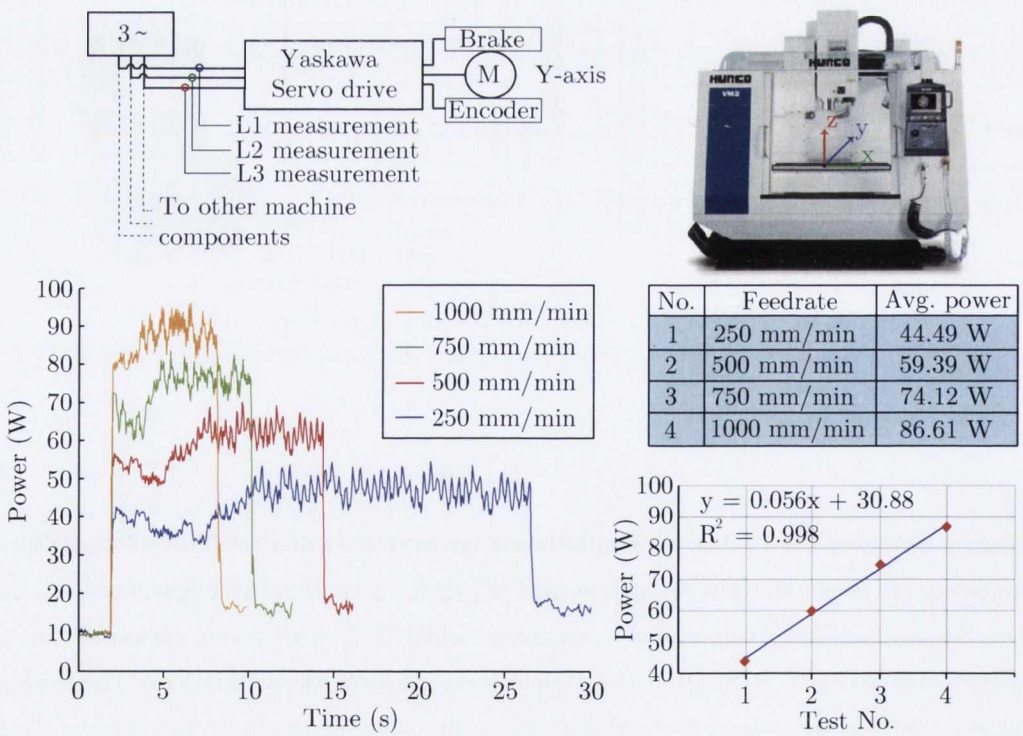

No.	Feedrate	Avg. power
1	250 mm/min	44.49 W
2	500 mm/min	59.39 W
3	750 mm/min	74.12 W
4	1000 mm/min	86.61 W

Figure 4.19 – Y-axis power consumption

An analysis of the current consumption characteristics of the x-axis during rapid and standard speed traversals was conducted. During this test the measurement device was installed at the x-axis servo drives input terminals and each test was repeated three times. Phase one and phase three were observed to supply power to the x-axis servo drive at all times but phase two only contributed to the system during rapid traversal. This phenomena is a characteristic of the Yaskawa x, y, and z axis servo drives which only load all three phases during high load conditions, as experienced during rapid axis accelerations. Figure 4.20 illustrates a sample of the findings from the x-axis current consumption characterisation.

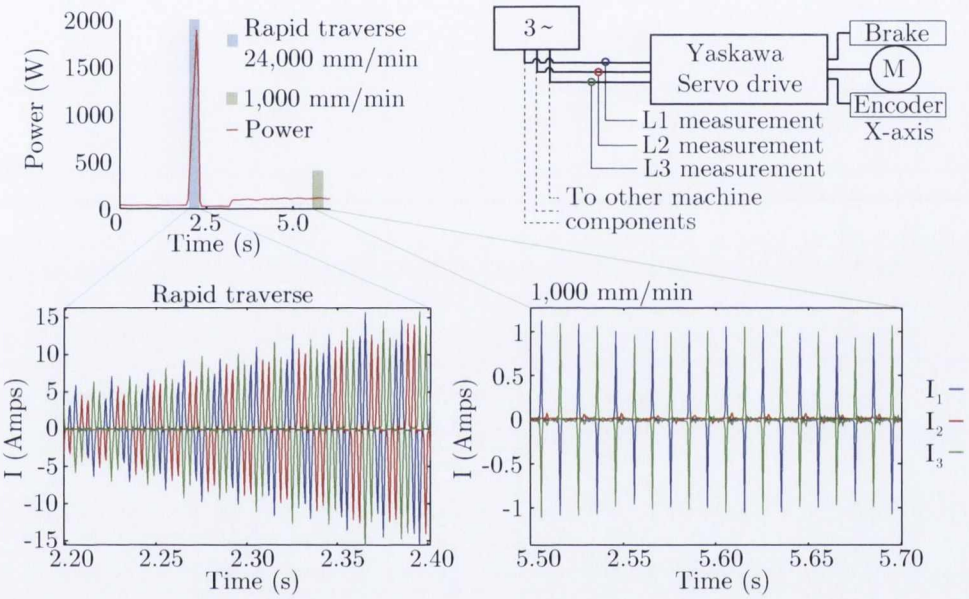

Figure 4.20 – X-axis power consumption

The z-axis carries the machine tool spindle and its positional accuracy ensures accurate depths of cut at the workpiece. The z-axis is driven by a 2.0 kW Yasakawa servo motor. The maximum feed rates for cutting and rapid motion are 7.6 m/min and 19 m/min respectively. During the assessment of z-axis power consumption the measurement device was installed at the input terminals of the axis servo drive, as illustrated in Figure 4.21, and therefore only measured the power consumed directly by the z-axis. The power consumption of horizontal axes is a function of a number of variables including friction losses in guideways, bearings, and cutting forces. Abele et al. [100] noted that vertical axes must also consider the influence of gravity which opposes upward motion and supports downward motion.

The z-axis system requires a baseline power consumption of 290 Watts in order to maintain the position of the spindle unit. The power consumption of the servo system decreases below the baseline as the spindle head is lowered towards the work table. In order to lower the z-axis

downwards at 100 mm/min the average power consumption is 260 Watts. Raising the z-axis at a rate of 100 mm/min requires an average of 360 Watts. The most energy intensive movement of the z-axis is the rapid traversal of the spindle head from the work table towards its home position. The average power required to rapidly raise and lower the spindle head at its maximum feed rate, 19,000 mm/min, is 2.68 kW and 18 W respectively. Figure 4.21 illustrates the power consumption of the z-axis servo drive under a variety of different loading conditions.

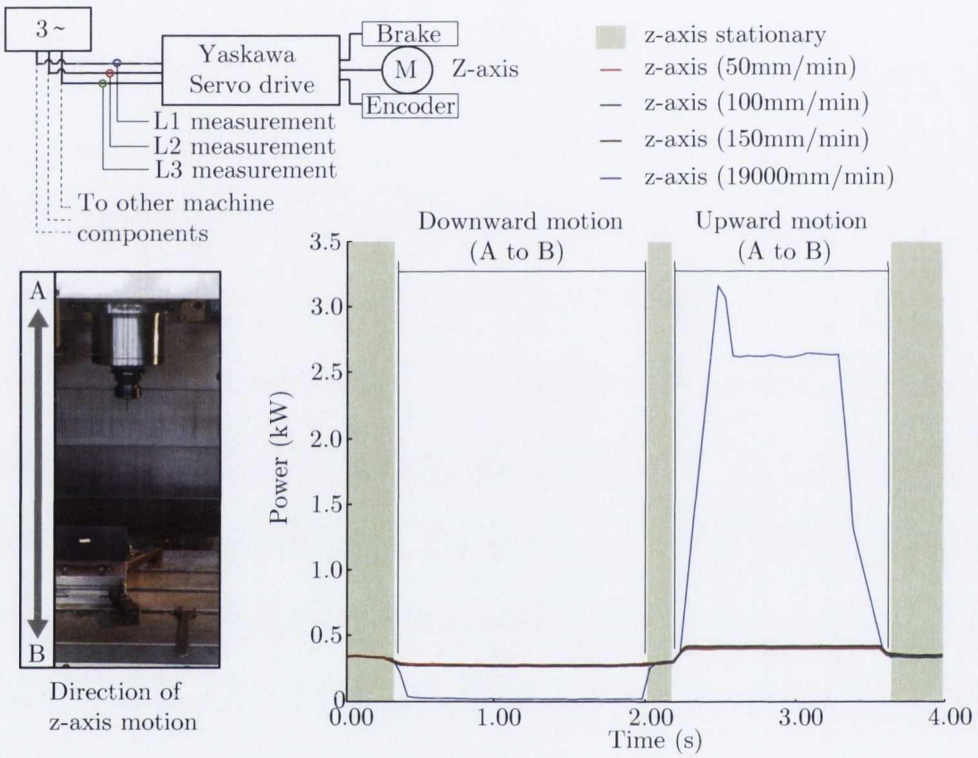

Figure 4.21 – Z-axis power consumption

4.4.3 Auxiliary components

Coolant system

Although current research studies are focused on minimising the use of coolant, wet cutting is still widely used in industry [118]. The VM2 machine tool coolant system is self contained and consists of a flood coolant nozzle, washdown hose, and an externally mounted spray gun to clean chips from the inside of the enclosure. Used coolant is filtered free of chips, oil, and other contaminants before being recirculated into the coolant tank. To assess the power consumed by the coolant system the measurement device was installed at the main incomer of the machine tool. Figure 4.22 illustrates the power profile associated with activating the coolant pump; the power profile shows the mean and standard deviations of 3 coolant pump activations. The power profile shows an initial turn

on transient which is then followed by a constant level power requirement while the coolant pump remains active.

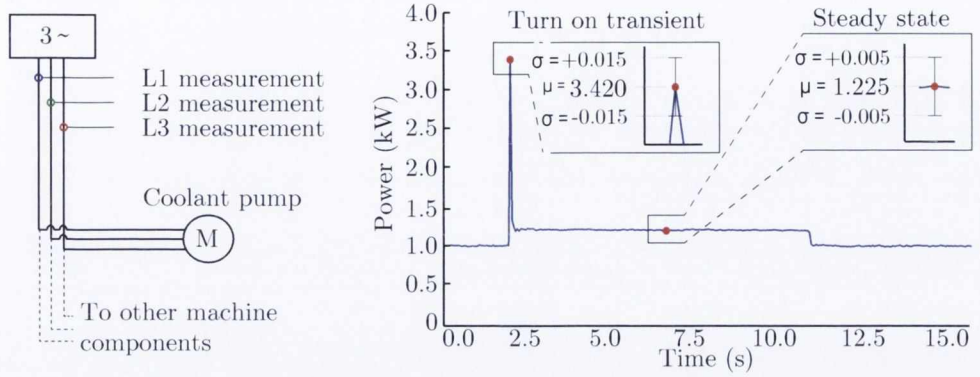

Figure 4.22 – Coolant pump analysis

Tool change

The VM2 automatic tool change (ATC) operation uses a swinging arm tool changing mechanism to load and unload tools from a vertically orientated tool change magazine. When a tool is requested the appropriate pocket rotates 90° making the tool available to the swing arm. The tool changing arm then rotates to simultaneously grab the tool in the magazine pocket and also the tool in the spindle. The spindle then unclamps the tool allowing the tool change arm to motion downwards and simultaneously pull the tools out of the spindle and the magazine pocket. The tool change arm then rotates through 180°, swapping the tools and allowing the spindle to clamp the new tool. Finally, the tool change arm and the magazine pocket return to their original position. To assess the power consumed during a tool change operation the measurement device was installed at the main incomer of the machine tool. Figure 4.23 illustrates the power requirements of a tool change; the power profile shows the mean and standard deviations of 3 tool change operations.

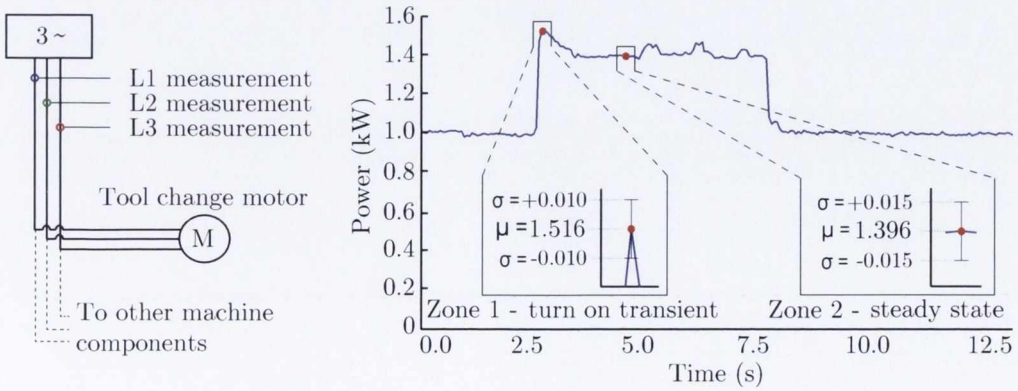

Figure 4.23 – Tool change analysis

4.4.4 Idle mode

In order to quantify the idle power consumption of the test machine the measurement device was initially installed at the machine tool isolator. Each component was then assessed individually to achieve an accurate breakdown. The measurement device recorded the power consumption of each component for a period of five minutes during idle mode. The study showed that the Hurco VM2 requires approximately 1.01 kW of power during idle periods; Figure 4.24 illustrates the component level idle power breakdown.

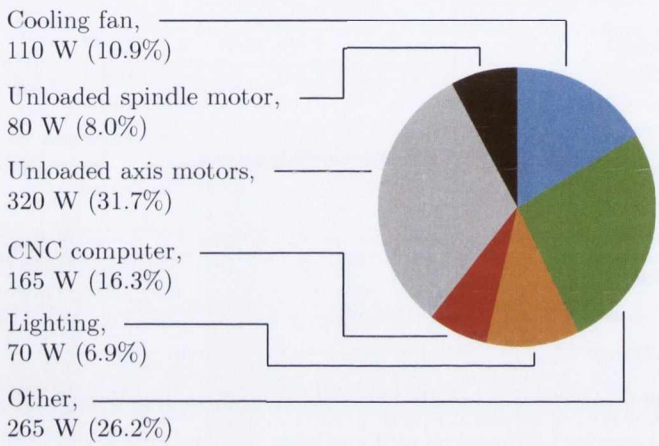

Figure 4.24 – Hurco VM2 idle power consumption

The idle power consumption of the Hurco VM2 is comprised of a number of individual consumers including machine tool lighting, the CNC console, unloaded axis drives, a heat exchanging fan, and additional peripheral equipment. Recent research studies have shown that the idle power consumption of machine tools is highly variable and is not related to the size of the machine. A study presented by Behrendt et al. [188] suggested that there is no relationship between machine size and idle power consumption however, machine tool complexity was observed to exhibit a direct relationship with idle power consumption. Current state of the art research studies in the area of energy efficient machine tools are focusing on green mode machines that reduce standby power consumption. Already there are a large number of multinational machine developers releasing green machines into the marketplace. One example of this is Sinumerik Ctrl-Energy, a range of solutions developed by Siemens allowing machine tools to operate effectively while reducing energy consumption [93].

4.5 Material removal analysis

In an attempt to quantify the energy required to remove material a series of machining tests were performed. In the first machining test, all machining parameters remained constant as the depth of

cut was changed during the machining of an aluminium (6060) workpiece; each test was replicated three times. Figure 4.25 illustrates power increasing linearly as the depth of cut increases. This trend supports the findings of recent research studies from within the literature which suggest there is an almost linear relationship between power and depth of cut during milling processes [88].

Figure 4.25 also shows that the constant power required to keep the machine in a 'ready state' dominates the overall power requirement. This observation supports the results of a study conducted by Diaz et al. [88] that highlighted machining time as the dominant energy consumption parameter for high tare machine tools. The additional energy required to cut workpiece material represents only a small fraction of the total energy required. Again this finding aligns with work presented by Balogun and Mativenga [183], Gutowski et al. [79], and Dahmus and Gutowski [84] who found that the energy required to remove material was responsible for less 15% of the total energy in certain studies.

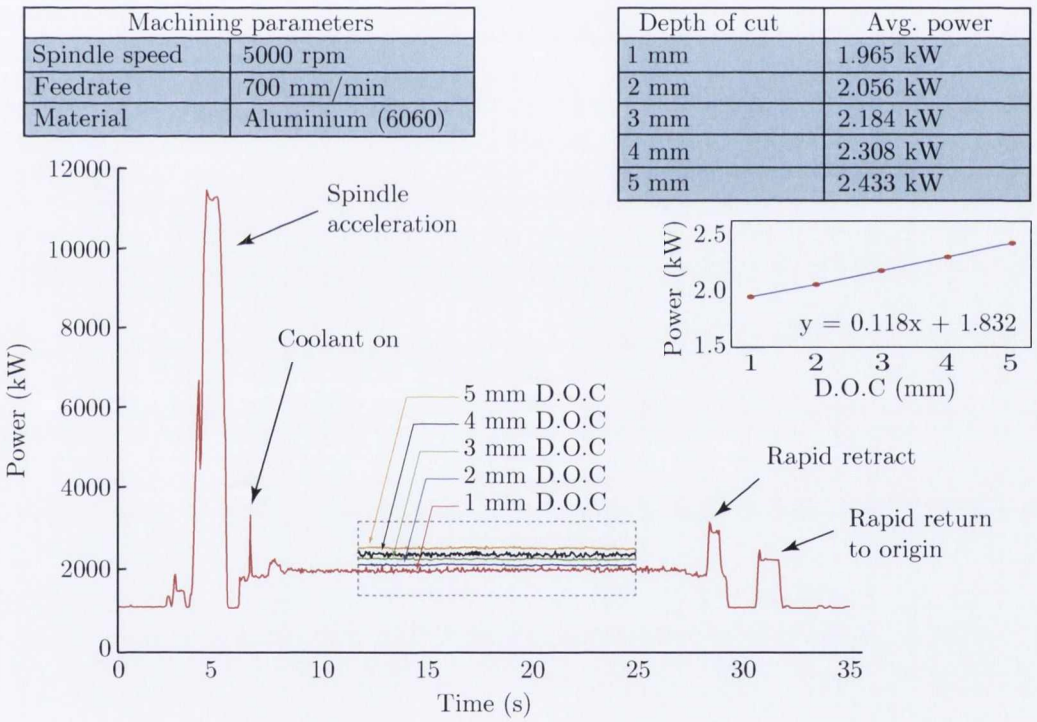

Figure 4.25 – Aluminium DOC analysis

Specific energy is a fundamental parameter derived from the power and machining conditions in machining processes. In this section specific energy consumption (SEC) is defined as the energy consumption of a machine tool to remove 1 cm^3 of material in accordance with the research work of Kara and Li [118]. The use of a standardised metric such as SEC allows different machine tools and different processing parameters to be accurately compared. Research studies suggest using SEC is a preferable method to assess the energy required to remove material because it is a simple

concept to apply and it takes account of both the static and dynamic components of machine tool power consumption [183]. Specific energy consumption can also be used to quantify the efficiency of a machine tool during processing; the SEC can then be used as an optimisation metric.

The power consumption values used in the SEC calculation described here only include the power consumed during processing. The energy required for machine start up, clamping, and workpiece positioning are not included. The tests performed here involved machining a slot into an aluminium (6060) workpiece and varying the depth of cut. The material removal rate was calculated by multiplying the width of cut, depth of cut, and feed rate. The SEC was then calculated by integrating the power consumed during the relevant machining test over the duration of time taken to remove 1 cm^3 of material. Figure 4.26 illustrates the findings of this test; there is an inverse relationship between material removal rate (MRR) and SEC. This finding aligns with the research work of Diaz et al. [88] who demonstrated an inverse relationship between specific energy and material removal rates during a milling process. Similarly, Kara and Li [118] observed an inverse relationship between specific energy and material removal rate for a variety of different machine tools with varying parameters.

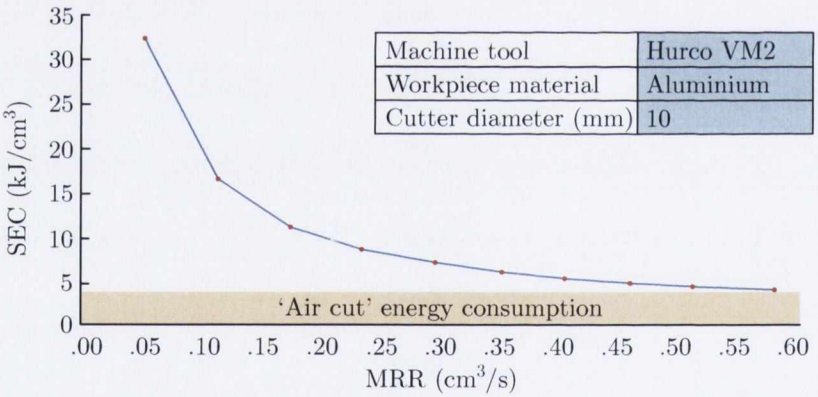

Figure 4.26 – SEC analysis

The findings observed here suggest that from the perspective of energy consumption the most efficient machining strategies are those which remove the maximum quantity of material in the minimum amount of time. Theoretically this is true, but in reality it is not an optimal solution as excessive feed rates and cutting speeds have been shown to cause rapid tool wear resulting in rough work finishes [95]. State-of-the-art machining strategies are being developed by machine tool builders who are actively seeking to reduce the power consumption of their products in a number of novel ways, for example; adjusting the acceleration profiles of spindle motors, developing adaptive pecking cycles, and selectively deactivating non-continuously required devices [9, 95].

4.6 Summary

A power measurement system was designed and developed to facilitate a machine tool electrical energy characterisation. The measurement system was calibrated against sate-of-the-art commercially available power monitoring devices. The R^2 values of $> 95\%$ obtained during machining tests verified that the system was accurate and reliable. The primary source of error which lead to discrepancies during the verification tests was intrinsically linked to the performance of the HT-Italia calibration device which zeroed all current readings with a magnitude of less than 1 Amp.

An energy consumption characterisation was performed on a Hurco VM2 3-axis CNC milling machine by applying the power measurement device to the main electrical incomer of the machine and mapping the machines internal electricity distribution system. Individual machine components were characterised by activating each component three times under various loading conditions in order to obtain statistically significant results. The most energy intensive machine tool component was observed to be the spindle motor, with an instantaneous power consumption of 11.89 kW observed during spindle acceleration when the motor must overcome forces resulting from inertia and frictional resistance.

Machining tests were performed to investigate two phenomena; the relationship between power consumption and depth of cut, and also the relationship between specific energy consumption and material removal rate. During the first set of machining tests, the parameters were held constant with a spindle speed of 5000 rpm and a feedrate of 700 mm/min; the depth of cut increased from 1 mm to 5 mm in steps of 1 mm. The material workpiece was aluminium (6060). Machine tool power consumption was observed to increase almost linearly with depth of cut with approximately 0.118 kW of additional power required for each 1 mm increase in depth of cut. These observed results align with recent research studies describing a linear relationship between power consumption and depth of cut [88].

The second set of machining tests also used an aluminium (6060) workpiece. The machining parameters were held constant with a spindle speed of 4000 rpm and a feedrate of 500 mm/min. The depth of cut increased from 0.5 mm to 5 mm in steps of 0.5 mm in order to vary the material removal rate. Each machining operation was performed three times. An inverse relationship was observed between specific energy consumption (kJ/cm^3) and material removal rate (cm^3/s). The results obtained in these tests match the findings of similar studies that have recently been published within the CIRP community and also within the broader research community [88, 183].

Chapter 5

Nonintrusive machine tool load monitoring

5.1 Motivation

One of the key motivations behind the development of a nonintrusive intelligent energy sensor is the development of unit process level energy consumption transparency; identified by the Knowledge, Awareness, and Prediction (KAP) EU-FP7 funded research project as a key enabler of energy efficiency optimisations [194]. Within the KAP research framework, techniques including complex event processing and data stream analysis are proposed as methods capable of achieving the important levels of innovation that are required to optimise energy consumption in manufacturing facilities [194].

Traditionally an intrusive approach to load monitoring has been employed to assess the energy consumption of manufacturing equipment [142]. The intrusive monitoring approach requires a large number of sensors to be deployed on each component in order to monitor and control the energy usage. The context-aware approach to industrial energy metering proposed by Herrmann et al. [15] is an example of an approach that relies on information emanating from energy measurement devices and additional sources - including manual inputs from operators - in order to derive higher quality information from the available metering data. The potential of reduced-cost data acquisition has motivated the development of nonintrusive load monitoring (NILM) systems. The ability of NILM systems to associate observed electrical waveforms with the operation of particular devices makes it an attractive alternative to complex arrays of intrusive monitoring sensors [195]. Reducing the scope of sensor deployment overcomes many of the drawbacks associated with multi-sensor arrays. Traditional multi-sensor arrays increase the difficulty and the cost of installation, particularly for short term or temporary monitoring [135].

Within the literature researchers have proposed a variety of NILM systems based on the steady state and/or transient load characteristics of individual components. Both transient and steady state based NILM systems have associated benefits and drawbacks. The development of a NILM system based solely on steady state detection is much less demanding than a system requiring the capture and analysis of transient phenomena. A limitation of steady state systems is the impossibility of distinguishing between two different appliances with identical steady state signatures. A

typical drawback associated with the deployment of a transient based NILM is the high sampling rates required in order to obtain transient information. Since both steady state and transient NILM systems have their own strengths and weaknesses, considering both for a study is an interesting approach that has been explored within the literature; for example Chang et al. [144] and Norford et al. [155]. The main steps in a non intrusive load monitoring system are (a) the acquisition of electrical signals, (b) extraction of the important events and (c) production of a component classifier, see Figure 5.1. Leeb et al. [156] noted that the likely success of any NILM system is related to the rate of event generation at a particular point. A machine tool is therefore a suitable application due to the sequential nature of CNC machining.

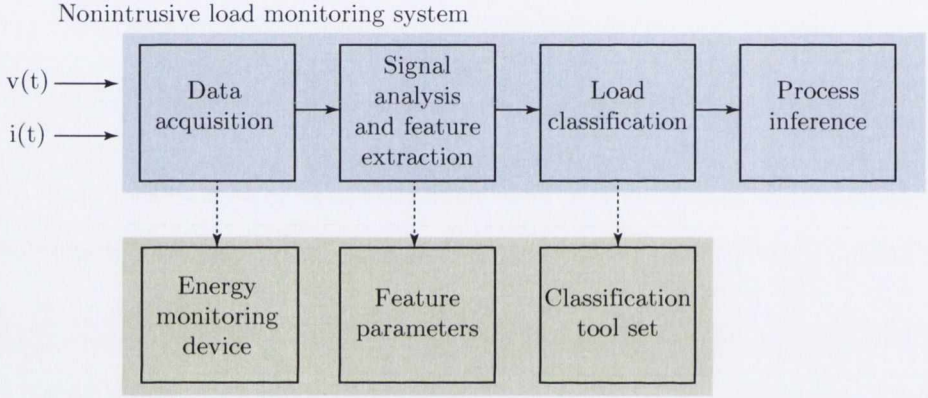

Figure 5.1 – Nonintrusive load monitoring system

The power measurement device that is used to acquire the electrical signals has been highlighted as one of the most important facets of a non intrusive load monitoring application. Within the literature there exists several examples of NILM studies which use defective measurement equipment. Figuieredo et al. [196] developed a NILM system that obtained power measurements via a prototype meter from ISA- Intelligent Sensing Anywhere. The meter was only capable of reporting one parameter value at any moment in time and this resulted in the existence of a delay between the reporting of variables. Further to this, the meter randomly failed to export data points causing measurement errors [196]. According to Chang et al. [144] a robust, reliable, and accurate NILM system can only be realised if a custom measurement device has been developed. Chapter 4 has previously described the development, calibration, and verification of the measurement device used in this research study. The intelligent energy sensor proposed here is a novel approach to the industrial smart metering issue described by Herrmann et al. [15].

5.2 Nonintrusive intelligent machine energy sensor

The intelligent energy sensor combines a two-tiered nonintrusive load monitoring system with condition based inference algorithms to quantify the energy consumption and operational status

of the test machine during machining. The primary goal of the intelligent energy sensor described here is to accurately quantify the duration of time and the energy consumed by a machine tool in each of the three machining states:

- Idle mode - machine is powered on but not ready for production
- Run-time mode - machine is "ready" for production with spindle motor activated
- Production mode - machine is removing material

The intelligent energy sensor also aims to identify the spindle speed during machining, the number of tool changes, coolant pump activations, and important summary statistics including peak power demand. A flow chart describing how the system operates is included in Figure 5.2 and an in-depth explanation is included within Section 5.3.

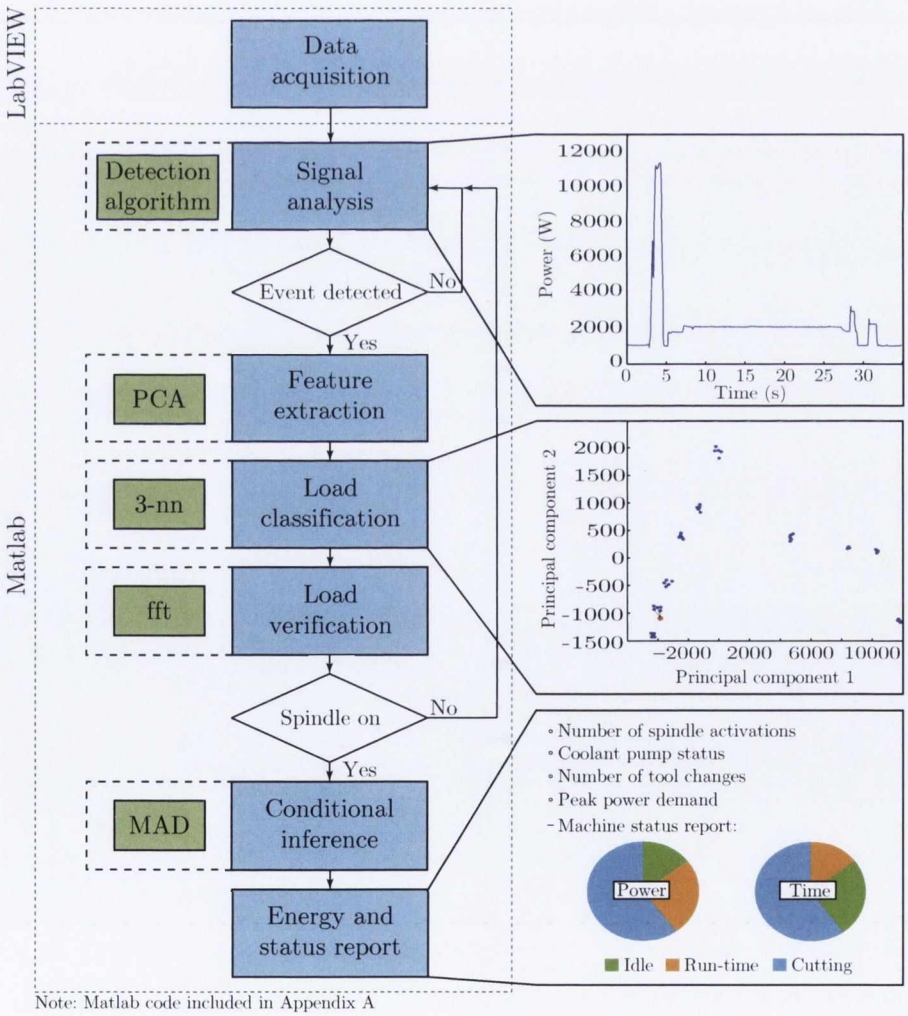

Figure 5.2 – Intelligent energy sensor flow chart

Initially the system analyses the RMS power waveform and searches for activations using an event detection algorithm. Each recorded load signature is normalised, dimensionally reduced, and plot in a two-dimensional signature space before it is compared against a library of training signatures. Frequency information from the current waveforms is then used to verify the initial classification decision. Expanding NILM systems to include harmonic data as described here is a scheme that has been deployed within the literature in order to improve the accuracy of usage disaggregation tools [143]. Once a spindle activation has been detected and verified, a series of condition based statements are employed in order to calculate the power consumed and time spent in each of the three operational states. All of the data is initially acquired using LabVIEW hardware and software; the data processing and analysis is implemented in Matlab.

5.3 Time domain

5.3.1 Training

The NILM segment of the intelligent energy sensor is trained using a supervised learning process where training data is labelled with a predefined class. To illustrate an example of the learning process, the spindle and coolant pump training processes are described below. The measurement device is installed at the main electrical service entry to the machine, as shown in Figure 5.3, and the component in question is activated five times. The coefficient of determination, R^2, tables included in Figure 5.3 and Figure 5.4 highlight the repeatability of each component activation. The spindle acceleration process occurs in parallel with a rapid z-axis motion from the machines home position to the work table. The spindle acceleration training process illustrated in Figure 5.4 therefore includes this rapid z-axis motion.

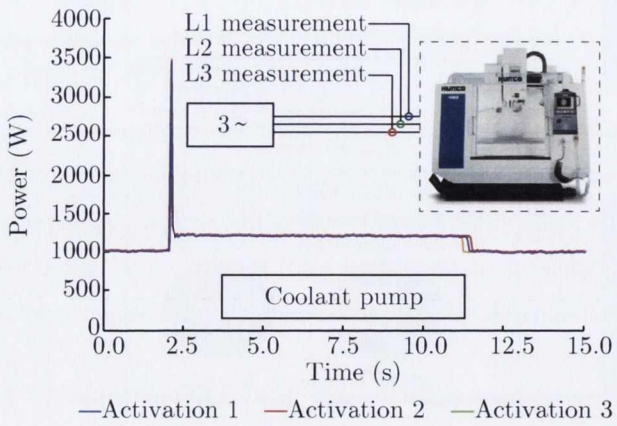

	Activation No.				
Activation No.	1	2	3	4	5
1		96.4	96.7	97.4	97.2
2	96.4		98.4	97.3	98.8
3	96.7	98.4		97.9	98.6
4	97.4	97.3	97.9		98.9
5	97.2	98.8	98.6	98.9	

R^2 table (All values %)

Figure 5.3 – Coolant pump activation training data

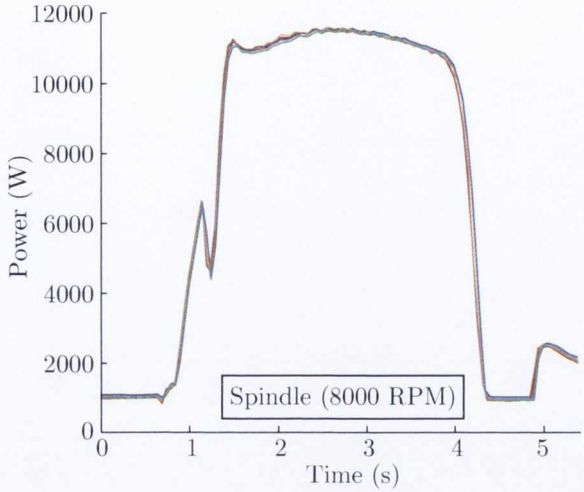

		Activation No.				
		1	**2**	**3**	**4**	**5**
Activation No.	**1**		97.2	97.7	96.9	97.9
	2	97.2		98.1	97.8	98.0
	3	97.7	98.1		97.6	97.7
	4	96.9	97.8	97.6		97.9
	5	97.9	98.0	97.7	97.9	

R^2 table (All values %)

Figure 5.4 – Spindle (8000 rpm) activation training data

A series of n features - a number of measurements that represent the original data - are recorded for each load signature and a class label is assigned. The feature parameters used in this study are included in Table 5.1. The selected features are a superset of those used by researchers attempting to apply pattern recognition tools to domestic and industrial applications [77, 195]. Figure 5.5 illustrates the signature recorded by the activation detection algorithm and also the normalised load signature for an 8000 rpm spindle acceleration. Figure 5.5 also includes the features associated with the 8000 rpm spindle acceleration load signature.

Feature	**Equation**	**Description**
Data	P_k	RMS power values
P_{min}	min (P_k)	Minimum value of the window
$Pnorm_{max}$	max (P_k) - min (P_k)	Maximum value of the feature
$Pnorm_{rms}$	$\sqrt{\frac{1}{n}\sum(P_k - P_{min})^2}$	Root mean square of the feature
$Pnorm_{avg}$	$\frac{1}{n}\sum(P_k - P_{min})$	Mean value of feature
$Pnorm_{SD}$	$\sqrt{\frac{1}{n}\sum((P_k - (P_{min}) - P_{avg})^2}$	Standard deviation of the feature
$Pnorm_{CF}$	$Pnorm_{max}/Pnorm_{rms}$	Crest factor
$Pnorm_{FF}$	$Pnorm_{rms}/Pnorm_{avg}$	Form factor
The index k is from *(t-(n-1)) to (t)*		
n = number of points in each window		

Table 5.1 – Feature parameters

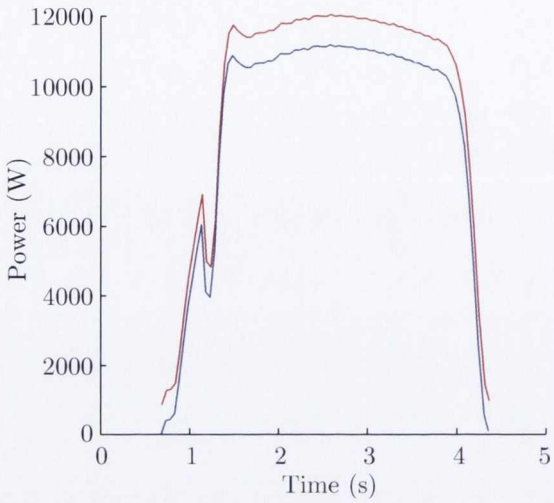

Feature	Value
$Pnorm_{max}$	11.15 kW
$Pnorm_{rms}$	9.56 kW
$Pnorm_{avg}$	8.94 kW
$Pnorm_{std}$	3.41 kW
$Pnorm_{time}$	3.5 seconds
$Pnorm_{CF}$	1.16
$Pnorm_{FF}$	1.07
Class label	spin8

Figure 5.5 – 8000 rpm spindle activation energy signature

At this point each load signature is represented by 7 features, i.e. the data is seven-dimensional. A principle component analysis is performed in order to reduce the dimensionality of the data. Principal component analysis is a mathematical decomposition of variance that assumes the dimensionality of a dataset can be reduced by linear transformation. With respect to the PCA proposed here, this assumption is not unreasonable. Within manufacturing systems there are examples of non-linearities, the spindle power-speed analysis presented in Section 4.4.1 is an example of one such non-linearity. However, when all existing relationships are aggregated, it is reasonable to consider a manufacturing system as a linear system. Although this assumption is not unreasonable, it is critical to exercise caution when using PCA based approaches to extrapolate beyond the training region.

A PCA transforms the initial data points into a rotated orthogonal coordinate system where the origin is the mean of the data points and the axes are described by the eigenvectors. In order to effectively implement a PCA the data set must be normalised in order to obtain a dataset with a mean of zero. Achieving this is done by subtracting the mean from each dimension, i.e. all of the data in the first dimension d_1 have $\bar{d_1}$ subtracted, and all of the data in the second dimension d_2 have $\bar{d_2}$ subtracted etc.,.

The covariance matrix of the dataset is then calculated. For an n dimensional dataset the covariance matrix will have n rows and n columns. Each entry in the matrix is the result of calculating the covariance between two separate dimensions with the exception of the diagonal of the matrix which represents the variance of each dimension. The covariance matrix calculated for the seven-dimensional data recorded in this study takes the form:

$$C = \begin{pmatrix} cov(d_1,d_1) & cov(d_1,d_2) & cov(d_1,d_3) & cov(d_1,d_4) & cov(d_1,d_5) & cov(d_1,d_6) & cov(d_1,d_7) \\ cov(d_2,d_1) & cov(d_2,d_2) & cov(d_2,d_3) & cov(d_2,d_4) & cov(d_2,d_5) & cov(d_2,d_6) & cov(d_2,d_7) \\ cov(d_3,d_1) & cov(d_3,d_2) & cov(d_3,d_3) & cov(d_3,d_4) & cov(d_3,d_5) & cov(d_3,d_6) & cov(d_3,d_7) \\ cov(d_4,d_1) & cov(d_4,d_2) & cov(d_4,d_3) & cov(d_4,d_4) & cov(d_4,d_5) & cov(d_4,d_6) & cov(d_4,d_7) \\ cov(d_5,d_1) & cov(d_5,d_2) & cov(d_5,d_3) & cov(d_5,d_4) & cov(d_5,d_5) & cov(d_5,d_6) & cov(d_5,d_7) \\ cov(d_6,d_1) & cov(d_6,d_2) & cov(d_6,d_3) & cov(d_6,d_4) & cov(d_6,d_5) & cov(d_6,d_6) & cov(d_6,d_7) \\ cov(d_7,d_1) & cov(d_7,d_2) & cov(d_7,d_3) & cov(d_7,d_4) & cov(d_7,d_5) & cov(d_7,d_6) & cov(d_7,d_7) \end{pmatrix}$$

The eigenvectors of this covariance matrix are then calculated. The eigenvector with the largest eigenvalue is known as the first principle component and the eigenvector with the second highest eigenvalue is the second principle component and so on. Typically only the M largest eigenvalues are retained which significantly reduces the dimensionality of the data. Duda et al. [172] observed that in many cases there are only a small number of large eigenvalues, and this implies that M, the number of principal components chosen, is the inherent dimensionality of the subspace governing the signal.

Although a certain amount of information is lost by ignoring the principal components with the smallest eigenvalues it is generally not significant as the vast majority of the variation within the data is accounted for by the M largest principal components [197]. In the case of the data in this study the first and second principal components account for over 95% of the variation in the data and the first three principal components account for over 99% of the variation.

The new dimensionally reduced dataset is calculated by multiplying the mean adjusted data by the derived transformation matrix, Equation 5.3. Choosing the first two principal components will result in a transformation matrix containing the eigenvectors associated with the two largest eigenvalues as columns, Equation 5.1, and choosing the first three principal components will result in a transformation matrix containing the eigenvectors associated with the three largest eigenvalues, Equation 5.2.

$$Tm = (eig_1\ eig_2) \tag{5.1}$$

$$Tm = (eig_1\ eig_2\ eig_3) \tag{5.2}$$

$$Final\ Data = Tm\ x\ AdjustedData \tag{5.3}$$

Figure 5.6 and Figure 5.7 illustrate a sample of the most important component activations transformed into two-dimensional and three-dimensional feature spaces. This methodology of mapping manufacturing machine tool component activations onto a PCA transformed feature space represents a novel contribution to this research area.

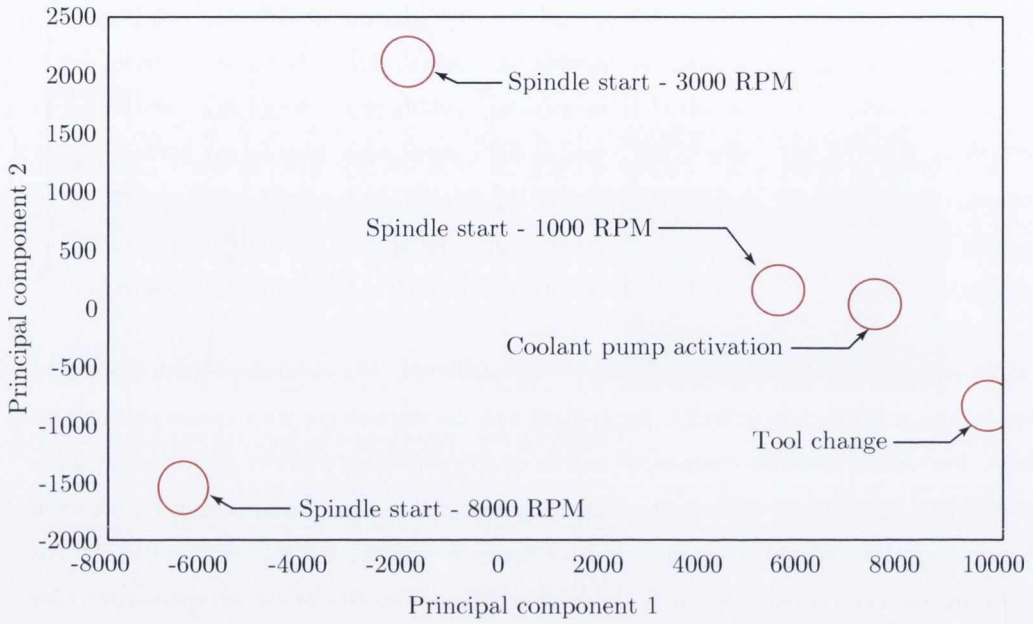

Figure 5.6 – PCA data representation (2D feature space)

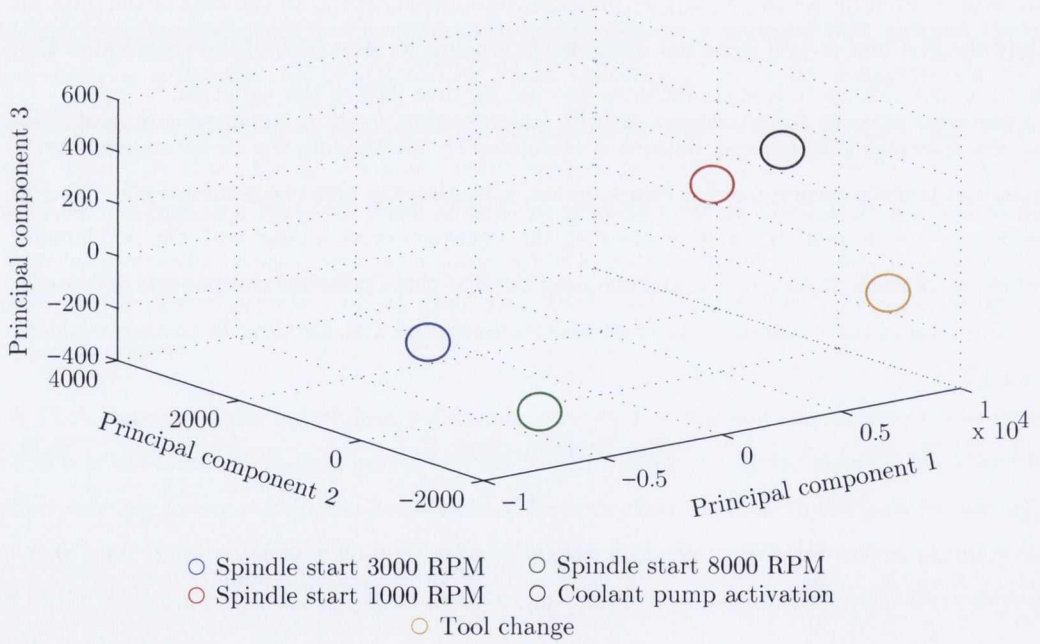

Figure 5.7 – PCA data representation (3D feature space)

Choosing the correct number of principal components is typically done by implementing some sort of visual heuristic; in this case a Pareto chart is used, Figure 5.8. The eigenvalues eig_1, eig_2,..., eig_n are placed in a bar graph with the cumulative total represented by the line graph. An elbow

point is identified in Figure 5.8 between the second and third eigenvalues. Choosing the number of principal components is a decision made by the system designer and in this case, the first two principle components are deemed to adequately represent the original data, accounting for over 95% of the total variance in the original dataset.

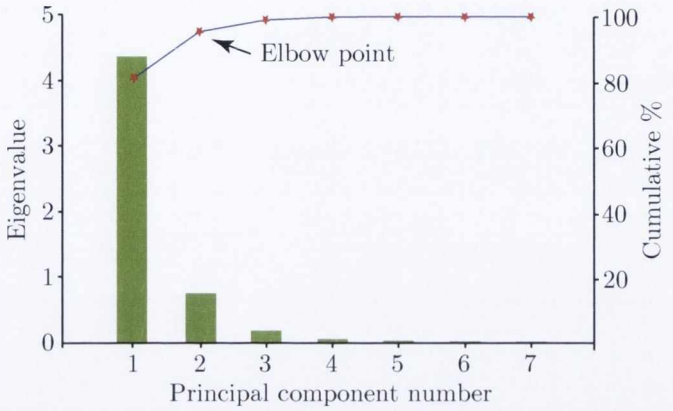

Figure 5.8 – Scree plot

5.3.2 Classification methodology

The intelligent energy sensor described in this research study uses a k-nearest neighbour classifier to classify query samples recorded in the time domain. Several NILM systems utilise k-nn classifiers including the studies presented by Lin and Tsai [142] and Tsai and Lin [198]. Within k-nn based systems classification is achieved by identifying the nearest neighbours to a query example and using those neighbours to determine the class of the query [199]. Details of the k-nn classification framework are included in Section 2.5.4.1.

Within this research study there is a training dataset D containing $(x_i)_{i \in |1,|D||}$ training samples, collected as described in Section 5.3.1. Each training sample is described by a set of F features and labelled with a class label $y_j \in Y$. The classification objective is to categorise each unknown sample u. A variety of metrics exist that can be used to calculate the distance between u and x_i for each $x_i \in D$. The chosen distance metric in this study is Euclidean distance and the k nearest neighbours are identified based on this metric.

$$d_{Euclidean}(x, y) = \sqrt{\Sigma_i (x_i - y_i)^2} \tag{5.4}$$

The most basic approach to assigning a class to a query sample is the majority rule which classifies the unknown sample based on the majority class among the unknown samples nearest neighbours [199]. This study uses a distance weighted voting technique where the vote of each nearest neighbour is weighted by the inverse of its distance to the query.

$$vote(y_j) = \frac{1}{\sqrt{\Sigma_i (x_i - y_i)^2}} \tag{5.5}$$

5.4 Frequency domain

The intelligent sensor system proposed here can be customised to monitor and record harmonics up to and including the 249^{th} order across all three phases if necessary. In order to verify the initial time domain classification, a series of key harmonic relationships can be assessed which can identify the spindle status. The key relationships allow the identification of three discrete spindle states; off, accelerating, and rotating at constant speed. The key harmonic relationships that are observed in the analysis of the machine tool current waveforms are the relative magnitudes of the 3^{rd}, 5^{th}, and 7^{th} harmonics. When the machine tool spindle is not energised the magnitude of the 3^{rd} harmonic is greater than that of the 5^{th} and 7^{th} harmonics.

When the machine tool spindle is energised this relationship is inverted as a result of the frequency inverter design described in Section 4.4.1. In addition to this, during periods of spindle acceleration the magnitude of the 5^{th} and 7^{th} harmonics is over two times the magnitude of the 3^{rd} harmonic. Figure 5.9 illustrates this changing relationship during different spindle operating conditions. Figure 5.9 also illustrates the amplitude changes of the 11^{th} and 13^{th} harmonics during the different spindle operating conditions. Both of these observed results are expected as the 5^{th}, 7^{th}, 11^{th}, and 13^{th} harmonics are all characteristic harmonics of the Hurco VM2's Yaskawa F7 six pulse frequency inverter. Although the key harmonic relationships exist within all three current phases only the I_1 harmonics are used to verify the spindle status in order to avoid redundancy.

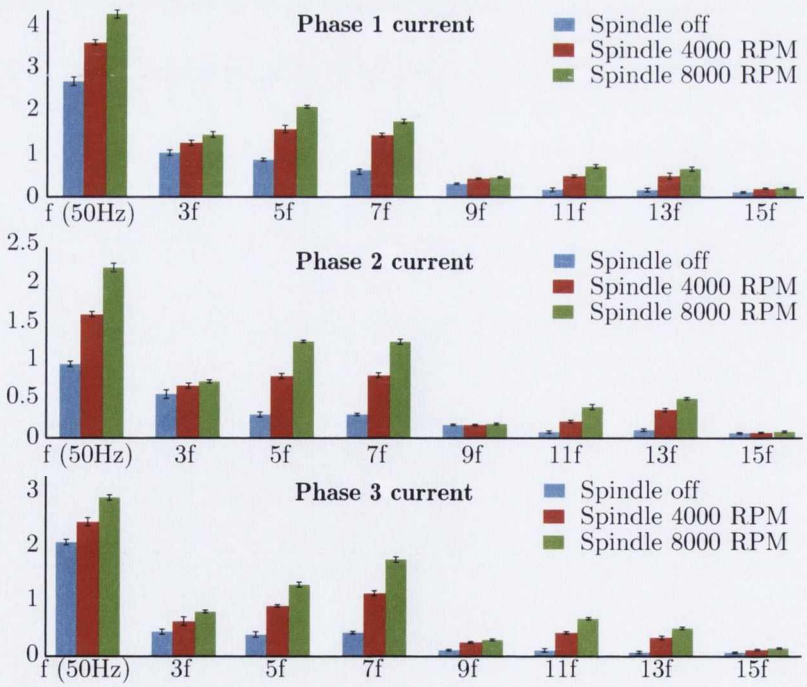

Figure 5.9 – Harmonic analysis

5.5 Conditional inference

Once the intelligent energy sensor has detected, classified, and verified a spindle activation, the system waits a set stabilisation period which is determined by the spindle speed. Figure 5.10 illustrates the stabilisation period for a sample 7000 rpm spindle acceleration and Figure 5.10 also includes a table listing the duration of the stabilisation periods for each of the eight spindle speeds analysed in this study.

Spindle speed (RPM)	Stabilisation period (s)	
	mean	std. deviation
1000	0	0
2000	0.55	0.05
3000	0.95	0.03
4000	1.00	0.07
5000	1.05	0.03
6000	1.15	0.08
7000	1.50	0.05
8000	1.65	0.05

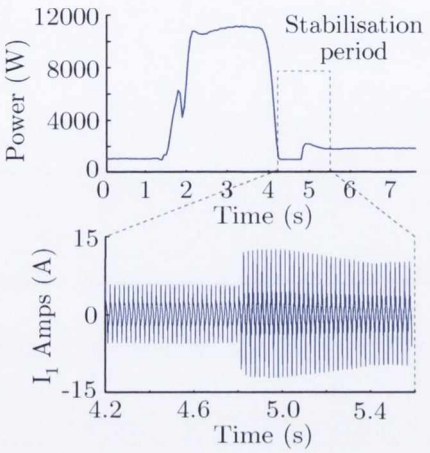

Figure 5.10 – Spindle stabilisation periods

At this point the machine is in a machining ready position and the system searches for a power consumption increase signifying the beginning of a machining process. The system implements a change of mean detection algorithm in order to identify and record a consumption increase resulting from material removal. The detection of mean changes in a measured time series data set can be posed as a hypothesis testing problem in which the null hypothesis (H_0) is that there is no change of mean in the data and the alternate hypothesis (H_1) is that a mean change exists within the data set. In reality, either the null or alternate hypothesis will be true and the change of mean detection algorithm will indicate which hypothesis is true.

The median absolute deviation (MAD) algorithm reported in studies by Leys [200] and Adekeye and Azubuike [201] is used here. The median (Md), is a measure of central tendency similar to the mean, however the median offers the significant advantage of not being strongly influenced by the presence of outliers [201]. Using the MAD is a more robust approach to the measurement of statistical dispersion than comparable methods as it displays a strong resilience to outliers due to its basis on the median rather than the mean. Commonly used statistics including standard deviation place heavier weights on outliers as the distances from the mean are squared.

The median is calculated by sorting observations in ascending order and calculating the mean rank of the observations. The median absolute deviation is calculated using Equation 5.6. A more

comprehensive description of how to calculate the MAD which includes example applications is provided by Leys [200].

$$MAD(X) = Median(|X - Median(X)|) \tag{5.6}$$

Calculating the MAD therefore requires the following steps:

1. Calculate the median of the original data series
2. Subtract this median from each value in the original data series values to obtain a new data series
3. Calculate the median of this new data series

Selecting the length of the sliding window, w, that is used for the cutting detection algorithm is important. The optimal window length is one that is sufficiently large that it does not recognise outliers as structural changes within the data set. However, it is crucial that w is not set too large which would have the effect of smoothing out all changes in the recorded time series. In this study the sliding window includes four data points. The window shift is 1 data point (50 ms) per time slice. Therefore, at each time t, the content of the window is:

$$w_t = (P_{t-3},\ P_{t-2},\ P_{t-1},\ P_t) \tag{5.7}$$

The robustness of the cutting detection algorithm is improved by incorporating slope information in order to allow rapid axis motions which may occur during typical machining operations to be separated from material removal. The first change point representing the beginning of material removal is detected by the cutting detection algorithm when the MAD statistic breaches a threshold, δ_{MAD}, and the slope, $\frac{\Delta y}{\Delta x}$, is below a threshold value, δ_m. These machine tool specific threshold values were obtained during an extensive training period that assessed the algorithms effectiveness at identifying cutting zones, using different threshold values, during a series of machining operations. The power consumption at this point is recorded. Following this, each change point detected by the cutting detector alternates the system between a 'cutting' and 'not cutting' condition. Material removal is adjudged to have ceased when the power consumption decreases below the threshold defined by the initial change point detected by the MAD.

5.6 Test workpieces

Assessing the energy efficiency of multiple machine tools has been identified as a key research area within the literature. Researchers have concluded that the development of a standard test piece is a necessity if accurate comparisons are to be made between machine tools. The definition of these standard workpieces remains an unsolved problem that will be addressed in parts three and four of ISO 14955: Machine tools - environmental evaluation of machine tools [184]. While researchers

await the introduction of internationally accepted workpieces, they will continue to design their own test workpieces.

Behrendt et al. [188] recently designed a test piece based on the Japanese Standards Associations (JSA) existing guideline. Mild steel (AISI 1018) was used as the workpiece material and the test included seventeen different features incorporating face milling, pocketing, and drilling operations. Another test that requires the completion of three milling operations performed with an 18 mm diameter carbide tipped cutter on a steel workpiece was proposed by a different CIRP research team [184]. Further to the two mentioned CIRP approaches, Avram and Xirouchakis [17] presented an energy consumption testing strategy that involved performing numerous milling operations under various loading conditions on an aluminium (7022) test piece. This study assesses the performance of the intelligent energy sensor by testing it on two workpieces described in Section 5.7.

5.7 Experimental results

5.7.1 Workpiece one

The first test uses a 10 mm carbide cutting tool to machine a slot with a 2 mm depth of cut into an aluminium (6060) workpiece. During this test there are no tool changes and the machine operates without coolant. The relevant machining information for this test is included in Figure 5.11.

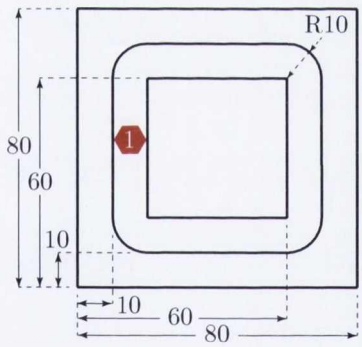

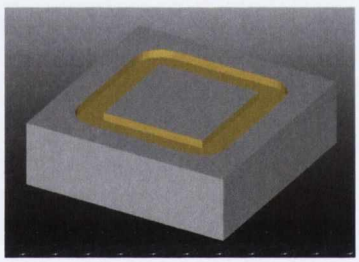

Operation #	1
Depth of cut (mm)	2
X feed rate (mm/min)	500
Y feed rate (mm/min)	500
Z feed rate (mm/min)	100
Spindle speed (RPM)	5000

Figure 5.11 – Workpiece one

Figure 5.12 illustrates the initial spindle acceleration detection and classification. An activation is detected when the slope, $\frac{\Delta y}{\Delta x}$, increases by more than a predefined value, δ_1. The system continues to record this load signature until a combination of conditions are met; firstly the slope, $\frac{\Delta y}{\Delta x}$, decreases by more than a predefined value, δ_2, and the relationships between $Power_{RMS}(x)$ and $Power_{RMS}((x)-5)$, and $Power_{RMS}(x)$ and $Power_{RMS}((x)-1)$ meet certain conditions signifying a consumption decrease followed by a stabilisation. The machine tool specific activation detection values were obtained during the initial component level training phase. The chosen values were the most effective at repeatedly isolating similar signatures for each component activation during the training phase.

The recorded activation is then normalised by subtracting the minimum value, P_{min}, from each of the activation values. Each of the seven features described in Section 5.3 are then computed for the normalised activation and a feature vector of the form $Fv = [F_1 \ F_2 \ F_3 \ ... \ F_7]$ is produced. At this point the feature vector, Fv, is multiplied by the transformation matrix, Tm, in order to transform it into the feature space shown in sub plot 3 of Figure 5.12.

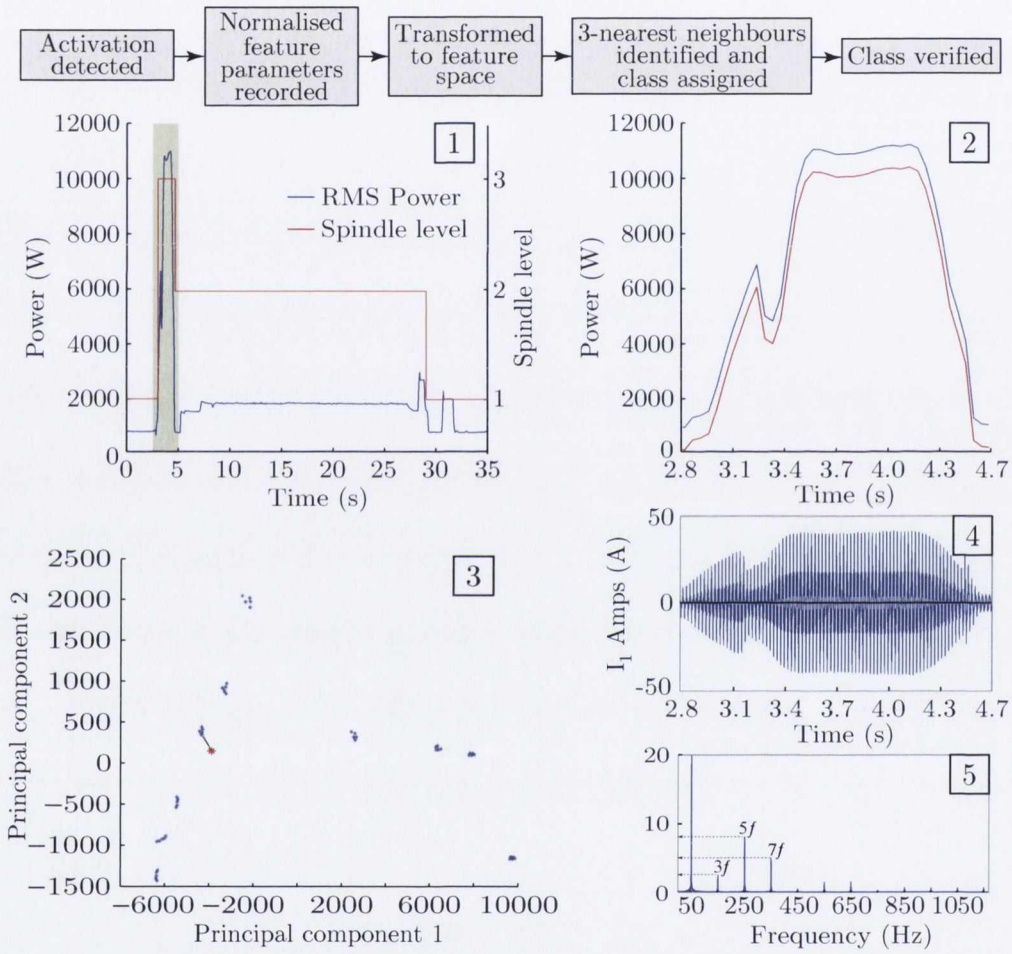

Figure 5.12 – Spindle activation identification and classification

The red point within sub plot 3 of Figure 5.12 represents the detected activation described above. The system now computes the inverse Euclidean distance between the test point and each of the training samples within the feature space. The inverse Euclidean distances between the test point and its three nearest neighbours, calculated using $1/d_{Euclidean}(x, y) = \frac{1}{\sqrt{\Sigma_i (x_i - y_i)^2}}$, are included in Table 5.2. The tabulated results show the activation has been correctly classified as a 5000 rpm spindle acceleration.

k-nn	Euclidean distance	Inverse Euclidean distance	Class label
k=1	453.74	0.0022	Spin5
2	489.94	0.0020	Spin5
3	530.08	0.0018	Spin5

Table 5.2 – Detected activation (i), 3-nearest neighbours

The I_1 current profile, illustrated in sub plot 4 of Figure 5.12, also recorded during the event detection process is used to verify the assigned class using the method described in Section 5.4. This validation test operates by monitoring the relationship between the spindle frequency inverter's characteristic harmonics and non-characteristic harmonics. The spindle level plot included in sub plot 1 of Figure 5.12 includes the spindle level for the duration of the test. The plotted values are the results of a sliding window fft test in accordance with the following:

- level 1 - $3^{rd} > 5^{th}$ & $3^{rd} > 7^{th}$
- level 2 - $5^{th} > 3^{rd}$ & $7^{th} > 3^{rd}$
- level 3 - $5^{th} > 2 * (3^{rd})$ & $7^{th} > 2 * (3^{rd})$

In the case of the activation currently under consideration the magnitude of the 5^{th} harmonic, 7.62, and the magnitude of the 7^{th} harmonic, 4.19, are both more than double the 3^{rd} harmonic magnitude of 1.88. This supports the findings of the initial classification tool which labelled the test sample as a spindle acceleration. Following the identification of a 5000 rpm spindle acceleration the system waits 1.05 seconds for the power consumption to stabilise in accordance with the table included in Figure 5.10. At this point the system searches for a consumption increase resulting from material removal by implementing the cutting detection algorithm described in Section 5.5.

The cutting tool is adjudged to have made contact with the workpiece - in accordance with the conditions set out in Section 5.5 - 1.45 seconds after the spindle has stabilised at 5000 rpm. The power consumption increase is recorded by the cutting detection system. The algorithm continues to run until the spindle is powered off; this occurs approximately 22.15 seconds after the cutting process begins. Within the spindle on zone the cutting detection algorithm identifies two periods of material removal and a rapid axis acceleration, illustrated in Figure 5.13. In order to validate the sensors observation that the spindle is powered off, a further verification test is performed using the frequency information as described in Section 5.4. In this case, the magnitude of the 5^{th} harmonic, 0.85, and the magnitude of the 7^{th} harmonic, 0.66, are both below the 3^{rd} harmonic magnitude of 1.62 providing further validation that the spindle has been powered off.

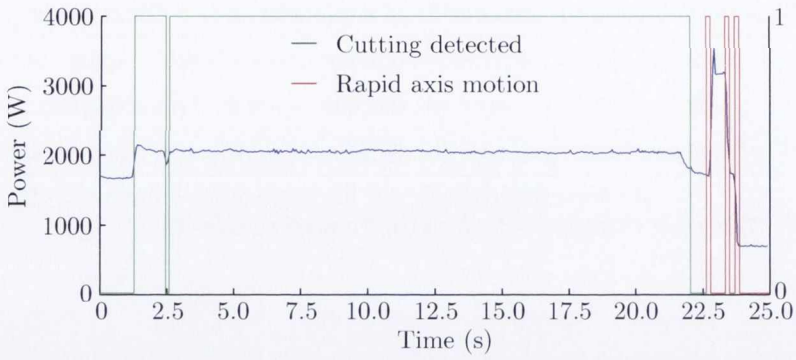

Figure 5.13 – Workpiece one material removal detection

Figure 5.14 includes the data provided by the intelligent energy sensor summary report for the first test workpiece. The test lasts for a total time of 35.2 seconds and 20.55 Wh are consumed by the machine tool during this period.

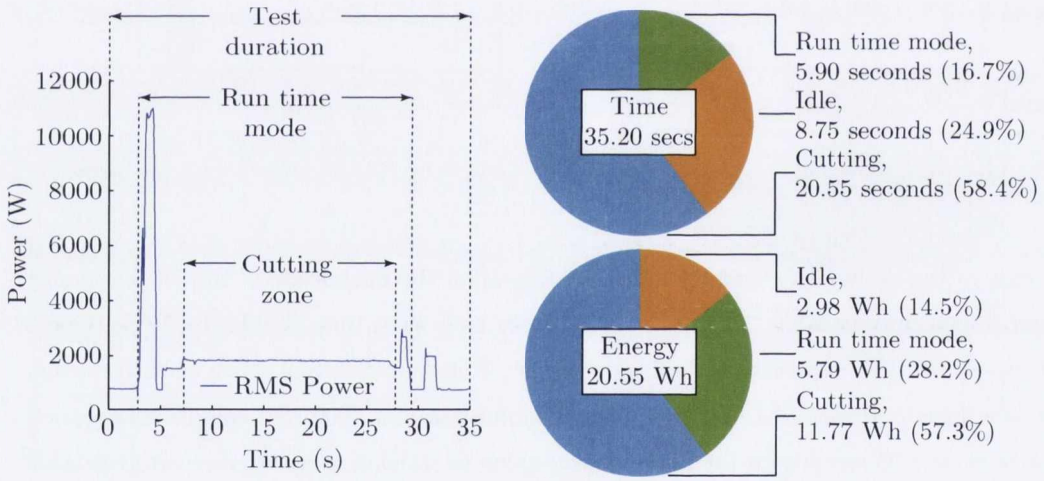

Figure 5.14 – Workpiece one machine state power and time breakdown

5.7.2 Workpiece two

The second workpiece incorporates facets of the test strategies developed within the literature described in Section 5.6. The workpiece material is mild steel (AISI 1018). Multiple operations are performed with varying machining parameters. During this test there are two tool changes and the machine operates with and without coolant for different operations. The following is a list of the three operations included for the second test workpiece test:

- 10 mm cutting tool to machine a slot with a 4 mm depth of cut, operation number 1 in Figure 5.15;

- 8 mm cutting tool to machine a slot with a 2 mm depth of cut, operation number 2 in Figure 5.15;
- 6 mm cutting tool to drill a 6 mm diameter hole to a depth of 10 mm - 2 mm pecking distance - operation number 3 in Figure 5.15.

The relevant machining information for this test is included in Figure 5.15.

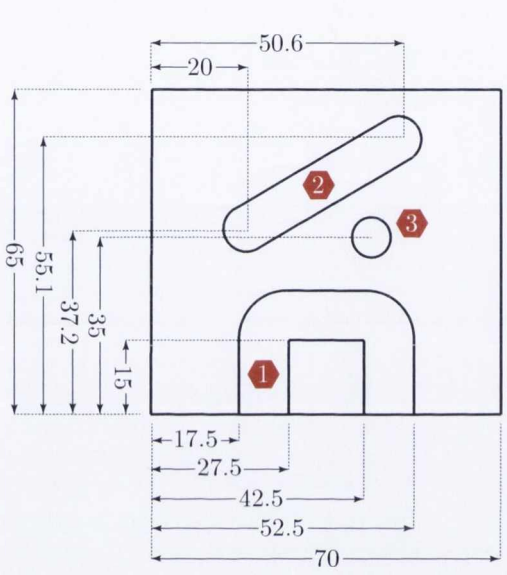

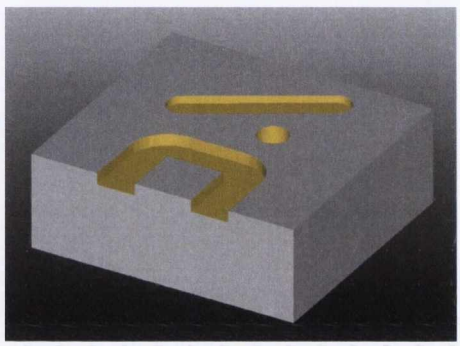

Operation #	1	2	3
Depth of cut (mm)	4	2	10
X feed rate (mm/min)	500	250	N/A
Y feed rate (mm/min)	500	250	N/A
Z feed rate (mm/min)	100	100	125
Spindle speed (RPM)	4000	7000	7000

Figure 5.15 – Workpiece two

The initial spindle acceleration, detection, and classification diagrams are included in Figure 5.16. The activation, detected when the slope, $\frac{\Delta y}{\Delta x}$, increases by more than a predefined value, δ_1, continues to be recorded until a combination of conditions are met. Firstly the slope, $\frac{\Delta y}{\Delta x}$, must be observed to decrease by more than a predefined value, δ_2, and the relationships between $Power_{RMS}(x)$ and $Power_{RMS}((x) - 5)$, and $Power_{RMS}(x)$ and $Power_{RMS}((x) - 1)$ must also meet certain conditions signifying a consumption decrease followed by a stabilisation.

The recorded activation is then normalised as described previously by subtracting the minimum value, P_{min}, from each of the activation values. Each of the seven features described in Section 5.3 are then computed for the normalised activation and a feature vector of the form $Fv = [F_1 \ F_2 \ F_3 \ \ldots \ F_7]$ is produced. At this point the feature vector, Fv, is multiplied by the transformation matrix, Tm, in order to transform it into the feature space shown in sub plot 3 of Figure 5.16.

The highlighted point within sub plot 3 of Figure 5.16 represents the detected activation described above. The inverse Euclidean distances between the test point and each of the training samples within the feature space is then recorded. The recorded distance between the test point and

its three nearest neighbours are included in Table 5.3. The tabulated results show the activation has been correctly classified as a 4000 rpm spindle acceleration.

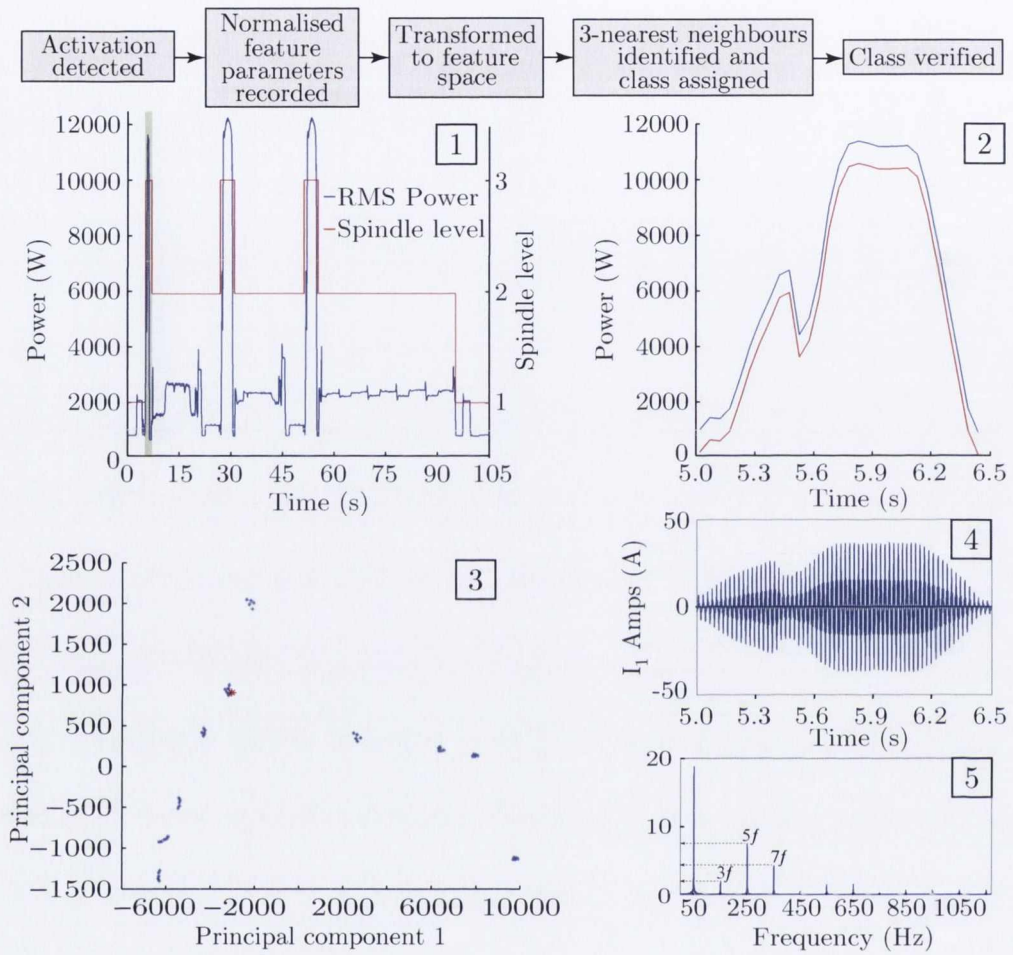

Figure 5.16 – Spindle activation identification and classification

k-nn	Euclidean distance	Inverse Euclidean distance	Class label
k=1	66.75	0.0149	Spin4
2	82.13	0.0121	Spin4
3	91.44	0.0109	Spin4

Table 5.3 – Detected activation (ii), 3-nearest neighbours

The I_1 current profile, illustrated in sub plot 4 of Figure 5.16, also recorded during the event detection process is used to verify the assigned class using the method described in Section 5.4. In the case of the activation currently under consideration the magnitude of the 5^{th} harmonic, 7.13, and the magnitude of the 7^{th} harmonic, 4.11, are both more than double the 3^{rd} harmonic

magnitude of 1.98. This supports the findings of the initial classification tool which labelled the test sample as a spindle acceleration. Following the identification of a 4000 rpm spindle acceleration the system waits 1.00 seconds for the power consumption to stabilise in accordance with the table included in Figure 5.10 before searching for a material removal process.

The detection algorithm observes another event and records an additional load signature within the spindle stabilisation zone. The recorded activation, normalised activation, and feature space mapping are all included in Figure 5.17. The intelligent energy sensor classifies this load signature as a coolant pump activation. The red point within sub plot 3 of Figure 5.17 represents the detected activation described above.

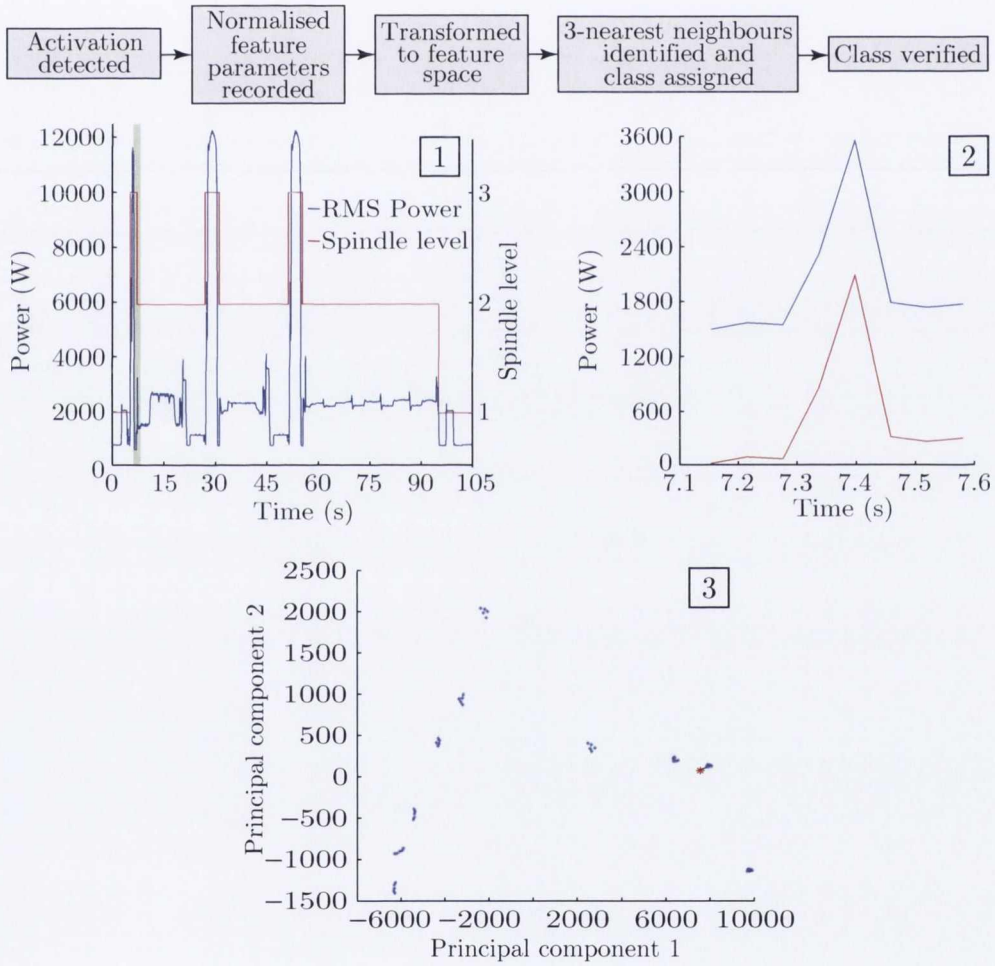

Figure 5.17 – Coolant pump activation identification and classification

The system now computes the inverse Euclidean distance between the test point and each of the training samples within the feature space. The inverse Euclidean distance between the test point and its three nearest neighbours, calculated using $1/d_{Euclidean}(x, y) = \frac{1}{\sqrt{\Sigma_i (x_i - y_i)^2}}$, are

included in Table 5.4. The tabulated results show the activation has been correctly classified as a coolant pump activation.

k-nn	Euclidean distance	Inverse Euclidean distance	Class label
k=1	121.54	0.0082	Cool
2	128.22	0.0077	Cool
3	165.39	0.0060	Cool

Table 5.4 – Detected activation (iii), 3-nearest neighbours

After the stabilisation period has elapsed the system searches for a consumption increase resulting from material removal by using the cutting detection algorithm described in Section 5.5. The cutting tool makes contact with the workpiece 3.45 seconds after the coolant pump has been activated and the associated increase is recorded and stored. The machining operation is adjudged to have ceased when the power consumption returns to the static level observed before material removal was detected, a period of 7.45 seconds. The algorithm continues to run until the spindle is powered off; this occurs approximately 10.75 seconds after the cutting process begins. Within the spindle on zone, the cutting detection algorithm identifies three periods of material removal and two rapid axis accelerations, illustrated in Figure 5.18.

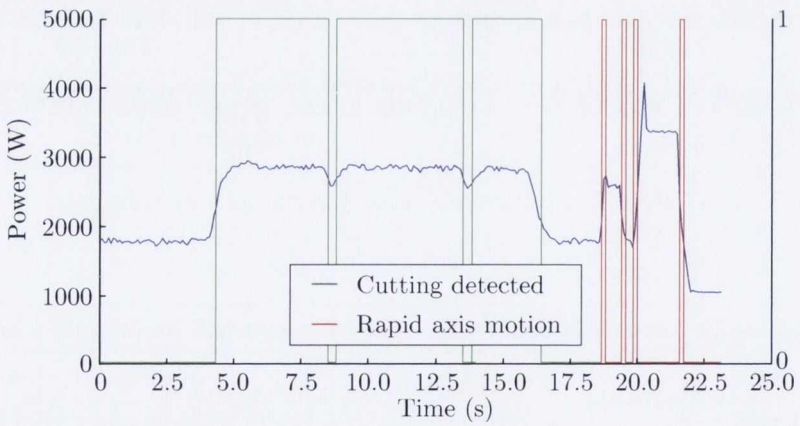

Figure 5.18 – Workpiece two - operation one material removal detection

The spindle is deemed to have been powered off when the power consumption returns to the recorded level during idle mode. At this point the verification test is performed as described within Section 5.7.1 covering the first test workpiece. The magnitude of the 5^{th} harmonic, 0.89, and the magnitude of the 7^{th} harmonic, 0.62, are both below the 3^{rd} harmonic magnitude of 1.58 at this point validating the identified spindle off status.

The next activation detected by the intelligent energy sensor after the machine tool spindle is powered off is included in Figure 5.19. The figure includes the initial recorded activation, normalised activation, I_1 current waveform, harmonic study, and feature space mapping. Following the steps outlined above this activation is identified as a tool change operation. The frequency verification test is useful here as the tool change process represents one of the few operations that can only occur whilst the spindle is powered off. Therefore, assessing the spindle status during the tool change operation provides a level of component verification.

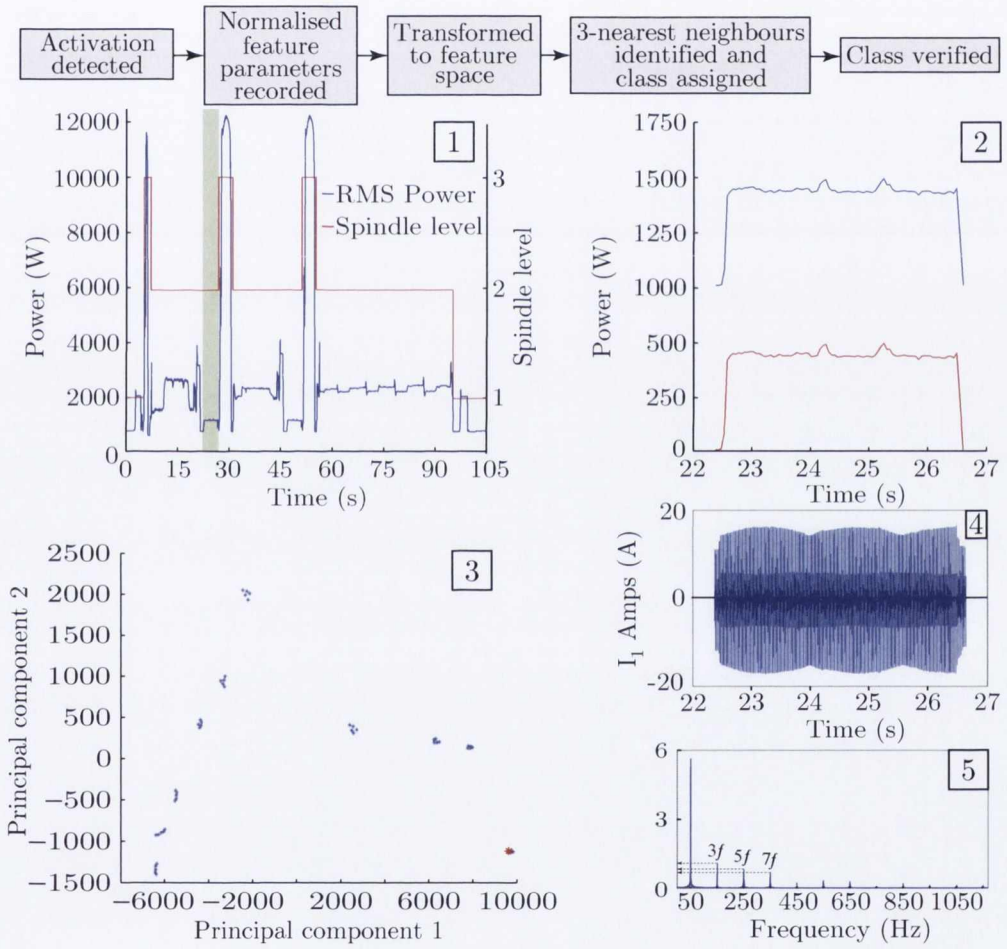

Figure 5.19 – Tool change identification and classification

The system computes the inverse Euclidean distance between the test point and each of the training samples as previously described. The inverse Euclidean distance between the test point and its three nearest neighbours, calculated using $1/d_{Euclidean}(x, y) = \frac{1}{\sqrt{\Sigma_i (x_i - y_i)^2}}$, are included in Table 5.5. The tabulated results show the activation has been classified as a tool change operation.

k-nn	Euclidean distance	Inverse Euclidean distance	Class label
k=1	21.56	0.0464	Tool
2	22.21	0.0450	Tool
3	31.77	0.0314	Tool

Table 5.5 – Detected activation (iv), 3-nearest neighbours

The intelligent sensor follows the same procedure for the rest of the recorded power profile identifying an additional two spindle activations, both 7,000 rpm, and another tool change activation. The system also quantifies the duration of material removal within each run time zone. Figure 5.20 includes a summary of the data provided by the intelligent energy sensor for the second test workpiece.

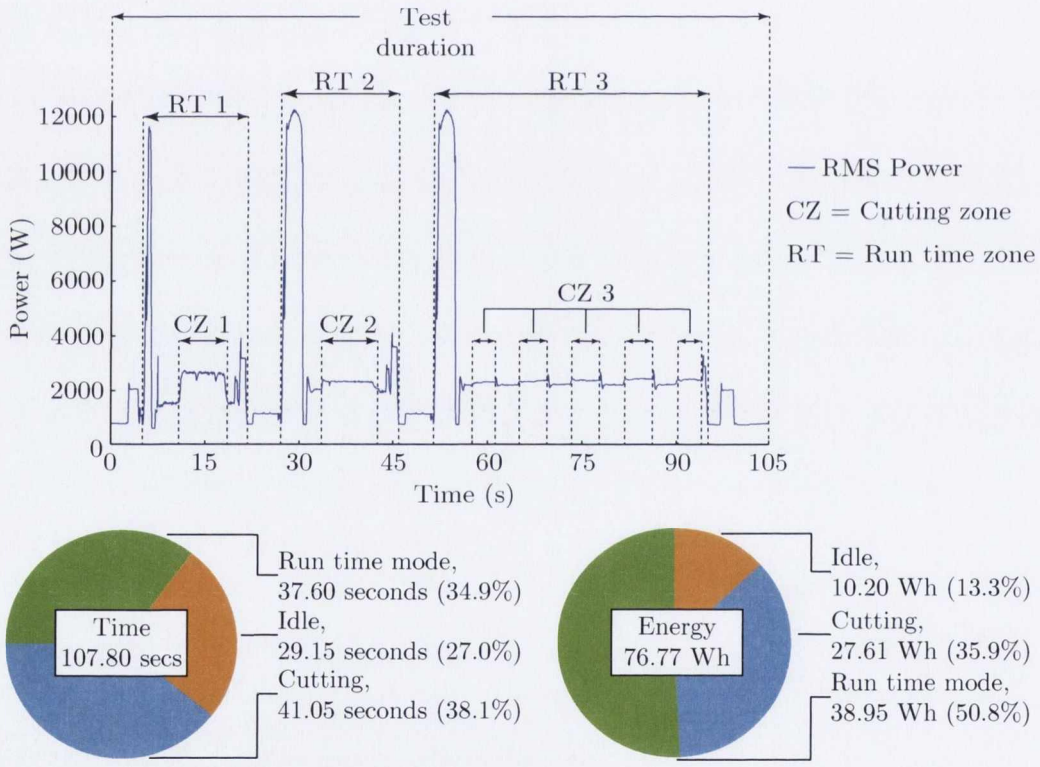

Figure 5.20 – Workpiece two machine state power and time breakdown

5.8 Summary

Numerous researchers, including Vijayaraghavan and Dornfeld [19] and Dahmus and Gutowski [84], have identified the duration of time a machine tool spends in each operational state during processing as an important research area; Vikhorev et al. [77] observed that the time production

machines spend in idle represents 20% - 30% of the energy losses in a manufacturing facility. The intelligent energy sensor described in this chapter combines a nonintrusive load monitoring system with condition based inference algorithms in order to quantify the energy consumption and operational status of the test machine during machining. Herrmann et al. [15] suggest that obtaining transparency on machine tool status during operational periods will increase the level of motivation to alter behaviour and reduce the energetic impacts of machining.

The NILM segment of the intelligent energy sensor was trained using a supervised learning process where training data is labelled with a predefined class. A selection of features were collected for each component activation. Each machine tool activation was then mapped onto a PCA transformed feature space; a process that has not previously been reported in the literature. During testing periods query activations were mapped onto the feature space and a 3-nn classification tool was employed to classify the unknown query. A median absolute deviation algorithm was applied to identify material removal zones.

The combination of algorithms which form the intelligent energy sensor and their application to a cutting machine tool are novel contributions to the research area. The developed sensor was applied to a Hurco VM2 3-axis CNC milling machine. The proposed sensor is a low cost solution which can support the expansion of unit process life cycle inventory databases and assist the industry transition towards sustainable manufacturing. The intelligent energy sensor was tested on two workpieces. The design of the workpieces was inspired by workpieces from the literature, in particular the workpieces described by Behrendt et al. [188] and Avram and Xirouchakis [17] were influential. The intelligent energy sensor reports strong results, accurately identifying individual component activations as well as the operational status of the machine tool during machining.

Chapter 6

Conclusions and recommendations for future work

6.1 Summary

This research work has highlighted the importance of developing a holistic understanding of energy consumption within manufacturing facilities at each hierarchical level. The need for this understanding has been driven by the rising cost of energy, the fact that energy has become a major cost driver within manufacturing facilities, and the widespread implementation of environmental legislation. Developing a more comprehensive understanding of how energy is consumed within manufacturing facilities is a core component of research efforts aiming to advance industrial energy efficiency.

This study presents an array of tools which consider energy consumption at all levels of the manufacturing facility hierarchy. One of the critical challenges facing plant managers is the need to gain transparency inside the complex energy distribution networks of their manufacturing plants. Studies within the literature have identified submetering as a necessary task in order to develop the level of energy transparency required. The industrial case study presented in this work describes an effective energy metering system implementation strategy. The case study describes a decision support tool that identifies where metering devices are needed and also develops energy performance indicators based on the data emanating from the installed metering system.

The design and development of a custom power measurement tool facilitated a detailed machine tool energy characterisation. Component level transparency was achieved by assessing individual components under various loading conditions and recording the consumption characteristics. The machine tools dynamic behaviour was also analysed with a series of machining tests. The machining tests were performed in order to investigate two phenomena; the relationship between power consumption and depth of cut, and also the relationship between specific energy consumption and material removal rate.

Quantifying the duration of time a machine tool spends in each operational state has also been identified as an important research area. Obtaining transparency on machine tool status during machining will motivate improvements that can reduce the energetic impacts of machining. This study presents a novel nonintrusive intelligent energy sensor that combines a nonintrusive load

monitoring system with condition based inference algorithms in order to identify the operational status of a machine tool during machining. The intelligent energy sensor is novel in terms of both its design and application.

6.1.1 Manufacturing process chain electrical energy characterisation

An industrial case study was undertaken to investigate the energy consumption of a complex manufacturing facility at various hierarchial levels. A wireless-state-of-the-art metering system was installed in order to improve the level of energy transparency within the facility. In an effort to ensure energy measurement devices were installed at appropriate locations a generic metering installation strategy was developed that assessed the magnitudes and trends that existed within the power profiles of each piece of equipment. Although researchers have previously highlighted the importance of electrical energy measurement within manufacturing facilities [59,120]; the metering infrastructure that is now installed in the test facility represents the cutting edge in this area and similar projects have not been reported in the literature to date.

The information emanating from the energy metering system was used to develop energy performance indicators allowing the effectiveness of energy projects to be accurately quantified as well as optimising energy cost savings from the perspectives of both procurement and end use. At a facility level the test site consumes over 17 GWh of electricity each year. Initial results disaggregated this total facility consumption into the most significant energy users with production (42%), compressed air (15%), and dust extraction (11%) representing the most significant consumers. Other notable contributors included HVAC (9%), chilled water (8%), and office spaces (3%).

A detailed investigation into the electrical energy requirements of process chains was conducted. This section of the study focused on one value stream that produced two separate products. The process chains for both products were mapped out from an energy perspective and the requirements of each process were quantified. In terms of direct energy consumption, product A required 2.26 kWh/unit and product B required 2.49 kWh/unit. The product A line included seven processes while the product B line included ten processes. The most energy intensive processes for product A were the clean line (51.99%), milling (32.07%), and in process cleaning (6.32%). The most energy intensive processes for product B were inspection (38.23%), the clean line (28.51%), and turning (17.18%). One of the most interesting results observed at this juncture was the portion of the overall energy consumption that is associated with non-value adding operations such as cleaning and inspection.

A unit process level investigation was performed on a single piece of manufacturing equipment, a Mazak FH-4800 milling machine. A holistic quantification methodology was developed which accounted for the energy required directly and indirectly by the machine tool. The results of this section observed that overheads, in the form of lighting and HVAC accounted for 10.37% of the total energy required. The provision of coolant accounted for approximately 9.24%, with the

machine tool itself requiring 80.39% of the total required energy. The results observed in this section of the research were in line with studies from within the CIRP community as well as other relevant academic journals [19, 85, 118].

It can be concluded that a structured methodology is necessary to allow the discrimination between energy consumers in complex manufacturing facilities due to the level of complexity inherent in modern manufacturing sites with primary and supporting energy, various hierarchical levels, as well as multiple processing steps. The methodology developed herein allowed a complete disaggregation of the energy consumed within a complex manufacturing facility.

6.1.2 Machine tool electrical energy characterisation

A power measurement tool was designed and developed to facilitate a machine tool energy characterisation study. The measurement system was calibrated against a sate-of-the-art commercially available power monitoring device. The R^2 values of $> 95\%$ obtained during verification tests proved that the system was accurate and reliable. The primary source of error which lead to discrepancies during the verification tests was intrinsically linked to the performance of the calibration device. The HT-Italia power meter used in conjunction with HT-FLEX33 current transformers zeroed all current readings with a magnitude of less than 1 Amp.

An energy investigation was performed on a 3-axis Hurco VM2 CNC milling machine. The electrical distribution network that exists within the machine tool was mapped. Individual machine components were then characterised by activating each component three times under various loading conditions in order to obtain statistically significant results. The spindle was the component requiring the most power, with a maximum instantaneous power consumption of 11.89 kW observed during spindle acceleration. A power-speed analysis found a dynamic relationship between spindle speed and power consumption depending on the operating range. Both the x and y axis are powered by 1.3 kW servo motors, with the z axis being driven by a larger 2.0 kW servo motor primarily due to the increased mass carried by the z axis.

Auxiliary components including the coolant pump and tool change motor were also analysed. The coolant pump required a peak power of 3.42 kW during its initial turn on transient, and then 1.22 kW during steady state operation. The tool change motor required a peak power of 1.52 kW during its initial turn on transient, and then 1.39 kW during steady state operation. The contribution of peripheral equipment to the machine tools idle power requirement was also quantified. Unloaded motors (39.7%) and cooling fans (10.53%) represented the most energy intensive pieces of idle mode equipment.

Machining tests were performed in an attempt to investigate two phenomena; the relationship between power consumption and depth of cut, and also the relationship between specific energy consumption and material removal rate. The machining tests were performed on an aluminium (6060) workpiece. During testing the machining parameters were held constant - with a spindle

speed of 5000 rpm and a feedrate of 700 mm/min - and the depth of cut was increased from 1 mm to 5 mm in steps of 1 mm. Each machining operation was performed three times. A linear relationship between power consumption and depth of cut was observed. Approximately 0.118 kW of additional power were required for each 1 mm increase in depth of cut. The results of these machining tests aligned with recent research studies that also described a linear relationship between power consumption and depth of cut [88].

The second set of machining tests also used an aluminium (6060) workpiece. The machining parameters were held constant - with a spindle speed of 4000 rpm and a feedrate of 500 mm/min - while the depth of cut increased from 0.5 mm to 5 mm in steps of 0.5 mm in order to vary the material removal rate. Each machining operation was performed three times. An inverse relationship was observed between specific energy consumption (kJ/cm^3) and material removal rate (cm^3/s). The results obtained during these machining tests matched the findings of similar studies that have recently been reported in the literature [88, 183].

The hierarchical approach ultimately leads to the unit process level, and raises the question of the capability of energy and power data to characterise machine tool performance, considering that consumption levels can be low, under 0.1 kW, and difficult to measure. The methodology developed based on metering multiple machine tool subcomponents demonstrated that the measurement of energy and power is a viable approach to resolve component level consumption in certain circumstances. This approach is not without limitation and its effectiveness may be reduced as depth of cut decreases below 0.5 mm and if small diameter tools are used.

6.1.3 Nonintrusive machine tool load monitoring

The potential of reduced-cost data acquisition has motivated development of nonintrusive electrical load monitoring devices. The devices have primarily been deployed in domestic buildings [137], but their use in commercial and industrial facilities is increasing [155]. This work, distinct in both its approach and application area focused on an individual milling machine tool. A novel nonintrusive intelligent energy sensor was designed, developed, and tested. The system deployed voltage and current sensing elements at the main incomer of the machine tool and assessed the current machine tool status based on the patterns existent within the acquired data.

The implementation of the intelligent energy sensor, based on measurements at a single point, required feature extraction and classification techniques in order to separate individual loads. The proposed intelligent energy sensor combines a NILM approach with conditional inference algorithms in order to identify the machine tools operational status as well as individual component activations.

An activation detection algorithm is used to detect when a machine component has been energised; when an activation is detected the system records the relevant waveforms and collects a series of time domain and frequency domain features. The time domain features included maximum power, RMS power, crest factor, form factor, etc.,. Frequency domain features included the

3^{rd}, 5^{th}, and 7^{th} harmonics. Training the system was completed by activating the machine tool components five times and recording all features.

In order to maximise the separation distance between each machine component activations time domain features a principal component analysis was performed. The results of the principal component analysis showed that including the first two principal components described 96% of the variation, and the first three principal components accounted for 99% of the variation. A scree plot identified the first two principal components as the most important components to be included and this allowed the seven time domain features to be transformed and visualised in a 2-D space that accounted for 96% of the original data variation.

Classification of the time domain signals was performed by a three-nearest neighbours tool. K-nn based classification systems find application in many NILM systems due to their simplicity in computation and implementation. Classification of the frequency domain information was performed by comparing the relative magnitudes of characteristic harmonics. A median absolute deviation algorithm was then deployed in order to identify material removal zones. The intelligent energy sensor was tested on two workpieces based on existing workpieces from the literature.

An intrusive approach to metering involving the deployment of multiple sensors is advantageous in lab arrangements, however the potential to undertake a detailed examination of the global machine tool power consumption in an intelligent manner presents the advantages of reducing the hardware cost and installation difficulty of the metering system. The methodology developed based on PCA and MAD algorithms demonstrated it was possible to discriminate between machine states and recognise certain component activations. Therefore it can be concluded that with the appropriate analysis architecture, and the appropriate level of training for the algorithm, a nonintrusive and intelligent approach to energy metering provides a viable alternative to multi-sensor arrangements.

6.2 Recommendations for future work

The areas where future work could be undertaken include:

- Developing alternatives to traditional cleaning/inspection processes
- Further investigations into the relationship between process parameters and energy consumption
- Identifying machine tool components by injecting electrically intrusive signatures
- Developing an intelligent energy sensor that interfaces with state-of-the-art machine tool controllers

There is an opening in the literature for studies that investigate alternatives to the traditional non-value adding operations including cleaning and inspection. The results observed within this

study highlighted the energy intensive nature of conventional biomedical device cleaning processes and the impact they have on the overall energy consumption for each part. Studies that propose methods that either change or remove standard cleaning and inspection operations from biomedical process chains have the potential to make significant energy savings.

There is an opportunity for research projects that investigate the effects of adapting machining process plans in order to reduce energy consumption. There are currently a small number of research publications that address this area however, there is scope for the development of environmental process plan optimisation strategies that can be applied to multiple machining processes. Also, within the literature there is still not a complete understanding of the relationship that exists between machining parameters and energy consumption. Although unit process energy databases do exist there is a need for a comprehensive database created by multiple stake holders that can assist in the development of a thorough understanding of how process parameters impact on energy consumption.

Further work on the intelligent energy sensor developed here could include an on-line solution which could report on the machine status in real-time. As the existing system operates on a conventional computer platform there is also scope to connect the intelligent energy sensor to a variety of communication networks, including the web; allowing the machine tool status to be monitored remotely.

The development of a more comprehensive machine tool component activation tool capable of identifying individual axis movements could be facilitated by injecting an electrical signal onto each device. For example, in order to differentiate two identical axis positioning servo motors, a different voltage harmonic or transient could be injected into the servo motors electrical signals.

An additional opportunity for future work results from current developments in machine tool controllers. As more and more controllers provide access to energy consumption information there is scope for an application that interfaces directly with machine tool controllers in order to infer the operational status of the machine tool. The development of a generic intelligent energy sensor that is capable of learning machine tool signals from different machines would represent a major contribution to the research area that could evolve into a valuable commercialisation project.

References

[1] IEA, *"World Energy Outlook"*, OECD/International Energy Agency, Paris, 2009. Available at: http://www.worldenergyoutlook.org/2009.asp/ [Accessed on 15/09/2009].

[2] WEC, *"World Energy Resources"*, World Energy Council, London, 2010. Available at: http://www.worldenergy.org/publications/2010/survey-of-energy-resources-2010 [Accessed on 12/02/2013].

[3] EIA, *"Annual Energy Outlook 2006 With Projections to 2030"*, United States Energy Information Administration, Washington, DC, 2006. Available at: http://www.eia.gov/oiaf/archive/aeo06/index.html/ [Accessed on 18/10/2010].

[4] IEA, *"Key World Energy Statistics"*, OECD/International Energy Agency, Paris, 2010. Available at: http://www.oecd-library.org/energy/key-world-energy-statistics-2010_9789264095243-en [Accessed on 12/09/2011].

[5] IEA, *"World Energy Outlook"*, OECD/International Energy Agency, Paris, 2012. Available at: http://www.iea.org/weo/docs/weo2012/factsheets.pdf [Accessed on 10/03/2013].

[6] EWEA, *"EU Energy Policy to 2050 - Achieving 80-95 percent emissions reductions"*, European Wind Energy Association, Brussels, 2011. Available at: http://www.ewea.org/fileadmin/ewea_documents/documents/publications/reports/ewea_energy_policy_to_2050.pdf [Accessed on 1/5/2012].

[7] SEAI, *"Energy in Ireland: 1990-2010"*, Sustainable Energy Authority of Ireland, Cork, 2011. Available at: http://www.seai.ie/publications/statistics_publications/EPSSU_publicatio-ns/energy_in_Ireland_1990_-_2010_-_2011_report.pdf [Accessed on 15/09/2011].

[8] R. Saidur, "A review on electrical motors energy use and energy savings," *Renewable and Sustainable Energy Reviews*, vol. 14, no. 3, pp. 877–898, 2010.

[9] J. Duflou, J. Sutherland, D. Dornfeld, C. Herrmann, J. Jeswiet, S. Kara, M. Hauschild, and K. Kellens, "Towards energy and resource efficient manufacturing: A process and systems approach," *CIRP Annals - Manufacturing Technology*, vol. 61, pp. 587–609, 2012.

[10] IEA, *"Key World Energy Statistics"*, OECD/International Energy Agency, Paris, 2012. Available at: http://www.iea.org/publications/freepublications/publication/kwes.pdf [Accessed on 22/11/2012].

[11] C. Herrmann, S. Thiede, S. Kara, and J. Hesselbach, "Energy oriented simulation of manufacturing systems - concept and application," *CIRP Annals - Manufacturing Technology*, vol. 60, no. 1, pp. 45–48, 2011.

[12] S. Bonilla, C. Almeida, B. Gianetti, and D. Huisingh, "The roles of cleaner production in the sustainable development of modern societies," *Journal of Cleaner Production*, vol. 18, pp. 1–5, 2010.

[13] J. Klemes and D. Huisingh, "Economic use of renewable resources, LCA, cleaner batch processes and minimising emissions and wastewater," *Journal of Cleaner Production*, vol. 16, pp. 159–163, 2008.

[14] M. Despeisse, P. Ball, S. Evans, and A. Levers, "Industrial ecology at factory level - a conceptual model," *Journal of Cleaner Production*, vol. 31, pp. 30–39, 2012.

[15] C. Herrmann, S. Suh, G. Bogdanski, A. Zein, J. Cha, J. Um, S. Jeong, and A. Guzman, "Context-aware analysis approach to enhance industrial smart metering," in *proceedings of the 18th CIRP International Conference on Life Cycle Engineering*, pp. 323–328, Braunschweig, 2011.

[16] R. Saidur, N. A. Rahim, H. H. Masjuki, S. Mekhilef, H. W. Ping, and M. F. Jamaluddin, "End-use energy analysis in the Malaysian industrial sector," *Energy*, vol. 34, no. 2, pp. 153–158, 2009.

[17] O. Avram and P. Xirouchakis, "Evaluating the use phase energy requirements of a machine tool system," *Journal of Cleaner Production*, vol. 19, pp. 699–711, 2011.

[18] S. Hu, F. Liu, Y. He, and T. Hu, "An on-line approach for energy efficiency monitoring of machine tools," *Journal of Cleaner Production*, vol. 27, pp. 133–140, 2012.

[19] A. Vijayaraghavan and D. Dornfeld, "Automated energy monitoring of machine tools," *CIRP Annals - Manufacturing Technology*, vol. 59, no. 1, pp. 21–24, 2010.

[20] P. Thollander and M. Ottoson, "Energy management practices in Swedish energy-intensive industries," *Journal of cleaner production*, vol. 18, pp. 1125–1133, 2010.

[21] C. Herrmann and S. Thiede, "Process chain simulation to foster energy efficiency in manufacturing," *CIRP Journal of Manufacturing Science and Technology*, vol. 1, no. 4, pp. 221–229, 2009.

[22] K. Kellens, W. Dewulf, and J. Duflou, "Machine tool oriented ecodesign perspectives based on systematic manufacturing process impact assessment," in *proceedings of the 6th International Symposium on Environmentally Conscious Design and Inverse Manufacturing*, pp. 741–746, Sapporo, 2009.

[23] G. Ingarao, R. Di-Lorenzo, and F. Micari, "Sustainability issues in sheet metal forming processes: an overview," *Journal of Cleaner Production*, vol. 19, pp. 337–347, 2011.

[24] T. Thepsonthi, M. Hamdi, and K. Mitsui, "Investigation into minimal cutting fluid application in high-speed milling of hardened steel using carbide mills," *International Journal of Machine Tools and Manufacture*, vol. 49, pp. 156–162, 2009.

[25] Y. Seow and S. Rahimifard, "A framework for modelling energy consumption within manufacturing systems," *CIRP Journal of Manufacturing Science and Technology*, vol. 4, pp. 258–264, 2011.

[26] P. Jean-Baptiste and R. Ducroux, "Energy policy and climate change," *Energy Policy*, vol. 31, no. 2, pp. 155–166, 2003.

[27] C. C. Lee and C. P. Chang, "Energy consumption and GDP revisited: A panel analysis of developed and developing countries," *Energy Economics*, vol. 29, no. 6, pp. 1206–1223, 2007.

[28] SEAI, *"Energy in Ireland - Key Statistics"*, Sustainable Energy Authority of Ireland, Cork, 2008. Available at: http://www.seai.ie/publications/statistics_publications/EPSSU_publications/energy_in_Ireland_key_statistics/energy_in_Ireland_key_statistics_2008.pdf [Accessed on 15/03/2010].

[29] OPEC, *"World Oil Outlook"*, Organisation of the Petroleum Exporting Countries, Vienna, 2012. Available at: http://www.opec.org/opec_web/downloads/publications/woo2012.pdf [Accessed on 27/06/2013].

[30] IEA, *"World Energy Outlook"*, OECD/International Energy Agency, Paris, 2010. Available at: http://www.iea.org/media/weo2010.pdf [Accessed on 27/11/2011].

[31] R. Wakeford, "And now, fukushima," *Journal of Radiological Protection*, vol. 31, pp. 167–176, 2011.

[32] P. Fairley, "Fukushima's positive impact," *IEEE Spectrum*, 04 April 2011.

[33] F. Manzano-Agugliaro, A. Alcayde, F. Montoya, A. Zapata-Sierra, and C. Gil, "Scientific production of renewable energies worldwide: An overview," *Renewable and Sustainable Energy Reviews*, vol. 18, pp. 134–143, 2013.

[34] EWEA, *"Wind in Power: 2012 European Statistics"*, European Wind Energy Association, Brussels, 2013. Available at: http://www.ewea.org/fileadmin/files/library/publications/statistics/wind_in_power_annual_statistics_2012.pdf [Accessed on 1/06/2013].

[35] GWEC, *"Global Wind Statistics"*, Global Wind Energy Council, Brussels, 2012. Available at: http://www.gwec.net/uploads/2013/02/gwecprstats2012_english.pdf [Accessed on 15/05/2013].

[36] C. Archer and M. Jacobson, "Evaluation of global wind power," *Journal of Geophysical Research*, vol. 110, p. 20, 2005.

[37] EWEA, *"Pure Power, Wind Energy Targets for 2020 and 2030"*, European Wind Energy Association, Brussels, 2009. Available at: http://www.ewea.org/fileadmin/ewea_documents/documents/publications/reports/pure_power_full_report.pdf [Accessed on 1/05/2012].

[38] EIA, *"Annual Energy Outlook 2013"*, United States Energy Information Administration, Washington, DC, 2013. Available at: http://www.eia.gov/forecasts/aeo/ [Accessed on 18/07/2013].

[39] D. Turney and V. Fthenakis, "Environmental impacts from the installation and operation of large-scale solar plants," *Renewable and Sustainable Energy Reviews*, vol. 15, no. 6, pp. 3261–3270, 2011.

[40] O. Negro, F. Alkemande, and M. Hekkert, "Why does renewable energy diffuse so slowly? a review of innovation system problems," *Renewable and Sustainable Energy Reviews*, vol. 16, pp. 3836–3846, 2012.

[41] SEAI, *"Renewable Energy in Ireland"*, Sustainable Energy Authority of Ireland, Cork, 2010. Available at: http://www.seai.ie/publications/statistics_publications/renewable_energy_in_Ireland/re_in_Ire_2010update.pdf [Accessed on 22/06/2011].

[42] EPA, *"The Lean and Energy Toolkit, Achieving Process Excellence Using Less Energy"*, United States Environmental Protection Agency, Washington, DC, 2007. Available at: http://www.epa.gov/lean/environment/toolkits/energy [Accessed on 10/05/2011].

[43] A. Zein, *Sustainable Production, Life Cycle Engineering and Management - Transition Towards Energy Efficient Machine Tools.* Springer Berlin Heidelberg, 2011.

[44] ISO, *ISO 50001 - Energy Management Systems: Requirements with Guidance for Use*, International Standards Organisation, 2011. Available at: http://www.iso.org/ [Accessed on 10/05/2012].

[45] J. M. Cullen and J. M. Allwood, "The efficient use of energy: Tracing the global flow of energy from fuel to service," *Energy Policy*, vol. 38, no. 1, pp. 75–81, 2010.

[46] IEA, *"Worldwide Trends in Energy Use and Efficiency"*, OECD/International Energy Agency, Paris, 2008. Available at: http://www.iea.org/ [Accessed on 20/01/2011].

[47] D. A. Muller, F. M. A. Marechal, T. Wolewinski, and P. J. Roux, "An energy management method for the food industry," *Applied Thermal Engineering*, vol. 27, no. 16, pp. 2677–2686, 2007.

[48] B. Taylor, "Encouraging industry to assess and implement cleaner production measures," *Journal of cleaner production*, vol. 14, pp. 601–609, 2006.

[49] P. Rohdin and P. Thollander, "Barriers to and driving forces for energy efficiency in the non-energy intensive manufacturing industry in Sweden," *Energy*, vol. 31, no. 12, pp. 1836–1844, 2006.

[50] K. Gillingham, R. G. Newell, and K. Palmer, "Energy efficiency economics and policy, NBER working paper no. 15031," in *the National Bureau of Economic Research*, 2009.

[51] M. Altmann, J. Michalski, A. Brenninkmeijer, and P. Tisserand, *Overview of Energy Efficiency measures of European Industry.* European Parliment, Directorate-General for Internal Policies, 2010.

[52] ADEME, *"Energy Efficiency Trends and Policies in the Industrial Sector in the EU-27", The French Environment and Energy Management Agency*, 2009. Available at: http://www.odyssee-indicators.org/publications/pdf/brochures/industry.pdf [Accessed on 17/09/2010].

[53] A. Thumann, W. J. Younger, and T. Niehus, *Handbook of energy audits.* Fairmont Press; Distributed by CRC Press/Taylor and Francis, 2010.

[54] P. Solding and P. Thollander, "Increased energy efficiency in a swedish iron foundry through the use of discrete event simulation," in *proceedings of the 2006 Winter Simulation Conference*, pp. 1971–1976, California, 2006.

[55] P. Sandberg and M. Solderstrom, "Industrial energy efficiency: the need for investment decision support from a manager perspective," *Energy Policy*, vol. 31, no. 15, pp. 1623–1634, 2003.

[56] H. de Groot, E. Verhoef, and P. Nijkamp, "Energy saving by firms: decision-making, barriers and policies," *Energy Economics*, vol. 23, no. 6, pp. 717–740, 2001.

[57] B. Mecrow and A. Jack, "Efficiency trends in electric machines and drives," *Energy Policy*, vol. 36, no. 12, pp. 4336–4341, 2008.

[58] S. Thiede, G. Posselt, and C. Herrmann, "SME appropriate concept for continuously improving the energy and resource efficiency in manufacturing companies," *CIRP Journal of Manufacturing Science and Technology*, vol. 6, pp. 204–211, 2013.

[59] S. Kara, G. Bogdanski, and W. Li, "Electricity metering and monitoring in manufacturing systems," in *Proceedings of the 18th CIRP International Conference on Life Cycle Engineering*, pp. 1–10, Braunschweig, 2011.

[60] S. Rahimifard, Y. Seow, and T. Childs, "Minimising embodied product energy to support energy efficient manufacturing," *CIRP Annals - Manufacturing Technology*, vol. 59, no. 1, pp. 25–28, 2010.

[61] SEAI, *"Electricity and Gas Prices in Ireland"*, Sustainable Energy Authority of Ireland, Cork, 2011. Available at: http://www.seai.ie/publications/statistics_publications/EPSSU_publications/electricity_and_gas_prices/ [Accessed on 11/01/2012].

[62] J. Hesselbach, C. Hermann, R. Detzer, L. Martin, S. Thiede, and B. Ludedmann, "Energy efficiency through optimised coordination of production and technical building services," in *proceedings of the 15th CIRP International Conference on life Cycle Engineering*, Sydney, 2009.

[63] J. Kopac and F. Pusavec, "Sustainability spirit in manufacturing/machining processes," in *proceedings of the 2009 Portland International Conference on Management of Engineering and Technology*, pp. 1197–1205, Oregon, 2009.

[64] P. Naughton, "New tool for targeting energy improvements in semiconductor manufacturing equipment," in *proceedings of the 17th IEEE/SEMI Advanced Semiconductor Manufacturing Conference*, pp. 428–432, Massachusetts, 2006.

[65] T. Smith and J. Schmidt, "Northstar initiative: Global supply-chain energy efficiency in small and medium sized enterprises," tech. rep., University of Minnesota, December 2007.

[66] S. Kara and S. Ibbotson, "Embodied energy of manufacturing supply chains," *CIRP Journal of Manufacturing Science and Technology*, vol. 4, no. 3, pp. 317–323, 2011.

[67] F. Vanek and Y. Sun, "Transportation versus perishability in life cycle energy consumption: a case study of the temperature controlled food product supply chain," *Transportation research part D: Transport and environment*, vol. 13, no. 6, pp. 383–391, 2008.

[68] J. Pearse, S. Johnson, and G. Grant, "3D-mapping optimisation of embodied energy of transportation," *Resources, Conservation, and Recycling*, vol. 51, no. 2, pp. 435–453, 2007.

[69] T. Nuortio, J. Kytojoki, H. Niska, and O. Braysy, "Improved route planning and scheduling of waste collection and transport," *Expert systems with applications*, vol. 30, no. 2, pp. 223–232, 2006.

[70] R. Pachero, J. Ordez, and G. Martinez, "Energy efficient design of buildings: A review," *Renewable and Sustainable Energy Reviews*, vol. 16, no. 6, pp. 3559–3573, 2012.

[71] E. Mathews, C. Botha, D. Arndt, and A. Malan, "HVAC control strategies to enhance comfort and minimise energy usage," *Energy and Buildings*, vol. 8, no. 3, pp. 853–863, 2001.

[72] M. Fasiuddin and I. Budaiwi, "HVAC system strategies for energy conservation in commercial buildings in saudi arabia," *Energy and Buildings*, vol. 43, no. 12, pp. 3457–3466, 2011.

[73] W. R. Ryckaert, C. Lootens, J. Geldof, and P. Hanselaer, "Criteria for energy efficient lighting in buildings," *Energy and Buildings*, vol. 42, no. 3, pp. 341–347, 2010.

[74] H. J. Han, Y. I. Jeon, S. H. Lim, W. W. Kim, and K. Chen, "New developments in illumination, heating and cooling technologies for energy-efficient buildings," *Energy*, vol. 35, no. 6, pp. 2647–2653, 2010.

[75] BSI, *"Energy Performance of Buildings - Energy Requirements for lighting"*, British Standards Institution, 2006. Available at: http://www.bsigroup.com/ [Accessed on 1/04/2011].

[76] L. Harvey, "Reducing energy consumption in the buildings sector: Measures, costs, and examples," *Energy Efficiency*, vol. 2, no. 2, pp. 139–163, 2009.

[77] K. Vikhorev, R. Greenough, and N. Brown, "An advanced energy management framework to promote energy awareness," *Journal of Cleaner Production*, vol. 43, pp. 103–112, 2013.

[78] C. F. Murphy, J. P. Laurent, and D. T. Allen, "Life cycle inventory development for wafer fabrication in semiconductor manufacturing," in *proceedings of the 2003 IEEE International Symposium on Electronics and the Environment*, pp. 276–281, Massachusetts, 2003.

[79] T. Gutowski, G. Dahmus, and A. Thiriez, "Electrical energy requirements for manufacturing processes," in *proceedings of the 13th CIRP International Conference on Life Cycle Engineering*, pp. 623–628, Leuven, 2006.

[80] A. Pechmann and I. Schoeller, "Optimising energy costs by intelligent production scheduling," in *proceedings of the 18th CIRP International Conference on Life Cycle Engineering*, pp. 293–298, Braunschweig, 2011.

[81] T. Devoldere, W. Dewulf, W. Deprez, B. Willems, and J. Duflou, *Improvement Potential for Energy Consumption in Discrete Part Production Machines*, pp. 311–316. Springer London, 2007.

[82] F. Jovane, Y. Koren, and C. Boer, "Present and future of flexible automation: Towards new paradigms," *CIRP Annals - Manufacturing Technology*, vol. 52, no. 2, pp. 543–560, 2003.

[83] H. W. Lau, E. M. Cheng, C. M. Lee, and G. S. Ho, "A fuzzy logic approach to forecast energy consumption change in a manufacturing system," *Expert Systems with Applications*, vol. 34, no. 3, pp. 1813–1824, 2008.

[84] J. Dahmus and T. Gutowski, "An environmental analysis of machining," in *proceedings of the 2004 ASME International Mechanical Engineering Conference*, California, 2004.

[85] M. F. Rajemi, P. T. Mativenga, and A. Aramcharoen, "Sustainable machining: selection of optimum turning conditions based on minimum energy considerations," *Journal of Cleaner Production*, vol. 18, no. 10-11, pp. 1059–1065, 2010.

[86] A. De-Filippi, R. Ippolito, and G. Micheletti, "NC machine tools as electric energy users," *CIRP Annals - Manufacturing Technology*, vol. 30, no. 1, pp. 323–326, 1981.

[87] S. Anderberg and S. Kara, "Energy and cost efficiency in CNC machining," in *proceedings of the 7th International CIRP Conference on Sustainable Manufacturing*, Chennai, 2009.

[88] N. Diaz, E. Redelsheimer, and D. Dornfeld, "Energy consumption characterisation and reduction strategies for milling machine tool use," in *proceedings of the 18th CIRP International Conference on Life Cycle Engineering*, pp. 263–267, Braunschweig, 2011.

[89] F. Draganescu, M. Gheoghe, and C. Doicin, "Models of machine tool efficiency and specific consumed energy," *Journal of Materials Processing Technology*, vol. 141, pp. 9–15, 2003.

[90] D. Fratila, "Evaluation of near dry machining effects on gear milling process efficiency," *Journal of Cleaner Production*, vol. 17, pp. 839–845, 2009.

[91] F. Pusavec, P. Krajnik, and J. Kopac, "Transitioning to sustainable production - part I: application on machining technologies," *Journal of Cleaner Production*, vol. 18, no. 2, pp. 174–184, 2010.

[92] A. Dietmair and A. Verl, "Energy consumption forecasting and optimisation for tool machines," *2009 Modern Machinery Science Journal*, pp. 63–67, 2009.

[93] Siemens Group, *Sinumerik Ctrl-Energy*, 2010. Available at: //http:www.automation.siemens.com/ [Accessed on 15/01/2012].

[94] M. Sulitka, L. Novotny, J. Sveda, P. Strakos, J. Hudec, J. Smolik, and P. Vlach, "Machine tool lightweight design and control techniques," *2008 Modern Machinery Science Journal*, pp. 29–34, 2008.

[95] M. Mori, M. Fujishima, Y. Inamusa, and Y. Oda, "A study on energy efficiency improvement for machine tools," *CIRP Annals - Manufacturing Technology*, vol. 60, pp. 145–148, 2011.

[96] G. Byrne, D. Dornfeld, I. Inasaki, G. Ketteler, W. König, and R. Teti, "Tool condition monitoring - the status of research and industrial application," *CIRP Annals - Manufacturing Technology*, vol. 44, pp. 541–567, 1995.

[97] Y. Altintas, "Prediction of cutting forces and tool breakage in milling from feed drive current measurements," *Transactions of the ASME Journal of Engineering for Industry*, vol. 114, pp. 386–392, 1992.

[98] P. Bhattacharyya, D. Sengupta, S. Mukhopadhyay, and A. Chattopadhyay, "On-line tool condition monitoring in face milling using current and power signals," *International Journal of Produciton Research*, vol. 46, pp. 1187–1201, 2008.

[99] N. Diaz, M. Helu, A. Jarvis, D. Tonissen, S. amd Dornfeld, and R. Schlosser, "Strategies for minimum energy operation for precision machining," in *proceedings of the MTTRF Annual Meeting*, Shanghai, 2009.

[100] E. Abele, Y. Altintas, and C. Brecher, "Machine tool spindle units," *CIRP Annals - Manufacturing Technology*, vol. 59, pp. 781–802, 2010.

[101] S. Chen, Y. Juan, C. Tang, C. Chang, and T. Chen, "Analysis of the harmonic losses and bearing load for motorised high speed spindles," in *proceedings of the 17th IEEE Conference on Industrial Engineering and Engineering Management*, pp. 772–777, Xiamen, 2010.

[102] G. Wakelih, "Harmonics in rotating machines," *Electric power systems research*, vol. 66, pp. 31–37, 2003.

[103] D. Dornfeld, "Standards for environmental performance in manufacturing," 2010. Available at: http://www.environmentalleader.com/, [Accessed on 28/07/2012].

[104] CECIMO, *"Report on the drivers of growth in the European machine tool industry"*, European Association of the Machine Tool Industries, Brussels, 2010. Available at: http://www.cecimo.eu/, [Accessed on 23/02/2013].

[105] D. Hagemann, "Status of ISO/TC39/WG12," *1st stakeholder meeting on machine tools and related machinery*, Brussels, July, 2012.

[106] C. Herrmann, L. Bergmann, S. Thiede, and A. Zein, "Energy labels for production machines - an approach to facilitate energy efficiency in production systems," in *proceedings of the 40th CIRP International Seminar on Manufacturing Systems*, Liverpool, 2007.

[107] K. Schischke, E. Hohwieler, R. Feitscher, J. Konig, S. Kreuschner, P. Wilpert, and N. Nissen, "Energy using product group analysis, Lot 5: Machine tools and related machinery," *Task 1 report*, Berlin, February, 2011.

[108] D. Pigosso, E. Zanette, A. Filho, A. Ometto, and F. Rozenfeld, "Ecodesign methods focused on remanufacturing," *Journal of Cleaner Production*, pp. 21–31, 2009.

[109] E. Westkamper and L. Alting, "Life cycle management and assessment: Approaches and visions towards sustainable manufacturing," *CIRP Annals - Manufacturing Technology*, vol. 49, no. 2, pp. 501–526, 2000.

[110] S. Kara, S. Manmek, and C. Herrmann, "Global manufacturing and the embodied energy of products," *CIRP Annals - Manufacturing Technology*, vol. 59, no. 1, pp. 29–32, 2010.

[111] J. L. Sullivan, "Life cycle inventory of a generic U.S. family sedan - overview of results of the USCAR AMP project," in *proceedings of the 1998 Total Life Cycle Meeting*, pp. 114–122, Graz, 1998.

[112] T. Gutowski, "The carbon and energy intensity of manufacturing," in *proceedings of the 40th CIRP International Seminar on Manufacturing Systems*, Liverpool, 2007.

[113] Y. Umeda, S. Takata, F. Kimura, T. Tomiyama, J. Sutherland, S. Kara, C. Herrmann, and J. Duflou, "Toward integrated product and process life cycle planning - an environmental perspective," *CIRP Annals - Manufacturing Technology*, vol. 61, pp. 681–702, 2012.

[114] H. Cao, H. Li, H. Cheng, Y. Luo, R. Yin, and Y. Chen, "A carbon efficiency approach for life-cycle carbon emissions characteristics of machine tools," *Journal of Cleaner Production*, vol. 37, pp. 19–28, 2012.

[115] B. Linke, Y. Huang, and D. Dornfeld, "Establishing greener products and manufacturing processes," *International Journal of Precision Engineering and Manufacturing*, vol. 13, no. 7, pp. 1029–1036, 2012.

[116] J. Kelly Kissock and C. Eger, "Measuring industrial energy savings," *Applied Energy*, vol. 85, no. 5, pp. 347–361, 2008.

[117] A. De-Filippi, R. Ippolito, and G. Micheletti, "Forecast of the electric energy requirement in a mechanical plant by using a stochastic model," *CIRP Annals - Manufacturing Technology*, vol. 29, no. 1, pp. 285–288, 1980.

[118] S. Kara and W. Li, "Unit process energy consumption models for material removal processes," *CIRP Annals - Manufacturing Technology*, vol. 60, no. 1, pp. 37–40, 2011.

[119] R. Larek, E. Brinksmeier, D. Meyer, T. Pawletta, and O. Hagendorf, "A discrete-event simulation approach to predict power consumption in machining processes," *Production Engineering*, vol. 5, no. 5, pp. 575–579, 2011.

[120] S. Wang, C. Yan, and F. Xao, "Quantitative energy performance assessment methods for existing buildings," *Energy and Buildings*, vol. 55, pp. 873–888, 2012.

[121] D. Gordic, M. Babic, N. Jovicic, V. Sustersic, D. Koncalovic, and D. Jelic, "Development of energy management system - case study of serbian car manufacturer," *Energy Conversion and Management*, vol. 51, no. 12, pp. 2783–2790, 2010.

[122] SEAI, *"I.S. EN 16001:2009, Energy Management Systems - Requirements with Guidance for Use"*, Sustainable Energy Authority of Ireland, Cork, 2009. Available at: http://www.seai.ie/your_business/energy_agreements/IS393_energy_management_systems/EN160001_technical_guideline.pdf [Accessed on 13/03/2010].

[123] M. H. Bollen, "What is power quality?," *Electric Power Systems Research*, vol. 66, no. 1, pp. 5–14, 2003.

[124] W. Koon, "Current sensing for energy metering," in *proceedings of the International IC China Conference and the Embedded Systems Conferences*, Shanghai, 2002.

[125] S. Ziegler, R. Woodward, H. Iu, and L. Borle, "A review of current sensing techniques," *IEEE Sensors Journal*, vol. 9, no. 4, pp. 354–376, 2009.

[126] P. Ripka, "Electric current sensors: a review," *Measurement Science and Technology*, vol. 21, no. 11, pp. 112001–112024, 2010.

[127] W. McLyman, "Reviewing current transformers and current transducers," in *proceedings of the 2007 Electrical Insulation Conference and Electrical Manufacturing Expo.*, pp. 360–365, Tennessee, 2007.

[128] IEEE, *"*IEEE *1159 - Recommended Practice for Monitoring Electric Power Quality"*, Institute of Electrical and Electronics Engineers, 1995. Available at: http://www.ieeexplore.ieee.org/ [Accessed on 15/04/2013].

[129] D. Saxena, K. Verma, and S. Singh, "Power quality event classification: an overview and key issues," *International Journal of Engineering, Science and Technology*, vol. 2, no. 3, 2010.

[130] Y. Seow, *A framework for modelling embodied product energy to support energy efficient manufacturing.* PhD thesis, Loughborough University, 2011.

[131] S. Bhattacharyya, J. Myrzik, and W. Kling, "Consequences of poor power quality - an overview," in *proceedings of the 42nd International Universities Power Engineering Conference*, pp. 651–656, Brighton, 2007.

[132] J. Bickel, "Selecting the right power quality meter," *Electrical construcion and maintenance*, vol. 2, pp. 46–51, 2003.

[133] T. Hoevanaars, K. LeDoux, and M. Colosino, "Interpreting IEEE STD 519 and meeting its harmonic limits in VFD applications," in *proceedings of the 50th IEEE Petroleum and Chemical Industry Conference*, pp. 145–150, Texas, 2003.

[134] A. Delle-Femine, D. Gallo, C. Landi, and M. Luiso, "Power quality monitoring instrument with FPGA transducer," *IEEE Transactions on instrumentationa and measurement*, vol. 58, pp. 3149–3158, 2009.

[135] S. R. Shaw, *System identification techniques and modeling for nonintrusive load diagnostics.* PhD thesis, Massachusetts Institute of Technology, 2000.

[136] H. Pihala, "Non-intrusive appliance load monitoring system based on a modern kWh-meter." Technical Research Centre of Finland, Licentiate Thesis, 1998.

[137] G. W. Hart, "Nonintrusive appliance load monitoring," *Proceedings of the IEEE*, vol. 80, no. 12, pp. 1870–91, 1992.

[138] S. Drenker and A. Kader, "Nonintrusive monitoring of electric loads," *IEEE Computer Applications in Power*, vol. 12, no. 4, pp. 47–51, 1999.

[139] A. G. Ruzzelli, C. Nicolas, A. Schoofs, and G. P. O'Hare, "Real-time recognition and profiling of appliances through a single electricity sensor," in *proceedings of the 7th Annual IEEE Communications Society Conference on Sensor Mesh and Ad Hoc Communications and Networks*, pp. 1–9, Massachusetts, 2010.

[140] S. B. Leeb, *A conjoint pattern recognition approach to nonintrusive load monitoring.* PhD thesis, Massachusetts Institute of Technology, 1993.

[141] H. H. Chang, K. L. Chen, Y. P. Tsai, and W. J. Lee, "A new measurement method for power signatures of nonintrusive demand monitoring and load identification," *IEEE Transactions on Industry Applications*, vol. 48, pp. 764–771, 2012.

[142] Y. H. Lin and M. S. Tsai, "Applications of hierarchical support vector machines for identifying load operation in nonintrusive load monitoring systems," in *proceedings of the 2011 World Congress on Intelligent Control and Automation*, pp. 688–693, Taipei, 2011.

[143] C. Laughman, L. Kwangduk, R. Cox, S. Shaw, S. Leeb, L. Norford, and P. Armstrong, "Power signature analysis," *IEEE Power and amp; Energy Magazine*, vol. 1, no. 2, pp. 56–63, 2003.

[144] C. Hsueh-Hsien, L. Ching-Lung, and Y. Hong-Tzer, "Load recognition for different loads with the same real power and reactive power in a non-intrusive load-monitoring system," in

proceedings of the 12th International Conference on Computer Supported Cooperative Work in Design, pp. 1122–7, Xi'an, 2008.

[145] J. G. Roos, I. E. Lane, E. C. Botha, and G. P. Hancke, "Using neural networks for non-intrusive monitoring of industrial electrical loads," in *proceedings of the 1994 IEEE Instrumentation and Measurement Technology Conference*, vol. 3, pp. 1115–1118, Hamamatsu, 1994.

[146] D. C. Robertson, O. I. Camps, J. S. Mayer, and W. B. Gish, "Wavelets and electromagnetic power system transients," *IEEE Transactions on Power Delivery*, vol. 11, no. 2, pp. 1050–8, 1996.

[147] A. I. Cole and A. Albicki, "Data extraction for effective non-intrusive identification of residential power loads," in *proceedings of the 1998 IEEE Instrumentation and Measurement Technology Conference*, vol. 2, pp. 812–815, Minnesota, 1998.

[148] S. R. Shaw and C. R. Laughman, "A kalman-filter spectral envelope preprocessor," *IEEE Transactions on Instrumentation and Measurement*, vol. 56, no. 5, pp. 2010–17, 2007.

[149] S. R. Shaw, S. B. Leeb, L. K. Norford, and R. W. Cox, "Nonintrusive load monitoring and diagnostics in power systems," *IEEE Transactions on Instrumentation and Measurement*, vol. 57, no. 7, pp. 1445–1454, 2008.

[150] L. Farinaccio and R. Zmeureanu, "Using a pattern recognition approach to disaggregate the total electricity consumption in a house into the major end-users," *Energy and Buildings*, vol. 30, no. 3, pp. 245–59, 1999.

[151] M. Baranski and J. Voss, "Genetic algorithm for pattern detection in NIALM systems," in *proceedings of the 2004 IEEE International Conference on Systems, Man and Cybernetics*, pp. 3462–8, The Hague, 2004.

[152] D. Srinivasan, W. S. Ng, and A. C. Liew, "Neural-network-based signature recognition for harmonic source identification," *IEEE Transactions on Power Delivery*, vol. 21, no. 1, pp. 398–405, 2006.

[153] N. Kwak and C. Chong-Ho, "Input feature selection for classification problems," *IEEE Transactions on Neural Networks*, vol. 13, no. 1, pp. 143–59, 2002.

[154] M. Kudo and J. Sklansky, "Comparison of algorithms that select features for pattern classifiers," *Pattern Recognition*, vol. 33, no. 1, pp. 25–41, 2000.

[155] L. K. Norford and S. B. Leeb, "Non-intrusive electrical load monitoring in commercial buildings based on steady-state and transient load-detection algorithms," *Energy and Buildings*, vol. 24, no. 1, pp. 51–64, 1996.

[156] S. B. Leeb, S. R. Shaw, and J. L. Kirtley Jr, "Transient event detection in spectral envelope estimates for nonintrusive load monitoring," *IEEE Transactions on Power Delivery*, vol. 10, no. 3, pp. 1200–1210, 1995.

[157] S. Mekid, N. Schlegel, N. Aspragathos, and R. Teti, "Foresight formulation in innovative production, automation and control systems," *Foresight*, vol. 9, pp. 35–47, 2007.

[158] A. Cannata, M. Gerosa, and M. Taish, "SOCRADES: A framework for developing intelligent systems in manufacturing," in *proceedings of the 5th IEEE Conference on Industrial Engineering and Engineering Management*, pp. 1904–1908, Bangkok, 2008.

[159] R. Teti, K. Jemielniak, G. O'Donnell, and D. Dornfeld, "Advanced monitoring of machining operations," *CIRP Annals - Manufacturing Technology*, vol. 59, pp. 717–739, 2010.

[160] D. Kalla, J. Twomey, and M. Overcash, "Wichita State-MR4: Report on unit process life cycle inventory," tech. rep., Wichita State University, August 2009.

[161] N. Weinert, S. Chiotellis, and G. Seliger, "Methodology for planning and operating energy-efficient production systems," *CIRP Annals - Manufacturing Technology*, vol. 60, no. 1, pp. 41–44, 2011.

[162] A. Deshpande, J. Snyder, and D. Scherrer, "Feature level energy assessments for discrete part manufacturing," in *proceedings of the 2011 North American Manufacturing Research Institution SME Conference*, Pennsylvania, 2011.

[163] S. Chiotellis and M. Grismajer, "Analysis of electrical power data streams in manufacturing," in *proceedings of the 19th CIRP International Conference on life Cycle Engineering*, Berkeley, 2012.

[164] C. Pang, C. Le, O. Gan, X. Chee, D. Chang, M. Luo, H. Chan, and F. Lewis, "Intelligent energy audit and machine management for energy-efficient manufacturing," in *proceedings of the 5th International IEEE Conference on Cybernatics and Intelligent Systems*, pp. 142–147, Hangzhou, 2011.

[165] C. Bishop, *Pattern Recognition and Machine Learning.* New York: Springer Science and Business Media, 2006.

[166] C. M. Bishop, *Neural Networks for Pattern Recognition.* Oxford: Oxford University Press, 1995.

[167] A. K. Jain, R. P. Duin, and M. Jianchang, "Statistical pattern recognition: A review," *IEEE Transactions on Pattern Analysis and Machine Intelligence*, vol. 22, no. 1, pp. 4–37, 2000.

[168] M. Nadler and P. E. Smith, *Pattern Recognition Engineering.* Wiley-interscience, 1993.

[169] P. Cunningham, "UCD-CSI-2007-7:Report on dimension reduction," tech. rep., University College Dublin, August 2007.

[170] I. K. Fodor, "A survey on dimension reduction techniques," tech. rep., Center for Applied Scientific Computing, Lawrence Livermore National Laboratory, June 2002.

[171] R. Shalkoff, *Pattern Recognition, Statistical, Structural and Neural Approaches.* John Wiley & Sons, 1992.

[172] R. Duda, P. Hart, and D. Stork, *Pattern Classification.* Wiley-Interscience, 2nd ed., 2000.

[173] F. Tsung, "Statistical monitoring and diagnosis of automatic controlled processes using dynamic PCA," *International Journal of Production Research*, vol. 38, no. 3, pp. 625–637, 2000.

[174] G. Halligan and S. Jagannathan, "PCA-based fault isolation and prognosis with application to pump," *The International Journal of Advanced Manufacturing Technology*, vol. 55, no. 5-8, pp. 699–707, 2011.

[175] C. Elkan, "UCSD:Report on nearest neighbour classification," tech. rep., University of California, San Diego, January 2011.

[176] P. He and J. Wang, "Fault detection using the k-nearest neighbour rule for semiconductor manufacturing processes," *IEEE Transactions on Semiconductor Manufacturing*, vol. 20, pp. 345–354, 2007.

[177] D. Li and T. Liao, "Applications of fuzzy k-nn in weld recognition and tool failure monitoring," in *proceedings of the 28th Southeastern Symposium on System Theory*, pp. 222–226, Los Angeles, 1997.

[178] A. Webb, *Statistical pattern recognition.* West Sussex, UK: John Wiley & Sons Ltd., 2002.

[179] J. Duflou, K. Kellens, and W. Dewulf, "Unit process impact assessment for discrete part manufacturing: A state of the art," *CIRP Journal of Manufacturing Science and Technology*, vol. 4, no. 2, pp. 129–135, 2011.

[180] K. Bunse, M. Vodicka, P. Schonsleben, M. Brulhart, and F. Ernst, "Integrating energy efficiency performance in production management - gap analysis between industrial needs and scientific literature," *Journal of Cleaner Production*, vol. 19, pp. 667–679, 2011.

[181] UNIDO, *"Global Industrial Energy Efficiency Benchmarking Report,* United Nations Industrial Development Organisation, Vienna, 2010. Available at: http://www.unido.org/ [Accessed on 25/05/2011].

[182] P. Ball, M. Despeisse, S. Evans, and A. Levers, "Mapping manufacturing material, energy and waste process flows," in *proceedings of the 7th Global Conference on Sustainable Manufacturing*, pp. 349–354, Chennai, 2009.

[183] V. Balogun and P. Mativenga, "Modelling of direct energy requirements in mechanical machining processes," *Journal of Cleaner Production*, vol. 41, pp. 179–186, 2013.

[184] H. Gotze, H. Koriath, A. Kolesnikov, R. Lindner, and J. Paetzold, "Integrated methodology for the evaluation of the energy - and cost-effectiveness of machine tools," *CIRP Journal of Manufacturing Science and Technology*, vol. 5, pp. 151–163, 2012.

[185] N. Krishnan and P. Sheng, "Environmental verus conventional planning for machined components," *CIRP Annals - Manufacturing Technology*, vol. 49, no. 1, pp. 363–366, 2000.

[186] M. Sarwar, M. Persson, H. Hellbergh, and J. Haider, "Measurement of specific cutting energy for evaluating the efficiency of bandsawing different workpiece materials," *International Journal of Machine Tools and Manufacture*, vol. 49, no. 12-13, pp. 958–965, 2009.

[187] Hurco, *Hurco* VM*2 machining centre documentation - maintenance and safety manual*, 2009.

[188] T. Behrendt, A. Zein, and S. Min, "Development of an energy consumption monitoring procedure for machine tools," *CIRP Annals - Manufacturing Technology*, vol. 61, no. 1, pp. 43–46, 2012.

[189] A. Blondel, "Measurements of the energy of polyphase currents," *International Electrical Congress, Chicago*, pp. 112–117, 1893.

[190] S. Karni, *Applied Circuit Analysis*. New York: John Wiley & Sons, 1988.

[191] J. Kang, "White paper on multi-pulse rectifier solutions for input harmonics mitigation," tech. rep., Yaskawa, Inc., December 2005.

[192] B. Singh, G. Bhuvaneswari, and V. Garg, "A novel polygon based 18-pulse ac-dc converter for vector controlled induction motor drives," *IEEE Transactions on Power Electronics*, vol. 22, pp. 488–497, 2007.

[193] Y. Altintas, A. Verl, C. Brecher, L. Uriarte, and G. Pritschow, "Machine tool feed drives," *CIRP Annals - Manufacturing Technology*, vol. 60, pp. 779–796, 2011.

[194] KAP, *"Knowledge, Awareness, and Prediction (*KAP*) of Man, Machine, Material, and Method"*, Sap Research Dresden, 2013. Available at: http://www.kap-project.eu/index.php?id=340 [Accessed on 15/05/2013].

[195] G. Lin, S. Lee, J. Hsu, and W. Jih, "Applying power meters for appliance recognition on the electric panel," in *proceedings of the 5th* IEEE *Conference on Industrial Electronics and Applications*, pp. 2254–2259, Taichung, 2010.

[196] M. Figueiredo, A. Almeida, and B. Ribeiro, "An experimental study on electrical signature identification of non-intrusive load monitoring (NILM) systems," in *proceedings of the 2011 International Conference on Adaptive and Natural Computing Algorithms*, pp. 31–40, Ljubljana, 2011.

[197] L. Smith, "University of Otago: A tutorial on principle component analysis," tech. rep., University of Otago, Februaury 2002.

[198] M. Tsai and Y. Lin, "Development of a non-intrusive monitoring technique for appliance identification in electricity energy management," in *proceedings of the 2011 International Conference on Advanced Power System Automation and Protection*, pp. 108–113, Beijing, 2011.

[199] P. Cunningham, "UCD-CSI-2007-4: Report on k-nearest neighbour classifiers," tech. rep., University College Dublin, March 2007.

[200] C. Leys, "Detecting outliers: Do not use standard deviation around the mean, use absolute deviation around the median," *Journal of Experimental Social Pyschology*, 2013. http://dx.doi.org/10.1016/j.jesp.2013.03.013.

[201] K. Adekeye and P. Azubuike, "Derivation of the limits for control chart using the median absolute deviation for monitoring non-normal process," *Journal of Mathematics and Statistics*, vol. 8, pp. 37–41, 2012.

Appendix A

Intelligent energy sensor matlab code

```
close all;
clear all;
clc;
tic;
%%% DATA FILE
data01 = dlmread('wkp2dataset.txt');
%%% LOADING RAW DATA
len01 = length(data01);
time01 = data01(:,1);
I1_val01 = data01(:,7);
I2_val01 = data01(:,6);
I3_val01 = data01(:,5);
V1_val01 = data01(:,2);
V2_val01 = data01(:,3);
V3_val01 = data01(:,4);
I1_rms_val01 = data01(:,10);
I2_rms_val01 = data01(:,9);
I3_rms_val01 = data01(:,8);
%%% CALIBRATION FACTORS
ical = 148.17;
vcal = 3.03;
%%% CALIBRATED DATA
I101 = ical.*I1_val01;
I201 = ical.*I2_val01;
I301 = ical.*I3_val01;
I1_rms01 = ical.*I1_rms_val01;
I2_rms01 = ical.*I2_rms_val01;
I3_rms01 = ical.*I3_rms_val01;
V1_01 = vcal.*V1_val01;
V2_01 = vcal.*V2_val01;
V3_01 = vcal.*V3_val01;
%%% POWER CALCULATIONS
V3_01neg = V3_01.*-1; %% V3 negative
W1_01 = V2_01.*I101; %% Wattmeter 1
W2_01 = V3_01neg.*I301; %% Wattmeter 2
Power_01 = W1_01 + W2_01; %% Both Wattmeters
Powerrms_01 = rmseod(Power_01,100,0,1); %% RMS power
save = Powerrms_01';
%%% RMS POWER WAVEFORM PLOT
figure(1)
plot(Powerrms_01); hold on;
title('Power - workpiece test')
%%% PCA VARIABLES
A = dlmread('traindata_adj.txt'); %% Training data matrix
normal = dlmread('meandata.txt');  %% Normalisation mean vector
%%% PCA CALCULATION
A1 = A';
covariance_matrix = cov(A);
[eigenvectors eigenvalues] = eig(covariance_matrix);
p1 = eigenvectors(:,7);
p2 = eigenvectors(:,6);
p3 = eigenvectors(:,5);
feature_vect2 = [p1 p2]; %% Two dimensional transformation vector
feature_vector2 = feature_vect2'; %% Transposing two dimensional
transformation vector
final_data2D = feature_vector2 * A1;  %% Transformed training data set
b1 = final_data2D(1,:);
```

```
b2 = final_data2D(2,:);
%%% READ CLASS LABELS
fileID = fopen('datalabels.txt','rt');
labels_b = textscan(fileID,'%s %s %s %s %s %s %s %s %s %s %s %s %s %s %s %s %s
%s %s %s %s %s %s %s %s %s %s %s %s %s %s %s %s %s %s %s %s %s %s %s %s %s %s
%s %s %s %s %s %s %s %s','CollectOutput',true); %% loading class labels
fclose(fileID);
newdat = cat(1,labels_b{1});
%%% Stabilisation periods
stables = dlmread('stables.txt');  %% Stabilisation values for spindle
activations
%%% SETTING CONDITIONS
test_length = length(Powerrms_01);
t1=[0:1:length(Powerrms_01(1:test_length))];
t =t1';
event_start = [];
event_stop = [];
change_start = 0;
change_stop = 0;
location = [];
distances = [];
slope_store = [];
Fs = 2000;
activations = [];
%%% SETTING MAD CONDITIONS
store = [];
machining = 0;
cutting = [];
cutting_power = [];
spin_off =[];
slope_set = [];
RT_stop = [];
run_time = [];
run_time_duration = [];
run_time_power = [];
rapid_accel = 0;
spindle_off = 0;
change = 0;
%%% NAMING CLASSES
Spin1 = sym('Spin1');
Spin2 = sym('Spin2');
Spin3 = sym('Spin3');
Spin4 = sym('Spin4');
Spin5 = sym('Spin5');
Spin6 = sym('Spin6');
Spin7 = sym('Spin7');
Spin8 = sym('Spin8');
Cool = sym('Cool');
Tool = sym('Tool');
%%% Finds activations
pop = 1;   %%% Variables that control when the long if loop is triggered
popped = 1;   %%% Variables that control when the long if loop is triggered
%%% Figure counters
madplot = 10;
counter = 2;
for i=5:length(Powerrms_01(1:test_length))
slope_top = Powerrms_01(1,(i)) - Powerrms_01(1,(i-1));
```

```
slope_bottom = (i) - (i-1);
slope = slope_top/slope_bottom;
slope_store = [slope_store slope];
pop = pop;
if slope > 390 && change_start == 0
event_start = [event_start t(i-1)];
disp('change start')
change_start = 1;
change_stop = 0;
end
if change_start == 1 && Powerrms_01(1,(i)) < Powerrms_01(1,(i-5)) - 300 &&
abs(Powerrms_01(1,(i)) - Powerrms_01(1,(i-1))) < 100
event_stop = [event_stop t(i)];
disp('change stop')
change_start = 1;
change_stop = 1;
popped = pop + 1;
end
if change_start == 1 && change_stop == 1
change_start = 0;
change_stop = 0;
end
%%% Collect the start and stop points of each activation
if popped > pop  %% needs to only fire if an additional activation has
occured
pop = 1; %%% resetting the trigger variables
popped = 1; %%% resetting the trigger variables
for j = 1:length(event_stop)
eval(['event_start' num2str(j) ' = event_start(1,(j));']);
eval(['event_stop' num2str(j) ' = event_stop(1,(j));']);
%%% This section collects and collates all the features from each
%%% activation
%%% plots each activation - necessary only for visualisation
% figure((counter*2)-1);
% subplot(2,1,1);
% plot(I101(eval(['event_start' num2str(j) '*100: event_stop' num2str(j)
'*100;'])))  %% plots current waveform for each activation
% plot(Powerrms_01(eval(['event_start' num2str(j) ': event_stop' num2str(j)
';'])));  %% plots rms power waveform
% subplot(2,1,2);
% plot(I101(eval(['event_start' num2str(j) '*100: event_stop' num2str(j)
'*100;'])))
%%% FEATURES
eval(['template' num2str(j) ' = Powerrms_01(event_start' num2str(j) ':
event_stop' num2str(j) ');']) %% Collects the data plotted in each event
window
eval(['template_min' num2str(j) ' = min(Powerrms_01(event_start' num2str(j)
': event_stop' num2str(j) '));']) %% Minimum value of each window
eval(['norm_temp' num2str(j) ' = template' num2str(j) ' - template_min'
num2str(j) ';']) %% Normalises each window to zero position
eval(['x_max' num2str(j) ' = max(norm_temp' num2str(j) ');']) %% Maximum
value in the normalised window
eval(['x_rms' num2str(j) ' = rmseod(norm_temp' num2str(j) ' ,
length(norm_temp' num2str(j) ') ,0,1);']) %% rms value of the normalised
window
eval(['x_avg' num2str(j) ' = mean(norm_temp' num2str(j) ');']) %% Average
value in the normalised window
```

```
eval(['x_sd' num2str(j) ' = std(norm_temp' num2str(j) ');']) %% SD of the
normalised window
eval(['x_t' num2str(j) ' = (event_stop' num2str(j) ' - event_start'
num2str(j) ')/20;']) %% Length of each window in seconds
eval(['x_cf' num2str(j) ' = x_max' num2str(j) ' / x_rms' num2str(j) ';']) %%
CF of the normalised window
eval(['x_ff' num2str(j) ' = x_rms' num2str(j) ' / x_avg' num2str(j) ';']) %%
FF of the normalised window
eval(['x_features' num2str(j) ' = [ x_max' num2str(j) ' x_rms' num2str(j) '
x_avg' num2str(j) ' x_sd' num2str(j) ' x_t' num2str(j) ' x_cf' num2str(j) '
x_ff' num2str(j) '];']) %% Summary
eval(['test_vect' num2str(j) ' = x_features' num2str(j) ';']) %% Creates
test vectors
eval(['test' num2str(j) ' = x_features' num2str(j) ' - normal ;']) %%
Normalises each test vector
eval(['test_point' num2str(j) ' = test' num2str(j) '* feature_vect2 ;']) %%
Transforms each test vector by using the transofrmation matrix
%%%% DISTANCE CALCULATIONS
for m = 1:50
eval(['euclidean_distance = sqrt(( test_point' num2str(j) '(1,1) -
final_data2D(1,(' num2str(m) ')))^2 + ( test_point' num2str(j) '(1,2) -
final_data2D(2,(' num2str(m) ')))^2   ) ;'])
location = [location (m)];
distances = [distances euclidean_distance];
knn = [distances euclidean_distance; location (m)];
end
eval(['knn' num2str(j) ' = knn;'])
eval(['[Y, I] = sort(knn' num2str(j) '(1,:));'])
eval(['B' num2str(j) ' = knn' num2str(j) '(:,I);']);
%%% SAVING LOCATION - %% (2,1) gives location on nearest neighbour// (1,1)
%%% Distance closest neighbour is from test point
eval(['nearest1_activation' num2str(j) ' = B' num2str(j) '(2,1);'])
eval(['nearest2_activation' num2str(j) ' = B' num2str(j) '(2,2);'])
eval(['nearest3_activation' num2str(j) ' = B' num2str(j) '(2,3);'])
%%% SAVING DISTANCE
eval(['nearest1_activation_dist' num2str(j) ' = B' num2str(j) '(1,1);'])
eval(['nearest2_activation_dist' num2str(j) ' = B' num2str(j) '(1,2);'])
eval(['nearest3_activation_dist' num2str(j) ' = B' num2str(j) '(1,3);'])
%%% SAVING INVERSE DISTANCE
eval(['nearest1_inv_dist' num2str(j) ' = 1/B' num2str(j) '(1,1);'])
eval(['nearest2_inv_dist' num2str(j) ' = 1/B' num2str(j) '(1,2);'])
eval(['nearest3_inv_dist' num2str(j) ' = 1/B' num2str(j) '(1,3);'])
%%% Setting nearest neighbours (Euclidean distance)
eval(['nearest_1 = B' num2str(j) '(1,1);'])
eval(['nearest_2 = B' num2str(j) '(1,2);'])
eval(['nearest_3 = B' num2str(j) '(1,3);'])
%%% Setting nearest neighbours (inverse Euclidean distance)
eval(['nearest_1inv = 1/B' num2str(j) '(1,1);'])
eval(['nearest_2inv = 1/B' num2str(j) '(1,2);'])
eval(['nearest_3inv = 1/B' num2str(j) '(1,3);'])
%%% Finding location of nearest classes
eval(['nearest1_class = B' num2str(j) '(2,1);'])
eval(['nearest2_class = B' num2str(j) '(2,2);'])
eval(['nearest3_class = B' num2str(j) '(2,3);'])
location = [];
distances = [];
knn = [];
```

```
end
%%% ACTIVATION WITHIN CLASSIFICATION RADIUS
if nearest_1 < 580 && nearest_2 < 580
disp('system has identified an activation')
activations = [activations 1]; %%%% Activation counter
class_label1 = newdat{1,nearest1_class};
class_label2 = newdat{1,nearest2_class};
class_label3 = newdat{1,nearest3_class};
%%% KNN CONDITIONS
%%% ALL EQUAL
if class_label1 == class_label2 & class_label2 == class_label3
inv_euc_dist = nearest_1inv + nearest_2inv + nearest_3inv;
class = class_label1;
end
%%% 1st n and 2nd n equal
if class_label1 == class_label2
inv_euc_dist1 = nearest_1inv + nearest_2inv;
inv_euc_dist2 = nearest_3inv;
if inv_euc_dist1 > inv_euc_dist2
class = class_label1;
else if inv_euc_dist2 > inv_euc_dist1
class = class_label3;
end
end
end
%%% 2nd n and 3rd n equal
if class_label2 == class_label3
inv_euc_dist1 = nearest_1inv;
inv_euc_dist2 = nearest_2inv + nearest_3inv;
if inv_euc_dist1 > inv_euc_dist2
class = class_label1;
else if inv_euc_dist2 > inv_euc_dist1
class = class_label2;
end
end
end
%%% 1st n and 3rd n equal
if class_label1 == class_label3
inv_euc_dist1 = nearest_1inv + nearest_3inv;
inv_euc_dist2 = nearest_2inv;
if inv_euc_dist1 > inv_euc_dist2
class = class_label1;
else if inv_euc_dist2 > inv_euc_dist1
class = class_label2;
end
end
end
%%% ALL UNEQUAL
if class_label1 ~= class_label2 & class_label2 ~= class_label3
inv_euc_dist1 = nearest_1inv;
inv_euc_dist2 = nearest_2inv;
inv_euc_dist3 = nearest_3inv;
if inv_euc_dist1 > inv_euc_dist2 & inv_euc_dist1 > inv_euc_dist3
class = class_label1;
end
if inv_euc_dist2 > inv_euc_dist1 & inv_euc_dist2 > inv_euc_dist3
class = class_label2;
```

```
end
if inv_euc_dist3 > inv_euc_dist2 & inv_euc_dist3 > inv_euc_dist1
class = class_label3;
end
end
%%% DISPLAYING CLASS
nameidx = getnameidx(newdat, class); %%% Finds location of identified class
stabilisation_period = stables(nameidx,1);  %%% Choosing the correct
stabilisation period
stable_seconds = stabilisation_period/20;
disp(['Activation identified as:' class])
if class == Spin1 || class == Spin2 || class == Spin3 || class == Spin4 ||
class == Spin5 || class == Spin6 || class == Spin7 || class == Spin8 || class
== Tool
%%% FREQUENCY VERIFICATION
eval(['len_test = length(event_start' num2str(j) '*100: event_stop'
num2str(j) '*100);']) %% Gets length of current waveform
eval(['test_current = I101(event_start' num2str(j) '*100: event_stop'
num2str(j) '*100);']) %% Gets current waveform
eval(['test_time = time01(event_start' num2str(j) '*100: event_stop'
num2str(j) '*100);']) %% Gets time stamps
NFFT_test = 2^nextpow2(len_test);
YI_test = fft(test_current,NFFT_test)/len_test;
fI_test = Fs/2*linspace(0,1,NFFT_test/2+1);
%%%%% Plotting current and fft - only use if visualisation needed
% figure; hold on;
% subplot(2,1,1); hold on;
% plot(Fs*test_time,test_current);
% subplot(2,1,2); hold on;
% plot(fI_test,2*abs(YI_test(1:NFFT_test/2+1)))
%%%% SAVING HARMONIC MAGNITUDES
eval(['hars' num2str(j) ' = (2*abs(YI_test(1:NFFT_test/2+1)));'])
hars = (2*abs(YI_test(1:NFFT_test/2+1)));
if length(hars) == 2049
har1 = max(hars(50:150));
har3 = max(hars(250:350));
har5 = max(hars(450:550));
har7 = max(hars(650:750));
end
if length(hars) == 4097
har1 = max(hars(100:300));
har3 = max(hars(500:700));
har5 = max(hars(900:1100));
har7 = max(hars(1300:1500));
end
if length(hars) == 8193
har1 = max(hars(250:1000));
har3 = max(hars(750:1500));
har5 = max(hars(1800:2200));
har7 = max(hars(2600:3000));
end
%%%% Frequency conditions
if har3 > har5 && har3 > har7
disp('spindle off verified in frequency domain')
end
if har5 > har3 && har7 > har3 && har5 < 2*har3
disp('spindle active status verified in frequency domain')
```

```
end
if har5 > 2*har3
disp('spindle start up sequence verified in frequency domain')
end
end
%%% This if loop only allows the MAD analysis to begin if a spindle
%%% acceleration has been detected
if class == Spin1 || class == Spin2 || class == Spin3 || class == Spin4 ||
class == Spin5 || class == Spin6 || class == Spin7 || class == Spin8
disp(['This activation requires a stabilisation period of '
num2str(stable_seconds) ' seconds']) %% Displaying stabilisation period
disp('MAD analysis in process')
%%%% FIND MACHINING ZONE
eval(['mcstart' num2str(j) ' = event_stop' num2str(j) ' +
stabilisation_period ;']) %% Sets machining start time for each spindle
activation
eval(['low' num2str(j) ' = find(Powerrms_01(mcstart' num2str(j)
':length(Powerrms_01)) < 1200) ;']) %% Finding next time the spindle is
powered off...
eval(['mcstop' num2str(j) ' = low' num2str(j) '(1,1) ;']) %% Sets machining
start time for each spindle activation
eval(['madtest' num2str(j) ' = Powerrms_01(mcstart' num2str(j) ':mcstop'
num2str(j) ' + mcstart' num2str(j) ');']) %% Sets madtest array
figure(2*madplot);
plot((eval(['madtest' num2str(j) ';']))) %% Plots waveform for each machining
test zone
madtest = eval(['madtest' num2str(j) ';']); %% Setting madtest for each time
the MAD is calculated
%%% Collecting run time power consumption
for i = eval(['event_start' num2str(j) ':mcstart' num2str(j) ';']);
run_time_power = [run_time_power Powerrms_01(i)];
end
eval(['change_stamp' num2str(j) ' = [] ;'])
%%%% MAD analysis %%%%
for i = 4:length(madtest)
eval(['MAD_zone' num2str(j) ' = madtest' num2str(j) '(4:length(madtest'
num2str(j) '));'])
eval(['time' num2str(j) ' = [4:1:(length((madtest' num2str(j) ')))];'])
x = [ madtest(1,(i)-3) madtest(1,(i)-2) madtest(1,(i)-1) madtest(1,(i))];
val(i) = mad(x,1); %%% the '1' in column two forces medians to be used
store = [store val(i)];
MAD_zone = eval(['MAD_zone' num2str(j) ';']);
slope_top = madtest(1,(i-1)) - madtest(1,(i-2));
slope_bottom = (i-1) - (i-2);
slope = slope_top/slope_bottom;
slope_set = [slope_set slope]; %% Record all slopes
eval(['stable_power = Powerrms_01(mcstart' num2str(j) ');']) %% Sets stable
power value
threshold = stable_power + 80; %%% Sets threshold
if val(i) < 20 && machining == 0 && rapid_accel == 0;
eval(['change_stamp' num2str(j) ' = [ change_stamp' num2str(j) ' 0 ];'])
machining = 0;
rapid_accel = 0;
run_time_power = [run_time_power madtest(i)];
change = 1;
end
%%% Machining started
```

```
if change == 0 && val(i) > 20 && val(i) < 60 && slope > 40 && machining == 0
&& rapid_accel == 0 && madtest(i) > threshold;
eval(['change_stamp' num2str(j) ' = [ change_stamp' num2str(j) ' 1 ];'])
machining = 1;
cutting = [cutting 1];
cutting_power = [cutting_power madtest(i)];
rapid_accel = 0;
change = 1;
end
%%% CHANGE POINT
if change == 0 && machining == 1 && spindle_off == 0 && val(i) > 40 && slope
< -10;
eval(['change_stamp' num2str(j) ' = [ change_stamp' num2str(j) ' 0 ];'])
cutting = [cutting 0];
machining = 1;
rapid_accel = 0;
run_time_power = [run_time_power madtest(i)];
change = 1;
end
%%% Machining continuing
if change == 0 && machining == 1 && rapid_accel == 0 && madtest(i) >
threshold;
eval(['change_stamp' num2str(j) ' = [ change_stamp' num2str(j) ' 1 ];'])
machining = 1;
cutting = [cutting 1];
cutting_power = [cutting_power madtest(i)];
rapid_accel = 0;
change = 1;
end
%%% rapid accel
if change == 0 && val(i) > 50 && machining == 0 && rapid_accel == 0;
eval(['change_stamp' num2str(j) ' = [ change_stamp' num2str(j) ' 2 ];'])
machining = 0;
rapid_accel = 1;
run_time_power = [run_time_power madtest(i)];
change = 1;
end
if change == 0 & Powerrms_01 > 0 ;
eval(['change_stamp' num2str(j) ' = [ change_stamp' num2str(j) ' 0 ];'])
change = 1;
machining = 0;
rapid_accel = 0;
run_time_power = [run_time_power madtest(i)];
end
%%% RESET VARIABLES
change = 0;
contact = 0;
spin_off = 0;
end
figure;
eval(['plotyy(time' num2str(j) ', MAD_zone' num2str(j) ',time' num2str(j)
',change_stamp' num2str(j) ');'])
title('Power - workpiece test - machining zone')
%%% Find run-time mode duration
eval(['run_time = Powerrms_01(event_start' num2str(j) ':RT_stop);'])
run_time_duration = [run_time_duration length(run_time)];
disp('MAD analysis complete')
```

```
%%% Verify spindle off
eval(['offverify' num2str(j) ' = I101(mcstop' num2str(j) '*100 + mcstart'
num2str(j) '*100:mcstop' num2str(j) '*100 + mcstart' num2str(j) '*100 +
399);'])
eval(['len_test_off = length(offverify' num2str(j) ');'])
eval(['test_current_off = offverify' num2str(j) ';'])
eval(['test_time_off = time01(mcstop' num2str(j) '*100 + mcstart' num2str(j)
'*100:mcstop' num2str(j) '*100 + mcstart' num2str(j) '*100 + 399);']) %% gets
time stamps
NFFT_test_off = 2^nextpow2(len_test_off);
YI_test_off = fft(test_current_off,NFFT_test_off)/len_test_off;
fI_test_off = Fs/2*linspace(0,1,NFFT_test_off/2+1);
eval(['hars_off' num2str(j) ' = (2*abs(YI_test_off(1:NFFT_test_off/2+1)));'])
hars_off = (2*abs(YI_test_off(1:NFFT_test_off/2+1)));
if length(hars_off) == 257
har_off1 = max(hars_off(10:20));
har_off3 = max(hars_off(35:45));
har_off5 = max(hars_off(60:70));
har_off7 = max(hars_off(85:95));
end
%%%% Frequency conditions
if har_off3 > har_off5 && har_off3 > har_off7
disp('spindle off verified in frequency domain')
end
if har_off5 > har_off3 && har_off7 > har_off3 && har_off5 < 2*har_off3
disp('spindle active status verified in frequency domain')
end
if har_off5 > 2*har_off3
disp('spindle start up sequence verified in frequency domain')
end
end
%%%% Activation outside classification radius
else if nearest_1 > 580 && nearest_2 > 580
disp('system has not identified a recognisable activation')
end
end
%%% plot signature space - only needed for visualisation
% figure;%(counter*2)
% plot(b1,b2,'b*'); hold on;
% eval(['plot(test_point' num2str(j) '(1,1), test_point' num2str(j)
'(1,2),''r*'')'])
%%% INCREMENT COUNTERS
counter = counter + 1;
madplot = madplot + 1;
end
end
%%%% QUANTIFICATION CALCULATIONS
TL = test_length/20;  %%% TL = test length
POWER_TOTAL = mean(Powerrms_01);
ENERGY_TOTAL = (TL/3600)*POWER_TOTAL;
MR = length(cutting)/20; %%% MR = Material removal
CUT_POW = mean(cutting_power); %%% Average power consumption
CUT_ENERGY = (MR/3600)*CUT_POW;
RT = length(run_time_power)/20;
RT_POW = mean(run_time_power); %%% Average power consumption
RTZ = RT; %%% RTZ = Run time zone
RT_ENERGY = (RTZ/3600)*RT_POW;
```

```
IT = TL - (RT+MR); %%% IT = Idle time
MP = (max(Powerrms_01))/1000; %%% MP is maximum power during the test
CA = sum(activations); %%% This counts the total number of activations in a
given test
IDLE_ENERGY = ENERGY_TOTAL - (CUT_ENERGY + RT_ENERGY);
%%%% SUMMARY REPORT
disp('- - - - SUMMARY REPORT - - - -')
disp(['Total test duration: ' num2str(TL) ' seconds'])
disp(['Total test energy: ' num2str(ENERGY_TOTAL) ' Wh'])
disp(['Total idle time: ' num2str(IT) ' seconds'])
disp(['Total idle energy: ' num2str(IDLE_ENERGY) ' Wh'])
disp(['Total Run time duration: ' num2str(RTZ) ' seconds'])
disp(['Total Run time energy: ' num2str(RT_ENERGY) ' Wh'])
disp(['Total cutting time: ' num2str(MR) ' seconds'])
disp(['Total cutting energy: ' num2str(CUT_ENERGY) ' Wh'])
disp(['Number of component activations detected: ' num2str(CA) ])
disp(['Maximum power demand: ' num2str(MP) ' kW'])
toc
```

Command Window - Test 1

- - - - SUMMARY REPORT - - - -
Total test duration: 35.2 seconds
Total test energy: 20.5548 Wh
Total idle time: 8.75 seconds
Total idle energy: 2.9860 Wh
Total Run time duration: 5.90 seconds
Total Run time energy: 5.7952 Wh
Total cutting time: 20.55 seconds
Total cutting energy: 11.7736 Wh
Number of component activations detected: 1
Maximum power demand: 11.2429 kW

Command Window - Test 2

- - - - SUMMARY REPORT - - - -
Total test duration: 107.8 seconds
Total test energy: 76.7694 Wh
Total idle time: 29.15 seconds
Total idle energy: 10.2054 Wh
Total Run time duration: 37.6 seconds
Total Run time energy: 38.9525 Wh
Total cutting time: 41.05 seconds
Total cutting energy: 27.6114 Wh
Number of component activations detected: 6
Maximum power demand: 11.8967 kW

Appendix B

Associated publications

B.1 Journal articles

- O'Driscoll, E., O'Donnell, G.E., Industrial power and energy metering - a state-of-the-art-review, *Journal of Cleaner Production, 41:53-64*, 2013.
- O'Driscoll, E., Óg Cusack, D., O'Donnell, G.E., The development of energy performance indicators within a complex manufacturing facility, *International Journal of Advanced Manufacturing Technology, 68:2205-2214*, 2013.
- O'Driscoll, E., Óg Cusack, D., O'Donnell, G.E., The characterisation of energy consumption in manufacturing facilities - a hierarchical approach, *International Journal of Automation Technology, 7:727-734*, 2013.

B.2 Conference articles

- O'Driscoll, E., Óg Cusack, D., O'Donnell, G.E., Implementation of energy metering systems in complex manufacturing facilities - A case study in a biomedical facility, *Procedia CIRP, 1:524-529*, 2012.
- O'Driscoll, E., Kelly, K., Óg Cusack, D., O'Donnell, G.E., Characterising the energy consumption of machine tool actuator components using pattern recognition, 8^{th} *CIRP Conference on Intelligent Computation in Manufacturing Engineering, Ischia*, 2012.
- O'Driscoll, E., Óg Cusack, D., O'Donnell, G.E., Quantifying electrical energy consumption in manufacturing process chains, *Trinity College Dublin Journal of Postgraduate Research, 10:148-161*, 2011.
- O'Driscoll, E., Óg Cusack, D., O'Donnell, G.E., Environmental analysis of process chains - A biomedical case study, *International Manufacturing Conference 27, Galway*, 2010.